Synthetic Routes to Terminal and Backbone Functionalised Copolymer Materials

by

Edward Luke Malins

A thesis submitted in partial fulfilment of the requirements for the degree of

Doctor of Philosophy in Chemistry

Department of Chemistry

University of Warwick

September 2015

Table of Contents

List of Figures

List of Tables

List of Schemes

List of Abbreviations

AEBiB	2-Azidoethyl-2′-bromoisobutyrate
AIBN	2,2′-Azobis(2-methylpropionitrile)
AMS	α-Methyl styrene
ATRP	Atom transfer radical polymerisation
BDTMP	3-Butyl-2-(dodecylthiocarbonothioylthio)-2-methylpropionate
BiBB	α-Bromoisobutyryl bromide
CRP	Controlled radical polymerisation
$Đ$	Polymer dispersity
DMA	*N*,*N*-dimethylacrylamide
DMAEA	2-(Dimethylamino)ethyl acrylate
DMAEMA	2-(Dimethylamino)ethyl methacrylate
DMF	*N*,*N*-dimethylformamide
DMSO	Dimethyl sulfoxide
DP	Degree of polymerisation
DVM	Dispersant viscosity modifier
FT-IR	Fourier transform-infrared red
GC-FID	Gas chromatography – flame ionisation detection
GPC	Gel permeation chromatography

HEBiB	2-Hydroxyethyl-2-bromoisobutyrate
iPOx	2-Isopropenyl-2-oxazoline
MalA	Maleic anhydride
MALDI-TOF	Matrix-assisted laser desorption/ionisation time-of-flight
MEK	2-Butanone
M_n	Number average molecular weight
M_p	Peak molecular weight
M_w	Weight average molecular weight
n.d.	Not determined
NMP	Nitroxide mediated polymerisation
NMR	Nuclear magnetic resonance
PA	Propagyl alcohol
PFS	2,3,4,5,6-pentafluorostyrene
PIB	Polyisobutylene
PIBA	Polyisobutylene acrylate
PIBBiB	Polyisobutylene bromoisobutyrate
PIBBSA	Polyisobutylene bis(succinic anhydride)
PIBP	Polyisobutylene phenol
PIBSA	Polyisobutylene succinic anhydride

PMMA	Poly(methyl methacrylate)
ppm	Parts per million
PSy	Polystyrene
RAFT	Reversible addition fragmentation chain transfer
RID	Refractive index detector
SET-LRP	Single electron transfer living radical polymerisation
Sy	Styrene
TEA	Triethylamine
THF	Tetrahydrofuran
TMI	3-Isopropenyl-α,α-dimethylbenzyl isocyanate
TP	Thiophenol
UV-vis	Ultra violet-visible
V601	Dimethyl-2,2′-azobis(isobutyrate)
VWD	Variable wavelength detector

Acknowledgements

Learning how to perform research can not be achieved alone but requires the support of so many others. Therefore, I will take this opportunity to thank all of those who helped me so much throughout and I will do my very best not to miss anybody out along the way.

First and foremost I would like to thank my supervisors, Professor David Haddleton and Dr. Remzi Becer, for giving me the opportunity to work in their labs and be a part of their ever-changing groups. I would especially like to thank Remzi for his constant enthusiasm and guidance over the years. Without his guidance I am sure this thesis would be much thinner and I wouldn't have the same opportunities; both in the past and looking forward. Many thanks to Dr. Carl Waterson and Dr. Ian McRobbie of Innospec, who have provided much insight and advice throughout the entire project.

A huge thank you to the past and present members of the Haddleton group; James, Jamie, Stacy, Mat, Ant, George, Kay, Raj, Qiang, Athina, Chris W, Chris S, Ronan, Jenny, Alex, Paul. You were all so friendly and patient, I immediately felt welcome and no (stupid) question of mine went unanswered. Working with you guys was always a lot of fun whether it was a beer-glass-smashingly-good-night-out for James or that one time the corridor on floor two got gassed out, so many tears. A thank you to my fume hood neighbour Dan, for being the most hard-working person I know and making me feel so unproductive.

Moreover, it has been such a pleasure to be part of the Becer group and watching it grow from a dynamic duo to a vast group of talented people; Gokhan, Resat, Jacky, Dominic, Manuel, Suzan, Martin, Norlaily, Tian, Elham, Cigdem, David, Silvia,

Yamin and Ben. I am going to miss the familiar sound of einslive.de in the morning and the occasional ill-fated night out; looking at you summer BBQ and Oktoberfest. I am however happy to leave you all with the fridge that smells suspiciously like thiols and that rota. vap. which still doesn't have a condenser…..

Furthermore, there has been no end of technical staff who have so kindly given their time to me; Ant, Kay, Raj, Ivan, Edward, Phillip, Chris, Ben, Krystelle, Lingzhi. These people have been so patient and never refused to help me, whether I asked them to teach me how to use an instrument, replace a piece of glassware that was broken somehow, reteach me how to use that instrument, analyse mysterious data, the list goes on.

I would like to thank my entire family for supporting me through my "perpetual student life" and for humouring me whilst I talk about polymers, they really are so much more than just plastics! I will finish by thanking Nena who has been an ever-constant supply of encouragement during my PhD and was always on hand to offer some perspective when I got bogged down by polymers. You have been extremely patient waiting for me to finish writing up and join you in the adult world and as a reward you now have to live with me!

Declaration

This thesis is submitted to the University of Warwick in support of my application for the degree of Doctor of Philosophy. It has been composed by myself and has not been submitted in any previous application for any other degree, or at any other institution.

The work presented (including data generated and data analysis) was carried out by the author.

Parts of this thesis have been published by the author:

"Alternating copolymers of functionalized α-methyl styrene monomers and maleic anhydride" E. L. Malins, C. Waterson and C. R. Becer, *Polym. Chem.*, 2015, **6**, 6543.

"Controlled synthesis of amphiphilic block copolymers based on poly(isobutylene) macromonomers" E. L. Malins, C. Waterson and C. R. Becer, *J. Polym. Sci. Part A: Polym.* Chem., 2015, DOI: 10.1002/pola.20150544R1, accepted.

_____ Date:_____

Edward Luke Malins

Abstract

The main objective of this thesis was to design and synthesise, via a combination of controlled radical polymerisation and post-polymerisation modification, functional copolymers with a potential application as automotive additives. Pursuit of this objective resulted in the development of four novel syntheses of copolymers.

Block copolymers of polyisobutylene (PIB) and poly(2-(dimethylamino)ethyl methacrylate) (PDMAEMA) were prepared via two different synthetic pathways that exploited alternative end group modifications of olefin terminated PIB. A PIB macroinitiator was utilised for the single-electron transfer living radical polymerisation of DMAEMA as well as macromolecular coupling of a primary amine bearing PDMAEMA and a succinic anhydride terminated PIB.

Friedel-Crafts alkylation of phenol with olefin terminated PIB and subsequent esterification of the phenolic end group with acryloyl chloride furnished polyisobutylene functionalised with an acrylate end group (PIBA). PIBA was then successfully copolymerised with *N*,*N*-dimethylacrylamide (DMA), via reversible addition fragmentation chain transfer (RAFT) polymerisation, to synthesise random and block copolymers of PIBA and DMA.

Alternating copolymers were synthesised by the free radical copolymerisation of alkyl-functional α-methyl styrene (AMS) monomers and maleic anhydride (MalA). These copolymers could then be modified post-polymerisation, via imidisation of the MalA repeat units with a primary amine, to prepare alternating difunctional copolymers.

In the last Chapter original modifications and block copolymers of poly(2,3,4,5,6-pentafluorostyrene) (P(PFS)) were developed. Functionalisation of P(PFS) with a *para*-azide moiety by substitution of the *para*-fluorine with sodium azide was demonstrated. This substitution was then performed in combination with a *para*-fluoro thiol “click” reaction and a [4+2] azide-alkyne cycloaddition to subsequently modify a P(PFS) backbone multiple times. A P(PFS) macroRAFT agent, prepared by RAFT polymerisation, was successfully chain extended with DMA and 2-isopropenyl-2-oxazoline to prepare functional amphiphilic block copolymers.

1. Introduction

Polymers have existed in the form of natural products including carbohydrates, proteins and polynucleotides long before synthetic polymers became so ubiquitous throughout the modern world. Furthermore, these natural polymers have already established synthetic pinnacles in precision and efficiency for modern chemists to strive towards.

The first use of the term "polymer" was by Jöns Jakob Berzelius in 1833 to describe two or more compounds with the same relative compositional formula but different absolute formulas.[1] Therefore, the different properties observed between these compounds was attributed to total number of atoms present in the molecule (e.g. acetylene and benzene). However, this original definition of polymer was used inconsistently with other terms of isomerism; allotropic and metameric. In 1922 Hermann Staudinger coined a new term, "macromolecule", to describe a covalently bonded organic molecule that contains greater than 1000 atoms.[1] Since then the international union of pure and applied chemistry (IUPAC) has redefined both terms. Macromolecule is "a molecule of high relative molecular mass, the structure of which essentially comprises the multiple repetition of units derived, actually or conceptually, from molecules of low relative molecular mass", macromolecules may also be referred to as "polymer molecules".[2] A polymer is "a substance composed of macromolecules".[2] Therefore, a distinction between single macromolecules and a substance/material composed of multiple polymeric molecules now exists.

Since this inception of macromolecular species and establishment of polymer science as a field, synthetic polymer chemistry utilises increasingly sophisticated techniques to develop complex molecules and materials. Macromolecules are now synthesised

with control over molecular weight, monomer composition, monomer microstructure (alternating, block, random and gradient copolymers) and architecture (linear, star, graft and dendritic polymers) (Figure 1.01) so the macromolecule can be better tailored for a desired application.

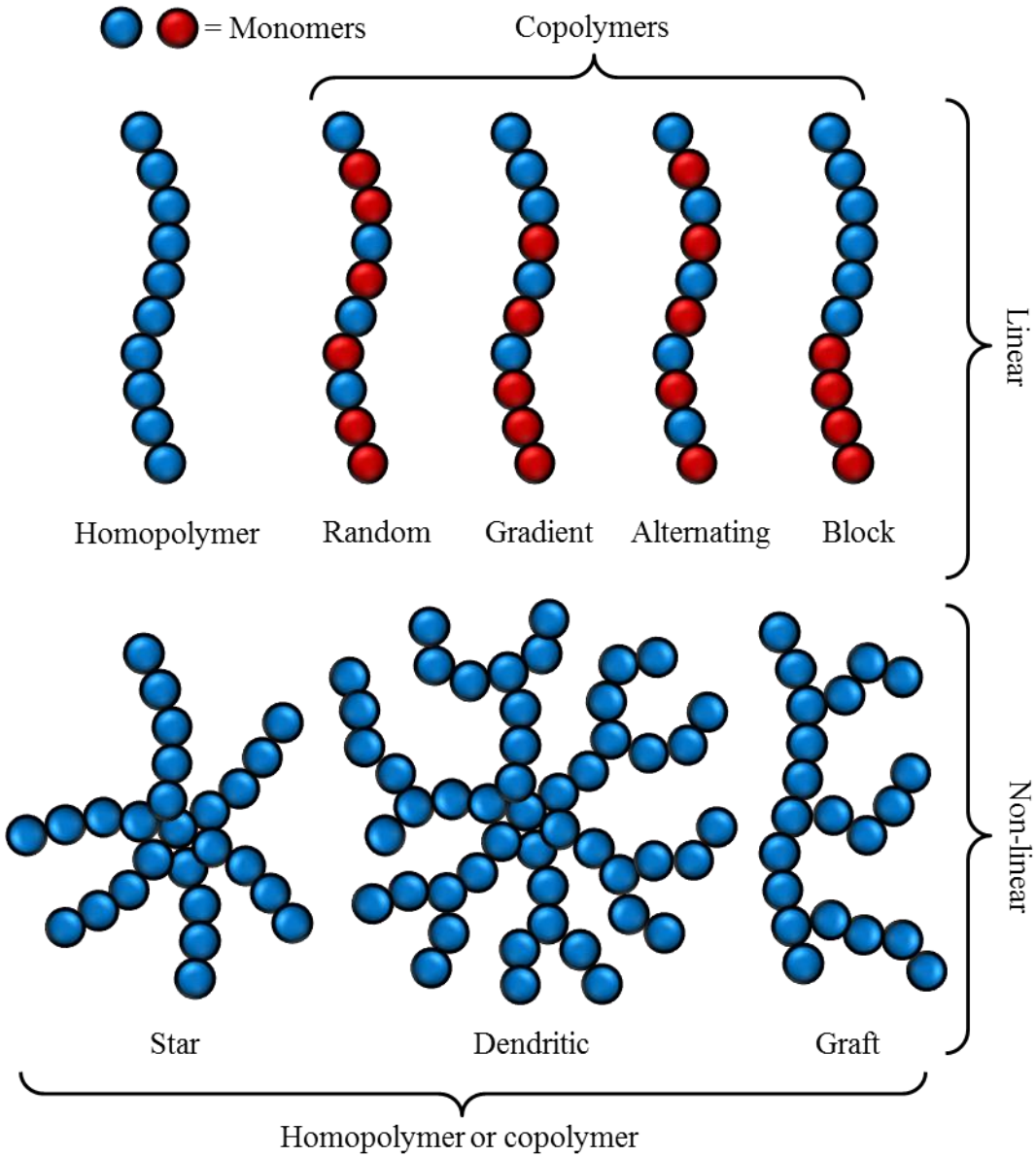

Figure 1.01. Representation of different copolymer compositions and (co)polymer architectures.

Traditional polymerisation techniques were condensation and addition polymerisation, which have since been renamed to step-growth and chain-growth polymerisation, respectively. Chain-growth polymerisation will now be introduced,

with a focus on radical polymerisation, as this will be the principle polymerisation technique utilised throughout this work.

1.1. Free radical polymerisation

Free radical polymerisation (FRP) is a well-established and widely utilised method of polymerising vinyl monomers.[3] This is partly due to FRP being tolerant towards many reaction conditions (temperature, reagent purity, solvents, functional groups, moisture, air etc.) and allowing polymerisation in bulk, in solution, in suspension or as an emulsion.[4]

Mechanisms governing FRP are well understood and can be classified into four stages; initiation, propagation, chain transfer and termination (Scheme 1.02).[4] Initiation is a two-step process which begins the growth of a polymer molecule, firstly free radicals ($I^{\bullet}$) are generated from an initiator molecule (I−I), this is commonly achieved by thermal decomposition (Scheme 1.01), photolysis and redox reactions.[4] These free radicals are then capable of adding a monomer unit and initiating the growth of a polymer molecule (Scheme 1.02).

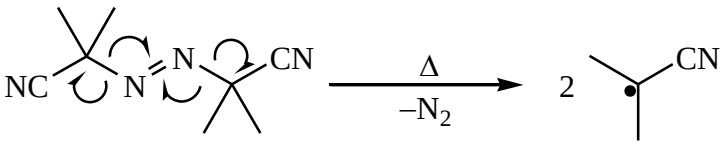

2,2′-Azobis(2-methylpropionitrile) (AIBN)

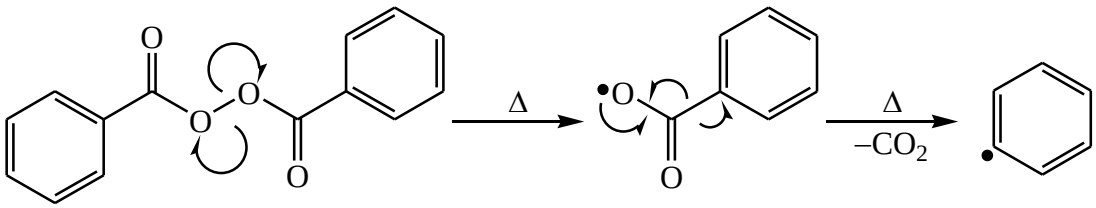

Dibenzoyl peroxide (BPO)

Scheme 1.01. Thermal decomposition of common free radical initiators to free radicals.

Propagation is the repeated addition of monomer units to the initiating radical species and formation of a propagating polymeric radical which continues to increase in chain length by addition of more monomers (Scheme 1.02).[3,4] Propagation continues until all monomer is consumed or chain transfer/termination of the polymeric radical occurs.[3]

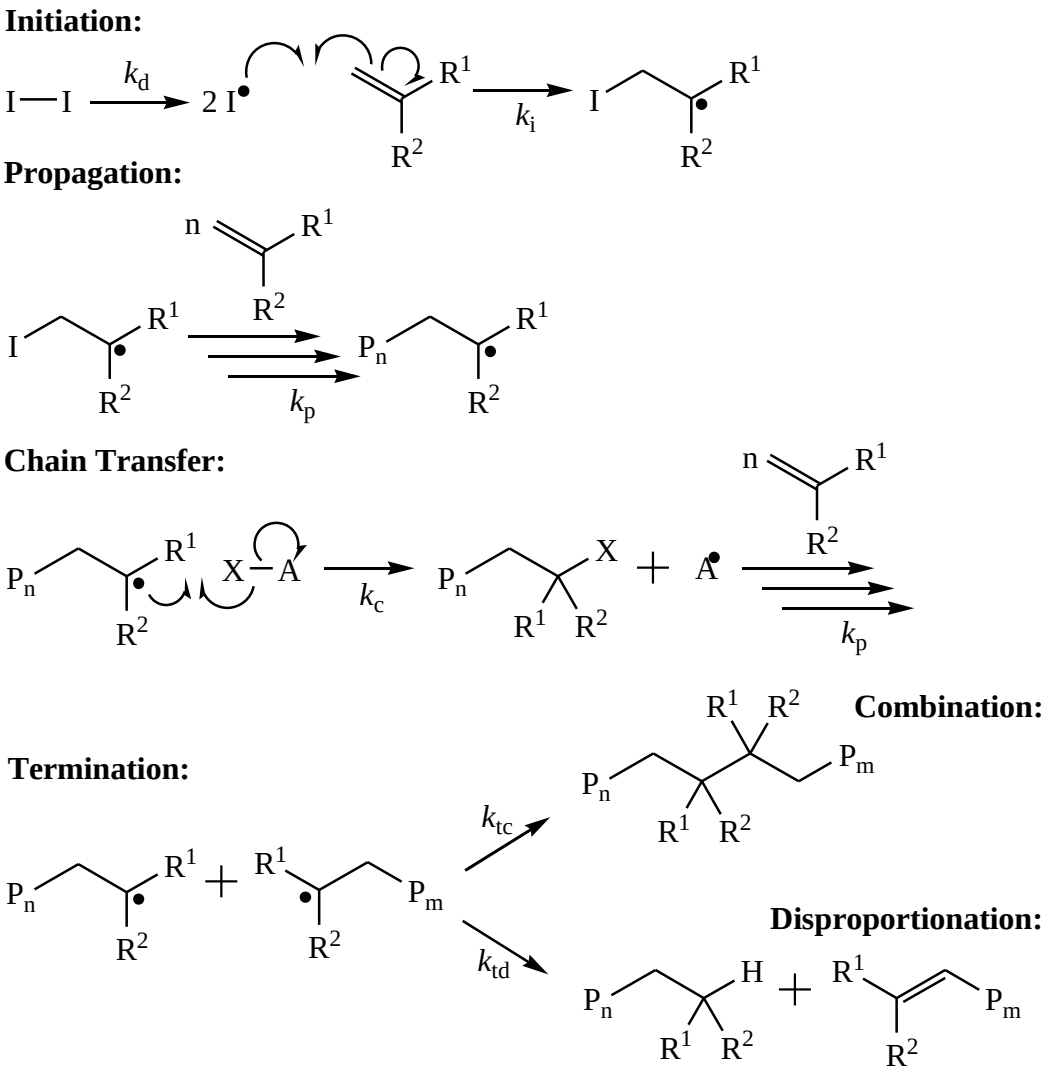

Scheme 1.02. General mechanism steps for free radical polymerisation: initiation, propagation, chain transfer and termination (combination and disproportionation).

Chain transfer is the process by which a propagating polymeric radical transfers the active centre (radical) to a new molecule.[3] This can occur by abstraction of hydrogen or another atom (X) from a number of species within the polymerisation; solvent, monomer, initiator, polymer or chain transfer agent (CTA).[4] Chain transfer results in

the termination of the propagating polymeric chain but does generate a new radical ($A^{\bullet}$), which may or may not be able to initiate a new propagating chain (Scheme 1.02).[4] Chain transfer results in the reduction of polymer molecular weight obtained when compared to polymerisation where no chain transfer occurs.[4] Mayo in 1943 developed the necessary theory to determine the chain transfer constant of a molecule from experimental measurements.[5]

Termination, the process by which a polymeric radical is consumed and no longer propagates, can occur by many different mechanisms. Bimolecular termination of radicals is most prevalent and often transpires between two polymeric radicals via two different mechanisms; combination or disproportionation.[4] Combination occurs when two separate polymeric chains meet and combine to form a new single polymer molecule with double the molecular weight.[4] Disproportionation also occurs when two separate propagating polymeric chains meet; however in this situation a hydrogen atom is abstracted from one polymer chain-end to the other polymer chain.[4] Disproportionation maintains two separate polymer molecules and as such does not double the molecular weight but does result in a mixture of saturated and unsaturated end groups (Scheme 1.02).[4] Termination may also occur via other mechanisms, such as combination of initiating radicals and polymeric radicals or reaction of polymeric radicals with molecular oxygen or radical inhibitors.

Owing to the high reactivity of radicals, termination and chain transfer side reactions are prominent in FRP which results in a less controlled polymerisation. Poor control of free radical polymerisation makes it difficult to synthesise polymer molecules with; predictable molecular weight, uniform molecular weight distribution and higher order architecture (block copolymers, stars, etc.). Furthermore, initiating and terminating species/mechanisms are less consistent throughout FRP which results in

poorly defined polymer end groups. Therefore, post-polymerisation functionalisation and chain extensions with further monomer are inefficient.

1.2. Living polymerisation and controlled radical polymerisation

Owing to certain limitations of FRP; controlling polymer molecular weight, maintaining a narrow polymer dispersity and certainty of the polymer end groups, living polymerisation was developed. Living polymerisation was first reported by Szwarc in 1956 for the polymerisation of styrene (Sy).[6,7] After polymerisation of Sy was complete, additional Sy was added to the system and subsequently polymerised and measured by an increase in viscosity.[6,7] Szwarc concluded that the polymer chains were "living" and capable of continuing to propagate as long as all sources of termination had been excluded from the polymerisation.[6,7] This discovery led to the field of living polymerisation and development of many living polymerisation techniques. However, many features of a polymerisation may define a polymerisation as "living", so Quirk and Lee detailed the following seven experimental criteria that must be fulfilled for a polymerisation to be "living":[8]

1. Polymerisation proceeds until all of the monomer has been consumed. Further addition of monomer results in continued polymerisation.
2. The number average molecular weight (M_n) is a linear function of monomer conversion.
3. The number of active polymer chains and active centres is constant.
4. M_n is controlled by the stoichiometry of the polymerisation.
5. Narrow molecular weight distribution polymers are produced.
6. Block copolymers can be prepared by sequential monomer addition.
7. Chain-end functionalised polymers can be prepared in quantitative yield.

Although living polymerisation enabled the synthesis of well-defined polymers, reaction conditions required are extremely stringent; monomer/solvent must be rigorously purified before polymerisation and all air/moisture must be excluded from the polymerisation. Furthermore, choice of monomer was limited by the functionality present and the active centre (cationic, anionic etc.) that forms for the polymerisation technique dictates which monomer classes can be polymerised. Therefore, a polymerisation technique was required that could synthesise polymers as well-defined as those synthesised by living polymerisation but is as tolerant as FRP is towards moisture, impurities, functionality etc.

A compromise between living polymerisation and FRP was achieved by the development of a new field of polymer synthesis, controlled radical polymerisation (CRP) which is also known as reversible-deactivation radical polymerisation (RDRP). Although CRP is often called living radical polymerisation, this is not strictly correct as termination always occurs by combination of radicals but CRP does manage to satisfy many of the living criteria outlined previously. Ionic living polymerisations do not undergo termination by combination as the propagating ionic polymer chains are unreactive with each other. However, propagating polymeric radicals are highly reactive with each other and potentially experience high amounts of bimolecular termination. Therefore, a major difficultly of CRP is suppressing bimolecular termination whilst still allowing propagation to occur at a reasonable rate. This can be achieved by utilising a mediating species to maintain a suitable radical concentration by reversibly activating an initiator/dormant polymer to an initiating radical/propagating polymeric radical. This mediating species will maintain the radical concentration by one of three general mechanisms; reversible termination by coupling, reversible termination by atom transfer and reversible chain transfer.[4]

Consequences of this reversible activation are that radical concentration is kept low (relative to dormant chains) and constant. As such many of the living polymerisation criteria are fulfilled and polymers with narrow dispersity, well-defined end groups, and predictable molecular weight which can be calculated by considering the stoichiometry and monomer conversion (Equation 1) are synthesisable.

$$M_{\mathrm{n.Theo}} = \rho \frac{[\mathrm{M}]_0}{[\mathrm{I}]} \mathrm{M_o} + \mathrm{I_o}$$

Equation 1. $M_{\mathrm{n.Theo}}$ = number average molecular weight, ρ = monomer conversion, $[\mathrm{M}]_0$ = initial monomer concentration, [I] = initiator concentration, $\mathrm{M_o}$ = monomer molecular weight and $\mathrm{I_o}$ = initiator molecular weight.

Compared to traditional living ionic polymerisation techniques, CRP offers many advantages; such as tolerance of many monomer/solvent functional groups, air and moisture tolerance and stringent purification of reagents is often not required. Owing to these benefits, CRP has been widely adopted and there are now a large number of CRP techniques that have been invented. The most widely studied and routinely employed CRP techniques will now be introduced.

1.2.1. Atom transfer radical polymerisation

Atom transfer radical polymerisation (ATRP) was independently developed by Sawamoto and Matyjaszewski in 1995, utilising ruthenium(II) and copper(I) catalysts respectively.[9-11] ATRP was developed from the atom transfer radical addition (ATRA) and the Kharasch reaction of the 1940s, which radically added halogens to olefins.[12,13] ATRP relies on the reversible activation of a dormant halogen capped polymer to an active polymeric radical by transfer of the halogen atom to and from a transition metal complex.[10,11] Said metal complex is in turn oxidised as it activates the dormant polymer chain and is reduced when deactivating an active polymer chain (Scheme 1.03).

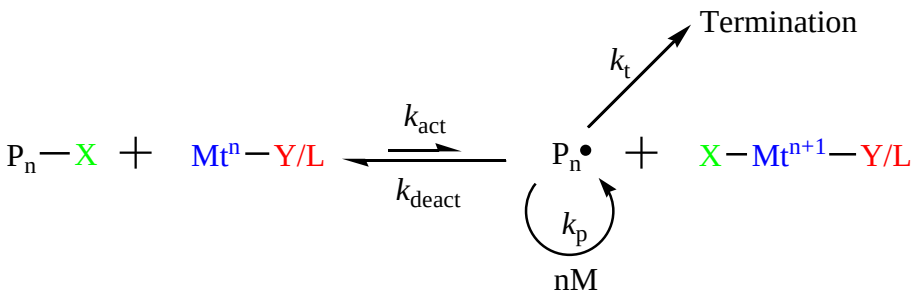

Scheme 1.03. Proposed mechanism for ATRP. Where P_n = polymeric molecule, X = halogen, Mt^n = transition metal with oxidation state of n, L = ligand, Y = ligand or counter ion and M = monomer.

Many transition metals have been utilised for ATRP (such as Re, Ru, Fe, Rh and Ni) but Cu(I) is still the most widely employed transition metal in ATRP, owing to its versatility and cost.[14] Cu(I) is only one component essential for mediating ATRP, careful consideration of ligand and polymerisation initiator is also vital to achieve a controlled polymerisation. A vast array of Cu(I)/ligand complexes have been examined by Matyjaszewski and co-workers to determine the activity of each complex and the resulting ATRP equilibrium constant.[15] It was shown that Cu(I)/ligand complex activity was highest when stabilised by ligands containing: alkyl amine ≈ pyridine > alkyl imine >> aryl imine > aryl amine.[15] It was also shown that complex activity decreased from tetradentate ligands to tridentate ligands and finally bidentate ligands.[15]

Matyjaszewski and co-workers also examined the ATRP equilibrium constants for a number of alkyl halide initiators.[15] Alkyl bromides are more active than the analogous alkyl chlorides.[15] Furthermore, activity was found to increase with the level of alkyl halide substitution, tertiary alkyl halide esters are most active whereas primary alkyl halide esters are the least active.[15] Finally, alternative initiator substituents for a given initiator type were examined and nitriles were found to increase activities more than benzyl derivatives.[15] Common ATRP ligands and initiators are shown in Figure 1.02.

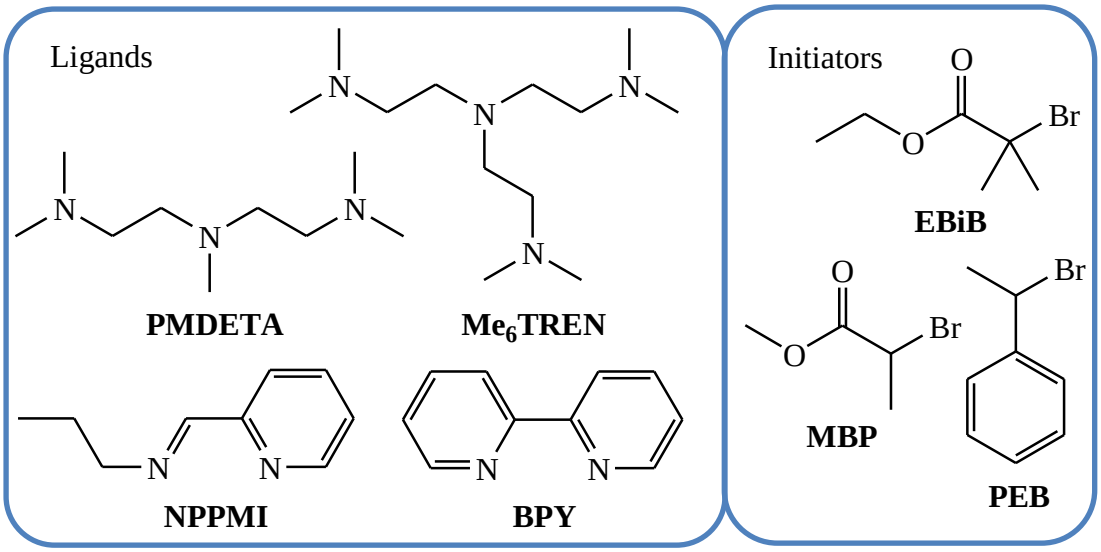

Figure 1.02. Structures of common ATRP ligands and initiators.

ATRP is typically performed in non-polar solvents or bulk[9-11] but polar-protic solvents have also been utilised as well as ionic liquids.[16,17] Although there are many variables influencing the ATRP equilibrium position and thus the control of the polymerisation, ATRP has proven to be an extremely versatile technique and can polymerise a wide range of monomers; (meth)acrylates, styrenes, (meth)acrylamides and acrylonitrile.[14] However, ATRP does require large quantities of copper complex catalyst and as such recent advances in ATRP have been focused on developing alternative ATRP techniques that reduce catalyst loading.

One such technique is initiators for continuous activator regeneration (ICAR) ATRP.[18] ICAR ATRP utilises small quantities of free radical initiators, such as AIBN, to reduce accumulated Cu(II) back to Cu(I) which can subsequently activate dormant polymer chains again.[18] ICAR ATRP has been limited in its application of synthesising block copolymers as some polymer chains will be initiated by the free radical initiator thus reducing the end group fidelity.[18] However, ICAR ATRP has been utilised to synthesise block copolymers by chain extending ATRP

macroinitiators whilst only generating a negligible quantity of free radical initiated homopolymers.[19]

Another technique designed to reduce accumulated Cu(II) back to Cu(I) and thus lower the quantity of catalyst required is activators regenerated by electron transfer (ARGET) ATRP.[20,21] ARGET ATRP regenerates Cu(I) by reduction of Cu(II) with a variety of compounds such as tin(II) 2-ethylhexanoate, glucose, ascorbic acid, phenols and hydrazine.[18,20-22] For ARGET ATRP to be most efficient reducing agents utilised should not directly or indirectly produce radicals which can initiate a polymerisation.[20,21] Deactivating species concentration should be suitably maintained so large concentrations of radicals are not generated and thus decreasing polymerisation control.[22]

UV/visible light irradiation has also been utilised to lower the quantity of copper catalyst, Cu(II) complexes are reduced to the active Cu(I) complexes in situ. This has been achieved with the presence of reducing agents such as methanol and without any reducing agents when irradiated at 350 nm at room temperature.[23,24] This methodology has been highly optimised so that only 100 ppm loadings of Cu(II) catalyst is required and polymerisations can be irradiated with LEDs at 392/450 nm or with sunlight to generate the necessary active Cu(I) catalyst to afford a controlled polymerisation.[25] Furthermore, monomer conversion could be stopped by removing the external light source, allowing the polymerisations to be switched on and off.[25]

Electrochemical potential has been exploited as an external stimulus to lower the quantity of copper catalyst required for ATRP.[26] Electrochemically mediated ATRP (eATRP) reversibly activates the Cu catalyst by reduction of Cu(II) complex to the active Cu(I) complex.[26] Controlled polymerisations could be maintained with

catalyst loadings as low as 50 ppm and polymerisation could be switched on and off by applying intermittent potentials.[26] eATRP has been extended to aqueous systems by the eATRP of oligo(ethylene glycol) methyl ether methacrylate (OEGMA).[27] Lately, Matyjaszewski and co-workers have aimed to broaden the appeal of eATRP by systematically optimising many electrochemical and polymerisation parameters such as, applied potential, catalyst concentration and choice of ligand as well as investigating Cu catalyst recycling.[28]

Zerovalent metals such as Fe(0) and Cu(0) have been added to ATRP containing $Fe(II)Br_2$ and $Cu(II)Br_2$, respectively, to (re)generate the active metal complexes.[29] This technique is also designed to limit the quantity of catalyst required by preventing the accumulation of deactivated metal salts. However, the exact role of Cu(0) and Cu(II) in the polymerisation mechanism is still debated and two proposed mechanisms exist.[30] Supplemental activator and reducing agent (SARA) ATRP describes Cu(0) as primarily a reducing agent for Cu(II) back to Cu(I) which is the principal activator of alkyl halides throughout polymerisation.[30] An alternative mechanism, single electron transfer living radical polymerisation (SET-LRP), maintains that Cu(0) is the only activator of alkyl halides as all Cu(I) undergoes rapid disproportionation to Cu(0) and Cu(II).[30] SET-LRP will now be introduced to highlight the differences from ATRP, particularly focusing on the alternative experimental conditions used to perform SET-LRP.

1.2.2. Single electron transfer living radical polymerisation

SET-LRP was first introduced in 2006 by Percec and co-workers wherein they polymerised acrylates, methacrylates and vinyl chloride utilising Cu(0) in the presence of *N*-containing ligands and polar solvents (water, alcohols, dimethyl sulfoxide (DMSO) etc.) at room temperature and initiated by alkyl/sulfonyl/*N*-

halides.[31] It was proposed that Cu(0) is the sole activator of initiator halides whilst Cu(I)Br rapidly disproportionates to the active "nascent" Cu(0) and Cu(II)Br_2.[31] Formation of the "nascent" Cu(0) nanoparticles have been demonstrated microscopically and by a series of visualisation experiments.[32,33] Cu(II)Br_2 remains a deactivating species as it is in ATRP, converting active propagating polymeric radicals back to the dormant alkyl halides (Scheme 1.04).[31] A crucial difference between SET-LRP and ATRP is that Cu(0) donates an electron via an outer-sphere electron-transfer mechanism (OSET) whereas ATRP proceeds via an inner-sphere electron-transfer mechanism (ISET).[31] OSET has lower activation energy than ISET and as such the polymerisations can be performed at lower temperature, whilst maintaining fast activation/deactivation and suppressing bimolecular termination even further.[31]

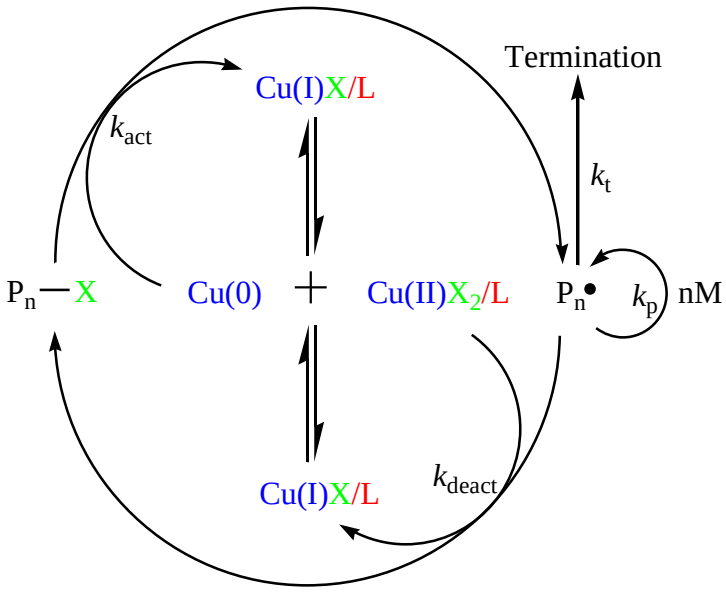

Scheme 1.04. Proposed mechanism of SET-LRP. Where P_n = polymeric molecule, X = halogen, L = ligand and M = monomer.

Disproportionation of Cu(I)Br to "nascent" Cu(0) and Cu(II)Br_2 is arguably the most important step of SET-LRP and therefore conditions that encourage disproportionation are highly favourable. Equilibrium of disproportionation is

dependent on ligand, solvent composition, counter ion and temperature.[34] Polar solvents are known to favour the disproportionation of Cu(I)Br and have been shown to be far more effective than non-polar alternatives when all other conditions remain constant.[35-37] Typical solvent choices include; DMSO, alcohols, water, ionic liquids, ethylene/propylene carbonate or binary mixtures thereof.[31,34,38,39] Furthermore, disproportionation can be promoted in less polar solvents by the addition of polar additives such as phenol and water.[40,41]

Correct choice of ligand is also vital for achieving high rates of disproportionation and as such ligand choice is more limited for SET-LRP than ATRP. Ligands that preferentially stabilise Cu(II) complexes are favoured as well ligands that distort the geometry of Cu(I) complexes, exposing coordination sites to water, solvents and monomer.[42] Common ligands that exhibit these qualities are ME_6TREN and PMDETA.[42]

Quality of the Cu(0) added to the polymerisation has a profound impact on SET-LRP. Firstly, use of Cu(0) wire instead of Cu(0) powder was shown to reduce the rate of polymerisation but allows for simple removal from the polymerisation.[31] Apparent rate constant of polymerisation was shown to increase with decreasing Cu(0) particle size.[43] Furthermore, activation of Cu(0) to remove the oxide layer present has been demonstrated as an effective method of allowing SET-LRP to proceed with no induction period.[44] Activation of Cu(0) has been achieved by pre-polymerisation treatment with acids (hydrochloric, glacial acetic, nitric), hydrazine and fluorinated alcohols.[37,44,45]

SET-LRP has been demonstrated to be a very tolerate polymerisation which is indeed very “living”, this has been highlighted by a series of experiments which

intentionally terminate and then reactive the SET-LRP.[46,47] Following intentional termination monomer conversion nearly ceases altogether and then resumes once the catalytic system is restored to its previous state, a controlled polymerisation is maintained throughout.[46,47] End group fidelity of polymers synthesised via SET-LRP has been demonstrated by various end group modifications and MALDI-TOF MS analysis to be perfect.[48] High end group fidelity has been exploited to synthesise highly ordered architectures such as; 32 armed polymer dendrimers after 4 generations via multiple end group modifications and subsequent polymerisations.[49]

Recently, SET-LRP has been utilised as an extremely effective tool for the synthesis of linear (multi)block copolymers by iterative additions of monomer to a living system with no intermittent purification required.[48] This has been reported for both the synthesis of acrylate[48,50-52] and acrylamide[34,53-55] linear/star (multi)block copolymers.

1.2.3. Reversible addition fragmentation chain transfer polymerisation

Reversible addition fragmentation chain transfer (RAFT) polymerisation was first reported by Moad and co-workers in 1998.[56] RAFT polymerisation differs from the other CRP techniques listed as it controls radical polymerisations via reversible chain transfer (also known as degenerative chain transfer).[56] RAFT polymerisation achieves reversible chain transfer by using thiocarbonylthio compounds, commonly known as RAFT agents, RAFT agents can be simplified to a generic structure (dithioester) (Figure 1.03).[56]

Two dynamic equilibria between active polymeric radicals and dormant thiocarbonylthio compounds is essentially for maintaining a controlled polymerisation via RAFT.[57] Scheme 1.05 depicts the proposed mechanism for a

RAFT polymerisation mediated by a RAFT agent with the generic dithioester structure.[57] Free radicals are generated via decomposition of an initiator molecule(s), such as the examples detailed in Section 1.1, free radicals are then capable of initiating monomer (M) to form an active propagating polymeric radical ($P_n^{\bullet}$). $P_n^{\bullet}$ can continue to propagate or establishes the RAFT pre-equilibrium by addition of the thiocarbonylthio compound which subsequently fragments and releases the RAFT agent's R group, forming a dormant polymeric thiocarbonylthio compound and a new free radical ($R^{\bullet}$).[57] $R^{\bullet}$ initiates monomer and subsequently propagates to form a second polymer radical ($P_m^{\bullet}$) before addition of $P_m^{\bullet}$ to the polymeric thiocarbonylthio to establish the RAFT main equilibrium.[57] Subsequent fragmentation of P_n/P_m forms a dormant polymer and an active polymeric radical which continues to propagate.[57] Fragmentation probability of P_n/P_m is equal and as such allows each polymeric radical equal probability of growing.[57] Termination can occur via the same mechanisms as for free radical but is suppressed by maintaining a lower concentration of active polymeric radicals.[57] This mechanism has been supported by ^{1}H-NMR spectroscopy and UV measurements of the thiocarbonylthio end group as well as direct observation of the intermediate radicals by electron spin resonance.[56,57]

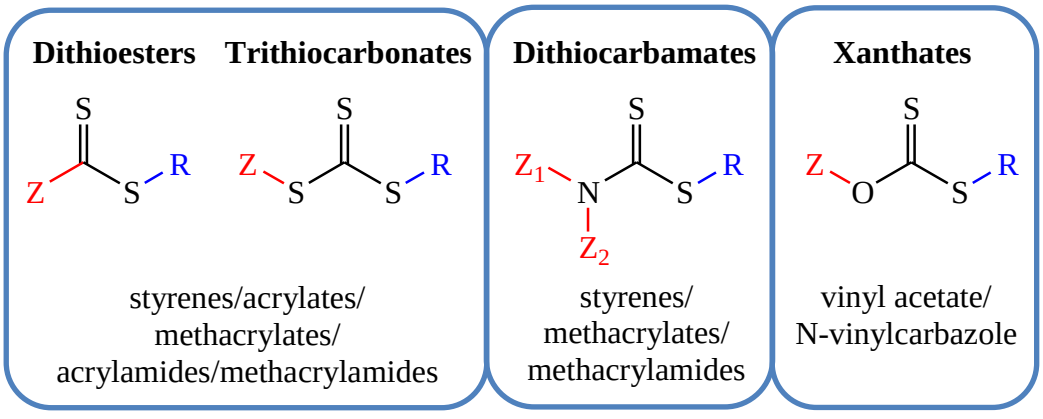

Figure 1.03. General structures of the four major varieties of RAFT agent and the monomer classes they are most suitable at mediating the polymerisations of.

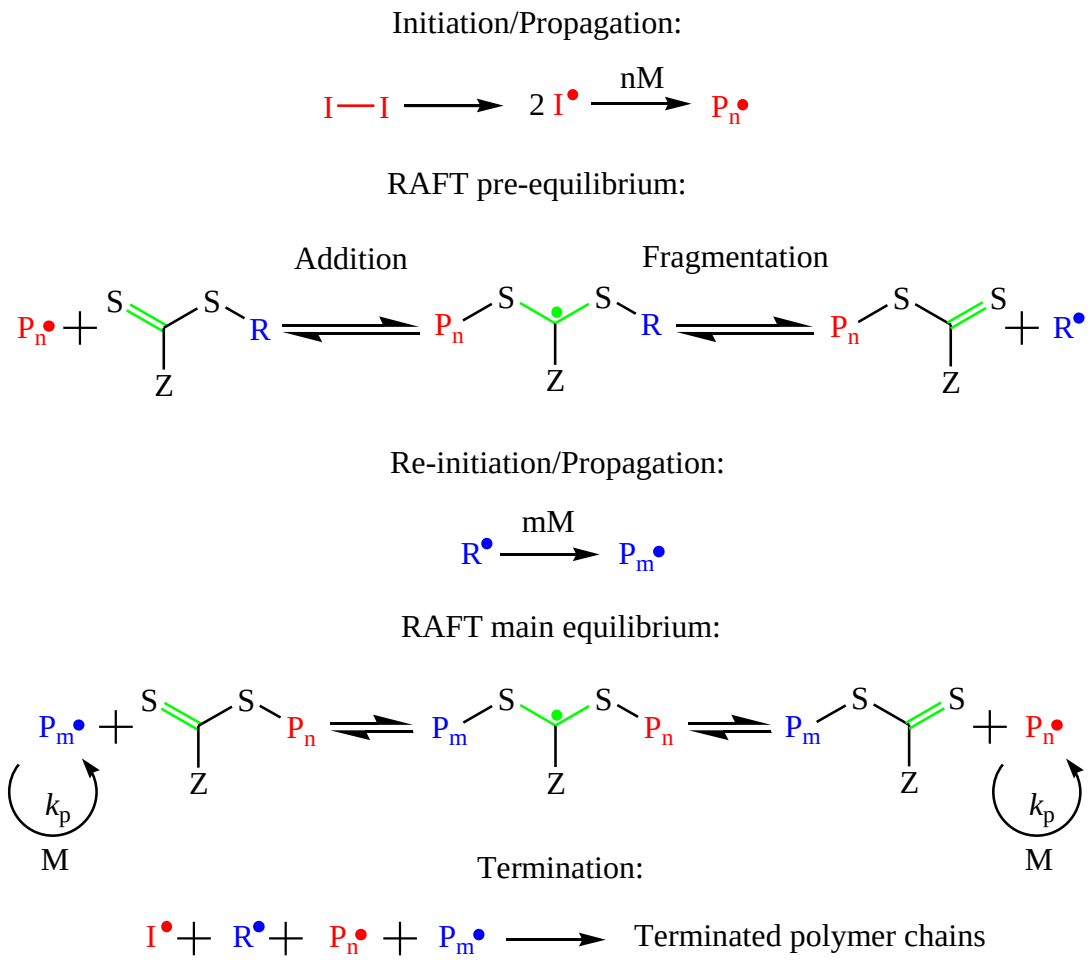

Scheme 1.05. Proposed mechanism for radical polymerisation mediated via RAFT.

RAFT agent Z and R groups are of paramount importance when selecting the most suitable RAFT agent to mediate the polymerisation of a desired monomer. The Z group is responsible for deactivation/activation of the C=S bond towards free radical addition as well as the stability of the resulting radical intermediate.[58] Therefore, Z group structure dictates the transfer coefficient of free radical addition to the C=S bond; transfer coefficients decrease when Z is Ph > SCH_2Ph ~ SMe ~ Me ~ $N(C_4H_4)$ >> OC_6F_5 > $N(C_4H_6O)$ > OC_6H_5 > $O(C_2H_5)$ >> $N(C_2H_5)_2$.[58] All of these Z groups fall into one of the four main varieties of RAFT agents; dithioesters,[56] trithiocarbonates,[59] dithiocarbamates[60] and xanthates[61,62] (Figure 1.03).

The R group must be a suitable radical leaving group but unstable enough that is capable of initiating another polymer chain.[63] R groups also influence the transfer

coefficient of a RAFT agent and is highly dependent on the monomer being polymerised.[63] For example, controlled polymerisation of MMA can only be achieved with R groups of structures related to $–C(CH_2)_3CN$ and $–C(CH_2)_3Ph$, as transfer constants are suitably high.[63] However, controlled polymerisation of styrenes/acrylates is possible with a much broader variety of R groups ($–C(CH_3)_2CN$, $–C(CH_3)_2Ph$, $–C(CH_3)_2COO(alkyl)$, $–C(CH_3)_2CONH(alkyl)$, $–C(CH_3)_3$, $–C(CH_3)HPh$, $–CH_2Ph$).[63] Therefore, transfer constants not only depend on R as a radical leaving group but also how the polymer acts as a radical leaving group.[63]

Careful consideration of Z and R groups typically meant that RAFT agents had to be specially selected to polymerise the desired monomer until a "universal" RAFT agent was designed.[64] Treatment of the "universal" RAFT agent with acid switched the RAFT agent from mediating the polymerisation of less activated monomers such as vinyl acetate, to suitably mediating polymerisations of more activated monomers such as styrenes and methacrylates.[64]

RAFT polymerisation has since been utilised to synthesise block copolymers by chain extension of polymers synthesised by RAFT, utilising the polymeric thiocarbonylthio end group to act as a so called macroRAFT agent.[59,64-66] Modification of polymeric end groups to macroRAFT agents and subsequent chain extension has combined RAFT polymerisation with a number of polymers unable to be radically synthesised such as, PEG[67] and polyolefins.[68,69] Furthermore, bifunctional RAFT agents capable of initiating/mediating two independent polymerisation techniques have been utilised to synthesise block copolymers.[70] Other polymer architectures such as stars and dendrimers have been synthesised by utilising RAFT agents that contain three or more thiocarbonylthio moieties.[65,71]

One disadvantage of polymers synthesised by RAFT polymerisation was the potential of malodourous compounds generated by degradation of the thiocarbonylthio moiety. Therefore, end group removal techniques were developed to remove the thiocarbonylthio end group whilst preserving the remaining polymer. There are two main strategies of end group removal to synthesise sulfur-free polymers. Thermal elimination simply requires high temperature to remove the thiocarbonylthio and generate an unsaturated end group.[72] Radical induced end group removal utilises a large excess of free radicals to cleave the thiocarbonylthio, generating a polymer radical which combines with a free radical or abstracts a hydrogen from a donor molecule.[73-75] Other end group modification techniques exist that do not totally remove all sulfur but can be used to add functionality to the polymer and as such will be discussed in Section 1.3.2.

Recently RAFT polymerisation has been utilised to synthesise highly ordered copolymer structures; acrylate oligomers by the consecutive addition of monomer[76] as well as acrylate/acrylamide multiblock copolymers that contain up to 20 blocks.[77] These multiblocks have been synthesised by exploiting the fast polymerisation of acrylamides whilst maintaining extremely low concentrations of initiator, thus minimising termination side reactions.[77] Perrier and co-workers have since optimised many aspects of this multiblock synthesis; short reaction times (2 hours per block),[78] non-stringent reactions conditions[79] and polymerisation at ambient temperature.[80] Quasi-multiblock copolymer synthesis has also been extended to automated synthesis for the facile synthesis of multiblock copolymer libraries.[81]

Finally, it is possible to combine two or more CRP techniques to synthesise polymers of unique structure, such as “bottle-brush” or “dual-brush” structures.[82-84] This can be achieved via the synthesis of initiator/mediator functionalised monomers

followed by selective polymerisation techniques to prepare the polymer back and then the polymer side chains.[82-84]

There are many more techniques utilised within CRP that fall outside the scope of this work. CRP techniques introduced; ATRP, SET-LRP and RAFT, illustrate how CRP is one facet of the synthetic polymer chemists' "toolbox" to design and synthesise complex macromolecular materials.

1.3. Post-polymerisation modification

Post-polymerisation modification is one of the most well-established and varied methods of introducing, removing, interchanging a selected functionality found within a polymer molecule. This section will introduce common methods used to perform post-polymerisation modification as well as the two major sites of modification on a polymer molecule; end-group and backbone.

1.3.1. "Click" chemistry

Sharpless and co-workers coined the term "click" chemistry in 2001 to describe an exclusive group of reactions that allowed for facile synthesis.[85] Reactions were only designated "click" if certain synthetic standards were maintained; modular, stereospecific, wide in scope, high yielding, solvent-free/benign solvent and no production of harmful by-products.[85] Purification of "click" reactions should also be very simple, ideally avoiding the use of chromatographic purification techniques if possible.[85] Sharpless describes these reactions as being 'spring-loaded for a single trajectory'.[85,86] "Click" reactions therefore exhibit many potential advantages such as reduced waste/by-products, low reaction duration, easily scalable, etc. "Click" chemistry was quickly adopted and utilised within multiple fields such as organic chemistry,[85] drug discovery[87] and polymer chemistry.[88-90] However, over time many

new reactions were developed and were often deemed "click" despite not fulfilling all of the criteria originally proposed by Sharpless.[86] More than twenty reactions were called "click" despite requiring tedious purification and not reaching high conversions.[86] Therefore, in an effort to prevent "click" becoming synonymous with "efficient" or just "successful", a group of polymer chemistry scientists looked to redefine and reaffirm the essential requirements for a reaction to qualify as a "click" within the context of macromolecular synthesis.[86] Figure 1.04 shows the original requirements proposed by Sharpless in 2001 (green), new macromolecular specific requirements that were proposed in 2011 (blue) and requirements that were adapted from Sharpless' original criteria to be macromolecular specific (yellow).[86]

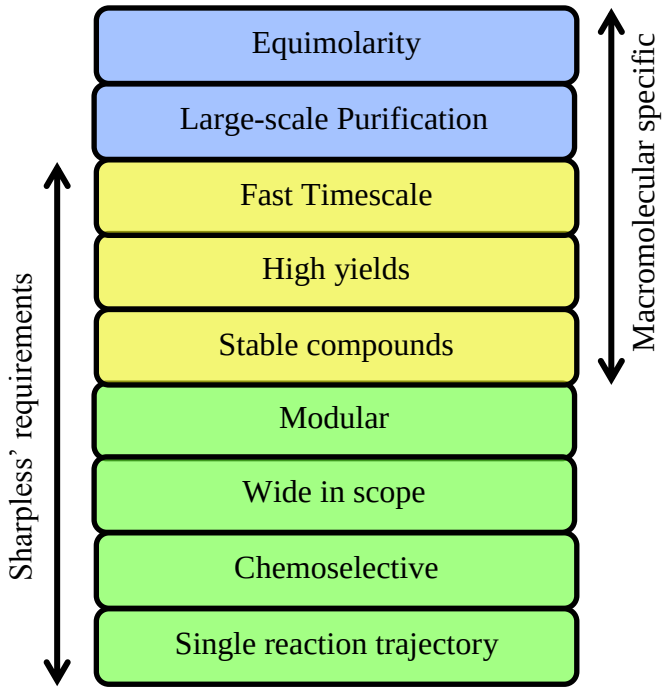

Figure 1.04. Synthetic requirements for "Click" reactions within macromolecular synthesis.[86]

Perhaps the most widely studied "click" reaction is the so-called Huisgen [4+2] 1,3-dipolar cycloaddition between an azide and alkyne, also commonly known as the copper(I)-catalysed azide-alkyne cycloaddition (CuAAC).[85,91] Without copper catalyst these cycloadditions proceed slowly and result in a mixture of 1,4- and 1,5-disubstituted 1,2,3-trizaole regioisomers.[91] When utilising a copper(I) catalyst

system the dipolar cycloaddition proceeds to high conversion under ambient conditions and affords only the 1,4-disubstituted product (Scheme 1.06).[85] Moreover, nitrile-azide dipolar cycloadditions and nitrile oxide-alkyne dipolar cycloaddition can functionalise polymers with tetrazoles[92] or isoxazole,[93] respectively (Scheme 1.06).

This reaction has been widely utilised within polymer science to synthesise; dendrimers,[89] dendronized polymers,[88] graft polymers,[90] and monomers.[52] Further benefits of the CuAAC is the potential to simultaneously perform a CuAAC and ATRP, to synthesise end/backbone functionalised polymers, as both reactions can utilise the same catalyst system (Cu(I)Br and *N*-based ligands such as PMDETA and NPPMI).[94,95]

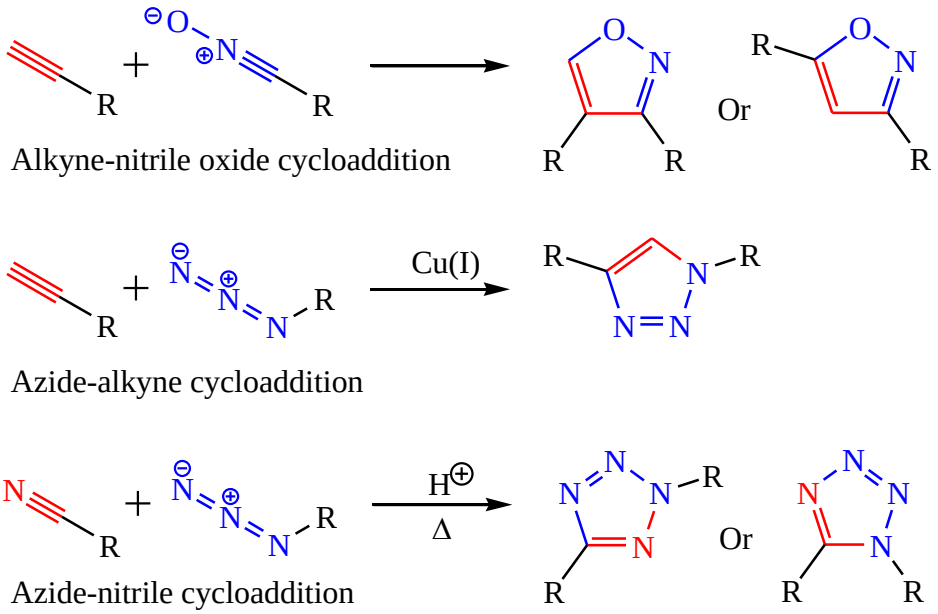

Scheme 1.06. Examples of 1,3-dipolar cycloaddition "click" reactions utilised in polymer chemistry.

However, the presence of copper catalysts is often undesirable and complete purification of the products can be challenging. As such there has always been a drive towards metal free azide-alkyne cycloadditions to remove the requirement for rigorous removal of the copper catalyst.[96] One method for metal-free cycloaddition is

the strain-promoted azide alkyne [4+2] cycloaddition (SPAAC) between cyclooctyne derivatives and azides.[97] SPAAC initially proceeded very slowly until the synthesis of monofluorinated and difluorinated cyclooctyne derivatives which exhibited accelerated rates of reaction.[98] Although SPAAC avoids the use of any metal catalyst during the cycloaddition, the synthesis of the cyclooctyne derivatives is very synthetically demanding. Metal-free azide-alkyne cycloaddition is also possible by utilising an alkyne possessing electron withdrawing substituents, such as acids or esters, these cycloaddition proceed to high conversion at ambient temperature in water.[99]

Thiols as a functional group have been widely utilised within "click" chemistry and are now routinely employed for the functionalisation of polymers. Addition of thiols to alkenes, more commonly known as the thiol-ene "click", proceeds via one of two mechanisms; radical addition and Michael addition (Scheme 1.07).

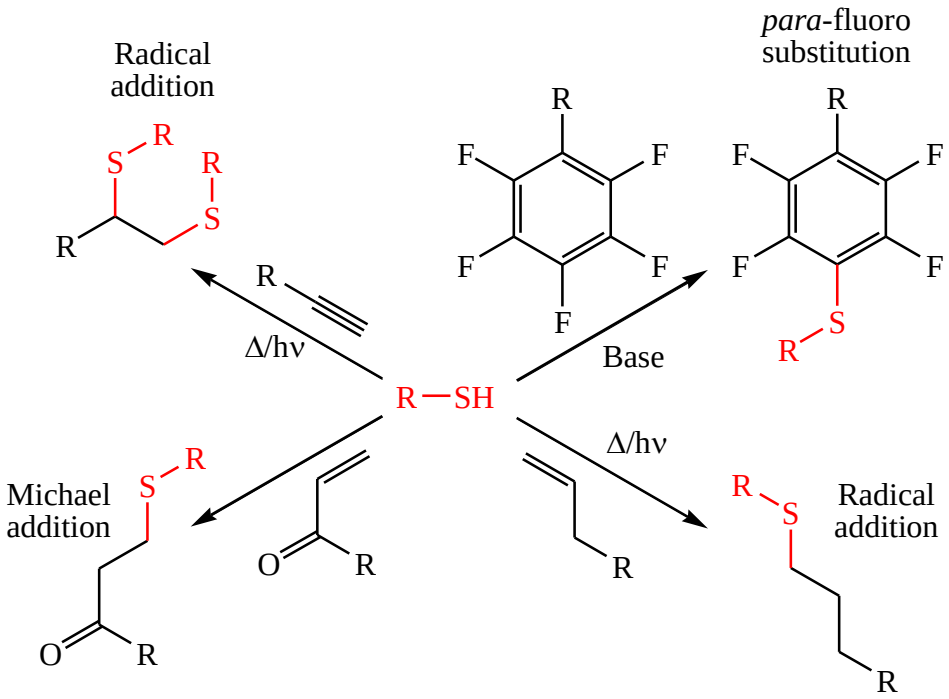

Scheme 1.07. Examples of different click reactions utilising thiols.

Radical addition of thiols can be achieved using thermal or photo radical initiators and has successfully functionalised polymers with alkene side groups[100,101] and end groups.[101] Moreover, radical addition of thiols to alkenes has been demonstrated as a suitable methodology of synthesising fourth generation dendrimers.[102] Furthermore, radical addition of thiols to alkynes (thiol-yne "click") proceeds in a similar fashion to radical thiol-ene but has the consequence that two thiols can add to one alkyne, increasing the potential for cross linking or incorporating more functionality.[103]

Michael addition of thiols to alkenes is possible if the alkene is suitably activated (Scheme 1.07), such as acrylates,[104] methacrylates[105] and maleimides.[106,107] Michael thiol-ene additions have been demonstrated to be suitable for functionalising polymer side chains[104] and end groups[106] as well and synthesising higher order structures such as cyclic polymers and polyfunctional materials.[107,108] Originally Michael type thiol-ene additions required large excesses of thiol and tertiary/primary amine catalyst relative to alkene to achieve high conversions. This technically disallowed Michael thiol-ene additions from being considered "click". Use of phosphine catalysts reduced the equivalents of thiol/catalyst required and thiol-ene additions proceeded to high conversions.[105] However, use of phosphine catalysts can also lead to unwanted side products such as addition of the phosphine to the alkene and as such should always be used in catalytic concentrations if possible.[105]

Finally, the labile *para*-fluorine substituent of pentafluorophenyl (C_6F_5) is known to undergo efficient nucleophilic substitution with thiols and various other nucleophiles (Scheme 1.07).[109,110] The so called thiol-*para* fluoro "click" reaction has been utilised to add functionality such as sugars (thiol-glycoside) and aromatic groups (thiolphenol) to (co)polymers of pentafluorostyrene (PFS).[111,112]

[4+2] cycloaddition of a conjugated diene and a substituted alkene (dienophile) to synthesise substituted cyclohexene, the Diels-Alder reaction, was discovered in 1928 and quickly expanded to include the synthesis of heterocycles by the hetero Diels-Alder reaction (Scheme 1.08).[113] Many desirable features of the (hetero) Diels-Alder reaction make it an ideal candidate for a "click" reaction, such as proceeding at ambient temperature without a catalyst. Some particularly impressive examples that utilise the (hetero) Diels-Alder reaction will be given.

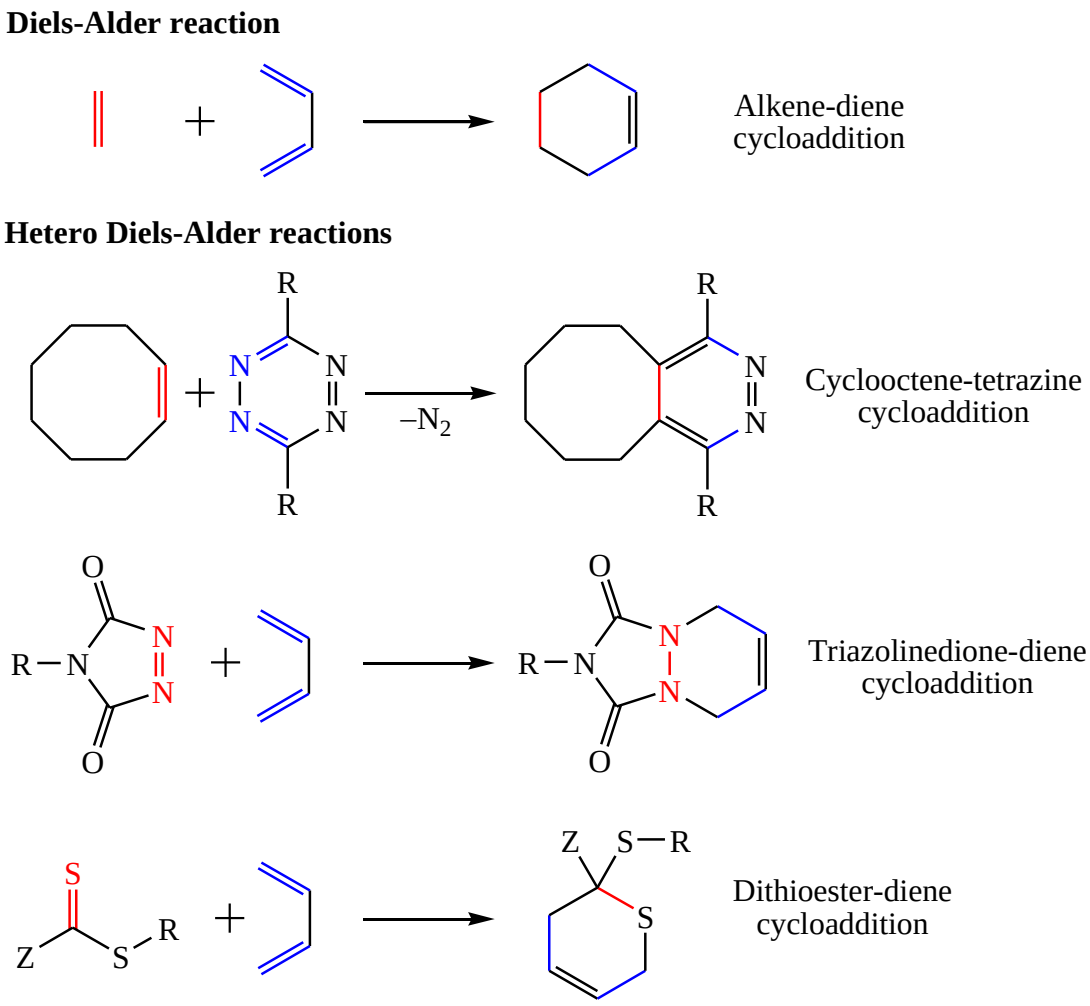

Scheme 1.08. Examples of (hetero) Diels-Alder "click" reactions.

Cyclooctenes and tetrazines undergo inverse-electron demand Diels-Alder and subsequent retro-[4+2] cycloaddition to form the substituted cyclooctane product (Scheme 1.08).[114] This reaction proceeds in as little as 5 minutes under ambient

conditions and the only by-product is N_2.[114] This extremely efficient reaction has been demonstrated as an effective technique for the coupling of two polymer chains, one functionalised with a tetrazine and the other with a norbornene.[115]

Triazolinediones (TAD) compounds have been shown to be promising candidates for "click" chemistry as they rapidly react, at ambient temperature and without catalyst, with indole compounds or undergo hetero Diels-Alder (Scheme 1.08) and ene reactions.[116] Most impressive is the rapid and orthogonal hetero Diels-Alder between TAD compounds and dienes which has been suitable at polymer-polymer coupling[116] as well as the layer-by-layer assembly of up to 58 individually linked molecular layers.[117]

Lastly, hetero Diels-Alder has been shown to be readily combined with RAFT polymerisation as a means of post-polymerisation modification. Dithioesters present as polymer end groups act as heterodienophiles and undergo [4+2] cycloaddition with dienes (Scheme 1.08).[118] This reactivity has been exploited to synthesise block copolymers by coupling a diene-terminated homopolymer with a dithioester terminated polymer synthesised in one step by RAFT polymerisation.[118]

1.3.2. Polymer end group modification

End group modification of polymers is one of the two major areas of polymer modification. With regards to free radical polymerisation, end group modification was challenging as the exact nature of initiating/terminating species was not always known and as such the final end group chemistry may be uncertain. However, end group functionality was introduced to polymers synthesised by free radical polymerisation by utilising a functional CTA.[119] Allylic sulfide CTAs substituted with carboxy, hydroxy, trialkoxysilyl and amino successfully end-capped polymers with the respective functionalities.[119] Furthermore, dimers of common α-methylvinyl

monomers were shown to be effective CTAs and synthesised polymers functionalised with a terminal substituted allyl end group.[120] Furthermore, catalytic chain transfer polymerisation (CCTP), free radical polymerisation which utilises a cobalt based catalyst, is another effective technique for the preparation of substituted allyl terminated polymers.[121] These terminal substituted allyl polymers, also called macromonomers, have also been demonstrated to be effective CTAs themselves and capable of synthesising block copolymers via free radical polymerisation.[122] End group modification of the terminal substituted allyl group is also possible and has been shown to be readily functionalised by Michael addition of thiols.[123-125]

CRP techniques not only allowed the synthesis of well-defined polymer distributions with tuneable molecular weights, CRP techniques also developed another means of synthesising polymers with well-defined α- and ω-terminal functionality. ATRP/SET-LRP initiated by an alkyl halide furnishes polymers with an alkyl halide functional group at the ω-terminus.[14] The ω-terminal bromine can be displaced by a number of nucleophilic species to impart new functionality at the chain end (Scheme 1.09). Common nucleophilic species utilised are thiols,[48,49] primary amines,[126] and azide anions.[127] Azide functionalised polymers are very versatile as they can be reduced to the corrosponding primary amine terminated polymer[127] or the azide can be utilised in a CuAAC for further functionalisation[128] or formation of higher order polymer architectures.[129]

Radical addition of a single monomer at the chain end can be performed if said monomer does not propagate via ATRP. Therefore, radical addition of allyl compounds has been utilised to add ω-terminal hydroxyl[126] and epoxy[130] functionality as well as other non-propagating monomers such as MalA.[131] Many

other end group modifications of polymers synthesised by ATRP/SET-LRP have been demonstrated and are summarised in Scheme 1.09.[14]

An effective method of introducing α-terminus end group functionality, although not technically an end group modification, is utilising a functional initiator to initiate ATRP/SET-LRP.[14] This method works well as ATRP/SET-LRP are tolerant of many functional groups.[14] These initiators are readily synthesised by esterification of a hydroxyl species with α-bromoisobutyryl bromide (BiBB) and functionalities such as monohydroxy,[132] phenolic esters,[133] maleimide etc.[134] have been incorporated via this approach.[14]

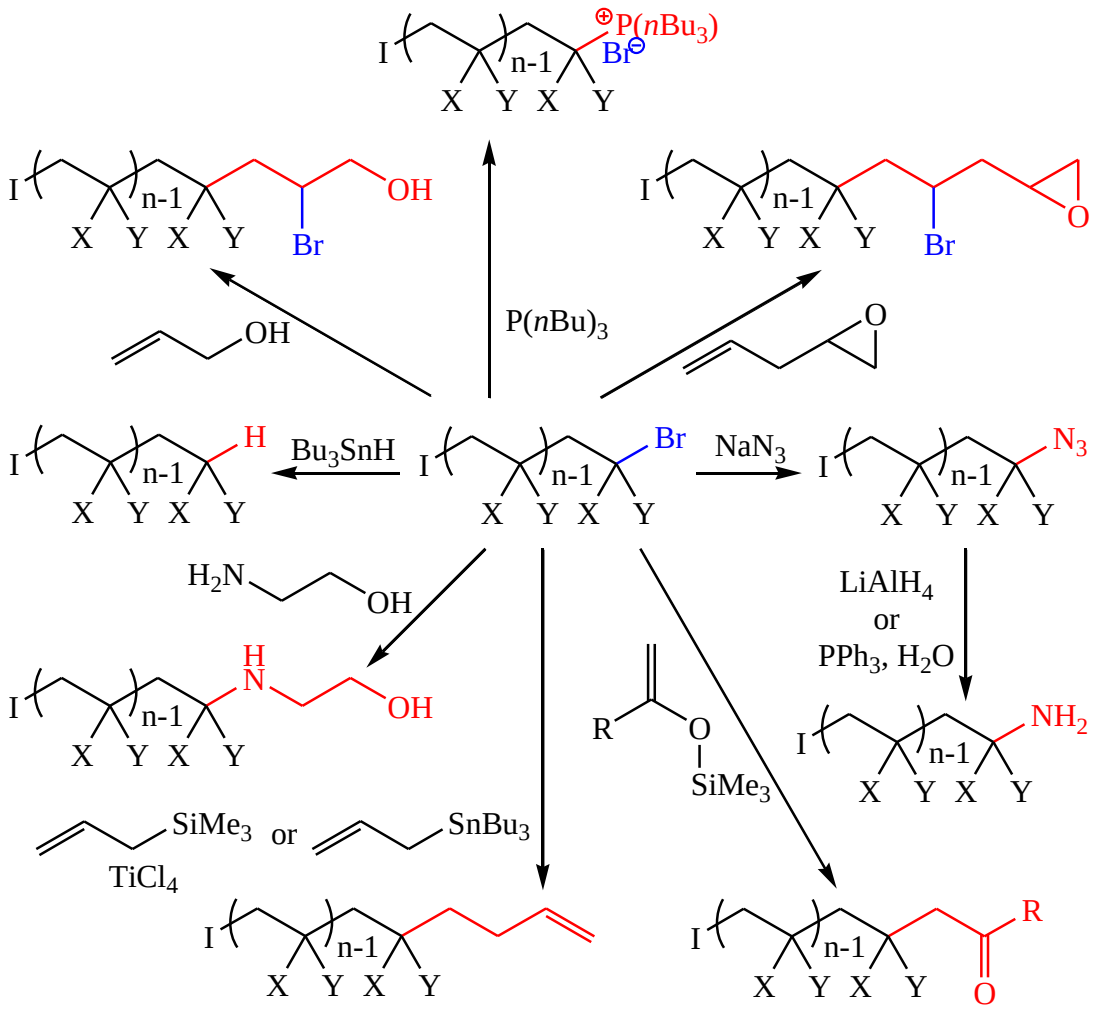

Scheme 1.09. Example of ω-end group modifications via displacement of the ω-terminal bromine of polymers synthesised by ATRP/SET-LRP.[14]

RAFT polymerisation furnishes polymers with a thiocarbonylthio functionality at the ω-terminus (Section 1.2.4). Removal of this functionality by thermolysis or radical induced reduction/addition was introduced in Section 1.2.4.[72-75] Other methods of RAFT end group modification exist which do not fully remove all sulfur but can add new functionality to the chain end. Aminolysis of a thiocarbonylthio end group is routinely performed to generate polymeric thiols after nucleophilic substitution with a primary/secondary amine (Scheme 1.10).[135-137] The polymeric thiol is then functionalised with activated alkenes; such as acrylates, methacrylates and maleimides, via Michael addition.[135-137] Although this process often utilises amines to furnish the polymeric thiol, said thiols can be generated after substitution with different nucleophiles such as sodium azide[138] or thiols.[139]

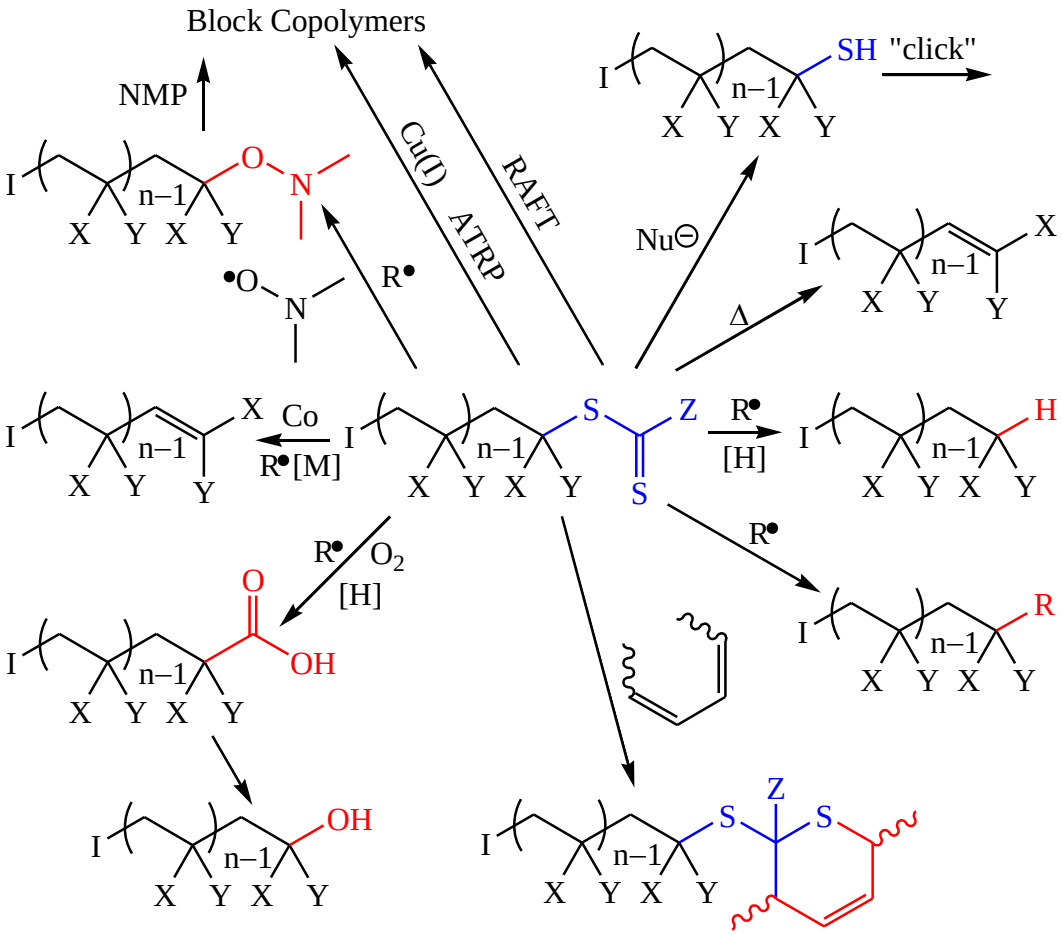

Scheme 1.10. Example end-group modifications via modification of the terminal thiocarbonylthio end group of polymers synthesised by RAFT.[140]

A recent advancement within RAFT end group modification is the hetero Diels-Alder between dithioester end groups and a diene, introduced in Section 1.3.1. (Scheme 1.10).[118] This has been demonstrated as an effective technique for coupling homopolymers to synthesise block copolymers[118,141] and has been highly optimised to utilise reactive photoenol dienes that couple at ambient temperature without catalyst when irradiated at 320 nm.[142] Many other end group modifications of polymers synthesised by RAFT have been demonstrated and are summarised in Scheme 1.10.[140]

End group functionality can be readily incorporated into a polymer synthesised by RAFT polymerisation by utilising a RAFT agent bearing a chosen functionality, such as carboxylic acid,[143] norbornene,[144] catechol etc.[145] Although this synthetic methodology is not technically end group modification it can be adapted so the RAFT agent bears a functionality which can be readily transformed to a new functionality which isn't tolerated by the reaction conditions. Phthalimide bearing RAFT agents can efficiently control the polymerisation of Sy and subsequent treatment of the phthalimide end group with hydrazine furnishes primary amine functionalised polystyrene.[146]

1.3.3. Polymer backbone modification

Functionalisation of the polymeric backbone is the second form of post-polymerisation modification and has a long history within polymer science of synthesising functional materials. Polymer backbone modification is simply the modification of a functional group within one or more repeat units to a new functional group. As such, backbone modification is arguably far more accessible then end group modification as there are many functional group containing monomers that can be readily polymerised (by radical, ionic or step-growth

polymerisation) without the need of protecting groups. Applications of post-polymerisation in the literature is extremely vast so choice examples of the commonly utilised functionalities will be presented.

Early examples of post-polymerisation modification utilised functional groups (such as anhydrides, epoxides and isocyanates) that were unreactive towards radicals but reactive towards nucleophilic species (such as hydroxyls, amines and thiols) (Scheme 1.11). As these functional groups are unreactive towards radicals they are ideal monomers to be (co)polymerised by FRP/CRP. Epoxide bearing monomers, glycidyl acrylate (GA) and glycidyl methacrylate (GMA) have been (co)polymerised by FRP, CCTP, SET-LRP and subsequently modified with hydroxyls,[147] amines,[125] thiols[125,148] and azide.[124]

Anhydride functionality is routinely incorporated into copolymer by the copolymerisation of MalA with other vinyl monomers. Copolymerisation of MalA is a doubly useful monomer owing to the reactive functionality it imparts and its tendency to polymerise alternately with more electron-rich monomers.[149] MalA containing copolymers are often ring opened with primary/secondary amines to form the corresponding amide-acid (Scheme 1.11).[150,151] Furthermore, given suitably high reaction temperatures (170-200 °C) and removal of water, primary amines and MalA furnish ring-closed maleimide functionality.[150,152]

Isocyanates are another reactive functionality that can be incorporated into a (co)polymer via (co)polymerisation of an isocyanate bearing monomer. However, isocyanates can be hydrolysised to a carboxylic acid which subsequently decarboxylates to a primary amine, this primary amine can then attack another isocyanate and potentially crosslink a polymer. Therefore, anhydrous solvents and

monomers are often required for polymerisation. Despite this (meth)acrylates and *α*-methylstyrenes bearing unprotected isocyanates have been (co)polymerised in a controlled manner and subsequently functionalised with hydroxyls,[153-155] amines[153] and thiols[153] to yield urethane, urea and thiourethane derivatives, respectively (Scheme 1.11).

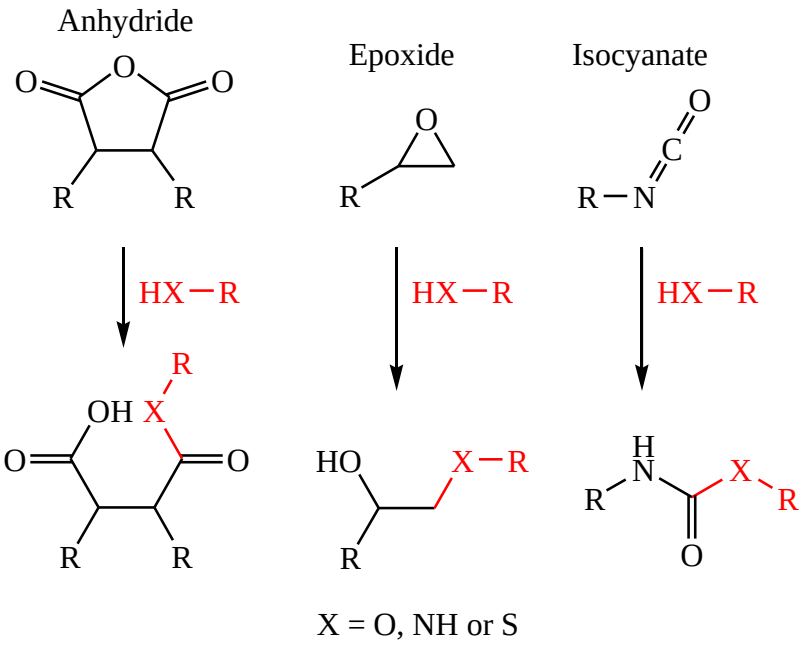

Scheme 1.11. General structures for anhydrides, epoxides and isocyanates and subsequent functionalisation with hydroxyls, primary amines or thiols.

Polymer backbone modification experienced a recent resurgence in interest and scope with the advent of "click" chemistry in 2001 (Section 1.3.1). All of the click reactions introduced in Section 1.3.1 have been utilised to functionalise polymer backbones by incorporating one of the reactive moieties necessary for the click reaction within the repeat unit before or after polymerisation. CuAAC has been utilised by polymerising protected and unprotected alkyne bearing (meth)acrylates before removal of the protecting group (if required) and then functionalised with azide compounds.[123,148] Other examples of alkyne functionalised polymers include poly(vinylacetylene) and poly(*α*-propargyl-*δ*-valerolactone).[88,90] Similarly, azide bearing polymers can be functionalised with alkyne compounds.[124]

Addition of thiols, by Michael and radical addition, to polymers bearing pendant alkenes has been widely reported.[100,101,104,156] Substitution of the *para*-fluorine on P(PFS) with thiols and primary amines has also proven to be another effective route of functionalising a polymer backbone with thiols.[111,112,157]

Post-polymerisation modification, at both the end group and backbone, is now a very well established field and represents another method in synthetic polymer chemists' "toolbox" to synthesise increasingly sophisticated materials.

1.4. Polymers as fuel additives

Increasing pressure from modern day environmental concerns and society's reliance on non-renewable fossil fuels continually drives improvement within the automotive industry. These advances come in many forms; from engine efficiency to combustion fuel purity. Another key area is the treatment of fuel with additives. Srivastava and Hancsók have identified six reasons why additives may be added to fuels.[158]

- To improve handling properties and stability of the fuel.
- To improve combustion properties of the fuel.
- To reduce emissions from fuel combustion.
- To provide engine protection and cleanliness.
- To increase the economic use of the fuel.
- To establish or enhance the brand image of a fuel.

There is a vast range of additives that may be added to fuel to fulfil one or more of the functions listed above; viscosity modifiers, anti-knocking agents, oxidation inhibitors, dispersants, detergents, dyes etc. Of those mentioned; oxidation inhibitors, dispersants and detergents make up the general class of additives known

as *stabilisers* or *deposit control agents*.[159] Demand for fuel additives is extremely high and in particular dispersants and detergents make up the single largest group of fuel additive consumed.[158] Estimated demand for different types of fuel additives in Europe in 1998 is shown in Table 1.01, dispersants and detergents make up nearly half of the total fuel additive demand at 44%.[158]

Table 1.01. Estimated demand for different types of fuel additives in Europe in 1998.[158]

Fuel Additive	Est. Demand (tonne)	Fuel Additive	Est. Demand (tonne)
Dispersants and detergents	70 000	Corrosion inhibitor	1 250
Cetane improver	20 000	Dehazer	2 550
Injector cleaning	25 600	Diesel stabiliser	200
Lubricity improver	5 250	Metal deactivator	200
Flow improver	30 000	Dyes, deodorants, etc.	400
Antioxidants	2 200	Lead antiknock	Nil after year 2000
Antistatic	50	Anti-valve seat recession	Nil

The fuel additive market continues to grow yearly. In 1998 the market value of fuel additives used in the USA was $625 million, this increased by 4.9% per year until the market was worth $795 million in 2003.[158] Market value continues to rise and was worth $1.1 billion in 2008, equating to a 6.4% rise year-to-year from 2003 to 2008.[158] As of 2012 the market value for fuel additives in the USA was $1.6 billion, a 9.8% increase per year from 2008, of the total $1.6 billion for all fuel additives $440 million was the market value of dispersant and detergent additives.[158]

Estimated quantity of dispersant and detergent fuel additives consumed was 1.683×10^3 t.[158] Therefore, better performing and more cost efficient fuel additives (especially dispersants/detergents) could be lucrative if they successfully capture a share of the continually growing fuel additives market.

1.4.1. Dispersants and detergents

Demand for fuel dispersants/detergents is so high because of the vital role they perform within a modern gasoline/diesel engine. Combustion of fuel may form deposits within an engine; these can take on the form of soot, sludge, lacquer and varnish. Deposits form due to incomplete combustion of the fuel, thermal degradation of other engine oils or attack from reactive species such as peroxides and radicals.[158] Oxidation inhibitors help to minimise the formation of deposit precursors, such as hydroperoxides and radicals.[159] Deposits are typically carbon rich but do contain oxygen and sulfur which increases their polarity, insolubility in fuel and attractiveness to each other.[159] This attraction causes the deposits to aggregate and eventually grow large enough that they partially block essential engine components, such as fuel injectors, intake valves, combustion chamber etc.[158] Blocked engine components may have many negative effects, such as loss of fuel economy, loss of engine power, increased rates of incomplete combustion leading to higher emissions of carbon monoxide and hydrocarbons.[158]

Dispersants and detergents are therefore added to fuel to remove deposits as they form (keep clean mode) or they are added in higher concentrations to the vehicle directly to help remove existing deposits (clean up mode).[158] If correctly treated, deposit formation will be minimised and engine efficiency maintained. High demand for dispersants and detergents additives is partially explained by the expectation of all automotive fuel to be treated with these additives.

Although detergents and dispersants perform very similar roles in automotive engines they differ in molecular structure and there are three significant ways in which detergents and dispersants do differ:[159]

1. Dispersants contain no metals whereas detergents do contain metals, such as magnesium and calcium. This is very important as combustion of detergents will lead to ash formation.
2. Dispersants have very poor acid neutralising ability whereas detergents are good at acid neutralisation. Dispersants may contain amine functionality (primary, secondary, tertiary or quaternary) which is slightly basic. However, this is weak compared to detergents which contain reserve metal bases such as metal hydroxides and carbonates which are significantly more basic.
3. Dispersants have a higher molecular weight than the organic portion of a detergent, approximately 4-15 times higher.

Considering the above criteria and that the compounds to be synthesised within this thesis will contain no added metals; they will be considered as dispersants. Therefore the remainder of the introduction will focus solely on dispersants and in particular their synthesis.

1.4.2. Dispersant mode of action

Dispersants are added to fuel and other engine oils to keep potentially harmful deposits well dispersed in the medium and prevent blockage of engine components. Deposit agglomeration is believed to be prevented via two mechanisms; steric and electrostatic stabilisation.[159] The generic structure of a dispersant additive facilitates these two mechanisms of stabilisation. Dispersants have general structure which is

similar to a surfactant, comprising of a polar head group, a connecting group and a non-polar hydrocarbon group (Figure 1.05).[159]

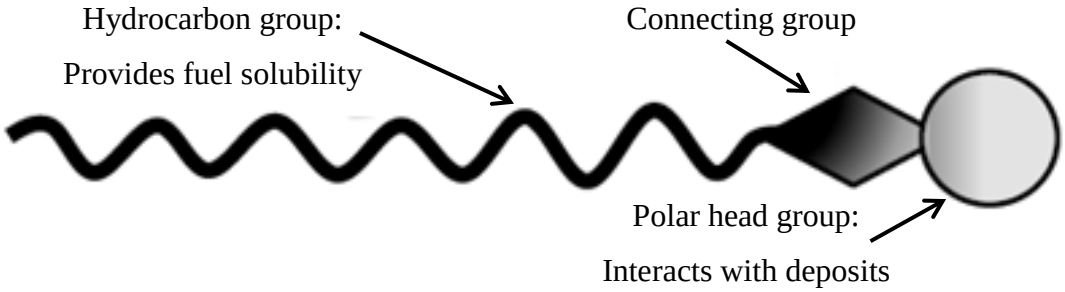

Figure 1.05. General structure of a fuel dispersant.

The non-polar hydrocarbon group, which is typically derived from poly olefins, is used to provide solubility in hydrophobic medium the dispersant molecule.[159] A connecting group is used to link a hydrocarbon group with a polar head group that will interact with fuel deposits.[159] Synthesis of typical hydrocarbon, connecting and polar head groups used for dispersants will be introduced in Section 1.4.3.

Dispersants hinder the agglomeration of deposits by two mechanisms; steric and electrostatic stabilisation. Steric stabilisation occurs when multiple dispersants adsorb onto the surface of a deposit via the polar head group. Deposits are then kept from agglomerating as the dispersants' hydrocarbon tails provide a physical barrier to attraction (Figure 1.06).[160] Electrostatic stabilisation occurs via deprotonation of acidic groups found on the deposit by weakly basic moieties (such as amines) utilised as the polar head group of a dispersant. This deprotonation subsequently introduces a charge to the deposit and prevents agglomeration of particles via electrostatic repulsion (Figure 1.07).[160]

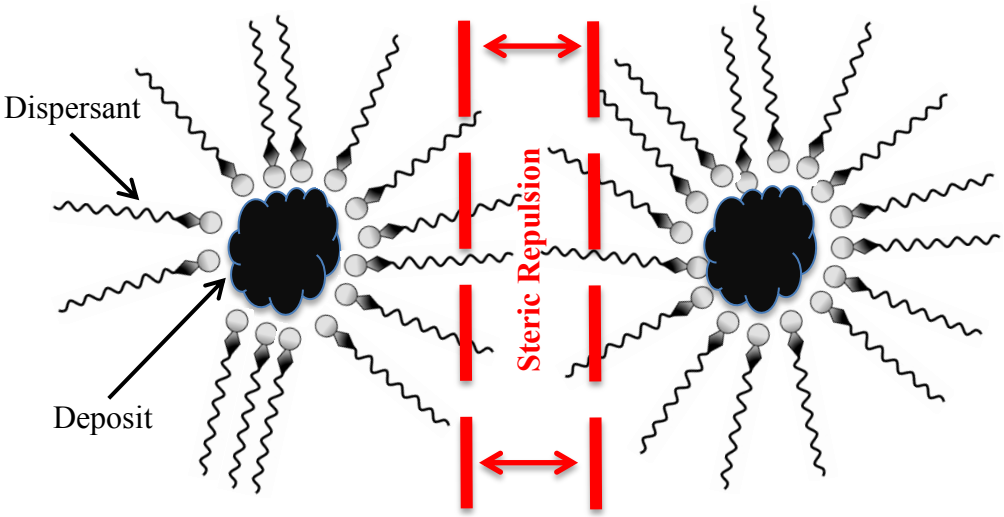

Figure 1.06. Steric stabilisation of a deposit by dispersant molecules.

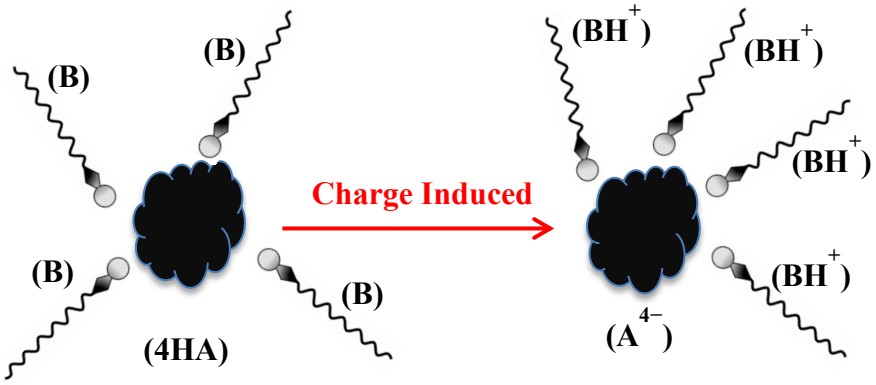

Figure 1.07. Electrostatic stabilisation of a deposit by dispersant molecules. Where B = base, A = acid, H = Hydrogen.

1.4.3. Fuel dispersant synthesis

As shown in Figure 1.05, dispersants have a general structure that is typically made up of three groups; a hydrocarbon group, connecting group and polar head group. Typical syntheses of these individual groups will now be introduced.

1.4.3.1. The hydrocarbon group

The hydrocarbon group is typically composed of polyisobutylene (PIB), although other olefin copolymers such as ethylene-propylene copolymers have been utilised.[161-164] PIB is traditionally synthesised via acid catalysed polymerisation of isobutylene (IB). This requires a strong Brønsted acid capable of protonating the

carbon-carbon double bond of IB to form a tertiary carbocation (Scheme 1.12), however the counter anion (A^-) of the acid used should be a sufficiently poor nucleophile that it does not immediately combine with the carbocation and prevent polymerisation.[4] Suitably strong acids include perchloric, sulfuric, phosphoric and trifluoromethanesulfonic.[4] Polymerisation proceeds by successive additions of IB to the carbocation before eventual termination of the carbocation and formation of an ω-terminal olefin.[4] PIB synthesised by strong Brønsted acids typically have low molecular weight and the terminal olefin shown in Scheme 1.12 is an over simplification as in reality a number of olefins are possible (Figure 1.08).[159]

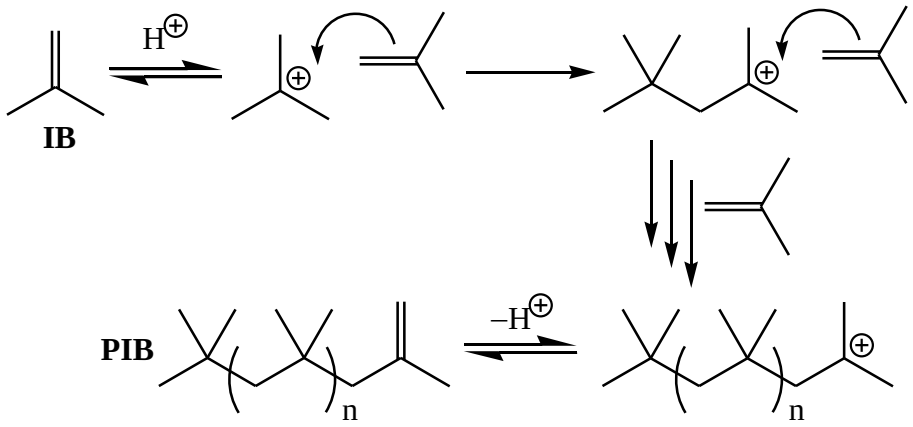

Scheme 1.12. Acid catalysed cationic polymerisation of IB to PIB.

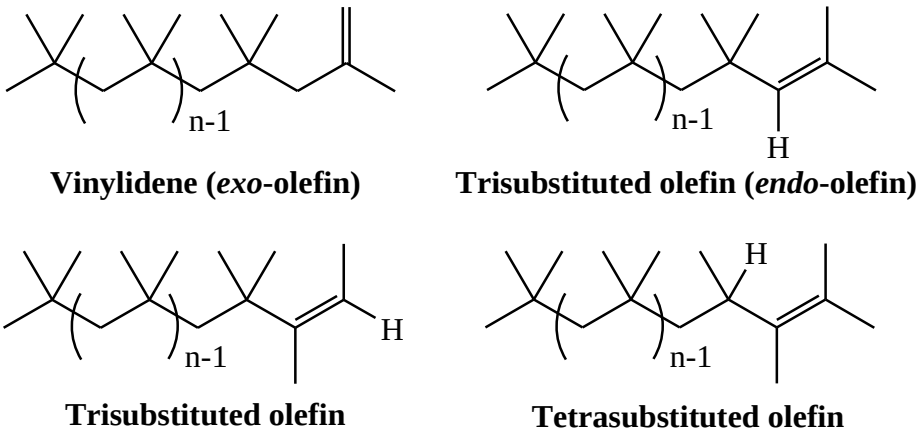

Figure 1.08. Potential PIB ω-terminal olefins after acid catalysed cationic polymerisation of IB.

A mixture of ω-terminal olefins is an undesirable quality for PIB, as different ω-terminal olefins exhibit different reactivity towards connecting group molecules such as MalA and phenol. Reactivity of the ω-terminal olefin typically decreases with increasing degree of substitution. However, it is possible to influence the relative concentrations of PIB ω-terminal olefins by cationic polymerisation of IB initiated with a Lewis acid instead of a traditional strong Brønsted acid. PIB produced by using boron trifluoride as catalyst contains an end group which is primarily the vinylidene (*exo*-olefine) and IB polymerised with aluminium trichloride as catalyst synthesises PIB which is functionalised with tri/tetra substituted terminal olefins.[160] Therefore, depending on which ω-terminal olefin is required for the subsequent synthetic step can be obtained by changing the catalyst for the cationic polymerisation of IB.

1.4.3.2. The connecting group

A connecting group is typically required for the synthesis of a dispersant as it can be difficult to couple a very non-polar hydrocarbon chain directly to a polar head group. Typical connecting groups in fuel dispersant synthesis are succinic esters, succinimides and phenols as well as other groups such as phosphonates.[159] Succinic esters and succinimides are formed by reacting succinic anhydrides with alcohols and primary amines, respectively.[159] A prevalent succinic anhydride used for fuel dispersant synthesis is polyisobutylene succinic anhydride (PIBSA), PIBSA is synthesised by reacting a PIB ω-terminal olefin with MalA.[160] However, PIB was shown in the last section to commonly be synthesised containing a mixture of ω-terminal olefins which have different reactivity towards MalA. Internal double bonds, such as the trisubstituted and tetrasubstituted olefins, require a chlorine-mediated process to first convert the terminal olefin into a more reactive diene that

will then undergo [4+2] cycloaddition with MalA to form the desired polyisobutylene tetrahydrophthalic anhydride (Scheme 1.13).[160,165] This chlorine-mediated process has certain merits; reaction rates are faster, proceed at a lower temperature and utilise PIB that contain higher concentrations of trisubstituted and tetrasubstituted ω-terminal olefins.[159]

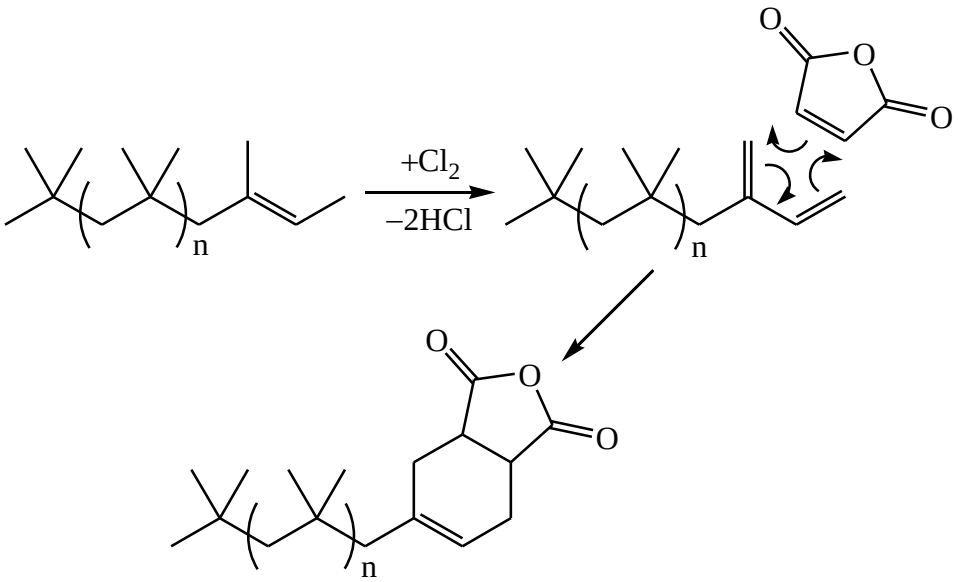

Scheme 1.13. Synthesis of a PIBSA via the chlorine-mediated process of a PIB terminated by a trisubstituted olefin and subsequent [4+2] cycloaddition of PIB diene with MalA.

However, the one major drawback of the chlorine-mediated process is the formation of HCl which may be present in the final product. One method of eliminating chlorinated substances from the final product is to simply not to use any chlorine throughout the synthesis. This can be achieved by utilising PIB that has a higher proportion of disubstituted ω-terminal olefin (*exo*-olefin) which reacts with MalA in the absence of catalyst and chlorine.[166] When PIB terminated by an *exo*-olefin (PIB_{exo}) and MalA are strongly heated (>200 °C), they undergo an ene reaction.[159] An ene reaction occurs between an alkene (PIB_{exo}) with an allylic hydrogen and an enophile (MalA) to form a new alkene shifted to the allylic position and the allylic hydrogen undergoing a 1,5 hydrogen shift (Scheme 1.14).

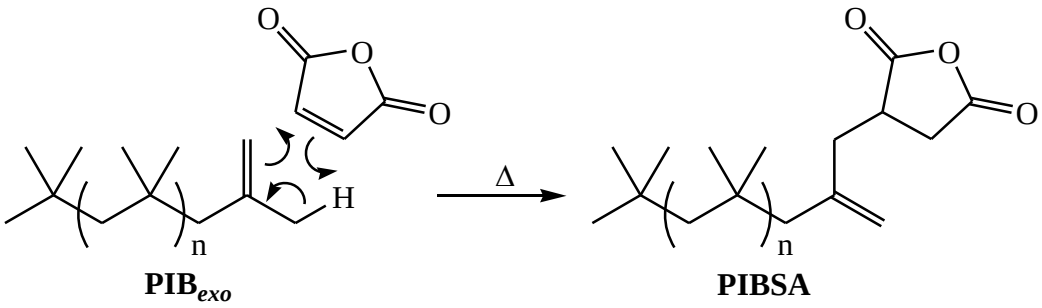

PIB*exo* **PIBSA**

Scheme 1.14. Synthesis of PIBSA via an ene reaction between PIB_{exo} and MalA.

However, ene reactions require a large excess of MalA and very high reaction temperature (>200 °C) which could potentially thermally degrade the PIB to smaller chain lengths. Furthermore, Scheme 1.14 only shows the formation of monofunctionalised PIB chain, in reality it is possible to synthesise difunctionalised PIB chains, polyisobutylene bis(succinic anhydride) (PIBBSA).[159] This depends on which allylic hydrogen is reacted first during the ene reaction.[159] Scheme 1.15 shows both potential pathways of the ene reaction between PIB_{exo} and MalA. Pathway A shifts an internal allylic hydrogen and as a result internalises the alkene, no further reaction is possible as trisubstituted terminal olefins require chlorine to react further as shown previously. Therefore, pathway A leads to monofunctionalised PIBSA. Alternatively, if an external allylic hydrogen is shifted this leads to an alkene that is still external and can undergo another ene reaction but now utilising an internal allylic hydrogen instead.[159] The Reaction proceeds no further after this point for the same reasons as for pathway A and therefore pathway B leads to difunctionalised product PIBBSA.[159] This a clear disadvantage when compared to the chlorine mediated process which only forms monofunctionalised products.

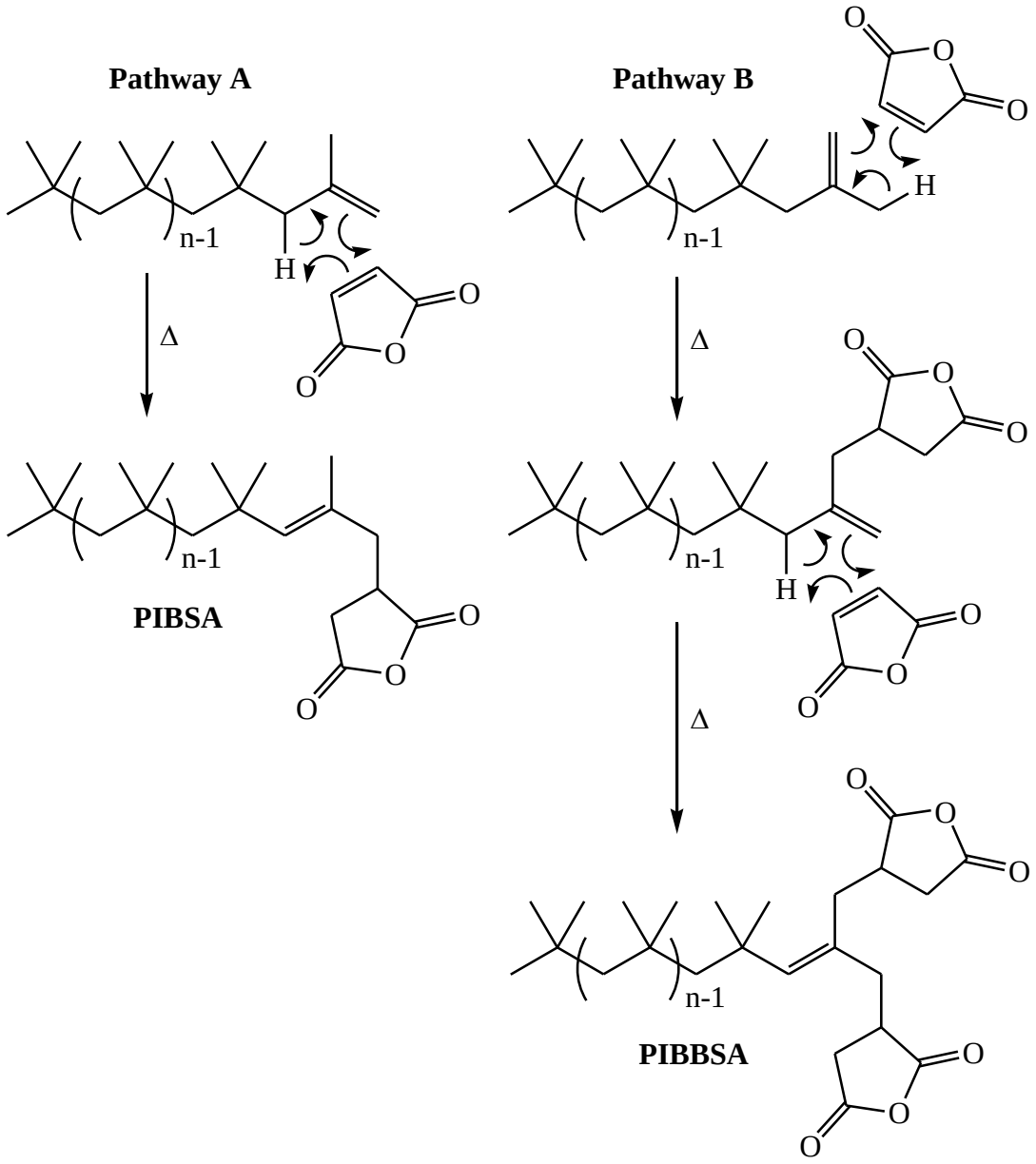

Scheme 1.15. Synthesis of mono (PIBSA) and di (PIBBSA) succinic anhydride functionalised PIB via an ene reaction between PIB_{exo} and MalA.

The final variety of connecting group chemistry used in fuel dispersant synthesis that will be introduced is alkylphenols. Polyisobutylene phenol (PIBP) is a common alkylphenol utilised in the fuel dispersant industry. PIBP is synthesised by a Friedel-Crafts alkylation of phenol with PIB terminated by an *exo*- and *endo*-olefin (PIB_{endo}) in the presence of a Lewis acid catalyst,[167] a strong Brønsted acid such as sulfuric acid,[168,169] or a cation exchange resin (Scheme 1.16).[170]

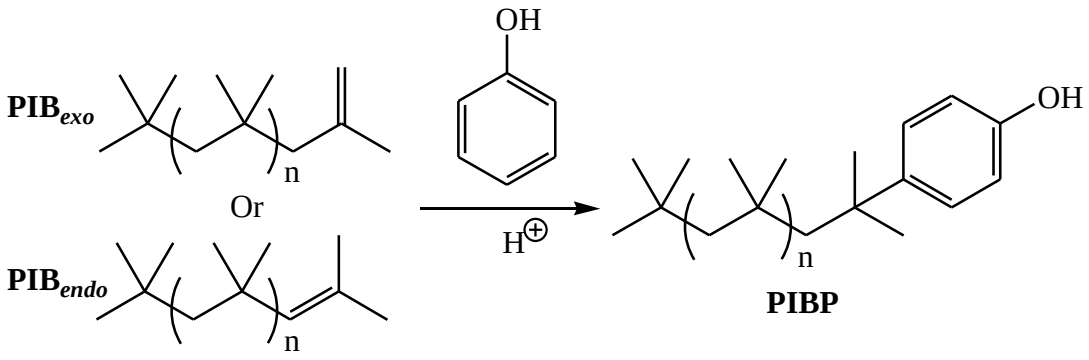

Scheme 1.16. Friedel-Crafts alkylation of phenol with PIB$_{exo}$ and PIB$_{endo}$ to synthesise PIBP.

The mechanism generally accepted is that firstly a proton adds to the vinylidene forming a tertiary carbocation, this is than subsequently attacked by the hydroxyl group of phenol giving a protonated phenyl ether.[171] The protonated phenyl ether can then rearrange to give an *ortho* or *para* alkylated phenol as well as the non-protonated phenyl ether.[171] *Para*-PIBP is the strongly favoured product; this has been demonstrated by analogous Friedel-Craft alkylations of phenol with isobutene,[172] furthermore multiple alkylations of phenol with PIB ω-terminal olefins have not been observed, even when PIB is in excess to phenol.[173]

1.4.3.3. The polar head group

Attachment of a polar head group, via the connecting group, to a hydrophobic group completes the synthesis of a fuel dispersant. The connecting and polar head group utilised categorises dispersants into one of the three major varieties; polyisobutylene succinic esters, polyisobutylene succinimides or Mannich-type dispersants.

Polyisobutylene succinic esters are formed by reacting alcohols, typically polyols, with PIBSA (Scheme 1.17). Polyols are useful reactants as a range of different dispersant products can be formed by simply changing the equivalents of polyol to PIBSA, products can be monoester, diester as well as coupled PIBSA chains (Scheme 1.17).[174]

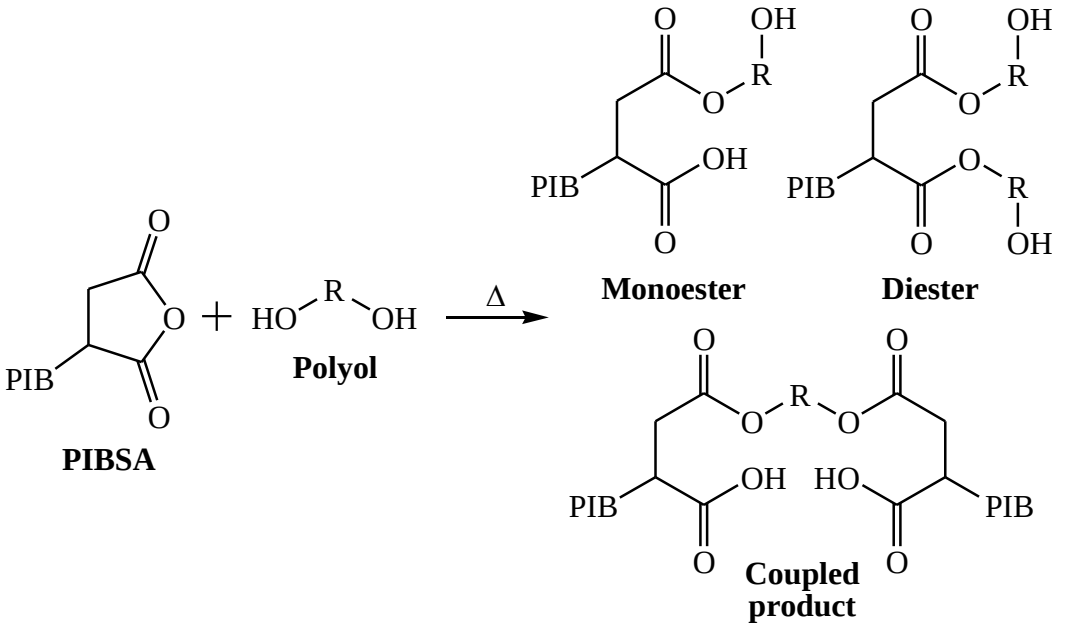

Scheme 1.17. Polyisobutylene succinic esters formed by reacting a polyol with PIBSA.

Polyisobutylene succinimides are synthesised by reacting PIBSA with a primary amine. These reactions require high temperatures ~200 °C to first ring open the cyclic anhydride to form a new amide bond and a carboxylic acid followed by cyclisation with loss of a water molecular to form the desired succinimides (Scheme 1.18). Common amines reacted with PIBSA to form the polar head group are polyamines such as; diethylenetriamine, triethylenetetramine and tetraethylenepentamine.[159,160,175] By selecting the appropriate polyamine it allows for a simple method to vary the quantity of nitrogen found on the polar head group.

Polyamines can be reacted with one or more PIBSA chains, allowing for another means of controlling the final quantity of nitrogen in the dispersant. Scheme 1.18 shows a reaction scheme between PIBSA and a generic polyamine, the polyamine is shown reacting with one, two and three PIBSA molecules to from the mono-succinimide, *bis*-succinimide and *tris*-succinimide respectively. This approach increases the ratio of polar head group to hydrophobic group from 1:1 to 2:1 to 3:1.

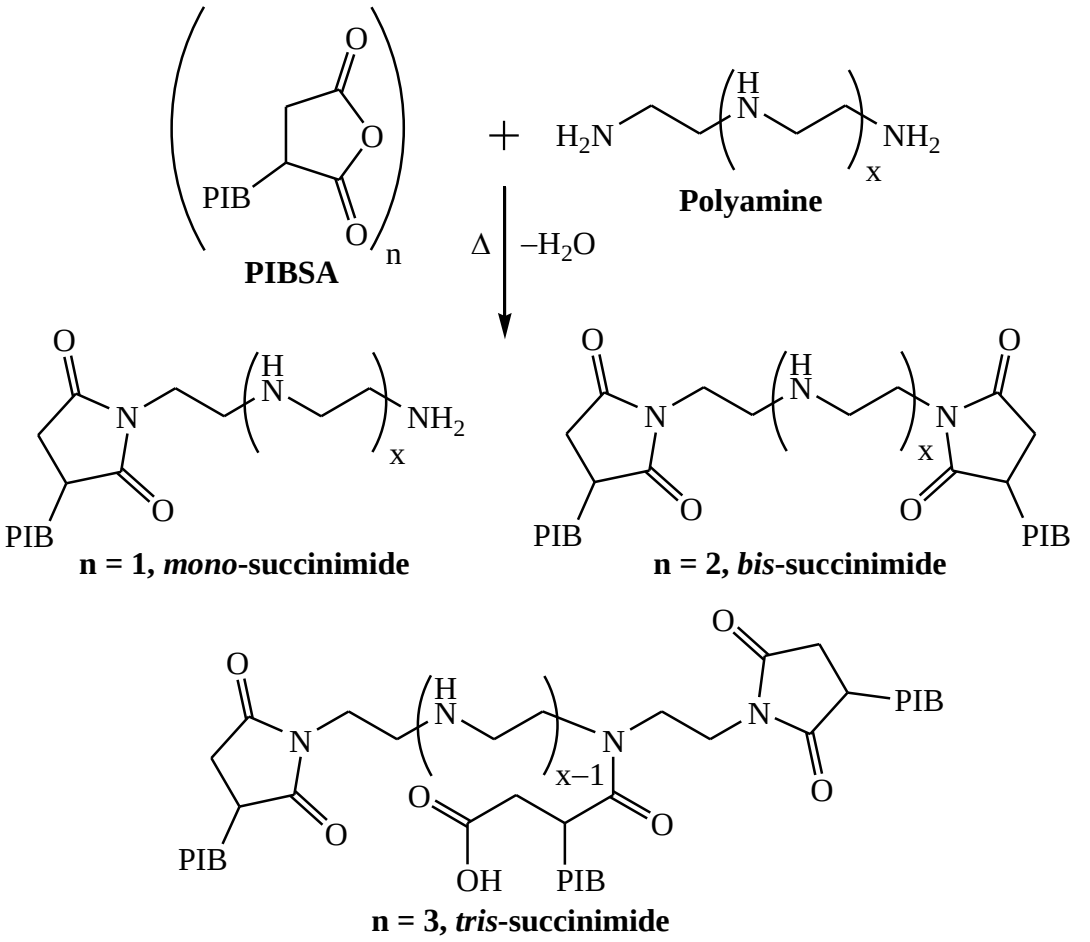

Scheme 1.18. Polyisobutylene succinimides synthesised by reacting a polyamine with different equivalents of PIBSA.

Polyisobutylene succinimides synthesis is not limited to just polyamines and other primary amines, containing extra functionalities such as tertiary amines,[176] alcohols,[177,178] ethers,[177] and esters[178] have been reacted with PIBSA to synthesise the corresponding polyisobutylene succinimides.

Mannich-type dispersants, named after the chemist who discovered the reaction used to synthesise these dispersants, are the final variety of dispersant introduced that are based on the general structure from Figure 1.05. These dispersants are synthesised by reacting PIBP with a primary amine and formaldehyde (Scheme 1.19).[179-181] These dispersants are commonly synthesised with the same polyamines introduced above and as such a mixture of dispersants can be produced which depends on the

equivalents of amine, formaldehyde and PIBP used. Therefore, a monofunctionalised, difunctionalised and a coupled product are possible.[179]

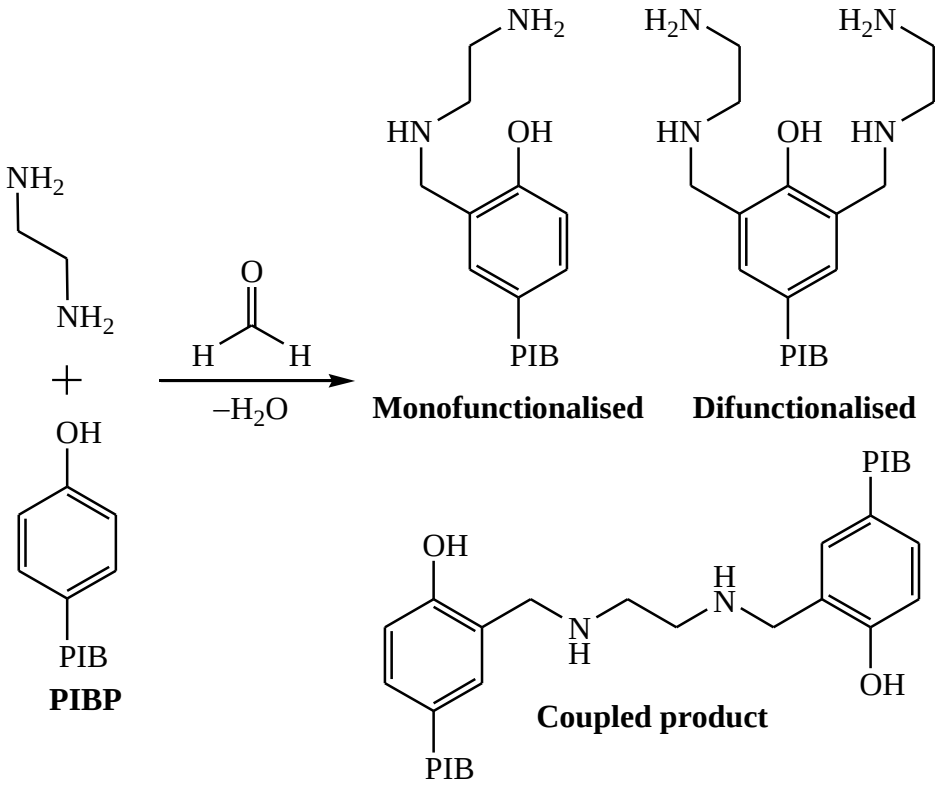

Scheme 1.19. Synthesis of Mannich-type dispersants by reacting PIBP with ethylenediamine in the presence of formaldehyde.

Therefore, an extremely diverse range of fuel dispersants are capable of being synthesised by different combinations of connecting and polar head groups. Furthermore, a range of dispersants can commonly be synthesised by simply changing the molar ratio of PIB precursor to the small molecule alcohol/amine.

1.4.4. Other polymeric fuel dispersants

Fuel dispersants are not limited to the general structure described earlier (Figure 1.05). A less uniform and potentially more advantageous family of dispersants are known as dispersant viscosity modifiers (DVMs).[159] These fuel additives are designed primarily as viscosity modifiers in engine oils but also have added functionality to provide dispersancy within the chosen medium.[159]

DVMs offer many advantages over traditional dispersants. Dispersancy-imparting monomers can be directly grafted to pre-existing polymers, such as grafting 4-vinylpyridine to an ethylene-propylene copolymer (Scheme 1.20).[182-185] Dispersancy-imparting functionalities may also be directly attached to reactive groups on pre-existing polymers, such as reacting primary amines/alcohols with MalA containing copolymers (Scheme 1.21).[186-188] DVMs may also be synthesised by grafting multiple functionalities to the same polymer.[189,190] Finally, DVMs can be synthesised in one step by copolymerisation of *n*-alkyl methacrylates and dispersancy-imparting monomers.[191,192]

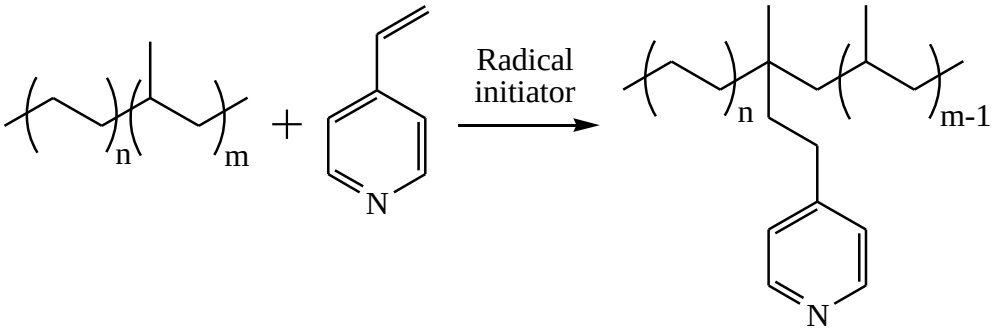

Scheme 1.20. DVM synthesised by grafting 4-vinylpyridine to an ethylene-porpylene copolymer.

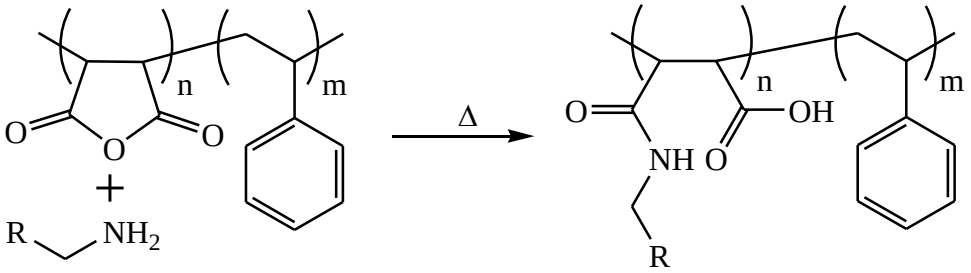

Scheme 1.21. DVM synthesised by reacting a primary amine with a MalA containing copolymer.

1.5. Aims and Objectives

This thesis aims to utilise the introduced polymerisation and post-polymerisation modification techniques to synthesis novel polymeric molecules and synthetic strategies. Furthermore, many of these new syntheses will draw from the discussed

synthesis of dispersants in an attempt to synthesise potential new dispersant molecules. Therefore, the following chapters will focus on fulfilling these objectives:

- Explore the possibilities of developing new synthetic strategies of preparing PIB block copolymers. By combining CRP techniques with end group modifications of PIB that is primarily terminated by an *exo*-olefin.
- Investigate the potential of developing a novel DVM system based on alternating copolymers of functionalised α-methyl styrene monomers and maleic anhydride. As well as post-polymerisation modification of the maleic anhydride repeat units.
- Preparation of a PIB macromonomer via end group modification of PIB, which is primarily terminated by an *exo*-olefin, before investigating said PIB macromonomers ability to be (co)polymerised via CRP techniques.
- Synthesise well defined block copolymers of 2,3,4,5,6-pentafluorostyrene and 2-isopropenyl-2-oxazoline via CRP. Investigate the potential of these block copolymers to be functionalised via multiple post-polymerisation modification routes.

1.6. References

1. W. B. Jensen, *J. Chem. Educ.*, 2008, **85**, 624.
2. A. D. Jenkins, P. Kratochvil, R. F. T. Stepto and U. W. Suter, *Pure & Appl. Chem.*, 1996, **68**, 2287.
3. P. J. Flory, *J. Am. Chem. Soc.*, 1937, **59**, 241.
4. G. Odian, *Principles of Polymerization*, John Wiley & Sons, 4th edn., 2004.
5. F. R. Mayo, *J. Am. Chem. Soc.*, 1943, **65**, 2324.
6. M. Szwarc, *Nature*, 1956, **178**, 1168.

7. M. Szwarc, M. Levy and R. Milkovich, *J. Am. Chem. Soc.*, 1956, **78**, 2656.
8. R. P. Quirk and B. Lee, *Polym. Int.*, 1992, **27**, 359.
9. M. Kato, M. Kamigaito, M. Sawamoto and T. Higashimura, *Macromolecules*, 1995, **28**, 1721.
10. J.-S. Wang and K. Matyjaszewski, *J. Am. Chem. Soc.*, 1995, **117**, 5614.
11. J.-S. Wang and K. Matyjaszewski, *Macromolecules*, 1995, **28**, 7901.
12. M. S. Kharasch, E. V. Jensen and W. H. Urry, *Science*, 1945, **102**, 128.
13. F. Minisci, *Acc. Chem. Res.*, 1975, **8**, 165.
14. K. Matyjaszewski and J. Xia, *Chem. Rev.*, 2001, **101**, 2921.
15. W. Tang, Y. Kwak, W. Braunecker, N. V. Tsarevsky, M. L. Coote and K. Matyjaszewski, *J. Am. Chem. Soc.*, 2008, **130**, 10702.
16. N. V. Tsarevsky, T. Pintauer and K. Matyjaszewski, *Macromolecules*, 2004, **37**, 9768.
17. A. J. Carmichael, D. M. Haddleton, S. A. F. Bon and K. R. Seddon, *Chem. Commun.*, 2000, 1237.
18. K. Matyjaszewski, W. Jakubowski, K. Min, W. Tang, J. Huang, W. A. Braunecker and N. V. Tsarevsky, *Proc. Natl. Acad. Sci. U.S.A.*, 2006, **103**, 15309.
19. L. Mueller, W. Jakubowski, W. Tang and K. Matyjaszewski, *Macromolecules*, 2007, **40**, 6464.
20. W. Jakubowski and K. Matyjaszewski, *Angew. Chem. Int. Ed.*, 2006, **45**, 4482.
21. W. Jakubowski, K. Min and K. Matyjaszewski, *Macromolecules*, 2006, **39**, 39.
22. K. Min, H. Gao and K. Matyjaszewski, *Macromolecules*, 2007, **40**, 1789.
23. M. A. Tasdelen, M. Uygun and Y. Yagci, *Macromol. Chem. Phys.*, 2010, **211**, 2271.

24. M. A. Tasdelen, M. Uygun and Y. Yagci, *Macromol. Rapid Commun.*, 2011, **32**, 58.
25. D. Konkolewicz, K. Schröder, J. Buback, S. Bernhard and K. Matyjaszewski, *ACS Macro Lett.*, 2012, **1**, 1219.
26. A. J. D. Magenau, N. C. Strandwitz, A. Gennaro and K. Matyjaszewski, *Science*, 2011, **332**, 81.
27. N. Bortolamei, A. A. Isse, A. J. D. Magenau, A. Gennaro and K. Matyjaszewski, *Angew. Chem. Int. Ed.*, 2011, **50**, 11391.
28. A. J. D. Magenau, N. Bortolamei, E. Frick, S. Park, A. Gennaro and K. Matyjaszewski, *Macromolecules*, 2013, **46**, 4346.
29. K. Matyjaszewski, S. Coca, S. G. Gaynor, M. Wei and B. E. Woodworth, *Macromolecules*, 1997, **30**, 7348.
30. D. Konkolewicz, Y. Wang, P. Krys, M. Zhong, A. A. Isse, A. Gennaro and K. Matyjaszewski, *Polym. Chem.*, 2014, **5**, 4396.
31. V. Percec, T. Guliashvili, J. S. Ladislaw, A. Wistrand, A. Stjerndahl, M. J. Sienkowska, M. J. Monteiro and S. Sahoo, *J. Am. Chem. Soc.*, 2006, **128**, 14156.
32. N. H. Nguyen, H.-J. Sun, M. E. Levere, S. Fleischmann and V. Percec, *Polym. Chem.*, 2013, **4**, 1328.
33. M. E. Levere, N. H. Nguyen, X. Leng and V. Percec, *Polym. Chem.*, 2013, **4**, 1635.
34. Q. Zhang, P. Wilson, Z. Li, R. McHale, J. Godfrey, A. Anastasaki, C. Waldron and D. M. Haddleton, *J. Am. Chem. Soc.*, 2013, **135**, 7355.
35. G. Lligadas and V. Percec, *J. Polym. Sci. Part A: Polym. Chem.*, 2008, **46**, 6880.

36. G. Lligadas, B. M. Rosen, M. J. Monteiro and V. Percec, *Macromolecules*, 2008, **41**, 8360.
37. N. H. Nguyen and V. Percec, *J. Polym. Sci. Part A: Polym. Chem.*, 2011, **49**, 4227.
38. G. Lligadas and V. Percec, *J. Polym. Sci. Part A: Polym. Chem.*, 2008, **46**, 2745.
39. S. Fleischmann and V. Percec, *J. Polym. Sci. Part A: Polym. Chem.*, 2010, **48**, 2243.
40. P. M. Wright, G. Mantovani and D. M. Haddleton, *J. Polym. Sci. Part A: Polym. Chem.*, 2008, **46**, 7376.
41. N. H. Nguyen, B. M. Rosen, X. Jiang, S. Fleischmann and V. Percec, *J. Polym. Sci. Part A: Polym. Chem.*, 2009, **47**, 5577.
42. B. M. Rosen and V. Percec, *J. Polym. Sci. Part A: Polym. Chem.*, 2007, **45**, 4950.
43. G. Lligadas, B. M. Rosen, C. A. Bell, M. J. Monteiro and V. Percec, *Macromolecules*, 2008, **41**, 8365.
44. N. H. Nguyen and V. Percec, *J. Polym. Sci. Part A: Polym. Chem.*, 2011, **49**, 4241.
45. S. R. Samanta, H.-J. Sun, A. Anastasaki, D. M. Haddleton and V. Percec, *Polym. Chem.*, 2014, **5**, 89.
46. X. Jiang, B. M. Rosen and V. Percec, *J. Polym. Sci. Part A: Polym. Chem.*, 2010, **48**, 2716.
47. M. E. Levere, N. H. Nguyen, H.-J. Sun and V. Percec, *Polym. Chem.*, 2013, **4**, 686.

48. A. H. Soeriyadi, C. Boyer, F. Nyström, P. B. Zetterlund and M. R. Whittaker, *J. Am. Chem. Soc.*, 2011, **133**, 11128.

49. B. M. Rosen, G. Lligadas, C. Hahn and V. Percec, *J. Polym. Sci. Part A: Polym. Chem.*, 2009, **47**, 3940.

50. M. R. Whittaker, C. N. Urbani and M. J. Monteiro, *J. Polym. Sci. Part A: Polym. Chem.*, 2008, **46**, 6346.

51. A. Anastasaki, C. Waldron, P. Wilson, C. Boyer, P. B. Zetterlund, M. R. Whittaker and D. Haddleton, *ACS Macro Lett.*, 2013, **2**, 896.

52. Q. Zhang, J. Collins, A. Anastasaki, R. Wallis, D. A. Mitchell, C. R. Becer and D. M. Haddleton, *Angew. Chem. Int. Ed.*, 2013, **52**, 4435.

53. Q. Zhang, Z. Li, P. Wilson and D. M. Haddleton, *Chem. Commun.*, 2013, **49**, 6608.

54. C. Waldron, Q. Zhang, Z. Li, V. Nikolaou, G. Nurumbetov, J. Godfrey, R. McHale, G. Yilmaz, R. K. Randev, M. Girault, K. McEwan, D. M. Haddleton, M. Droesbeke, A. J. Haddleton, P. Wilson, A. Simula, J. Collins, D. J. Lloyd, J. A. Burns, C. Summers, C. Houben, A. Anastasaki, M. Li, C. R. Becer, J. K. Kiviaho and N. Risangud, *Polym. Chem.*, 2014, **5**, 57.

55. F. Alsubaie, A. Anastasaki, P. Wilson and D. M. Haddleton, *Polym. Chem.*, 2015, **6**, 406.

56. J. Chiefari, Y. K. Chong, F. Ercole, J. Krstina, J. Jeffery, T. P. T. Le, R. T. A. Mayadunne, G. F. Meijs, C. L. Moad, G. Moad, E. Rizzardo and S. H. Thang, *Macromolecules*, 1998, **31**, 5559.

57. D. G. Hawthorne, G. Moad, E. Rizzardo and S. H. Thang, *Macromolecules*, 1999, **32**, 5457.

58. J. Chiefari, R. T. A. Mayadunne, C. L. Moad, G. Moad, E. Rizzardo, A. Postma and S. H. Thang, *Macromolecules*, 2003, **36**, 2273.

59. R. T. A. Mayadunne, E. Rizzardo, J. Chiefari, J. Krstina, G. Moad, A. Postma and S. H. Thang, *Macromolecules*, 2000, **33**, 243.

60. R. T. A. Mayadunne, E. Rizzardo, J. Chiefari, Y. K. Chong, G. Moad and S. H. Thang, *Macromolecules*, 1999, **32**, 6977.

61. D. Charmot, P. Corpart, H. Adam, S. Z. Zard, T. Biadatti and G. Bouhadir, *Macromol. Symp.*, 2000, **150**, 23.

62. M. Destarac, W. Bzducha, D. Taton, I. Gauthier-Gillaizeau and S. Z. Zard, *Macromol. Rapid Commun.*, 2002, **23**, 1049.

63. Y. K. Chong, J. Krstina, T. P. T. Le, G. Moad, A. Postma, E. Rizzardo and S. H. Thang, *Macromolecules*, 2003, **36**, 2256.

64. M. Benaglia, J. Chiefari, Y. K. Chong, G. Moad, E. Rizzardo and S. H. Thang, *J. Am. Chem. Soc.*, 2009, **131**, 6914.

65. Y. K. Chong, T. P. T. Le, G. Moad, E. Rizzardo and S. H. Thang, *Macromolecules*, 1999, **32**, 2071.

66. Y. Mitsukami, M. S. Donovan, A. B. Lowe and C. L. McCormick, *Macromolecules*, 2001, **34**, 2248.

67. S. Luo, J. Xu, Y. Zhang, S. Liu and C. Wu, *J. Phys. Chem. B*, 2005, **109**, 22159.

68. H. De Brouwer, M. A. J. Schellekens, B. Klumperman, M. J. Monteiro and A. L. German, *J. Polym. Sci. Part A: Polym. Chem.*, 2000, **38**, 3596.

69. A. J. D. Magenau, N. Martinez-Castro and R. F. Storey, *Macromolecules*, 2009, **42**, 2353.

70. M. Hales, C. Barner-Kowollik, T. P. Davis and M. H. Stenzel, *Langmuir*, 2004, **20**, 10809.

71. X. Hao, C. Nilsson, M. Jesberger, M. H. Stenzel, E. Malmström, T. P. Davis, E. Östmark and C. Barner-Kowollik, *J. Polym. Sci. Part A: Polym. Chem.*, 2004, **42**, 5877.
72. A. Postma, T. P. Davis, G. Moad and M. S. O'Shea, *Macromolecules*, 2005, **38**, 5371.
73. S. Perrier, P. Takolpuckdee and C. A. Mars, *Macromolecules*, 2005, **38**, 2033.
74. M. Chen, G. Moad and E. Rizzardo, *J. Polym. Sci. Part A: Polym. Chem.*, 2009, **47**, 6704.
75. Y. K. Chong, G. Moad, E. Rizzardo and S. H. Thang, *Macromolecules*, 2007, **40**, 4446.
76. J. Vandenbergh, G. Reekmans, P. Adriaensens and T. Junkers, *Chem. Commun.*, 2013, **49**, 10358.
77. G. Gody, T. Maschmeyer, P. B. Zetterlund and S. Perrier, *Nat. Commun.*, 2013, **4**, 2505.
78. G. Gody, T. Maschmeyer, P. B. Zetterlund and S. Perrier, *Macromolecules*, 2014, **47**, 3451.
79. G. Gody, R. Barbey, M. Danial and S. Perrier, *Polym. Chem.*, 2015, **6**, 1502.
80. L. Martin, G. Gody and S. Perrier, *Polym. Chem.*, 2015, **6**, 4875.
81. J. J. Haven, C. Guerrero-Sanchez, D. J. Keddie, G. Moad, S. H. Thang and U. S. Schubert, *Polym. Chem.*, 2014, **5**, 5236.
82. D. Zehm, A. Laschewsky, M. Gradzielski, S. Prévost, H. Liang, J. P. Rabe, R. Schweins and J. Gummel, *Langmuir*, 2010, **26**, 3145.
83. D. Zehm, A. Laschewsky, P. Heunemann, M. Gradzielski, S. Prevost, H. Liang, J. P. Rabe and J.-F. Lutz, *Polym. Chem.*, 2011, **2**, 137.

84. D. Zehm, A. Laschewsky, H. Liang and J. P. Rabe, *Macromolecules*, 2011, **44**, 9635.

85. H. C. Kolb, M. G. Finn and K. B. Sharpless, *Angew. Chem. Int. Ed.*, 2001, **40**, 2004.

86. C. Barner-Kowollik, F. E. Du Prez, P. Espeel, C. J. Hawker, T. Junkers, H. Schlaad and W. Van Camp, *Angew. Chem. Int. Ed.*, 2011, **50**, 60.

87. H. C. Kolb and K. B. Sharpless, *Drug Discov. Today*, 2003, **8**, 1128.

88. B. Helms, J. L. Mynar, C. J. Hawker and J. M. J. Fréchet, *J. Am. Chem. Soc.*, 2004, **126**, 15020.

89. P. Wu, A. K. Feldman, A. K. Nugent, C. J. Hawker, A. Scheel, B. Voit, J. Pyun, J. M. J. Fréchet, K. B. Sharpless and V. V. Fokin, *Angew. Chem. Int. Ed.*, 2004, **43**, 3928.

90. B. Parrish, R. B. Breitenkamp and T. Emrick, *J. Am. Chem. Soc.*, 2005, **127**, 7404.

91. R. Huisgen, *Angew. Chem. Int. Ed.*, 1968, **7**, 321.

92. N. V. Tsarevsky, K. V. Bernaerts, B. Dufour, F. E. Du Prez and K. Matyjaszewski, *Macromolecules*, 2004, **37**, 9308.

93. I. Singh, Z. Zarafshani, J.-F. Lutz and F. Heaney, *Macromolecules*, 2009, **42**, 5411.

94. G. Mantovani, V. Ladmiral, L. Tao and D. M. Haddleton, *Chem. Commun.*, 2005, 2089.

95. J. Geng, J. Lindqvist, G. Mantovani and D. M. Haddleton, *Angew. Chem. Int. Ed.*, 2008, **47**, 4180.

96. C. R. Becer, R. Hoogenboom and U. S. Schubert, *Angew. Chem. Int. Ed.*, 2009, **48**, 4900.

97. N. J. Agard, J. A. Prescher and C. R. Bertozzi, *J. Am. Chem. Soc.*, 2004, **126**, 15046.

98. J. M. Baskin, J. A. Prescher, S. T. Laughlin, N. J. Agard, P. V. Chang, I. A. Miller, A. Lo, J. A. Codelli and C. R. Bertozzi, *Proc. Natl. Acad. Sci. U.S.A.*, 2007, **104**, 16793.

99. Z. Li, T. S. Seo and J. Ju, *Tetrahedron Lett.*, 2004, **45**, 3143.

100. A. Gress, A. Völkel and H. Schlaad, *Macromolecules*, 2007, **40**, 7928.

101. L. M. Campos, K. L. Killops, R. Sakai, J. M. J. Paulusse, D. Damiron, E. Drockenmuller, B. W. Messmore and C. J. Hawker, *Macromolecules*, 2008, **41**, 7063.

102. K. L. Killops, L. M. Campos and C. J. Hawker, *J. Am. Chem. Soc.*, 2008, **130**, 5062.

103. B. D. Fairbanks, T. F. Scott, C. J. Kloxin, K. S. Anseth and C. N. Bowman, *Macromolecules*, 2009, **42**, 211.

104. J. Rieger, K. Van Butsele, P. Lecomte, C. Detrembleur, R. Jerome and C. Jerome, *Chem. Commun.*, 2005, 274.

105. G.-Z. Li, R. K. Randev, A. H. Soeriyadi, G. Rees, C. Boyer, Z. Tong, T. P. Davis, C. R. Becer and D. M. Haddleton, *Polym. Chem.*, 2010, **1**, 1196.

106. R. J. Pounder, M. J. Stanford, P. Brooks, S. P. Richards and A. P. Dove, *Chem. Commun.*, 2008, 5158.

107. M. J. Stanford, R. L. Pflughaupt and A. P. Dove, *Macromolecules*, 2010, **43**, 6538.

108. J. W. Chan, C. E. Hoyle and A. B. Lowe, *J. Am. Chem. Soc.*, 2009, **131**, 5751.

109. P. Battioni, O. Brigaud, H. Desvaux, D. Mansuy and T. G. Traylor, *Tetrahedron Lett.*, 1991, **32**, 2893.

110. X. Chen, L. Hui, D. A. Foster and C. M. Drain, *Biochemistry*, 2004, **43**, 10918.

111. C. R. Becer, K. Babiuch, D. Pilz, S. Hornig, T. Heinze, M. Gottschaldt and U. S. Schubert, *Macromolecules*, 2009, **42**, 2387.

112. C. R. Becer, K. Kokado, C. Weber, A. Can, Y. Chujo and U. S. Schubert, *J. Polym. Sci. Part A: Polym. Chem.*, 2010, **48**, 1278.

113. J. A. Norton, *Chem. Rev.*, 1942, **31**, 319.

114. M. L. Blackman, M. Royzen and J. M. Fox, *J. Am. Chem. Soc.*, 2008, **130**, 13518.

115. C. F. Hansell, P. Espeel, M. M. Stamenović, I. A. Barker, A. P. Dove, F. E. Du Prez and R. K. O'Reilly, *J. Am. Chem. Soc.*, 2011, **133**, 13828.

116. S. Billiet, K. De Bruycker, F. Driessen, H. Goossens, V. Van Speybroeck, J. M. Winne and F. E. Du Prez, *Nat. Chem.*, 2014, **6**, 815.

117. B. Vonhören, O. Roling, K. De Bruycker, R. Calvo, F. E. Du Prez and B. J. Ravoo, *ACS Macro Lett.*, 2015, **4**, 331.

118. S. Sinnwell, A. J. Inglis, T. P. Davis, M. H. Stenzel and C. Barner-Kowollik, *Chem. Commun.*, 2008, 2052.

119. G. F. Meijs, T. C. Morton, E. Rizzardo and S. H. Thang, *Macromolecules*, 1991, **24**, 3689.

120. B. Yamada, S. Tagashira and S. Aoki, *J. Polym. Sci. Part A: Polym. Chem.*, 1994, **32**, 2745.

121. N. S. Enikolopyan, B. R. Smirnov, G. V. Ponomarev and I. M. Belgovskii, *J. Polym. Sci.: Polym. Chem. Ed.*, 1981, **19**, 879.

122. J. Krstina, G. Moad, E. Rizzardo, C. L. Winzor, C. T. Berge and M. Fryd, *Macromolecules*, 1995, **28**, 5381.

123. L. Nurmi, J. Lindqvist, R. Randev, J. Syrett and D. M. Haddleton, *Chem. Commun.*, 2009, 2727.

124. Q. Zhang, S. Slavin, M. W. Jones, A. J. Haddleton and D. M. Haddleton, *Polym. Chem.*, 2012, **3**, 1016.

125. K. A. McEwan, S. Slavin, E. Tunnah and D. M. Haddleton, *Polym. Chem.*, 2013, **4**, 2608.

126. V. Coessens and K. Matyjaszewski, *Macromol. Rapid Commun.*, 1999, **20**, 127.

127. K. Matyjaszewski, Y. Nakagawa and S. G. Gaynor, *Macromol. Rapid Commun.*, 1997, **18**, 1057.

128. J.-F. Lutz, H. G. Börner and K. Weichenhan, *Macromol. Rapid Commun.*, 2005, **26**, 514.

129. N. V. Tsarevsky, B. S. Sumerlin and K. Matyjaszewski, *Macromolecules*, 2005, **38**, 3558.

130. V. Coessens, J. Pyun, P. J. Miller, S. G. Gaynor and K. Matyjaszewski, *Macromol. Rapid Commun.*, 2000, **21**, 103.

131. S. A. F. Bon, A. G. Steward and D. M. Haddleton, *J. Polym. Sci. Part A: Polym. Chem.*, 2000, **38**, 2678.

132. D. M. Haddleton, C. Waterson, P. J. Derrick, C. B. Jasieczek and A. J. Shooter, *Chem. Commun.*, 1997, 683.

133. D. M. Haddleton and C. Waterson, *Macromolecules*, 1999, **32**, 8732.

134. B. Gacal, H. Durmaz, M. A. Tasdelen, G. Hizal, U. Tunca, Y. Yagci and A. L. Demirel, *Macromolecules*, 2006, **39**, 5330.

135. X.-P. Qiu and F. M. Winnik, *Macromol. Rapid Commun.*, 2006, **27**, 1648.

136. C. Boyer, A. Granville, T. P. Davis and V. Bulmus, *J. Polym. Sci. Part A: Polym. Chem.*, 2009, **47**, 3773.

137. J. R. McKee, V. Ladmiral, J. Niskanen, H. Tenhu and S. P. Armes, *Macromolecules*, 2011, **44**, 7692.

138. Y. Wu, Y. Zhou, J. Zhu, W. Zhang, X. Pan, Z. Zhang and X. Zhu, *Polym. Chem.*, 2014, **5**, 5546.

139. S. Harrisson, *Macromolecules*, 2009, **42**, 897.

140. G. Moad, E. Rizzardo and S. H. Thang, *Polym. Int.*, 2011, **60**, 9.

141. A. J. Inglis, M. H. Stenzel and C. Barner-Kowollik, *Macromol. Rapid Commun.*, 2009, **30**, 1792.

142. K. K. Oehlenschlaeger, J. O. Mueller, N. B. Heine, M. Glassner, N. K. Guimard, G. Delaittre, F. G. Schmidt and C. Barner-Kowollik, *Angew. Chem. Int. Ed.*, 2013, **52**, 762.

143. J. T. Lai, D. Filla and R. Shea, *Macromolecules*, 2002, **35**, 6754.

144. M. M. Stamenović, P. Espeel, W. V. Camp and F. E. Du Prez, *Macromolecules*, 2011, **44**, 5619.

145. D. J. Phillips, I. Prokes, G.-L. Davies and M. I. Gibson, *ACS Macro Lett.*, 2014, **3**, 1225.

146. A. Postma, T. P. Davis, R. A. Evans, G. Li, G. Moad and M. S. O'Shea, *Macromolecules*, 2006, **39**, 5293.

147. D. Navarro-Rodriguez, F. J. Rodriguez-Gonzalez, J. Romero-Garcia, E. J. Jimenez-Regalado and D. Guillon, *Euro. Polym. J.*, 1998, **34**, 1039.

148. Q. Zhang, A. Anastasaki, G.-Z. Li, A. J. Haddleton, P. Wilson and D. M. Haddleton, *Polym. Chem.*, 2014, **5**, 3876.

149. B. Klumperman, *Polym. Chem.*, 2010, **1**, 558.

150. L. Coleman, J. Bork and H. Dunn, *J. Org. Chem.*, 1959, **24**, 135.

151. G. H. Hu and J. T. Lindt, *Polym. Bull.*, 1992, **29**, 357.

152. W.-F. Lee and C.-H. Lee, *Polymer*, 1997, **38**, 971.

153. J. D. Flores, J. Shin, C. E. Hoyle and C. L. McCormick, *Polym. Chem.*, 2010, **1**, 213.

154. R. M. Hensarling, S. B. Rahane, A. P. LeBlanc, B. J. Sparks, E. M. White, J. Locklin and D. L. Patton, *Polym. Chem.*, 2011, **2**, 88.

155. J. Moraes, T. Maschmeyer and S. Perrier, *J. Polym. Sci. Part A: Polym. Chem.*, 2011, **49**, 2771.

156. K. Kempe, R. Hoogenboom, M. Jaeger and U. S. Schubert, *Macromolecules*, 2011, **44**, 6424.

157. C. Ott, R. Hoogenboom and U. S. Schubert, *Chem. Commun.*, 2008, 3516.

158. S. P. Srivastava and J. Hancsok, in *Fuels and Fuel-Additives*, John Wiley & Sons, 1st edn., 2014, ch. 5, pp. 177-208.

159. L. R. Rudnick, in *Lubricant additives: Chemistry and Applications*, CRC Press, 2nd edn., 2009, ch. 5, pp. 143-166.

160. R. M. Mortier, M. F. Fox and S. Orszulik, in *Chemistry and Technology of Lubricants*, Springer, 3rd edn., 2010, ch. 7, pp. 213-236.

161. *US Pat.*, 5017299, 1991.

162. *US Pat.*, 5435926, 1995.

163. *US Pat.*, 6488723, 2002.

164. *US Pat.*, 6909018, 2005.

165. *US Pat.*, 4234435, 1980.

166. *US Pat.*, 361673, 1968.

167. *US Pat.*, 6875897, 2005.

168. C. Hongfa, J. Tian, H. S. Bazzi and D. E. Bergbreiter, *Org. Lett.*, 2007, **9**, 3259.

169. J. Li, S. Sung, J. Tian and D. E. Bergbreiter, *Tetrahedron*, 2005, **61**, 12081.

170. *US Pat.*, 5663457, 1997.

171. M. Ionescu and Z. S. Petrovic, *J. Serb. Chem. Soc.*, 2011, **76**, 591.

172. J. I. de Jong, *Recl. Trav. Chim. Pays-Bas*, 1964, **83**, 469.

173. D. E. Bergbreiter, C. Hobbs, J. Tian, H. Koizumi, H.-L. Su and C. Hongfa, *Pure Appl. Chem.*, 2009, **81**, 1981.

174. *US Pat.*, 3697428, 1972.

175. *US Pat.*, 7091306, 2006.

176. *US Pat.*, 7683120, 2010.

177. *US Pat.*, 6352566, 2002.

178. *US Pat.*, 5993497, 1999.

179. *US Pat.*, 3368972, 1968.

180. *US Pat.*, 3980569, 1976.

181. *US Pat.*, 6179885, 2001.

182. *US Pat.*, 4402843, 1983.

183. *US Pat.*, 4402844, 1983.

184. *US Pat.*, 6083888, 2000.

185. *US Pat.*, 20120178656A1, 2012.

186. *US Pat.*, 6117941, 2000.

187. *US Pat.*, 5429758, 1995.

188. *US Pat.*, 8168574B2, 2012.

189. *US Pat.*, 5439607, 1995.

190. *US Pat.*, 5698500, 1997.

191. *US Pat.*, 6124249, 2000.

192. *US Pat.*, 6331603B1, 2001.

2. Novel Synthetic Pathways to PIB-*b*-PDMAEMA Copolymers

2.1. Introduction

PIB based materials (block copolymers, graft copolymers, polymer networks etc.) continue to attract much attention and are widely utilised in a number of applications, such as the fuel additives detailed in Section 1.4. This is owing to PIB's versatile properties, including biostability, biocompatibility, low-temperature flexibility, gas-barrier and energy damping, chemical, thermal, and oxidative stability.[1] Previous accounts and recent advances for the synthesis of PIB block copolymers will be discussed.

PIB based block copolymers (which are copolymers that contain at least one discrete block of pure IB) can typically be synthesised via one of four synthetic approaches; sequential monomer addition, site transformation of the PIB end group, macromolecular coupling of homopolymers and dual-site initiators. Sequential monomer addition is achieved by direct addition of a second monomer following the living cationic polymerisation (LCP) of IB, a living PIB end group will initiate and subsequently polymerise said second monomer to furnish a block copolymer. Although this method is conceptually simpler it can be synthetically challenging as stringent reaction conditions are required and only monomers polymerisable via LCP are viable, such as styrene[2,3] and vinyl ethers.[4]

Alternatively, the site transformation methodology can be utilised to modify the PIB end group, following LCP of IB, to a range of initiators/mediators compatible with other polymerisation techniques. This is potentially a more versatile approach as polymerisation of many alternative monomer classes is possible.

For example, PIB has been combined with living anionic polymerisation by end capping living PIB with 1,1-diphenylethylene which was subsequently metalated with Na^+/K^+ and used to initiate the polymerisation of *tert*-butyl methacrylate (*t*BMA).[5] Alternatively, metalation with Li^+ synthesised a PIB macroinitiator suitable to initiate MMA.[5] PIB has also been combined with controlled radical polymerisation (CRP) techniques. Allyl terminated PIB was transformed to hydroxyl terminated PIB following hydroboration and oxidation. Hydroxyl terminated PIB was then subsequently esterified with α-bromoisobutyryl bromide (BiBB) in the presence of triethylamine (TEA) to synthesise a PIB macroinitiator. Said PIB macroinitiator was then utilised to polymerise *t*BMA or DMAEMA via ATRP.[6,7] Moreover, telechelic ATRP PIB macroinitiators have been used to synthesise ABCBA style pentablock copolymers of PIB, PMMA and poly(polyethylene glycol methacrylate) (PPEGMA).[8] Furthermore, 1-chloro-1-phenylethyl terminated PIB has been utilised as an ATRP macroinitiator for the polymerisation of styrene and *p*-acetoxystyrene.[9] Combining PIB with RAFT polymerisation has also been achieved by the synthesis of PIB macroRAFT agents. PIB macroRAFT agents are typically synthesised by hydroboration/oxidation of allyl terminated PIB[10-12] or nucleophilic substitution of allyl-halide terminated PIB with NaOH to furnish a hydroxyl terminated PIB.[13,14] Hydroxyl terminated PIB is then esterified with a RAFT agent bearing a carboxylic acid, such as cyano-4-(dodecylsulfanylthiocarbonyl)sulfanyl pentanoic acid, to synthesise a macroRAFT agent.[10-14] PIB macroRAFT agents have been successfully employed to mediate the polymerisation of styrene,[10] MMA,[10] amino acid-based monomers,[11] silsesquioxane containing monomers,[12] 2-(diethylamino)ethyl methacrylate (DEAEMA),[13] and *N*,*N*-diethylacrylamide,[14] and *N*-isopropylacrylamide,[15] to synthesise the corresponding PIB block copolymers.

Macromolecular coupling of reactive homopolymers requires the prior synthesis of quantitatively functionalised homopolymers with reactive moieties. Furthermore, these coupling reactions must proceed to high conversion under stoichiometric conditions otherwise block copolymer yield will be low or difficult block copolymer/homopolymers separation will be required. Despite these synthetic challenges macromolecular coupling has been utilised to synthesise PIB block copolymers. For example PIB-*b*-PMMA copolymers have been synthesised by coupling living homopolymers of PIB and PMMA, synthesised by cationic and group transfer polymerisation respectively.[16] Moreover, living poly(vinylferrocene) has been coupled with allyl-bromide/chlorosilyl terminated PIB to yield the block copolymer.[17] Furthermore, macromolecular coupling is possible between non-living polymers, PIB-*b*-PEG copolymers have been synthesised by CuAAC between an azide functionalised PIB and alkyne functionalised PEG.[18]

Finally, dual-site initiators have been developed to initiate both radical and cationic polymerisations separately for the synthesis of PIB-*b*-PMA copolymers.[19,20] The dual initiator possess a tertiary alkyl chloride to initiate the LCP of IB and a 2-bromo-2-methylpropionate to initiate the ATRP of MA.[19,20]

This chapter will contribute to the extensive field of PIB block copolymer synthesis by developing alternative pathways from the discussed examples to synthesise PIB copolymers. Alternative pathways to PIB copolymers include site transformation of olefin terminated PIB to synthesise a PIB macroinitiator which was subsequently employed in the SET-LRP of DMAEMA, thus combining PIB with another polymerisation technique. The second pathway utilises macromolecular coupling of PIBSA and primary amine functionalised PDMAEMA to synthesise PIB-*b*-PDMAEMA. PIB-*b*-PDMAEMA copolymers were chosen as a target PIB

based copolymer as these copolymers are suspected to be good candidates for fuel dispersants. PIB-*b*-PDMAEMA copolymers resemble the general fuel dispersant structure discussed in Section 1.4.2. (Figure 1.05). Fuel solubility will be provided by the PIB block and the DMAEMA block will act as the polar head group to interact with the fuel deposits. Control over the DP of both block lengths will allow for fine tuning the balance between fuel solubility and interaction with deposits.

2.2. Initial SET-LRP of DMAEMA studies

DMAEMA was chosen as a comonomer for the design of novel synthetic routes to PIB block copolymers as PDMAEMA has many desirable properties, such as pH responsiveness, temperature responsiveness, self-assembly behaviour,[21-23] and has been utilised in the fuel additive industry, which was the targeted application for the PIB-*b*-PDMAEMA copolymers in this thesis.[24,25]

ATRP of DMAEMA was initially reported with poorer than expected control, polymer dispersities were broad but high DMAEMA conversion (>90%) could be achieved.[26,27] Regarding block copolymer synthesis, DMAEMA was always polymerised last owing to the poor end group fidelity of the PDMAEMA.[28] Until Gan and co-workers reported an extremely effective polymerisation of DMAEMA methanol water mixtures initiated by *p*-toluenesulfonyl chloride.[28] PDMAEMA dispersity was as low as 1.07 and PDMAEMA was capable of being utilised as a macroinitiator for the ATRP of DEAEMA.[28]

Polymerisation of DMAEMA has also been attempted by SET-LRP, Grice found polymerisation was uncontrolled as polymer dispersity was high (>2) and DMAEMA conversion limited at ~80%.[29] However, this method of polymerising DMAEMA was attractive due to its utilisation of a tertiary alkyl bromide as initiator,

ethyl α-bromoisobutyrate (EBiB), as a wide range of functional alkyl bromide initiators are available to synthesise and incorporate into ATRP/SET-LRP.[30]

Therefore, previous conditions for SET-LRP of DMAEMA were adapted to observe if better control over the polymerisation was possible. Copper wire was used in place of the copper powder, as this has been shown to add control to SET-LRP kinetics and also makes the removal of copper from the reaction mixture simpler, 5/10 cm of activated Cu(0) wire was used for all polymerisations described in this section.[31,32] Furthermore, ligand to initiator ratio was reduced to 0.18:1, this has been shown to be an optimal ratio for minimising side reactions between the alkyl bromide end group and ligand.[33] 2-Hydroxyethyl-2-bromoisobutyrate (HEBiB) was used as initiator in place of EBiB to add a hydroxyl functionality to the PDMAEMA α-terminus (HO-PDMAEMA) (Scheme 2.01).

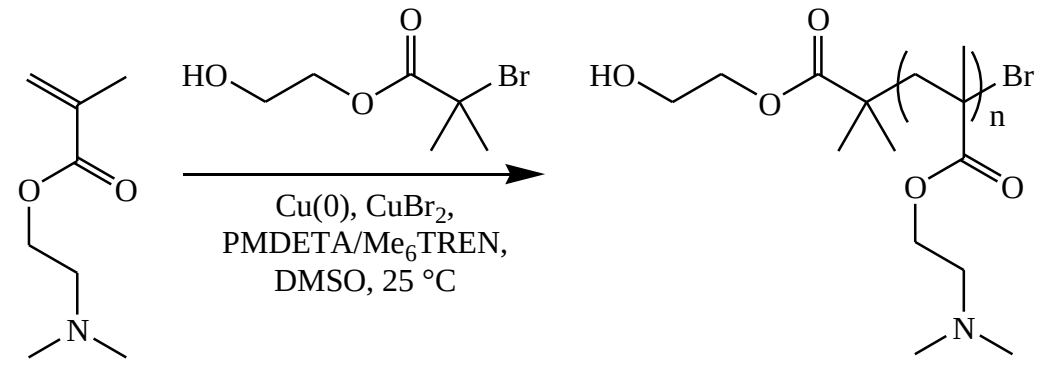

DMAEMA **HO-PDMAEMA**

Scheme 2.01. SET-LRP of DMAEMA initiated by HEBiB and mediated by Cu(0), $CuBr_2$, PMDETA/Me_6TREN in DMSO at 25 °C.

Firstly, Me_6TREN and PMDETA were compared to determine which ligand was better suited for the SET-LRP of DMAEMA (Table 2.01). PMDETA was found to be better suited for the chosen polymerisation system. However, PMDETA was only superior in terms of DMAEMA conversion over the 4 hour time scale, 55% compared to 19%. SET-LRP using Me_6TREN as ligand may have obtained lower conversion because it is the more active of the two ligands and as such generates

more radicals in the system. More radicals would result in more termination and as such propagation of DMAEMA would be suppressed. Essentially this would lower the initiator concentration in the polymerisation and increase the monomer to initiator ratio. This is supported by the theoretical M_n of PDMAEMA being significantly lower than the measured M_n even at low conversion (19%) of DMAEMA (Table 2.01, Sample P2.01). Polymer dispersity was approximately 1.3 for both ligands (Table 2.01). PDMAEMA was synthesised at a lower DP using by lowering the monomer to initiator ratio (P2.02).

Table 2.01. GPC characterisation and DMAEMA conversion for the SET-LRP of DMAEMA initiated by HEBiB and mediated by Cu(0), $Cu(II)Br_2$, PMDETA/Me_6TREN in DMSO at 25 °C.

Sample	DMAEMA Conversion$^{\alpha}$ (%)	$M_{n.Theo}{}^{\beta}$ ($g \cdot mol^{-1}$)	$M_{n.GPC}{}^{\gamma}$ ($g \cdot mol^{-1}$)	$Đ^{\gamma}$
P2.01$^{\delta}$	19	1700	3000	1.31
P2.02$^{\varepsilon}$	78	3300	4800	1.31
P2.03$^{\zeta}$	55	4500	5600	1.33

$^{\alpha}$Calculated from ^{1}H-NMR spectroscopy. $^{\beta}$Calculated from Equation 1. $^{\gamma}$THF + 2% TEA eluent, calibrated with PMMA standards.

$^{\delta}$[M]:[I]:[L]:[$Cu(II)Br_2$] = [DMAEMA]:[HEBiB]:[Me_6TREN]:[$Cu(II)Br_2$] = [50]:[1]:[0.18]:[0.05].

$^{\varepsilon}$[M]:[I]:[L]:[$Cu(II)Br_2$] = [DMAEMA]:[HEBiB]:[PMDETA]:[$Cu(II)Br_2$] = [25]:[1]:[0.18]:[0.05].

$^{\zeta}$[M]:[I]:[L]:[$Cu(II)Br_2$] = [DMAEMA]:[HEBiB]:[PMDETA]:[$Cu(II)Br_2$] = [50]:[1]:[0.18]:[0.05].

GPC traces for polymer samples P2.01 through P2.03 show a reasonably symmetrical peak with a slight tailing towards lower molecular weight (Figure 2.01).

These initial SET-LRPs of DMAEMA showed better control than those previously reported by Grice; low polymer dispersity was obtained, variable molecular weight was possible by targeting different DP of PDMAEMA and DMAEMA conversion was only slightly reduced. However, DMSO was difficult to effectively remove, partly because of its very high boiling point and its immiscibility with the *n*-hexane

which was used as a non-solvent for the precipitation of PDMAEMA. Therefore, an alternative reaction solvent was investigated that is equally suitable for the SET-LRP of DMAEMA but is easier to remove during purification.

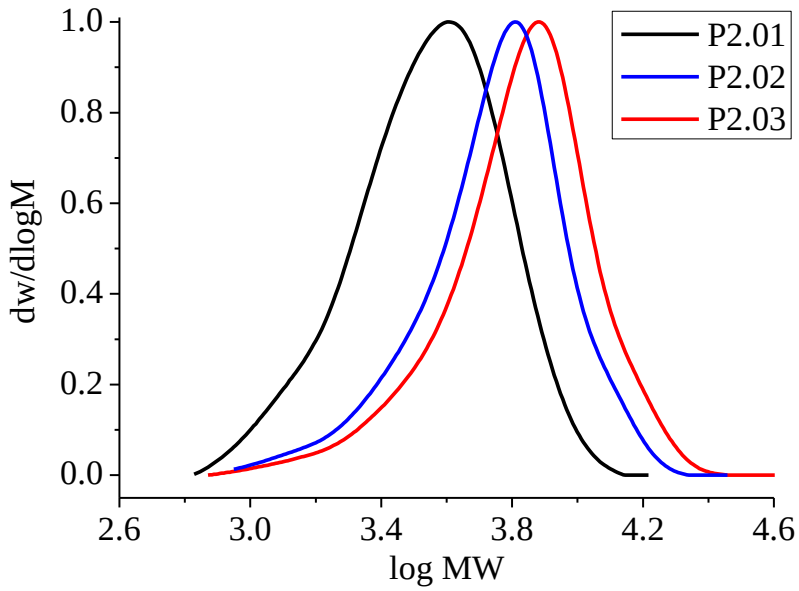

Figure 2.01. GPC traces of HO-PDMAEMA samples P2.01-P2.03.

Aliphatic alcohols and water have been previously employed in the ATRP/SET-LRP of DMAEMA and shown to be highly effective.[28,29] Methanol was substituted in place of DMSO and all other conditions remained the same from P2.02. As methanol is less polar than DMSO it may lead to a reduction in the rate of propagation which in turn could lead to greater control. As methanol is more volatile than DMSO it is expected to be easier to remove during purification.

Figure 2.02 shows the pseudo first-order kinetic plot obtained for SET-LRP of DMAEMA in methanol, an induction period is observed during the first 60 minutes of polymerisation which proceeds into a linear relationship between monomer conversion and time. Final conversion was lower at 61% compared to the analogous reaction in DMSO that had a final DMAEMA conversion of 78% after 4 hours. This was an expected result because of the decreased polarity of the reaction medium.

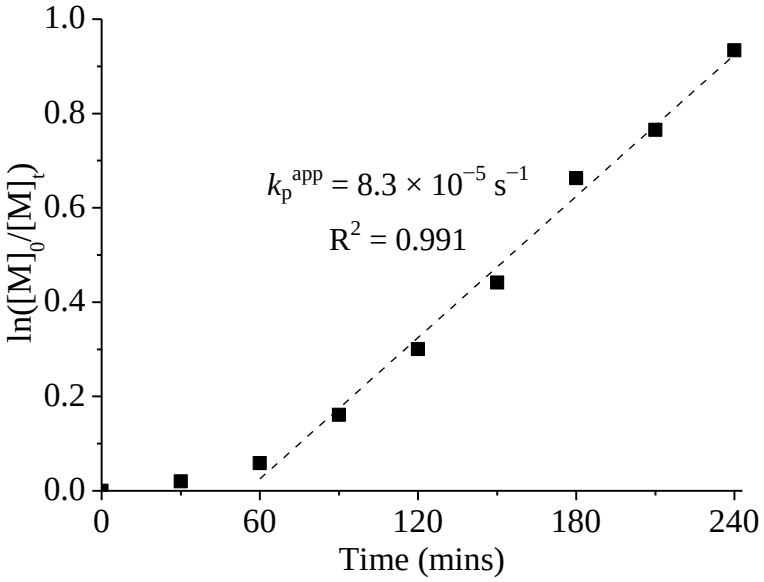

Figure 2.02. Semi-logarithmic kinetic plot for the SET-LRP of DMAEMA in methanol at 25 °C.

Molecular weight increases non-linearly with conversion (Figure 2.03). PDMAEMA M_n increases faster in the early stages of the polymerisation which is not predicted as conversions are still very low as a result of the induction period observed in Figure 2.02. As the polymerisation proceeds M_n increases slower and is a better fit to the theoretical M_n. Polymer dispersity increases throughout the polymerisation to ~1.5.

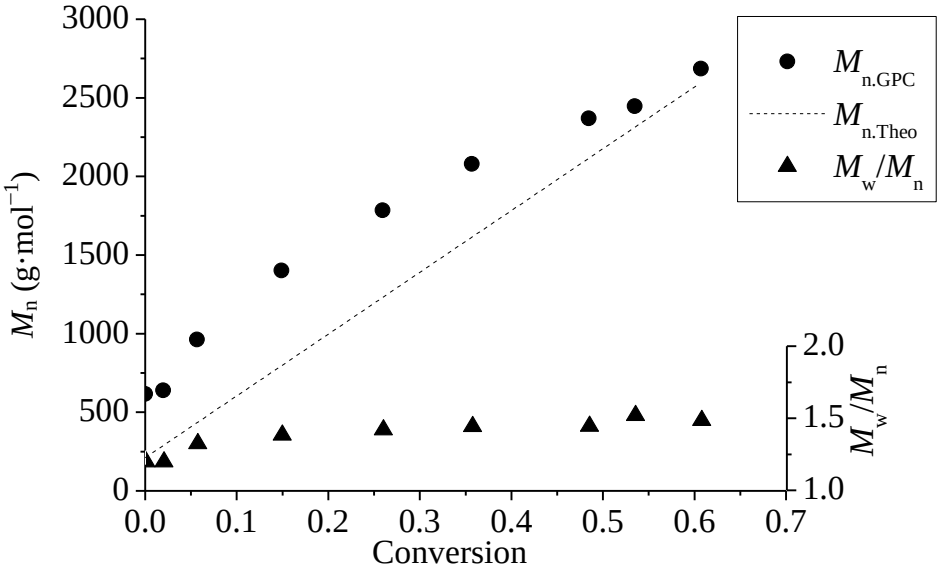

Figure 2.03. Evolution of M_n and dispersity versus DMAEMA conversion for SET-LRP of DMAEMA in methanol at 25 °C.

Evolution of HO-PDMAEMA M_n can also be shown by the GPC traces of individual time points shifting towards higher molecular weight (Figure 2.04). These GPC traces show tailing towards lower molecular weight that persists throughout the entirety of the polymerisation. Tailing potentially indicates that non-reversible termination is occurring or perhaps the PDMAEMA is interacting with the GPC column by adsorbing to the packing material and as such increasing the retention time of PDMAEMA. Figure 2.02 showed a linear relationship between DMAEMA conversion and reaction time which indicates no or little termination was occurring. 2% TEA added to the THF GPC eluent suppresses interactions between PDMAEMA and the GPC column packing material but perhaps a larger concentration is required to fully suppress interactions between PDMAEMA and GPC columns. However, it was not possible to increase or decrease the TEA concentration in the GPC eluent to test this hypothesis. Furthermore, Figure 2.04 shows all GPC traces contain a low molecular weight impurity that increases the measured polymer dispersity.

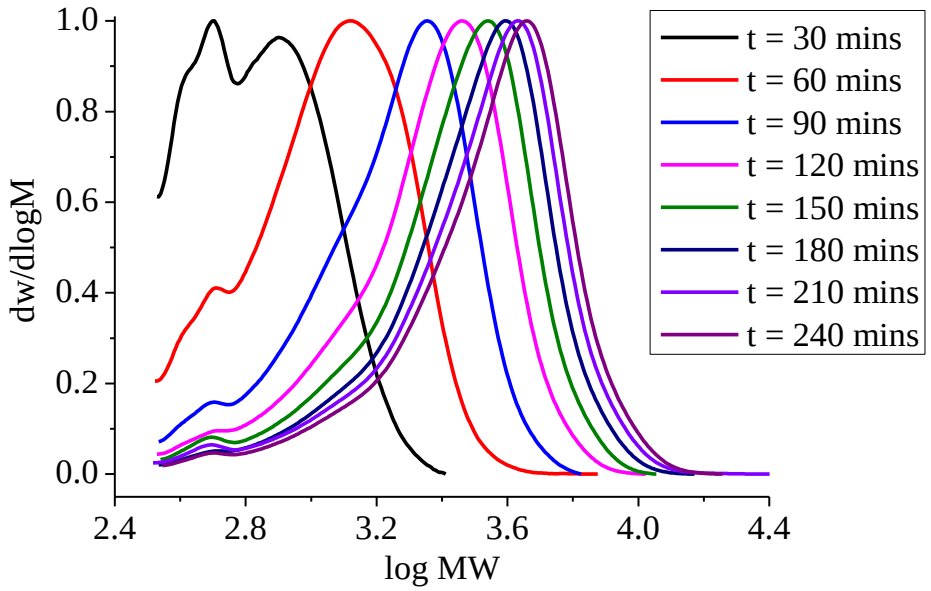

Figure 2.04. Evolution of GPC traces of HO-PDMAEMA (P2.04) throughout time.

SET-LRP of DMAEMA in methanol attained slightly lower conversion and had higher polymer dispersity than the analogous reaction performed in DMSO, however it was now possible to purify the PDMAEMA by precipitation. Final GPC characterisation of P2.04 is shown in Table 2.02, an increase in M_n and decrease in dispersity was measured as the low molecular weight impurity observed during polymerisation was removed by precipitation. Using methanol as a polymerisation solvent allowed for effective isolation of HO-PDMAEMA, therefore methanol was also used as solvent for the synthesis of PDMAEMA without hydroxyl functionality. Unfunctionalised PDMAEMA was synthesised by repeating the same procedure used for P2.04 but using EBiB as an initiator in place of HEBiB (Scheme 2.02).

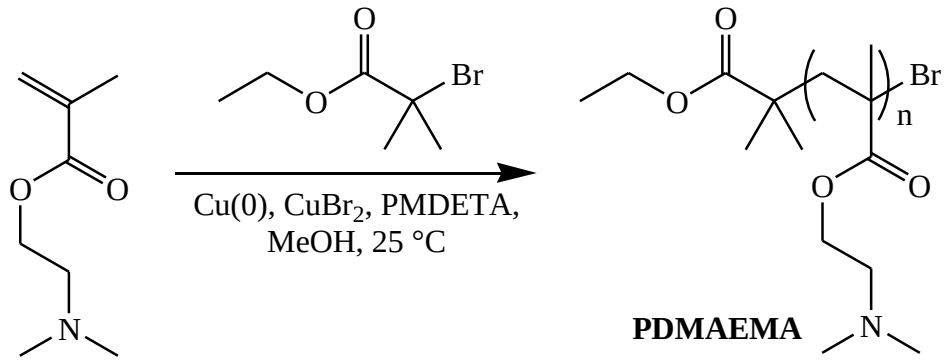

Scheme 2.02. SET-LRP of DMAEMA initiated by EBiB and mediated by Cu(0), $CuBr_2$, PMDETA in methanol at 25 °C.

PDMAEMA (P2.05) synthesised using EBiB as initiator proceeded to higher DMAEMA conversion, had a narrower dispersity (1.15) and higher M_n measured by GPC as predicated by the increased monomer conversion (Table 2.02). ^{1}H-NMR spectroscopy was utilised to confirm that purified PDMAMEA had been obtained. The ^{1}H-NMR spectrum of precipitated PDMAEMA (P2.05) showed no residual solvent or DMAEMA peaks (Figure 2.05). As effective purification of PDMAEMA samples was the primary reason for using methanol as a polymerisation solvent in place of DMSO, methanol was utilised for all remaining SET-LRP of DMAEMA in this chapter.

Table 2.02. GPC characterisation and DMAEMA conversion for the SET-LRP of DMAEMA initiated by HEBiB/EBiB and mediated by Cu(0), $Cu(II)Br_2$, PMDETA in methanol at 25 °C.

Sample	DMAEMA Conversion$^{\alpha}$ (%)	$M_{n.Theo}{}^{\beta}$ ($g \cdot mol^{-1}$)	$M_{n.GPC}{}^{\gamma}$ ($g \cdot mol^{-1}$)	$Đ^{\gamma}$
P2.04$^{\delta}$	61	2600	3600	1.34
P2.05$^{\varepsilon}$	81	3400	4100	1.15

$^{\alpha}$Calculated from ^{1}H-NMR spectroscopy. $^{\beta}$Calculated from Equation 1. $^{\gamma}$THF + 2% TEA eluent, calibrated with PMMA standards.

$^{\delta}$[M]:[I]:[L]:[$Cu(II)Br_2$] = [DMAEMA]:[HEBiB]:[PMDETA]:[$Cu(II)Br_2$] = [25]:[1]:[0.18]:[0.05].

$^{\varepsilon}$[M]:[I]:[L]:[$Cu(II)Br_2$] = [DMAEMA]:[EBiB]:[PMDETA]:[$Cu(II)Br_2$] = [25]:[1]:[0.18]:[0.05].

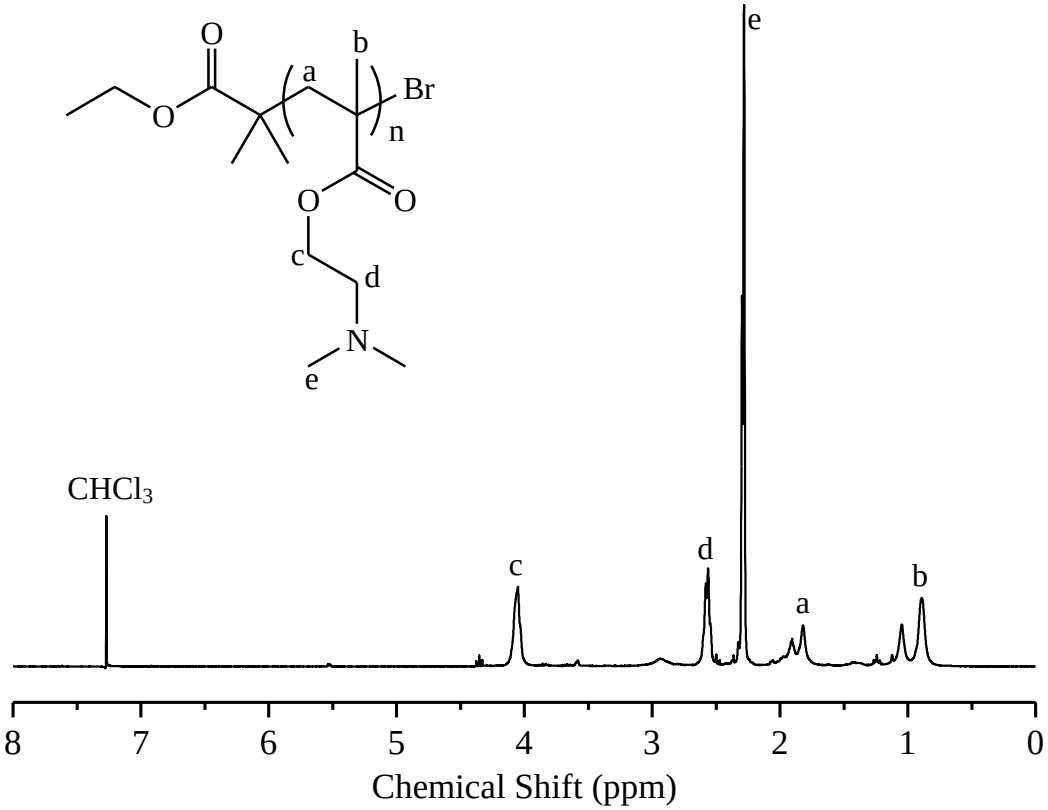

Figure 2.05. ^{1}H-NMR spectrum ($CDCl_3$, 400 MHz, 298 K) of purified PDMAEMA (P2.05).

Both HO-PDMAEMA (P2.04) and unfunctionalised PDMAEMA (P2.05) were synthesised to be reactively coupled with PIBSA to furnish PIB-*b*-PDMAEMA block copolymers. Section 2.4 will discuss the coupling of functional PDMAEMA and PIBSA in greater depth as well as the eventual system devised.

2.3. Synthesis of PIB-*b*-PDMAEMA copolymers using a PIB macroinitiator

SET-LRP of DMAEMA was performed with a PIB macroinitiator, in place of small molecular initiators, to synthesise PIB-*b*-DMAEMA block copolymers.

2.3.1. Synthesis of PIB macroinitiator (PIBBiB)

Transformation of PIB terminated by an *exo*-olefin (PIB_{exo}) to hydroxyl-polyisobutylene (PIBH) has been reported in the literature and is typically achieved by hydroboration and oxidation of the terminal olefin.[6,7,10,34] PIBH has been subsequently esterified with BiBB to yield an ATRP macroinitiator that was capable of initiating methacrylate monomers to yield the corresponding block copolymers.[6,7] Therefore, this methodology was reproduced using a commercial source of PIB that is primarily *exo*-olefin (PIB_{exo}) terminated, commonly known as "highly reactive" PIB.[35] It is worthy of note that a portion of the "highly reactive" PIB is *endo*-olefin (PIB_{endo}) terminated. Both of these terminal olefins undergo hydroboration and oxidation to the respective primary and secondary alcohols (Scheme 2.03).

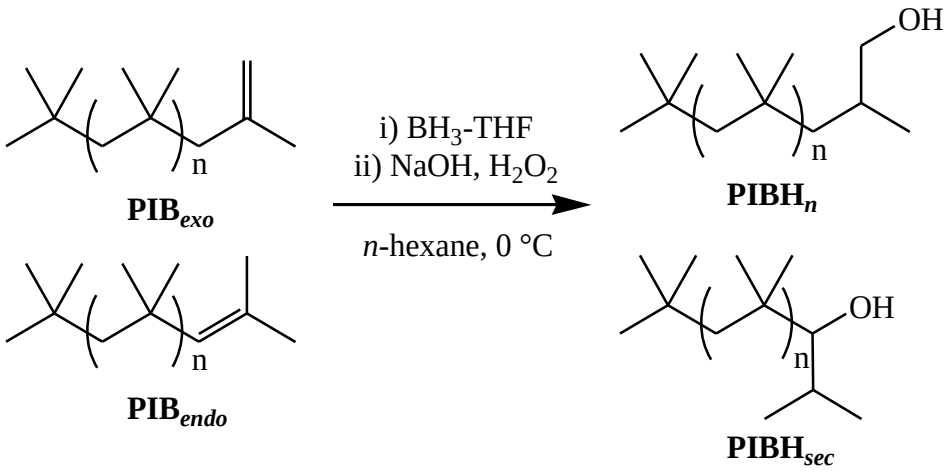

Scheme 2.03. Synthesis of PIBH via hydroboration and oxidation of PIB_{exo} and PIB_{endo}.

Hydroboration and oxidation of PIB converted 90% of the *exo*-olefin to the primary alcohol and 100% of the *endo*-olefin to the secondary alcohol. Conversion was calculated by relative integrations of the olefin protons to repeat unit protons H^b before and after hydroboration/oxidation (Figure 2.06). Therefore, relative concentrations of $PIBH_n$ to $PIBH_{sec}$ is 9:1.

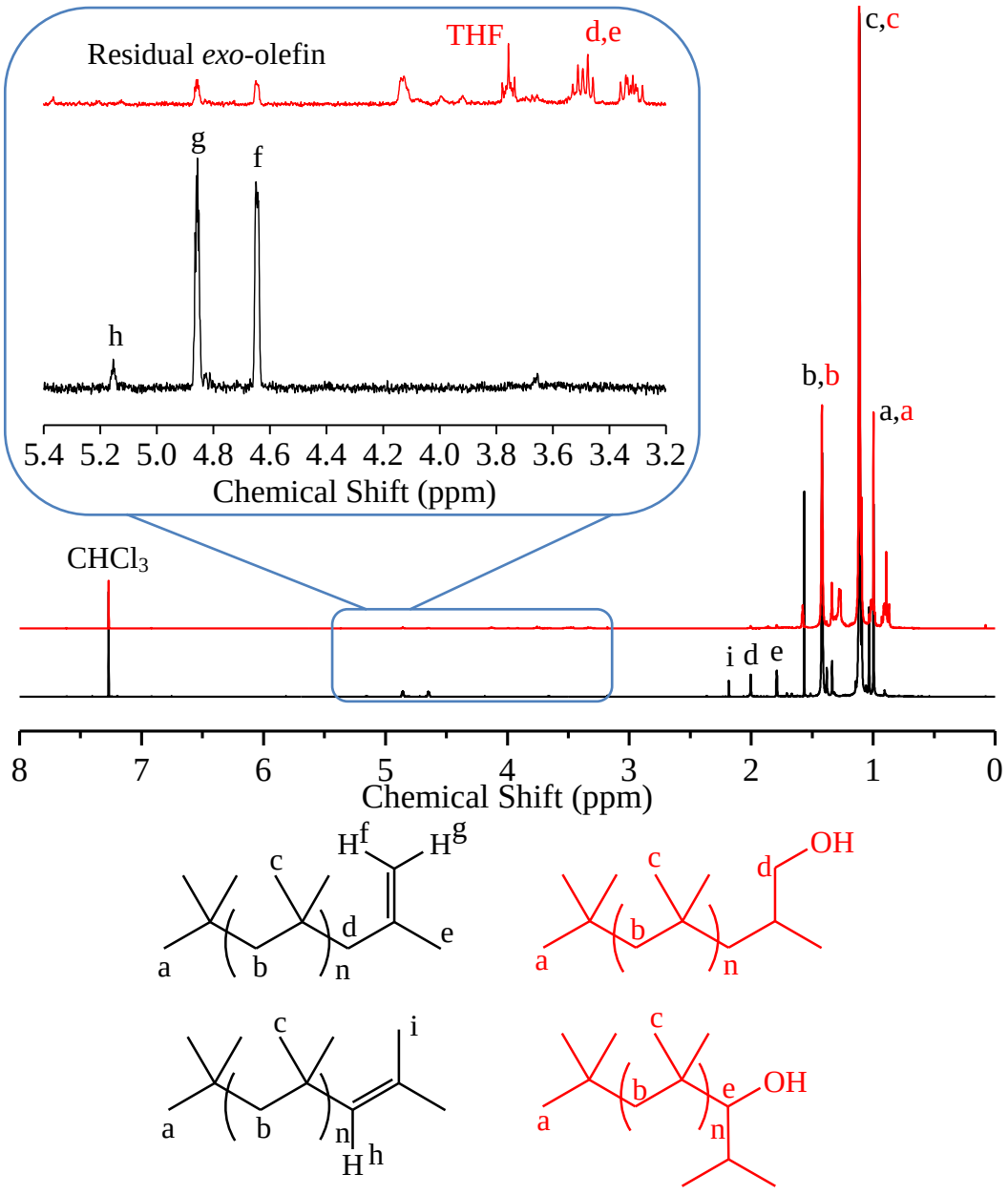

Figure 2.06. ^{1}H-NMR spectrum ($CDCl_3$, 300 MHz, 298 K) of PIB_{exo} and PIB_{endo} (black) and $PIBH_n$ and $PIBH_{sec}$ (red).

This reduction in olefinic protons and the appearance of new resonances between 3.2-3.6 ppm ($H^{d/e}$) corresponding to the methylene protons adjacent to the hydroxyl agree well with the adapted literature procedure (Figure 2.06).[34]

Following the hydroboration of PIB to PIBH, PIBH was esterified to an ATRP/SET-LRP macroinitiator, polyisobutylene bromoisobutyrate (PIBBiB), by reaction with BiBB and TEA as adapted from literature (Scheme 2.04).[6,7]

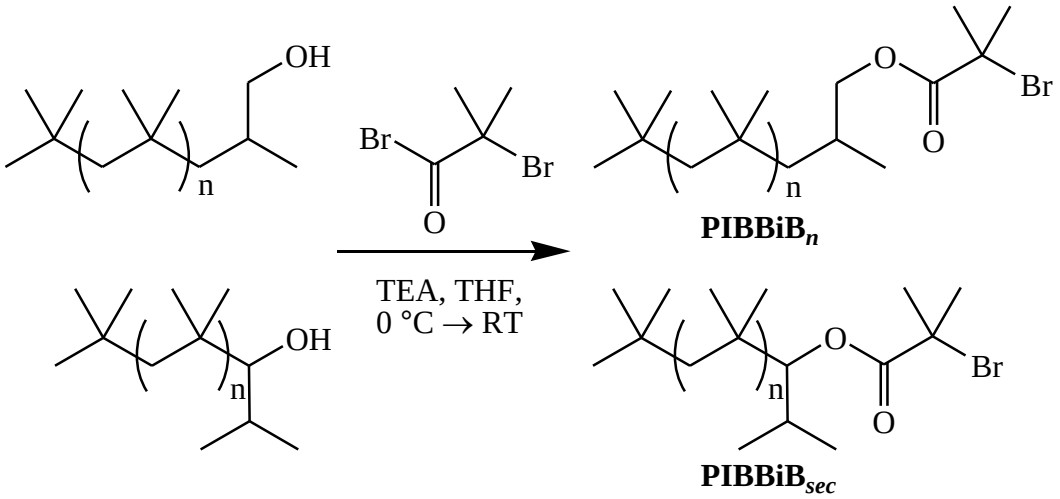

Scheme 2.04. Synthesis of PIBBiB by esterification of PIBH with BiBB.

^{1}H-NMR spectroscopy supports the structure of PIBBiB by appearance of a singlet at 1.97 ppm corresponding to the two methyl groups of the new initiating group (Figure 2.07). Integration of the methyl protons relative to repeat unit protons H^b indicate that 60% of the PIB chains are functionalised with the desired alkyl bromide initiating group. Furthermore, methylene protons adjacent to the hydroxyl of PIBH are shown to diminish after esterification (Figure 2.07). H^x is suspected to be an impurity caused by the hydrolysis of BiBB to the corresponding acid. A peak at similar chemical shift appears on the literature example that was reproduced, however it was not assigned in that instance.[6,7] Final yield of isolated PIBBiB was 78% and GPC showed a slight increase in molecular weight as expected and a reduction in the polymer dispersity, M_n: 1300 g·mol^{-1} and $Đ$: 1.44.

As PIBH was a mixture of secondary and primary alcohols there will also be a mixture of PIBBiB structures (Scheme 2.04) These two structures are expected to initiate and polymerise at a similar rate, therefore future structures of PIBBiB will simply be drawn as the more abundant PIBBiB$_n$ for schematic simplification.

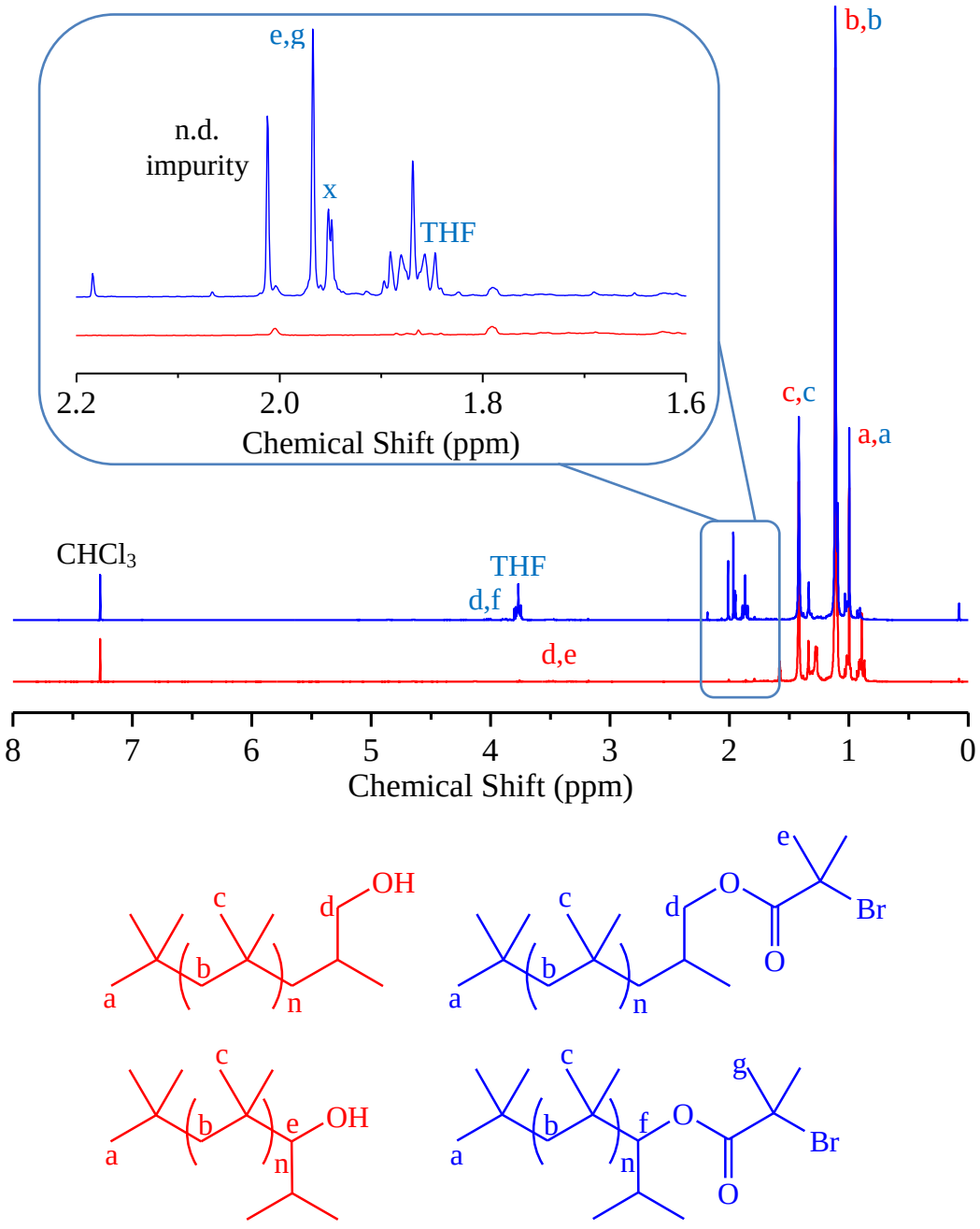

Figure 2.07. ^{1}H-NMR spectrum ($CDCl_3$, 300 MHz, 298 K) of PIBH$_n$ and PIBH$_{sec}$ (red) and PIBBiB$_n$ and PIBBiB$_{sec}$ (blue).

FT-IR spectra of PIB, PIBH and PIBBiB also qualitatively demonstrate the successive reactions by observing the disappearance and appearance of relevant

functional groups after hydroboration and esterification reactions (Figure 2.08). PIBH FT-IR spectrum no longer shows a signal for the C=CH_2 bond at 891 cm^{-1} and two new signals appear at 1072 cm^{-1} and 3404 cm^{-1} corresponding to the C-O and O-H bonds, respectively. PIBBiB FT-IR spectrum shows the appearance of peaks corresponding to the new ester group; 1738 cm^{-1} (C=O), 1273 cm^{-1} (C-O), 1165 cm^{-1} (C-O) and 1113 cm^{-1} (C-O).

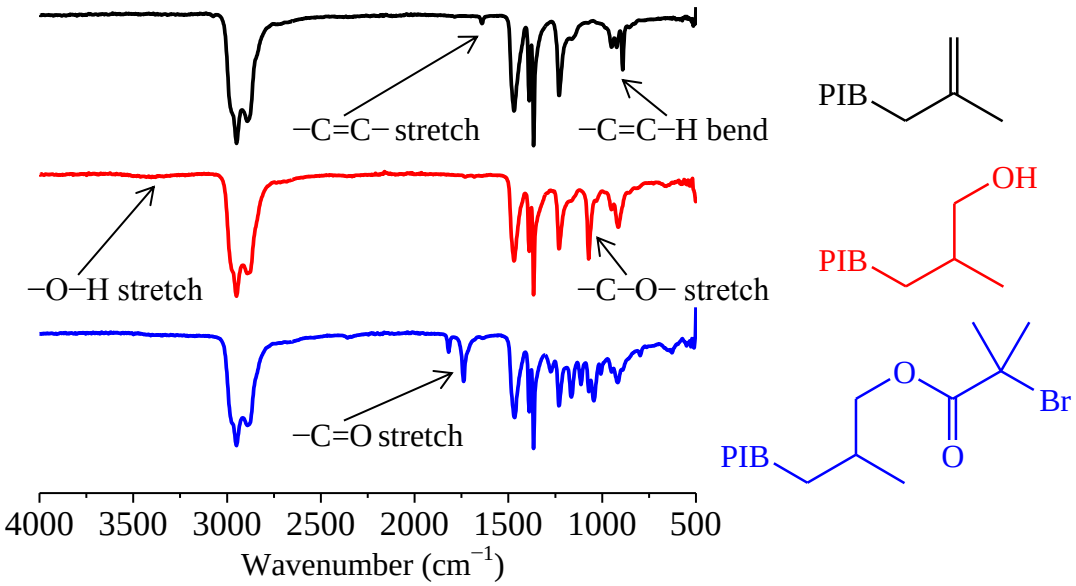

Figure 2.08. FT-IR spectra of PIB (black), PIBH (red) and PIBBiB (blue).

2.3.2. SET-LRP of DMAEMA using PIBBiB as initiator

Previous SET-LRP conditions of DMAEMA could not be reproduced when performing the polymerisation with PIBBiB as initiator; this is because PIBBiB was insoluble in the polymerisation medium, methanol. However, SET-LRP of less polar monomers has been reported, this is achieved by performing the polymerisation in a medium that is a mixture of polar and non-polar solvents[36-39] or a mixture of non-polar solvents and polar additives such as phenol.[39,40] Therefore, SET-LRP of a polar monomer (DMAEMA) using a hydrophobic macroinitiator (PIBBiB) is theoretically possible by using a mixed solvent system of methanol and toluene (1:1 volume

ratio). This solvent mixture would be suitably polar to disproportionate the Cu(I)Br to Cu(0) and Cu(II)Br_2 whilst fully solubilising PIBBiB. All other reaction conditions remained constant from previous SET-LRPs of DMAEMA (Scheme 2.05).

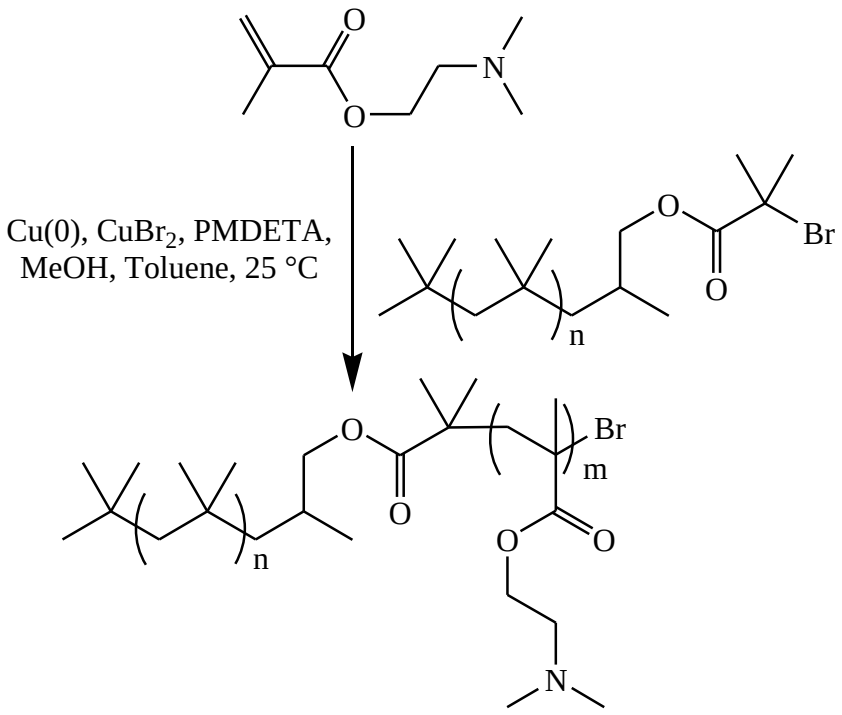

Scheme 2.05. SET-LRP of DMAEMA initiated by PIBBiB and mediated by Cu(0), $CuBr_2$, PMDETA in methanol and toluene at 25 °C.

Chain extension of PIBBiB with DMAEMA via SET-LRP to synthesise PIB-*b*-DMAEMA block copolymers was attempted at three different monomer to initiator ratios; 25:1, 15:1 and 5:1, with an aim to synthesise three different molecular weight block copolymers varying only in DP of the PDMAEMA block. DMAEMA conversion was consistent with previous SET-LRPs of DMAEMA (≥79%) for each chain extension and crude M_n measurements by GPC have increased as expected with increasing monomer to initiator ratio (Table 2.03).

Table 2.03. GPC characterisation and DMAEMA conversion for the SET-LRP of DMAEMA initiated by PIBBiB and mediated by Cu(0), Cu(II)Br_2, PMDETA in methanol and toluene at 25 °C.

Sample	DMAEMA Conversion$^{\alpha}$ (%)	$M_{n.Theo}{}^{\beta}$ (g·mol^{-1})	$M_{n.GPC}{}^{\gamma}$ (g·mol^{-1})	$Đ^{\gamma}$	$M_{n.GPC}{}^{\gamma}$ (g·mol^{-1})	$Đ^{\gamma}$
			Crude		Precipitated	
P2.06$^{\delta}$	80	1940	1600	2.15	3500	1.81
P2.07$^{\varepsilon}$	83	3260	2500	3.50	7900	1.80
P2.08$^{\zeta}$	79	4400	2900	3.43	8900	1.77

$^{\alpha}$Calculated from ^{1}H-NMR spectroscopy. $^{\beta}$Calculated from Equation 1. $^{\gamma}$THF + 2% TEA eluent, calibrated with PMMA standards.

$^{\delta}$[M]:[I]:[L]:[Cu(II)Br_2] = [DMAEMA]:[PIBBiB]:[PMDETA]:[Cu(II)Br_2] = [5]:[1]:[0.18]:[0.05]

$^{\varepsilon}$[M]:[I]:[L]:[Cu(II)Br_2] = [DMAEMA]:[PIBBiB]:[PMDETA]:[Cu(II)Br_2] = [15]:[1]:[0.18]:[0.05]

$^{\zeta}$[M]:[I]:[L]:[Cu(II)Br_2] = [DMAEMA]:[PIBBiB]:[PMDETA]:[Cu(II)Br_2] = [25]:[1]:[0.18]:[0.05]

However, GPC traces of crude PIB-*b*-PDMAEMA copolymers show a very ill defined, multi modal distribution with a significant low molecular weight shoulder that overlay with the distribution of PIBBiB (Figure 2.09-2.11). This low molecular weight shoulder could be due to the presence of many PIB species differing in *ω*-end group. As detailed in Section 2.3.1 and 1.4.3.1, olefin terminated PIB contains a mixture of terminal olefin *ω*-end groups, *exo*-olefin is the most prevalent, then *endo*-olefin, followed by a tetrasubstituted olefin. Tetrasubstituted olefins are very unreactive and as such would not be functionalised by the hydroboration/oxidation to give PIBH. This could help explain a significant portion of the low molecular weight impurity as well as subsequent functionalisations (hydroboration/oxidation and esterification of PIB) which did not proceed to full conversion. Furthermore, PIBBiB which fails to reinitiate would also contribute to the low molecular weight impurity. These possible PIB species could lead to the significant low molecular weight impurity seen in the crude GPC measurements of PIBBiB chain extension with DMAEMA.

Fortunately the PIB-*b*-PDMAEMA copolymers are insoluble in *n*-hexane and could be precipitated to remove the soluble low molecular weight PIB impurity which is soluble in *n*-hexane. GPC measurements of precipitated PIB-*b*-PDMAEMA copolymers show a dramatic increase in M_n as well as a lowering of the polymer dispersity (Table 2.03). Furthermore, GPC traces of precipitated PIB-*b*-PDMAEMA are now more symmetrical and mono-modal with less low molecular weight polymer impurities (Figure 2.09-2.11).

Despite successful removal of the PIB impurity by precipitation to yield purified PIB-*b*-DMAEMA copolymers, measured M_n was far greater than that of the theoretical M_n calculated (Table 2.03). This is caused by the absence of high end group fidelity of PIBBiB and results in a significantly different monomer to initiator ratio to what was targeted by the initial monomer feed ratio, thus synthesising a desired DP of the PDMAEMA block is very challenging via this synthetic pathway and as such a new pathway to PIB-*b*-DMAEMA copolymers was investigated.

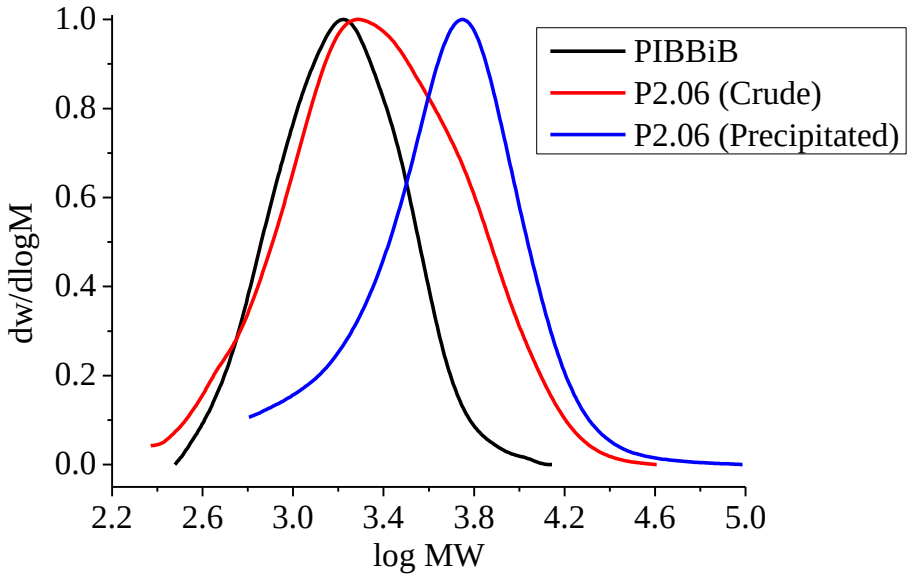

Figure 2.09. GPC traces of PIBBiB and PIB-*b*-PDMAEMA (P2.06) before and after precipitation.

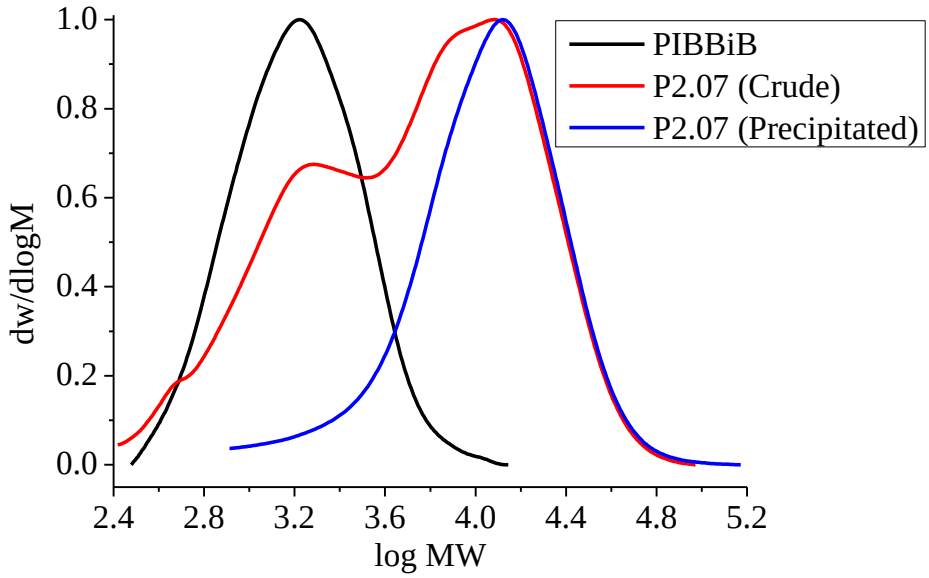

Figure 2.10. GPC traces of PIBBiB and PIB-*b*-PDMAEMA (P2.07) before and after precipitation.

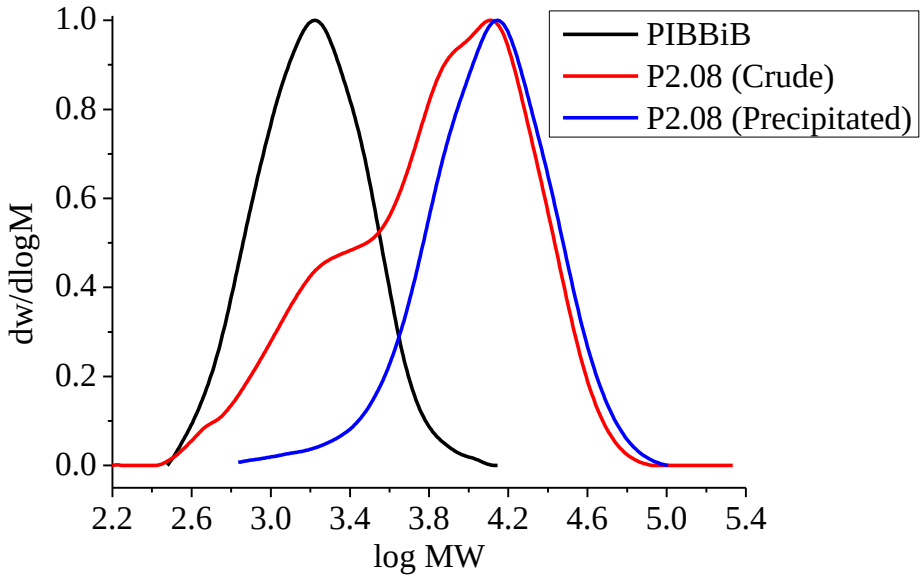

Figure 2.11. GPC traces of PIBBiB and PIB-*b*-PDMAEMA (P2.08) before and after precipitation.

2.4. Synthesis of PIB-*b*-PDMAEMA copolymers by macromolecular coupling of PIBSA and H_2N-PDMAEMA

Cyclic anhydrides can be quickly and efficiently ring-opened by primary amines. Firstly, the amine ring opens the cyclic anhydride to form an amide bond and a carboxylic acid; given sufficiently high temperature (~180 °C), long enough reaction

times and continual removal of water, the carboxylic acid and amide bond can cyclise with loss of water to form a cyclic imide. Reactions of cyclic anhydrides and secondary amines proceed only to the amide bond and a free carboxylic acid. One potential application of cyclic anhydride-primary amine reactions is the possibility to couple two homopolymers, one functionalised with a primary amine and the other a cyclic anhydride. Macosko and co-workers synthesised a range of polystyrene (PSy) that bare a single terminal functional group, including aliphatic primary amine, aromatic primary amine, cyclic anhydride, hydroxyl, carboxylic acid, epoxy and oxazoline.[41] After heating reactive pairs of these functionalities at 180 °C for 2 minutes, they found aliphatic primary amine-cyclic anhydride to be the most efficient as conversion was >99%, monitored by GPC.[41] This is compared to aromatic primary amine-cyclic anhydride (12.5% conversion) and carboxylic acid-epoxy (9% conversion), monitored by GPC.[41] This coupling approach will be utilised for the synthesis of PIB-*b*-PDMAEMA copolymers by synthesising an aliphatic primary amine functional PDMAEMA (H_2N-PDMAEMA) to couple with PIBSA.

2.4.1. Initial attempts at coupling PIBSA with functional PDMAEMA

Coupling of HO-PDMAEMA (P2.04) and PIBSA, provided by Innospec, to synthesise PIB-*b*-PDMAEMA copolymers was attempted first. This was performed by heating the HO-PDMAEMA with PIBSA to open the succinic anhydride thus forming an ester bond and furnishing the desired block copolymer (Scheme 2.06). Macosko and co-workers performed coupling reactions at 180 °C for 2 minutes, however the thermal stability of HO-PDMAEMA and PIBSA were unknown so coupling temperature was decreased to 90 °C and reaction duration was increased (24 hours) to allow for the decreased temperature.

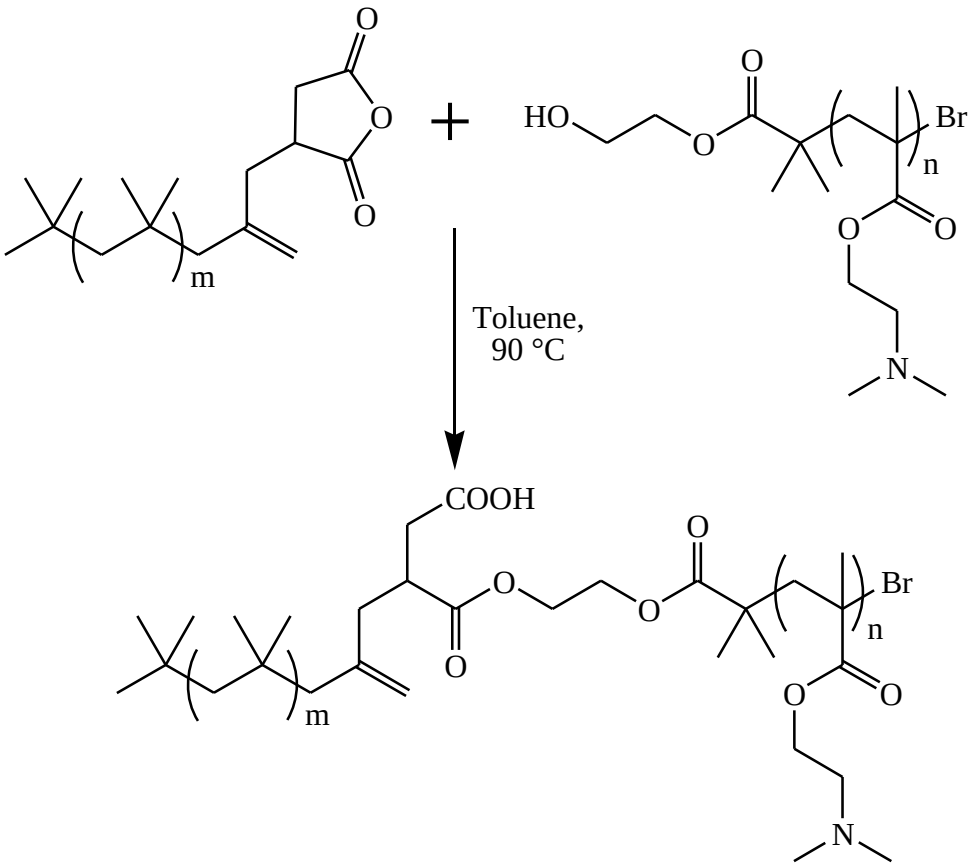

Scheme 2.06. Attempted synthesis of PIB-*b*-PDMAEMA via macromolecular coupling of HO-PDMAEMA and PIBSA.

However, GPC measurements suggested that HO-PDMAEMA (P2.04) did not shift to higher molecular weight after maintaining 90 °C for 24 hours. This agrees well with the result reported by Macosko who obtained 0% conversion after coupling a primary alcohol and cyclic anhydride at 180 °C.[41] As stated earlier primary amine-cyclic anhydride was shown to be the most efficient coupling reaction examined by Macosko, therefore synthesis of H_2N-PDMAEMA was required to couple with PIBSA.

The first synthetic pathway attempted to synthesise H_2N-PDMAEMA was to substitute the terminal alkyl bromide with an azide functionality after reaction with sodium azide (Scheme 2.07). The terminal azide would then be subsequently reduced to a primary amine. HO-PDMAEMA (P2.04) was not utilised for substitution with sodium azide as hydroxyl groups also have the potential to be

substituted by azide as alkyl bromides do, although the reaction is significantly slower it may result in doubly azide functionalised PDMAEMA.[42] Therefore, P2.05 was selected instead as it was synthesised with an unfunctionalised initiator.

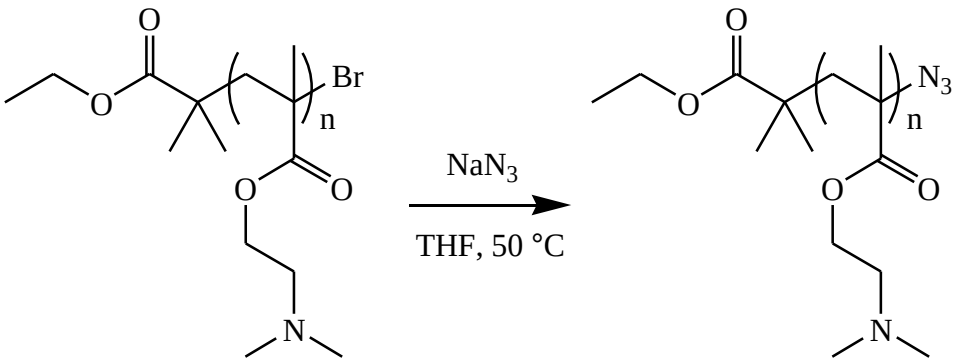

Scheme 2.07. Attempted synthesis of N_3-PDMAEMA via substitution of alkyl bromide with azide.

Despite prolonged reaction times (>48 hours) and increased reaction temperature (80 °C), no azide functionality could be observed by FT-IR spectroscopy, peak is expected to appear at ~2100 cm^{-1}, on the precipitated PDMAEMA. This indicates that either the chosen synthetic strategy is not suitable for functionalising PDMAEMA or that the PDMAEMA (P2.04) has low end group fidelity and as such cannot be functionalised to an observable degree. Therefore this synthetic strategy for synthesising H_2N-PDMAEMA, by modification of the *ω*–terminus, was abandoned and an alternative strategy to synthesise H_2N-PDMAEMA was investigated.

2.4.2. Synthesis of azide functional SET-LRP initiator

As the *ω*-terminal alkyl bromide of PDMAEMA could not be converted to an azide group, functionalising the *α*-terminus may be a more suitable route of incorporating azide functionality. This has been reported in the literature by use of an azide functional initiator in the ATRP of DMAEMA.[43,44] Therefore, an azide functionalised tertiary alkyl bromide ATRP initiator, 2-azidoethyl-2′-bromoisobutyrate (AEBiB), was reproduced from the literature (Scheme 2.08).[45,46]

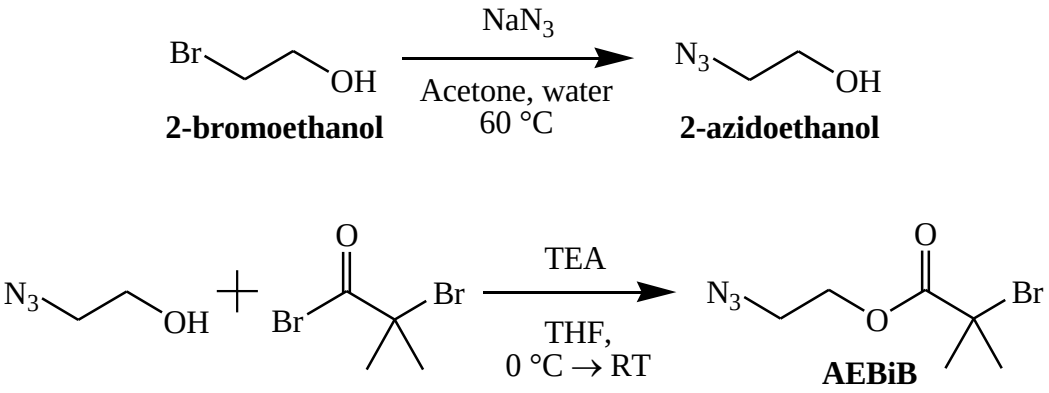

Scheme 2.08. Synthesis of 2-azidoethanol and 2-azidoethyl-2′-bromoisobutyrate (AEBiB).

Transformation of 2-bromoethanol to 2-azidoethanol was confirmed by ^{1}H-NMR spectroscopy (Figure 2.12). Triplets at 3.51 and 3.89 ppm shifted upfield to 3.41 and 3.75 ppm, respectively, after substitution of the alkyl bromide with azide and no residual 2-bromoethanol could be observed on the spectrum.[45]

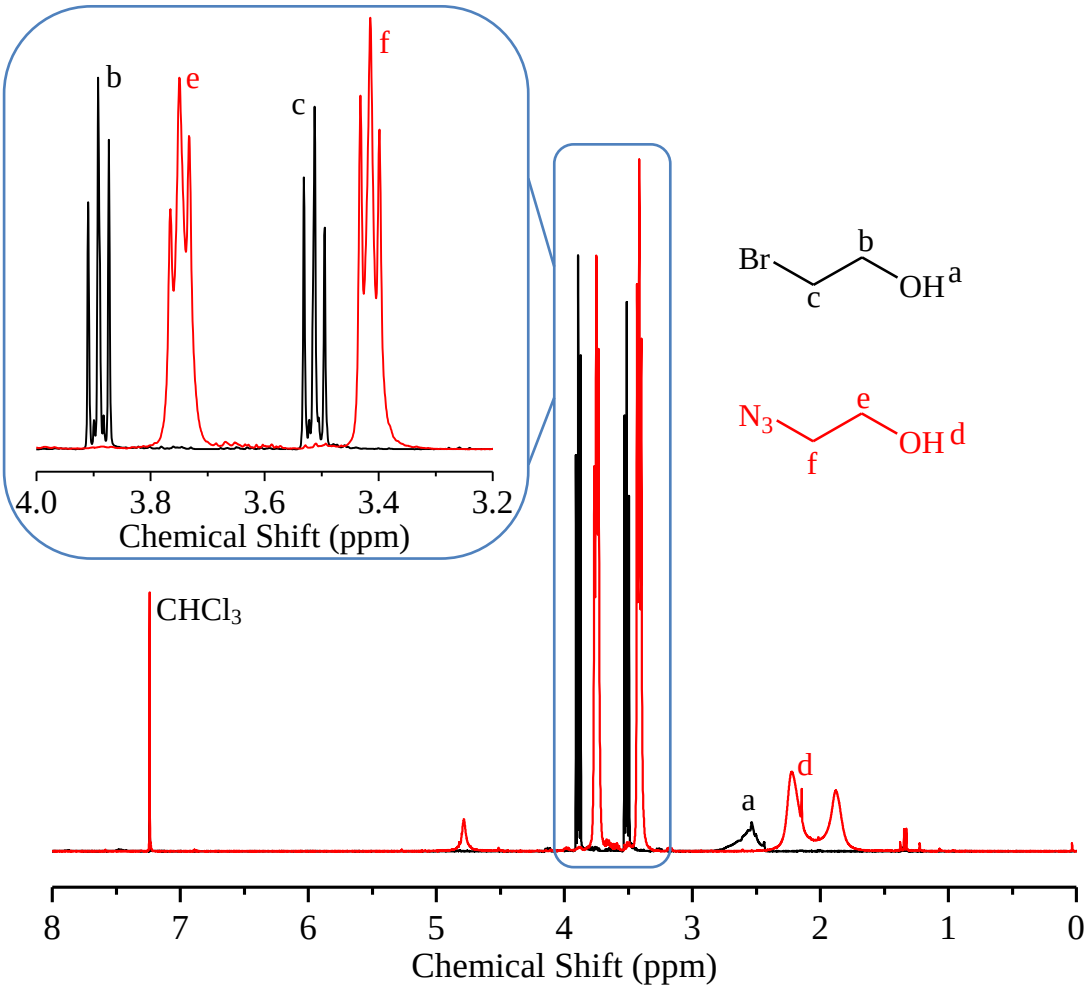

Figure 2.12. ^{1}H-NMR spectra ($CDCl_3$, 300 MHz, 298 K) of 2-bromoethanol (black) and 2-azidoethanol (red).

^{1}H-NMR spectroscopy can be used to confirm the esterification of 2-azidoethanol with BiBB, triplets at 3.41 and 3.75 ppm shifted downfield to 3.53 and 4.35 ppm, respectively, after formation of the ester (Figure 2.13). The chemical shifts and relative integrations match well with expected values from the literature procedure followed.[46] However, the ^{1}H-NMR spectrum of AEBiB also reveals a small amount of unreacted 2-azidoethanol is present in the final product, purity of AEBiB calculated from the ^{1}H-NMR is >95% and as such was deemed suitable for use in the SET-LRP of DMAEMA.

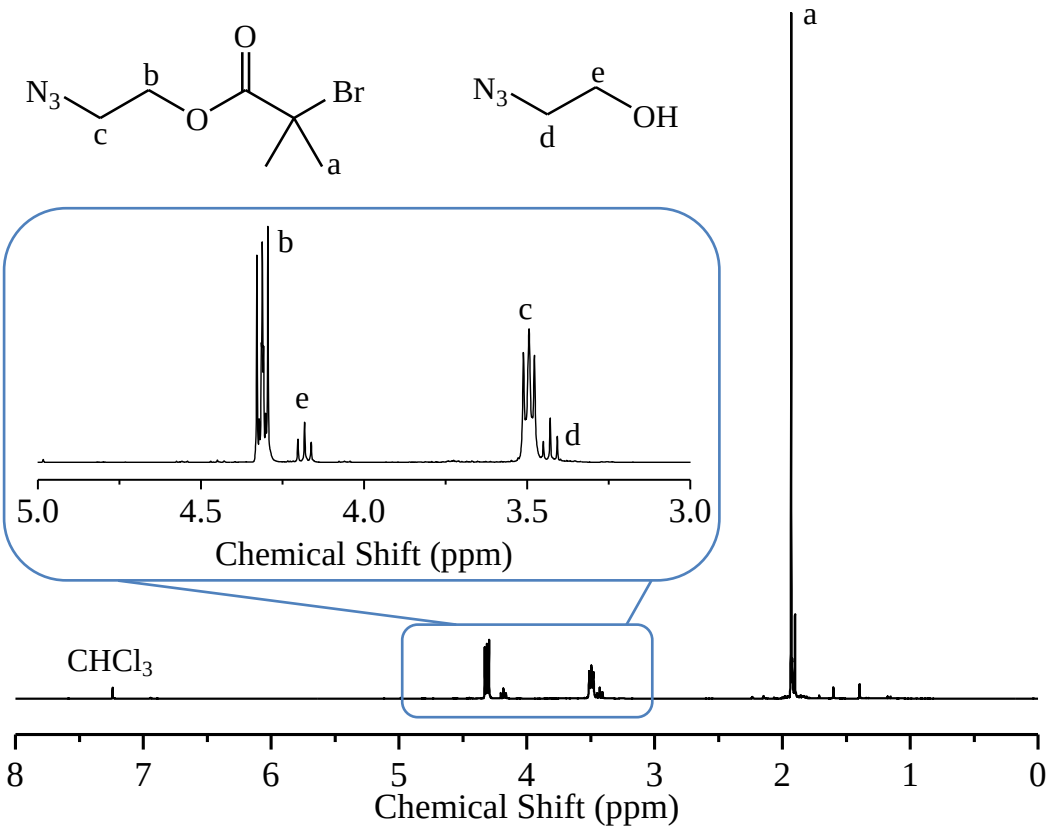

Figure 2.13. ^{1}H-NMR spectrum ($CDCl_3$, 300 MHz, 298 K) of 2-azidoethyl-2′-bromoisobutyrate and residual 2-azidoethanol.

FT-IR spectroscopy supports the substitution of bromine with azide by the appearance of a strong peak at 2094 cm^{-1} (Figure 2.14). Furthermore, following the esterification of 2-azidoethanol with BiBB the broad signal at 3345 cm^{-1} corresponding to the O−H stretch disappears and a new signal at 1734 cm^{-1} appears

that corresponds to the C=O stretch (Figure 2.14). The azide signal at 2094 cm^{-1} will be particularly useful when trying to identify if the PDMAEMA synthesised with this initiator do contain the desired azide functionality.

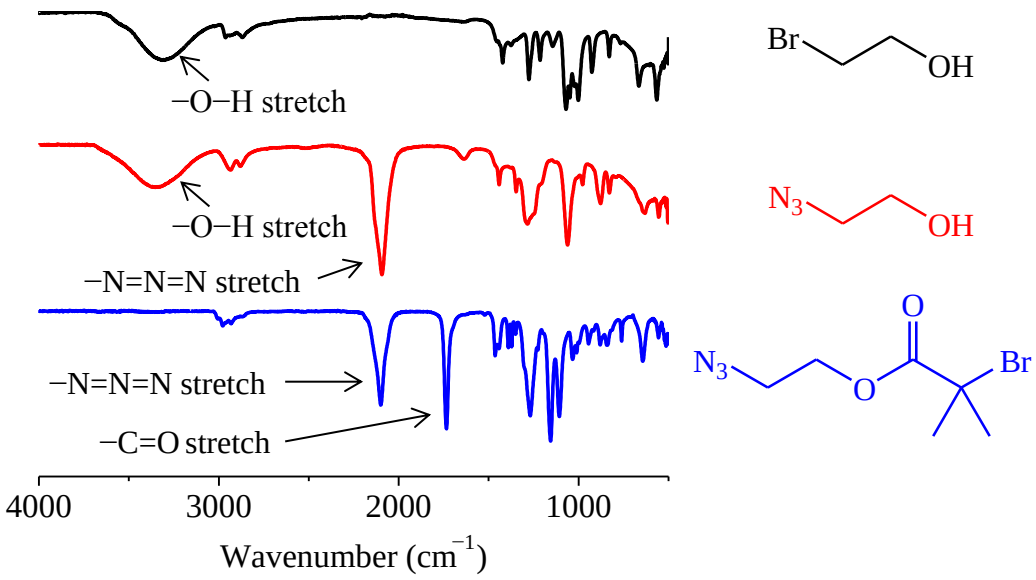

Figure 2.14. FT-IR spectra of 2-bromoethanol (black), 2-azidoethanol (red) and 2-azidoethyl-2′-bromoisobutyrate (blue).

2.4.3. SET-LRP of DMAEMA using AEBiB as initiator

SET-LRP of DMAEMA was performed using previous reaction conditions, substituting AEBiB in place of HEBiB as initiator (Scheme 2.09).

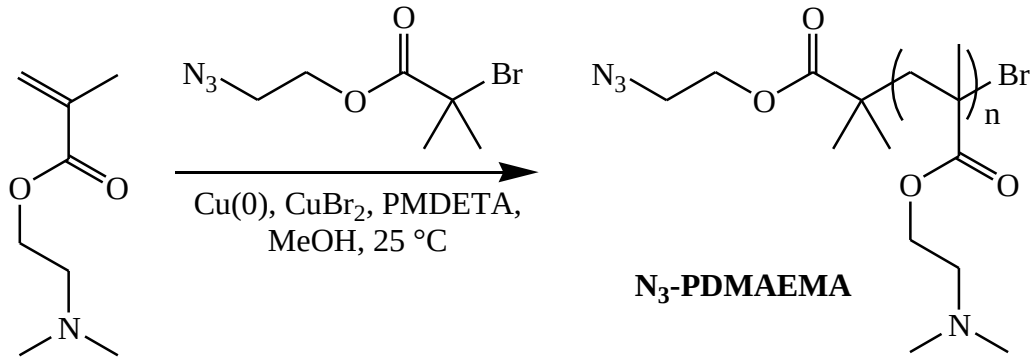

Scheme 2.09. SET-LRP of DMAEMA initiated by AEBiB and mediated by Cu(0), $CuBr_2$, PMDETA in methanol at 25 °C.

DMAEMA was successfully polymerised when using AEBiB as an initiator and mediated by the same Cu(0)/$CuBr_2$/PMDETA catalyst system as before. Three

different molecular weights of N_3-PDMAEMA were synthesised by increasing the monomer to initiator ratio. Measured M_n was greater than the theoretical M_n which is more significant when lower DP of PDMAEMA was targeted. DMAEMA conversion was ≥78% for each polymerisation and narrow polymer dispersity was maintained (Table 2.04). These results are consistent with previous SET-LRP of DMAEMA with small molecular initiators, such as EBiB and HEBiB.

Table 2.04. GPC characterisation and DMAEMA conversion for the SET-LRP of DMAEMA initiated by AEBiB and mediated by Cu(0), Cu(II)Br_2, PMDETA in methanol at 25 °C.

Sample	DMAEMA Conversion$^{\alpha}$ (%)	$M_{n.Theo}{}^{\beta}$ (g·mol^{-1})	$M_{n.GPC}{}^{\gamma}$ (g·mol^{-1})	$M_{p.GPC}{}^{\gamma}$ (g·mol^{-1})	$Đ^{\gamma}$
P2.09$^{\delta}$	78	900	2000	2600	1.21
P2.10$^{\varepsilon}$	82	2200	3400	4600	1.20
P2.11$^{\zeta}$	85	3600	4800	6600	1.26

$^{\alpha}$Calculated from ^{1}H-NMR spectroscopy. $^{\beta}$Calculated from Equation 1. $^{\gamma}$THF + 2% TEA eluent, calibrated with PMMA standards.

$^{\delta}$[M]:[I]:[L]:[Cu(II)Br_2] = [DMAEMA]:[AEBiB]:[PMDETA]:[Cu(II)Br_2] = [5]:[1]:[0.18]:[0.05]

$^{\varepsilon}$[M]:[I]:[L]:[Cu(II)Br_2] = [DMAEMA]:[AEBiB]:[PMDETA]:[Cu(II)Br_2] = [15]:[1]:[0.18]:[0.05]

$^{\zeta}$[M]:[I]:[L]:[Cu(II)Br_2] = [DMAEMA]:[AEBiB]:[PMDETA]:[Cu(II)Br_2] = [25]:[1]:[0.18]:[0.05]

N_3-PDMAEMA distributions were asymmetrical; displaying a tailing towards lower molecular weight which is consistent with previous synthesises of PDMAEMA by SET-LRP. GPC trace of P2.11 also displayed a slight high molecular weight shoulder potentially caused by recombination of propagating radicals (Figure 2.15).

The *α*-terminal azide present on the synthesised N_3-PDMAEMA is essential for the planned coupling reaction with PIBSA, the presence of the azide functionality can be observed at 2105 cm^{-1} by FT-IR spectroscopy (Figure 2.16).

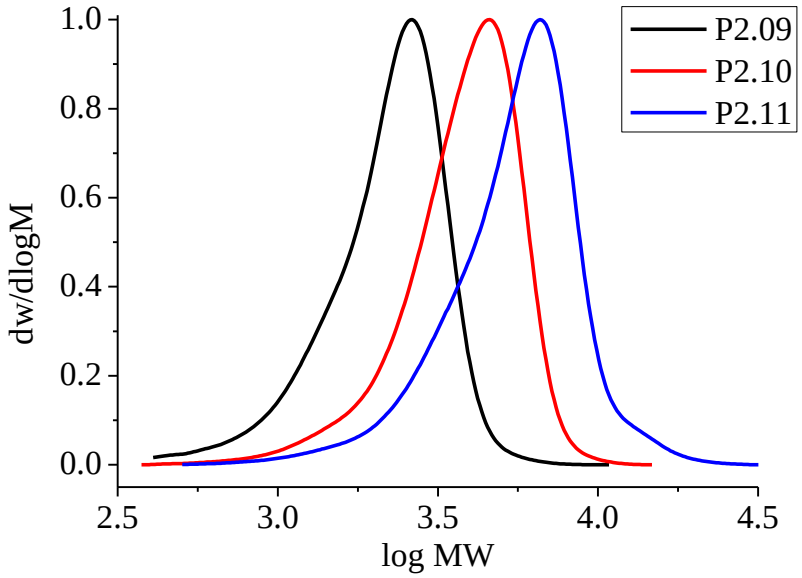

Figure 2.15. GPC traces of N_3-PDMAEMA samples P2.09-P2.11.

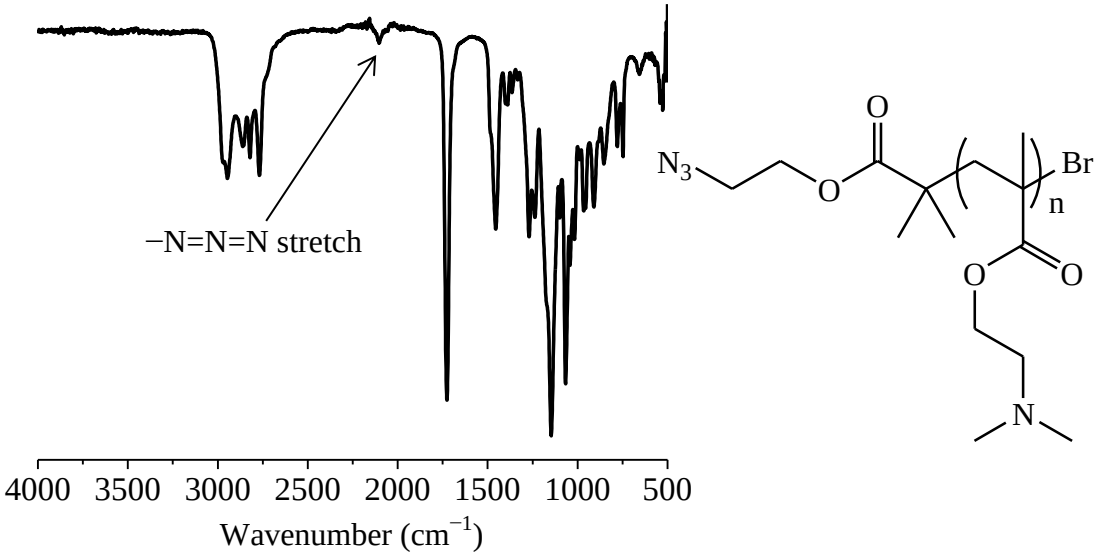

Figure 2.16. FT-IR spectrum of N_3-PDMAEMA sample P2.11.

Moreover, ^{1}H-NMR spectroscopy was utilised to measure the protons immediately adjacent to the azide group at 3.45 ppm on the purified N_3-PDMAEMA (Figure 2.17), this is in good agreement with the chemical shift reported for the same protons on AEBiB, 3.53 ppm. Both Figure 2.16 and 2.17 were of sample P2.11 which has a M_n of 4800 g·mol^{-1}, the highest molecular weight N_3-PDMAEMA sample

synthesised. Therefore, azide signals got stronger and clearer as the molecular weight of PDMAEMA was decreased.

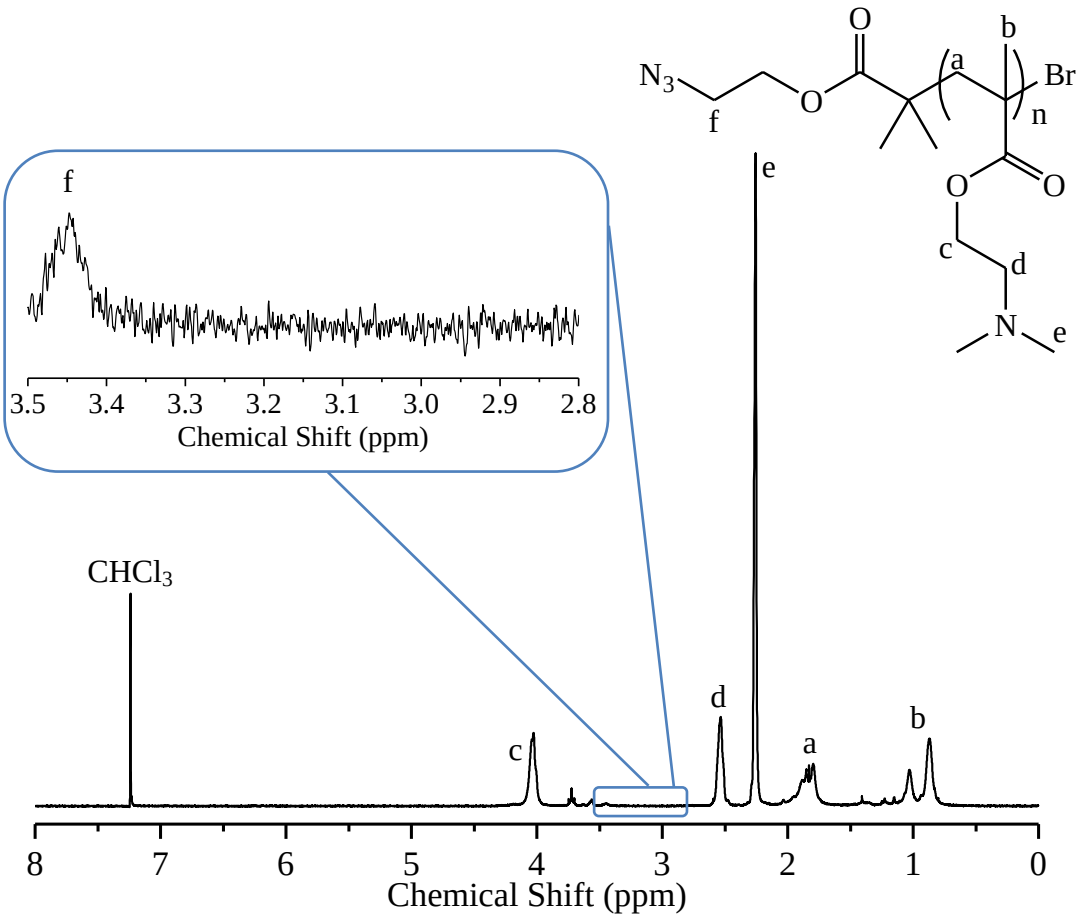

Figure 2.17. ^{1}H-NMR spectrum ($CDCl_3$, 300 MHz, 298 K) of N_3-PDMAEMA sample P2.11.

2.4.4. Reduction of N_3-PDMAEMA to H_2N-PDMAEMA

N_3-PDMAEMA was synthesised so that the azide could be reduced to a primary amine post-polymerisation, for later coupling to PIBSA. Azide groups can be converted to the corresponding primary amine by hydrogenation but another simple and mild method which has been widely used to prepare primary amine functionalised polymers is the Staudinger reaction.[30,47,48] Firstly, triphenylphosphine reacts with azide to generate a phosphazide which subsequently loses nitrogen gas and forms an iminophosphorane, a final aqueous work up forms the desired primary amine and triphenylphosphine oxide.[49] Reduction of N_3-PDMAEMA was performed using the Staudinger reaction (Scheme 2.10).

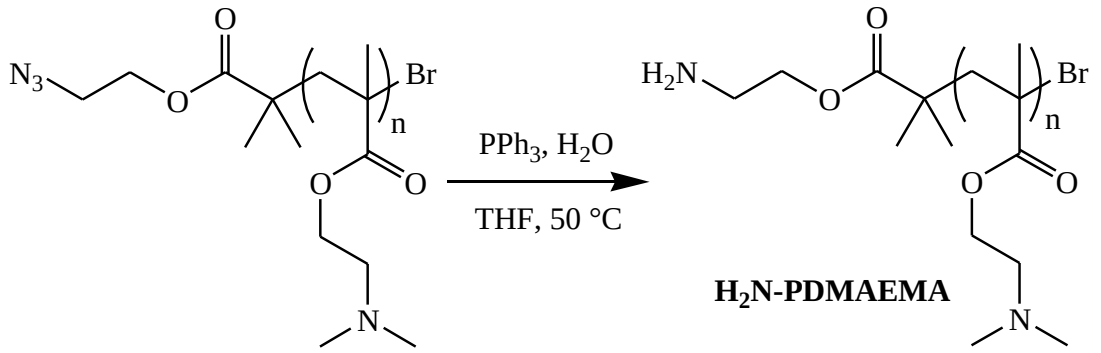

Scheme 2.10. Reduction of N_3-PDMAEMA to H_2N-PDMAEMA by a Staudinger reaction.

Reduction of the *α*-terminal azide to a primary amine was successful under the mild conditions outlined above, disappearance of the azide peak at 2105 cm^{-1} was observed by FT-IR spectroscopy (Figure 2.18).

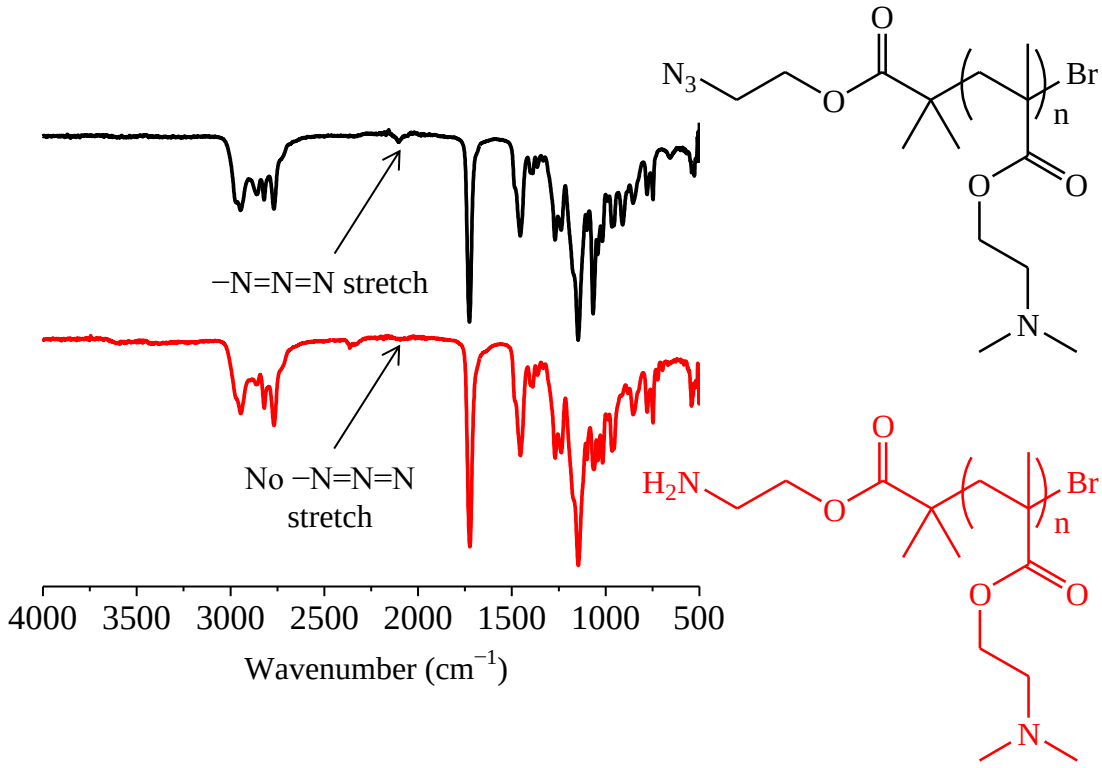

Figure 2.18. FT-IR spectra of N_3-PDMAEMA (P2.11) (black) and H_2N-PDMAEMA (P2.14) (red).

^{1}H-NMR spectroscopy also illustrates the transformation of azide to primary amine. A decrease in chemical shift of the protons adjacent to the azide group from 3.45 to 2.91 ppm occurs after transformation to a primary amine (Figure 2.19). As there is no signal at 3.45 ppm it is a good indication that complete consumption of the azide has occurred and agrees well with the FT-IR spectrum of P2.14.

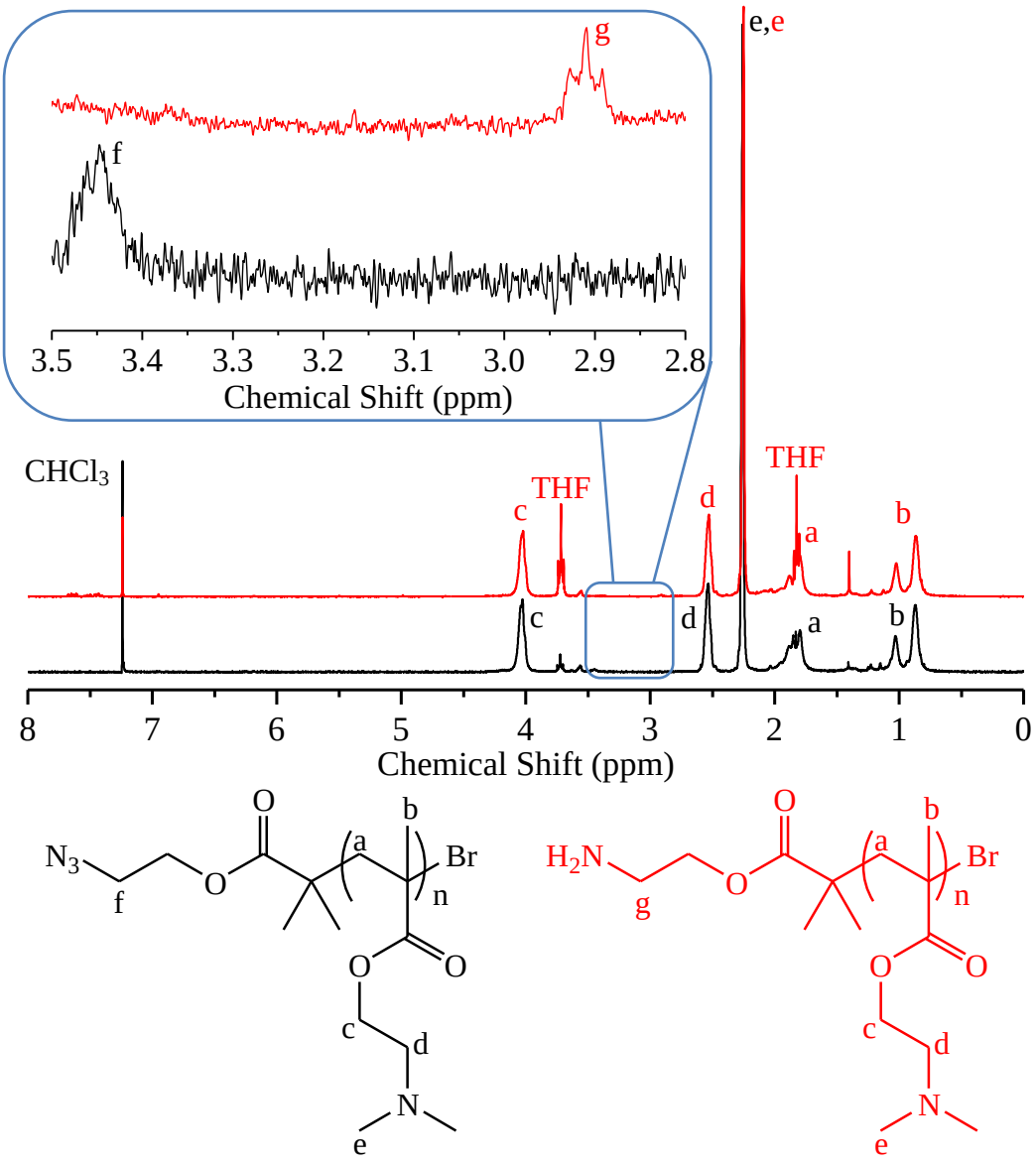

Figure 2.19. ^{1}H-NMR spectra ($CDCl_3$, 300 MHz, 298 K) of N_3-PDMAEMA (P2.11) (black) and H_2N-PDMAEMA (P2.14) (red).

GPC measured an increase in M_n and dispersity after reduction of N_3-PDMAEMA to H_2N-PDMAEMA (Table 2.05), this increase was most significant for P2.14; M_n increased by ~600 g·mol^{-1} and dispersity increased by 0.07. GPC traces show high molecular weight shoulders appearing on all three H_2N-PDMAEMA samples (Figure 2.20). This high molecular weight shoulder is responsible for the increase in measured M_n and dispersity as the remainder of the distribution overlays well with the N_3-PDMAEMA distribution and M_p values remain consistent (Table 2.05). This

high molecular weight shoulder may have occurred because of coupling between the new primary amine and any residual ω-alkyl bromide that was retained throughout the polymerisation. Such coupling reactions have been reported between small molecular primary amines and ω-alkyl bromides on polymers prepared by ATRP.[30]

Table 2.05. GPC characterisation of H_2N-PDMAEMA prepared by reduction of N_3-PDMAEMA.

Sample	Sample Reduced	$M_{n.Theo}^{\alpha}$ (g·mol^{-1})	$M_{n.GPC}^{\beta}$ (g·mol^{-1})	$M_{p.GPC}^{\beta}$ (g·mol^{-1})	$Đ^{\beta}$
P2.12	P2.09	900	2100	2600	1.24
P2.13	P2.10	2200	3400	4500	1.24
P2.14	P2.11	3600	5400	6700	1.33

[α]Calculated from Equation 1. [β]THF + 2% TEA eluent, calibrated with PMMA standards.

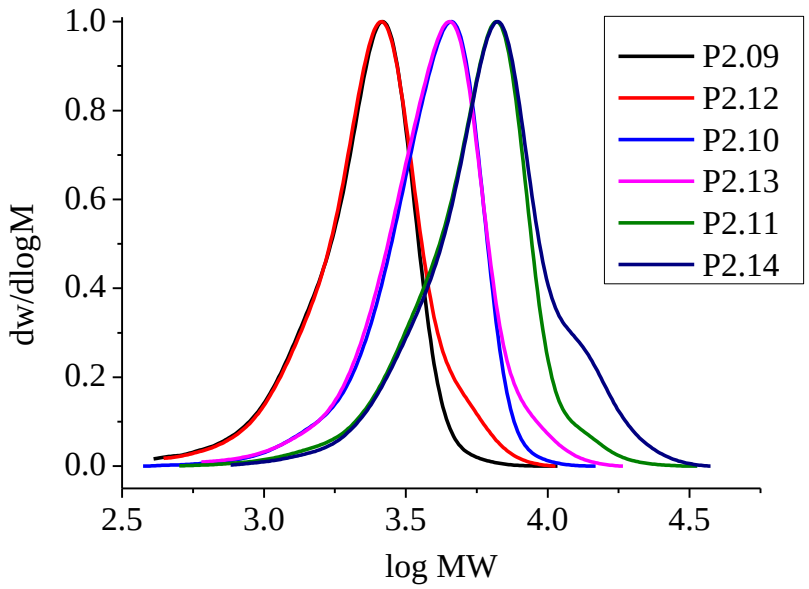

Figure 2.20. GPC traces of N_3-PDMAEMA (P2.09-P2.11) and H_2N-PDMAEMA (P2.12-P2.14).

2.4.5. Macromolecular coupling of H_2N-PDMAEMA and PIBSA

The Final stage of the planned synthesis of PIB-*b*-PDMAEMA copolymers is to couple H_2N-PDMAEMA with PIBSA. Described earlier, aliphatic primary amines and cyclic anhydride functionalised polymers react very quickly to form an amide bond, carboxylic acid and the corresponding block copolymer.[41] Reaction conditions

employed were the same as for the unsuccessful coupling of HO-PDMAEMA and PIBSA in Section 2.3.1 (Scheme 2.11).

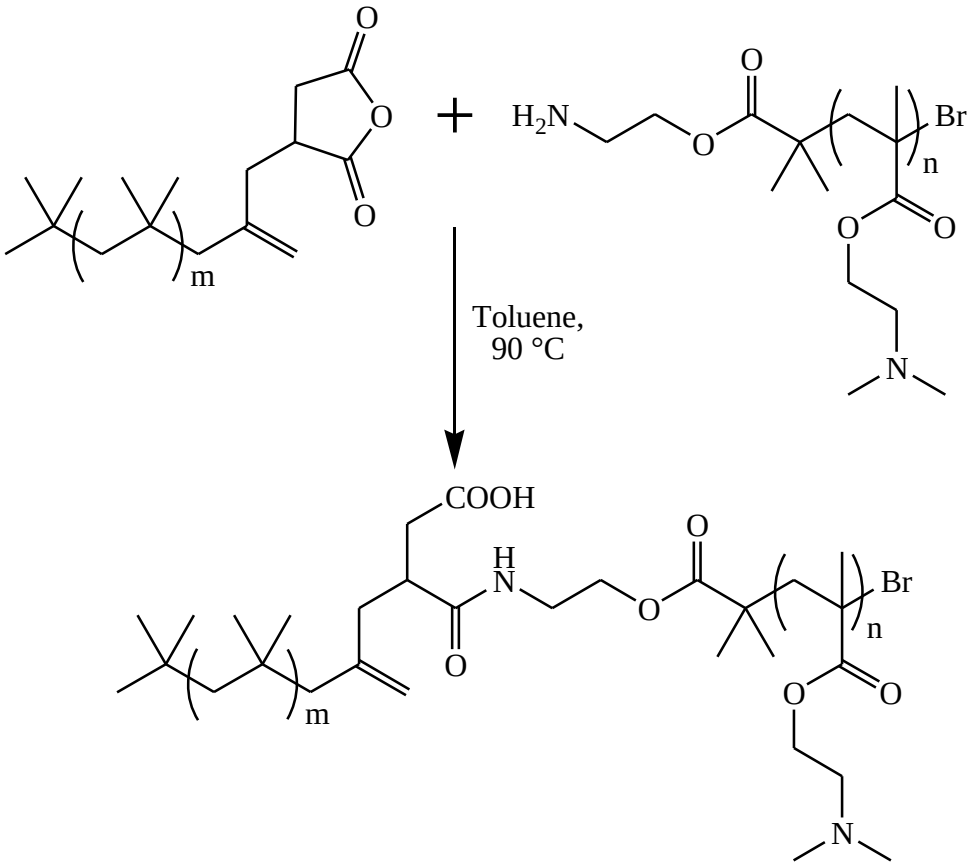

Scheme 2.11. Synthesis of PIB-*b*-PDMAEMA via macromolecular coupling of H_2N-PDMAEMA and PIBSA.

Macromolecular coupling was performed at 90 °C for two hours, after which the cooled reaction mixture was added to a large volume of *n*-hexane. Despite coupling H_2N-PDMAEMA with the hydrophobic PIB block, each PIB-*b*-PDMAEMA copolymer precipitated in *n*-hexane and the excess PIBSA could be removed from the product. Table 2.06 shows the final M_n and dispersity for the PIB-*b*-PDMAEMA copolymers synthesised. A shift towards higher molecular weight, shown by increased M_n and M_p, is observed from the original H_2N-PDMAEMA used to couple with PIBSA (Table 2.06). PIBSA M_n: 850 g·mol^{-1} M_w: 1600 g·mol^{-1} and $Đ$: 1.87 measured by GPC in THF +2% TEA and calibrated with PMMA standards. There is also a slight increase in the final block copolymer dispersity.

Table 2.06. GPC characterisation of PIB-*b*-PDMAEMA prepared by macromolecular coupling of H_2N-PDMAEMA and PIBSA.

Sample	Sample coupled	$M_{n.GPC}^{\alpha}$ (g·mol^{-1})	$M_{p.GPC}^{\alpha}$ (g·mol^{-1})	$Đ^{\alpha}$	$M_{n.GPC}^{\alpha}$ (g·mol^{-1})	$M_{p.GPC}^{\alpha}$ (g·mol^{-1})	$Đ^{\alpha}$
		Before Coupling			After Coupling		
P2.15	P2.12	2100	2600	1.24	2900	3500	1.37
P2.16	P2.13	3400	4500	1.24	4800	5800	1.43
P2.17	P2.14	5400	6700	1.33	7000	7500	1.45

[α]THF + 2% TEA eluent, calibrated with PMMA standards.

Figures 2.21 to 2.23 show the GPC traces of PIB-*b*-PDMAEMA overlaid against the respective H_2N-PDMAEMA used to couple with PIBSA. Each PIB-*b*-PDMAEMA trace shows a shift to higher molecular weight after the coupling reaction, as well as confirming the removal of excess PIBSA.

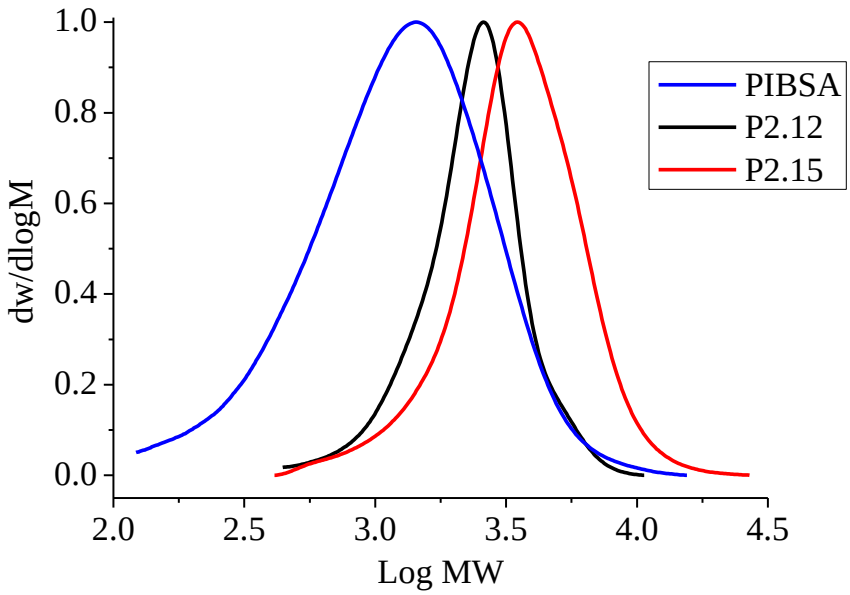

Figure 2.21. GPC traces of PIBSA, H_2N-PDMAEMA (P2.12) and PIB-*b*-PDMAEMA (P2.15).

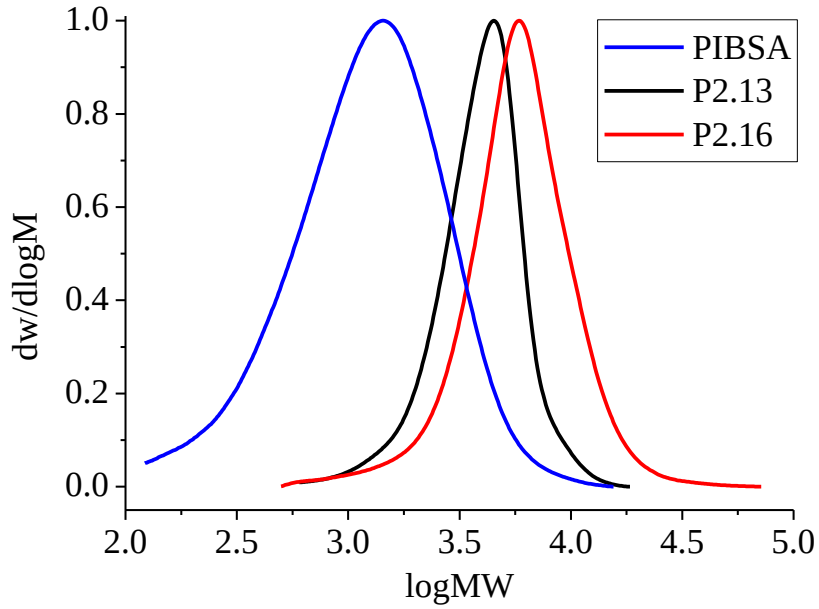

Figure 2.22. GPC traces of PIBSA, H_2N-PDMAEMA (P2.13) and PIB-*b*-PDMAEMA (P2.16).

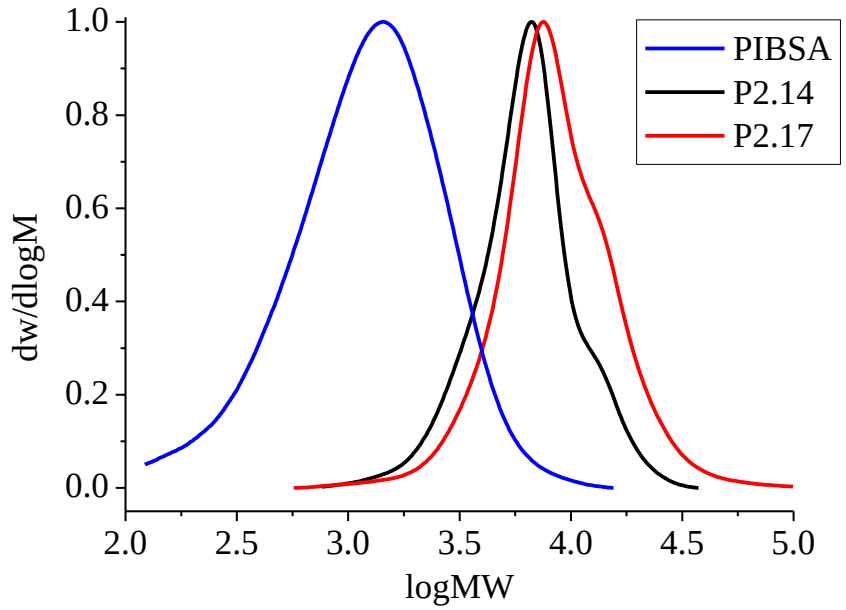

Figure 2.23. GPC traces of PIBSA, H_2N-PDMAEMA (P2.14) and PIB-*b*-PDMAEMA (P2.17).

GPC traces of PIB-*b*-PDMAEMA (Figure 2.21-2.23) also show the formation of a high molecular weight shoulder forming after coupling reactions. As described in Section 1.4.3.2 it is possible for PIBSA to be doubly functionalised with succinic anhydride groups, PIBBSA. PIBSA provided was quoted with a coupling ratio of 1.299 succinic anhydride groups per PIB chain. Therefore, PIBBSA could couple

with two H_2N-PDMAEMA chains and thus synthesise a higher molecular weight species than the desired block copolymer.

2.5. Conclusions

SET-LRP has been utilised to synthesise PDMAEMA homopolymers with hydroxyl and azide *α*-end group functionalities. Initial SET-LRP of DMAEMA was briefly optimised, with regard to ligand and reaction solvent. This methodology was continued to synthesise PIB-*b*-PDMAEMA copolymers by SET-LRP of DMAEMA using a PIB macroinitiator (PIBBiB), this is the first report utilising a PIB macroinitiator in conjunction with SET-LRP. PIB-*b*-PDMAEMA copolymers could be synthesised to different molecular weights, differing only in the block length of the PDMAEMA block length. However, M_n measured by GPC was approximately double the theoretical M_n. This was most likely caused by the low end group fidelity of PIBBiB, partly caused by the initial end group fidelity of the PIB starting material and subsequent end group modifications not proceeding to 100% functionalisation. This resulted in a different monomer to initiator ratio than the original ratio targeted and as such block copolymer M_n was much higher and crude PIB-*b*-PDMAEMA copolymers contained residual low molecular weight PIB impurities. Fortunately, this low molecular weight PIB impurity was removed during precipitation and purified block copolymers were obtained as was the initial aim of this chapter.

The second synthetic approach to synthesise PIB-*b*-PDMAEMA copolymers was macromolecular coupling of functionalised homopolymers; H_2N-PDMAEMA and PIBSA. H_2N-PDMAEMA was synthesised at different molecular weights by SET-LRP of DMAEMA using AEBiB as initiator, the terminal azide was subsequently reduced to a primary amine post-polymerisation. Reduction of terminal azide to

primary amine resulted in a slight broadening of polymer dispersity and presence of a high molecular weight shoulder. H_2N-PDMAEMA and PIBSA were then coupled at 90 °C to yield PIB-*b*-PDMAEMA copolymers. Coupling was shown to be successful by GPC as measured M_n of all H_2N-PDMAEMA samples increased after coupling. Furthermore, residual PIBSA was removed by precipitation of PIB-*b*-PDMAEMA in *n*-hexane. The presence of the difunctionalised PIBBSA is believed to have emphasised high molecular weight shoulders after macromolecular coupling as two H_2N-PDMAEMA chains could couple to one PIBSA.

Finally, PIB-*b*-PDMAEMA copolymers prepared via macromolecular coupling (P2.15-17) were submitted to Innospec to test for their performance as fuel dispersants using an undisclosed test method. All three PIB-*b*-PDMAEMA samples (P2.15-17) failed fuel dispersant performance testing performed by Innospec. It was suspected that P2.15-17 failed the performance test because the copolymers were not sufficiently soluble in the testing medium. Furthermore, P2.15-17 were all purified by precipitation into *n*-hexane which demonstrates their insolubility in aliphatic hydrocarbon solvents. Solubility of PIB-*b*-PDMAEMA in aliphatic hydrocarbon solvents could be improved multiple methods including, reducing the PDMAEMA block length, increasing the PIB block length, synthesising a PIB-*b*-PDMAEMA-*b*-PIB triblock copolymer or incorporating multiple PIB grafts along a PDMAEMA backbone. Incorporation of multiple PIB grafts along a single backbone, via polymerisation of a PIB macromonomer, was pursued in the next chapter to synthesise materials with increased solubility in aliphatic hydrocarbon solvents.

2.6. Experimental

2.6.1. Instrumentation

2.6.1.1. Gel permeation chromatography

Molecular weight averages and polymer dispersity was determined by GPC. GPC samples were prepared to a concentration of 1 mg·mL^{-1} and passed through 0.4 µm PTFE filters before injection. GPC measurements were performed on an Agilent 390-LC multi detector system equipped with a PL-AS RT autosampler, a PLgel 5 µm guard column (50 × 7.5 mm) and two PLgel 5 µm Mixed D columns (300 × 7.5 mm), a refractive index detector (RID) and a photodiode array UV-vis detector. Columns and RID were maintained at 40 °C. The system was eluted with THF and 2% v/v TEA at a flow rate of 1 mL·min^{-1} and the RID was calibrated with linear poly(methyl methacrylate) standards.

2.6.1.2. Nuclear magnetic resonance spectroscopy

^{1}H-NMR and ^{13}C-NMR spectra were measured using a Bruker DPX-300 or DPX-400. Chemical shifts are reported in parts per million (ppm) and all spectra are referenced against the residual solvent peak found in the deuterated NMR solvent. Abbreviations used for peak multiplicity are as follows; s = singlet, d = doublet, t = triplet, q = quartet and m = multiplet.

2.6.1.3. Fourier transform infrared spectroscopy

FT-IR spectra were recorded on a Bruker Vector-22 spectrometer using a Golden Gate diamond attenuated total reflection cell. All FT-IR spectra are plotted transmittance against wavenumbers (cm^{-1}).

2.6.2. Materials

Ethyl *α*-bromoisobutyrate (Aldrich, 98%), copper(II) bromide (Aldrich, 99%), *N,N,N′,N″,N″*-pentamethyldiethylenetriamine (Aldrich, 99%), borane tetrahydrofuran complex solution 1.0 M in THF (Aldrich), 2-bromoethanol (Aldrich, 95%), sodium azide (Aldrich, >99.5%), 2-hydroxyethyl 2-bromoisobutyrate (Aldrich, 95%) and *α*-bromoisobutyryl bromide (Aldrich, 98%) were used as received. *tris*[2-(dimethylamino)ethyl]amine was synthesised according to previous literature.[50] Olefin terminated PIB and PIBSA was donated by Innospec LTD and used as received.

2-(Dimethylamino)ethyl methacrylate (Aldrich, 98%) was destabilised by passing through a short column of basic aluminium oxide prior to polymerisation. Copper(0) wire (Cormax, 0.25 mm, 500 gms) was activated by washing with concentrated sulfuric acid prior to polymerisation.

2.6.3. Procedures

2.6.3.1. Synthesis of 2-azidoethanol

2-Bromoethanol (5.05 g, 0.04 mol, 1 eq.) and sodium azide (3.91 g, 0.06 mol, 1.5 eq.) were dissolved in a mixture of acetone (50 mL) and water (20 mL) before heating under reflux conditions at 60 °C for 18 hours. Acetone was removed in vacuo and the resulting aqueous layer was extracted with diethyl ether (5 × 20 mL). All organic layers were combined, dried over magnesium sulfate and filtered before removing all diethyl ether in vacuo.[45] ^{1}H-NMR ($CDCl_3$, 300 MHz, 298 K): δ (ppm) 3.40 (t, *J* = 4.7, 5.2 Hz, $N_3C\underline{H}_2CH_2OH$, 2H), 3.78 (t, *J* = 4.7, 5.1 Hz, $N_3CH_2C\underline{H}_2OH$, 2H). FT-IR (neat): ($cm^{-1}$) 3370 (br, m, O−H), 2940 (w), 2878 (w), 2093 (s, −N=N=N), 1633 (w), 1442 (w), 1284 (m), 1062 (m), 878 (m), 631 (m).

2.6.3.2. Synthesis of AEBiB

2-Azidoethanol (2.758 g, 0.032 mol, 1 eq.) was dissolved in THF (20 mL) and cooled to 0 °C before addition of TEA (5.3 mL, 0.038 mol, 1.2 eq.), followed by drop wise addition of *α*-bromoisobutyryl bromide (4.7 mL, 0.038 mol, 1 eq.) dissolved in THF (30 mL) over 2 hours, temperature was maintained at 0 °C for a further 2 hours before subsequently reaching room temperature and left to stand for 24 hours. THF was removed in vacuo and the crude product was dissolved in diethyl ether (30 mL). Organic layer washed with sat. $NaHCO_3$ sol. (3 × 30 mL), dried over magnesium sulfate and filtered before removing all diethyl ether in vacuo. Product dissolved in THF and passed through a column of basic aluminium oxide before solvent was removed in vacuo.[46] ^{1}H-NMR ($CDCl_3$, 300 MHz, 298 K): δ (ppm) 1.96 (s, $(-C\underline{H}_3)_2$, 6H,) 3.53 (t, *J* = 4.9, 5.3 Hz, $N_3C\underline{H}_2CH_2-$, 2H), 4.34 (t, *J* = 4.9, 5.1 Hz, $N_3CH_2C\underline{H}_2COO-$, 2H). FT-IR (neat): ($cm^{-1}$) 2977 (w), 2099 (s, −N=N=N), 1734 (s, C=O), 1467 (m), 1269 (s), 1155 (s), 1107 (s), 1034 (w), 945 (w), 841 (w), 643 (w).

2.6.3.3. SET-LRP of DMAEMA using small molecule initiators

Cu(0) wire, $CuBr_2$, solvent, ligand and DMAEMA were charged in that order into a Schlenk tube and degassed by gentle bubbling of N_2 gas. The Schlenk tube was then submerged into a water bath at 25 °C before the addition of degassed initiator via a degassed syringe. Samples were taken at desired time points via degassed syringe, diluted with THF and immediately passed through a short column of basic aluminium oxide to remove the catalyst. After 4 hours the remaining reaction mixture was diluted with THF and passed through a column of basic aluminium oxide. PDMAEMA was precipitated twice into *n*-hexane and dried in vacuo.

Table 2.11 displays the quantities of all individual substances (DMAEMA, initiator, ligand, $CuBr_2$, Cu(0) wire and solvent) used to synthesise all of the polymers (P2.01-P2.05 and P2.09-P2.11) prepared by general procedure above.

^{1}H-NMR ($CDCl_3$, 300 MHz, 298 K): δ (ppm) 0.78-1.17 (m, −C$\underline{H}_3$), 1.66-2.11 (m, −C$\underline{H}_2$−), 2.17-2.36 (s, −N(C$\underline{H}_3$)$_2$), 2.49-2.70 (m, −C$\underline{H}_2$N-), 3.91-4.18 (m, −COOC$\underline{H}_2$−). FT-IR (neat): (cm^{-1}) 2946 (w), 2820 (w), 2768 (w), 2100 (w, −N=N=N, P2.09-P2.11 only), 1726 (s), 1455 (m), 1269 (m), 1147 (s), 1061 (m), 1016 (m), 965 (m), 853 (w), 747 (w), 543 (w).

Table 2.07. GPC characterisation and DMAEMA conversion for PDMAEMA homopolymers prepared by SET-LRP.

Sample	DMAEMA Conversion$^{\alpha}$ (%)	$M_{n.Theo}$$^{\beta}$ (g·mol^{-1})	$M_{n.GPC}$$^{\gamma}$ (g·mol^{-1})	$M_{w.GPC}$$^{\gamma}$ (g·mol^{-1})	$Đ^{\gamma}$
P2.01	19	1710	3000	3900	1.31
P2.02	55	4540	5600	7400	1.33
P2.03	78	3270	4800	6300	1.31
P2.04	61	2600	3600	4800	1.34
P2.05	81	3400	4100	4700	1.15
P2.09	78	900	2000	2400	1.21
P2.10	82	2200	3400	4100	1.20
P2.11	85	3600	4800	6000	1.26

$^{\alpha}$Calculated from ^{1}H-NMR spectroscopy. $^{\beta}$Calculated from Equation 1. $^{\gamma}$THF + 2% TEA eluent, calibrated with PMMA standards.

2.6.3.4. Synthesis of PIBH

Borane tetrahydrofuran complex solution 1 M in THF (3.0 mL, 3.00 mmol, 1.2 eq.) and degassed *n*-hexane (10 mL) were added to a degassed flask. Olefin terminated PIB (2.685 g, 2.45 mmol, 1 eq.) was dissolved in *n*-hexane (10 mL), degassed by

gentle bubbling of N_2 gas for 30 minutes and added drop wise to the borane solution over 30 minutes at 0 °C. Mixture was maintained at 0 °C for a further 5 hours. Sodium hydroxide solution (0.5 M, 5 mL, 2.5 mmol, 1.02 eq.) was added drop-wise followed by 30% hydrogen peroxide solution (0.5 mL, 4.4 mmol, 1.8 eq.) and left for 2 further hours. Distilled water (40 mL) and *n*-hexane (20 mL) were added to the reaction mixture. Organic layer was separated and washed with distilled water (3 × 40 mL), dried over magnesium sulfate and filtered before removing all *n*-hexane in vacuo.[34] ^{1}H-NMR ($CDCl_3$, 300 MHz, 298 K): δ (ppm) 0.97-1.03 ((−C$\underline{H}_3$)$_3$, PIB *α*-terminus), 1.05-1.16 ((−C$\underline{H}_3$)$_2$, PIB repeat unit), 1.39-1.46 (s, −C$\underline{H}_2$−, PIB repeat unit), 1.79 (s, −C$\underline{H}_3$, residual vinylidene), 2.00 (s, −C$\underline{H}_2$−, residual vinylidene), 4.65 (s, −C=C$\underline{H}_f$H$_g$, residual vinylidene), 4.86 (q, −C=CH$_f$$\underline{H}_g$, residual vinylidene). FT-IR (neat): (cm^{-1}) 3404 (br), 2949 (s), 2878 (s), 1470 (m), 1365 (s), 1231 (m), 1072 (m, C−O), 914 (w). GPC: M_n 1200 g·mol^{-1}, M_w 1900 g·mol^{-1}, $Đ$ 1.56.

2.6.3.5. Synthesis of PIBBiB

Polyisobutylene hydroxyl (2.897 g, 2.4 mmol, 1 eq.) was dissolved in THF (20 mL) and degassed by gentle bubbling of N_2 gas for 30 minutes, cooled to 0 °C before the addition of triethylamine (0.73 mL, 5.2 mmol, 2.2 eq.) and degassed for a further 10 minutes. *α*-Bromoisobutyryl bromide (0.65 mL, 5.2 mmol, 2.2 eq.) diluted with THF (20 mL) was degassed for 30 minutes before adding drop-wise to the polyisobutylene hydroxyl solution at 0 °C. Reaction temperature was maintained at 0 °C for a further 4 hours before subsequently reaching room temperature and stirring for 2 days. Reaction mixture was diluted with *n*-hexane (60 mL) and extracted with distilled water (2 × 60 mL) and methanol (60 mL). Organic layer was dried over magnesium sulfate and filtered before removing all *n*-hexane in vacuo.[17,18] ^{1}H-NMR ($CDCl_3$, 300 MHz, 298 K): δ (ppm) 0.97-1.03 ((−C$\underline{H}_3$)$_3$, PIB *α*-terminus),

1.05-1.16 ((−C$\underline{H}_3$)$_2$, PIB repeat unit), 1.39-1.46 (s, −C$\underline{H}_2$−, PIB repeat unit), 1.79 (s, −C$\underline{H}_3$, residual vinylidene), 1.97 (s, –C(C$\underline{H}_3$)$_2$Br), 2.00 (s, −C$\underline{H}_2$−, residual vinylidene), 4.65 (s, −C=C$\underline{H}_f$H$_g$, residual vinylidene), 4.86 (q, −C=CH$_f$$\underline{H}_g$, residual vinylidene). FT-IR (neat): (cm^{-1}) 2947 (s), 2884 (s), 1819 (w), 1738 (m, C=O), 1466 (s), 1365 (s), 1273 (w, C−O), 1230 (m), 1165 (m, C−O), 1113 (m, C−O), 1044 (w), 916 (w). GPC: M_n 1300 g·mol^{-1}, M_w 1900 g·mol^{-1}, $Đ$ 1.44.

2.6.3.6. SET-LRP of DMAEMA using PIBBiB as initiator

Cu(0) wire, $CuBr_2$, methanol, PMDETA and DMAEMA were charged in that order into a Schlenk tube and degassed by gentle bubbling of N_2 gas. The Schlenk tube was submerged into a water bath at 25 °C before the addition of degassed PIBBiB dissolved in toluene via degassed syringe. After 4 hours the remaining reaction mixture was diluted with THF and passed through a column of basic aluminium oxide to remove the catalyst. PIB-*b*-PDMAEMA was precipitated twice into *n*-hexane and dried in vacuo.

Table 2.12 shows the quantities of all individual substances (DMAEMA, PIBBiB, PMDETA, $CuBr_2$, Cu(0) wire, methanol and toluene) used to synthesise the PIB-*b*-PDMAEMA copolymers (P2.06-P2.08) prepared by the procedure above.

^{1}H-NMR ($CDCl_3$, 300 MHz, 298 K): δ (ppm) 0.73-1.23 (m, −C$\underline{H}_3$, PDMAEMA repeat unit, (−C$\underline{H}_3$)$_2$, PIB repeat unit, (−C$\underline{H}_3$)$_3$, PIB *α*-terminus), 1.33-1.47 (m, −C$\underline{H}_2$−, PIB repeat unit), 1.66-2.11 (m, −C$\underline{H}_2$−, PDMAEMA repeat unit), 2.17-2.36 (s, −N(C$\underline{H}_3$)$_2$), 2.49-2.70 (m, −C$\underline{H}_2$N−), 3.91-4.18 (m, −COOC$\underline{H}_2$−).

Table 2.08. GPC characterisation and DMAEMA conversion for PIB-*b*-PDMAEMA copolymers (P2.06-P2.08) prepared by SET-LRP of DMAEMA using PIBBiB as initiator.

Sample	DMAEMA Conversion$^{\alpha}$ (%)	$M_{n.Theo}{}^{\beta}$ (g·mol^{-1})	$M_{n.GPC}{}^{\gamma}$ (g·mol^{-1})	$M_{w.GPC}{}^{\gamma}$ (g·mol^{-1})	$Đ^{\gamma}$
P2.06	80	1940	3500	6300	1.81
P2.07	83	3260	7900	14100	1.80
P2.08	79	4400	8900	15800	1.77

$^{\alpha}$Calculated from ^{1}H-NMR spectroscopy. $^{\beta}$Calculated from Equation 1. $^{\gamma}$THF + 2% TEA eluent, calibrated with PMMA standards.

2.6.3.7. Reduction of N_3-PDMAEMA to H_2N-PDMAEMA

N_3-PDMAEMA and triphenylphosphine were dissolved in THF (40 mL) and heated at 50 °C over night before the addition of distilled water (1 mL). Reaction heated at 50 °C for a further 2 hours. H_2N-PDMAEMA was precipitated twice into *n*-hexane and dried in vacuo.

Table 2.13 shows which N_3-PDMAEMA samples were reduced to produce the corresponding H_2N-PDMAEMA sample as well as the quantities of N_3-PDMAEMA, triphenylphosphine, THF and water used.

^{1}H-NMR ($CDCl_3$, 300 MHz, 298 K): δ (ppm) 0.78-1.17 (m, −C$\underline{H}_3$), 1.66-2.11 (m, −C$\underline{H}_2$−), 2.17-2.36 (s, −N(C$\underline{H}_3$)$_2$), 2.49-2.70 (m, −C$\underline{H}_2$N−), 3.91-4.18 (m, −COOC$\underline{H}_2$−). FT-IR (neat): (cm^{-1}) 2946 (w), 2820 (w), 2768 (w), 1726 (s), 1455 (m), 1269 (m), 1147 (s), 1061 (m), 1016 (m), 965 (m), 853 (w), 747 (w), 543 (w).

Table 2.09. GPC characterisation of H_2N-PDMAEMA (P2.12-P.14) prepared by reduction of N_3-PDMAEMA (P2.09-P2.11).

Sample	$M_{n.Theo}$ [α] (g·mol^{-1})	$M_{n.GPC}$ [β] (g·mol^{-1})	$M_{w.GPC}$ [β] (g·mol^{-1})	$Đ$ [β]
P2.12	900	2100	2600	1.24
P2.13	2200	3400	4200	1.24
P2.14	3600	5400	7200	1.33

[α]Calculated from Equation 1. [β]THF + 2% TEA eluent, calibrated with PMMA standards.

2.6.3.8. Macromolecular coupling of H_2N-PDMAEMA and PIBSA

H_2N-PDMAEMA and PIBSA were dissolved in toluene (50 mL) and heated at 90 °C for 2 hours before cooling to room temperature. PIB-*b*-PDMAEMA was precipitated twice into *n*-hexane and dried in vacuo.

Table 2.14 shows which H_2N-PDMAEMA samples were used to couple with PIBSA to synthesise the corresponding PIB-*b*-PDMAEMA samples as well as the quantities of H_2N-PDMAEMA, PIBSA and toluene used.

^{1}H-NMR ($CDCl_3$, 300 MHz, 298 K): δ (ppm) 0.73-1.23 (m, −C$\underline{H}_3$, PDMAEMA repeat unit, (−C$\underline{H}_3$)$_2$, PIB repeat unit, (−C$\underline{H}_3$)$_3$, PIB *α*-terminus), 1.33-1.47 (m, −C$\underline{H}_2$−, PIB repeat unit), 1.66-2.11 (m, −C$\underline{H}_2$−, PDMAEMA repeat unit), 2.17-2.36 (s, −N(C$\underline{H}_3$)$_2$), 2.49-2.70 (m, −C$\underline{H}_2$N−), 3.91-4.18 (m, −COOC$\underline{H}_2$−).

Table 2.10. GPC characterisation of PIB-*b*-PDMAEMA copolymers (P2.15-P2.17) prepared by macromolecular coupling of H_2N-PDMAEMA and PIBSA.

Sample	$M_{n.Theo}$[α] (g·mol^{-1})	$M_{n.GPC}$[β] (g·mol^{-1})	$M_{w.GPC}$[β] (g·mol^{-1})	$Đ$[β]
P2.15	1900	2900	4000	1.37
P2.16	3200	4800	6900	1.43
P2.17	4600	7000	10200	1.45

[α]Calculated from Equation 1. [β]THF + 2% TEA eluent, calibrated with PMMA standards.

Table 2.11. Monomer, initiator, ligand, $CuBr_2$, Cu(0) wire and solvent quantities used to prepare polymers P2.01-P2.05 and P2.09-P2.11 by SET-LRP.

Sample	Monomer			Initiator			Ligand			$CuBr_2$			Cu(0)	Solvent
	(mL)	(mmol)	(eq.)	(mg)	(mmol)	(eq.)	(µL)	(mmol)	(eq.)	(mg)	(mmol)	(eq.)	(cm)	(mL)
P2.01		DMAEMA			HEBiB			Me_6TREN						DMSO
	5	29.7	50	127	0.594	1	29	0.107	0.18	6.5	0.0297	0.05	5	5
P2.02		DMAEMA			HEBiB			PMDETA						DMSO
	5	29.7	50	126	0.594	1	22	0.107	0.18	6.6	0.0297	0.05	5	5
P2.03		DMAEMA			HEBiB			PMDETA						DMSO
	5	29.7	25	253	1.19	1	45	0.214	0.18	13.4	0.0594	0.05	5	5
P2.04		DMAEMA			HEBiB			PMDETA						MeOH
	5	29.7	25	251	1.19	1	45	0.214	0.18	13.4	0.0594	0.05	5	5
P2.05		DMAEMA			EBiB			PMDETA						MeOH
	5	29.7	25	230	1.19	1	45	0.214	0.18	13.3	0.0594	0.05	5	5
P2.09		DMAEMA			AEBiB			PMDETA						MeOH
	10	59.3	25	561	2.37	1	89	0.427	0.18	26.1	0.117	0.05	10	10
P2.10		DMAEMA			AEBiB			PMDETA						MeOH
	10	59.3	15	931	3.94	1	148	0.712	0.18	44.0	0.195	0.05	10	10
P2.11		DMAEMA			AEBiB			PMDETA						MeOH
	10	59.3	5	2820	11.9	1	445	2.135	0.18	133	0.585	0.05	10	10

Table 2.12. DMAEMA, PIBBiB, PMDETA, $CuBr_2$, Cu(0) wire, methanol and toluene quantities used to prepare block copolymers P2.06-P2.08 by SET-LRP.

Sample	DMAEMA			PIBBiB			PMDETA			$CuBr_2$			Cu(0)	MeOH/Toluene
	(mL)	(mmol)	(eq.)	(g)	(mmol)	(eq.)	(µL)	(mmol)	(eq.)	(mg)	(mmol)	(eq.)	(cm)	(mL)
P2.06	1	5.93	25	0.310	0.238	1	9	0.043	0.18	2.6	0.0117	0.05	5	1/1
P2.07	1	5.93	15	0.515	0.396	1	15	0.072	0.18	4.4	0.020	0.05	5	1/1
P2.08	1	5.93	5	1.495	1.15	1	45	0.216	0.18	13.2	0.059	0.05	5	2/2

Table 2.13. Quantities of N_3-PDMAEMA, triphenylphosphine, THF and water used to synthesise samples P2.12-P2.14.

Sample	N_3-PDMAEMA Reduced	PDMAEMA		Triphenylphosphine			THF	Water
		(g)	(eq.)	(g)	(mmol)	(eq.)	(mL)	(mL)
P2.12	P2.09	7.885	1	0.529	1.99	1.2	40	1
P2.13	P2.10	7.704	1	0.719	2.74	1.2	40	1
P2.14	P2.11	7.283	1	1.179	4.49	1.2	40	1

Table 2.14. Quantities of NH_2-PDMAEMA, PIBSA and toluene used to synthesis samples P2.15-P2.17.

Sample	H_2N-PDMAEMA Coupled	PDMAEMA		PIBSA		Toluene
		(g)	(eq.)	(g)	(eq.)	(mL)
P2.15	P2.12	8.126	1	1.559	1.25	50
P2.16	P2.13	7.703	1	2.302	1.25	50
P2.17	P2.14	7.319	1	3.634	1.25	50

2.7. References

1. J. P. Kennedy and M. Hiza, *J. Polym. Sci. Part A Polym. Chem.*, 1983, **21**, 1033.
2. R. F. Storey and B. J. Chisholm, *Polymer*, 1996, **37**, 2925.
3. B. Iván, X. Chen, J. Kops and W. Batsberg, *Macromol. Rapid Commun.*, 1998, **19**, 15.
4. T. Pernecker, J. P. Kennedy and B. Iván, *Macromolecules*, 1992, **25**, 1642.
5. J. Feldthusen, B. Iván and A. H. E. Muller, *Macromolecules*, 1998, **31**, 578.
6. Z. Fang and J. P. Kennedy, *J. Polym. Sci. Part A Polym. Chem.*, 2002, **40**, 3662.
7. Z. Fang and J. P. Kennedy, *J. Polym. Sci. Part A Polym. Chem.*, 2002, **40**, 3679.
8. Á. Szabó, A. Wacha, R. Thomann, G. Szarka, A. Bóta and B Iván, *J. Macromol. Sci., Pure Appl. Chem.*, 2015, **52**, 252.
9. X. Chen, B. Iván, J. Kops and W. Batsberg, *Macromol. Rapid Commun.*, 1998, **19**, 585.
10. A. J. D. Magenau, N. Martinez-Castro and R. F. Storey, *Macromolecules*, 2009, **42**, 2353.
11. K. Bauri, P. De, P. N. Shah, R. Li and R. Faust, *Macromolecules*, 2013, **46**, 5861.
12. U. Haldar, K. Bauri, R. Li, R. Faust and P. De, *J. Polym. Sci. Part A Polym. Chem.*, 2015, **53**, 1125.
13. C. Ren, X. Jiang, G. Lu, X. Jiang and X. Huang, *J. Polym. Sci. Part A Polym. Chem.*, 2014, **52**, 1478.
14. C. Ren, X. Liu, X. Jiang, G. Sun and X. Huang, *J. Polym. Sci. Part A Polym. Chem.*, 2015, **53**, 1143.
15. A. J. D. Magenau, N. Martinez-Castro, D. A. Savin and R. F. Storey, *Macromolecules*, 2009, **42**, 8044.

16. A. Takacs and R. Faust, *Macromolecules*, 1995, **28**, 7266.
17. T. Higashihara and R. Faust, *Macromolecules*, 2007, **40**, 7453.
18. W. H. Binder and R. Sachsenhofer, *Macromol. Rapid Commun.*, 2008, **29**, 1097.
19. Y. Zhu and R. F. Storey, *Macromolecules*, 2010, **43**, 7048.
20. Y. Zhu and R. F. Storey, *Macromolecules*, 2012, **45**, 1217.
21. C. Pietsch, U. Mansfeld, C. Guerrero-Sanchez, S. Hoeppener, A. Vollrath, M. Wagner, R. Hoogenboom, S. Saubern, S. H. Thang, C. R. Becer, J. Chiefari and U. S. Schubert, *Macromolecules*, 2012, **45**, 9292.
22. M. Li, G. L. Li, Z. Zhang, J. Li, K.-G. Neoh and E.-T. Kang, *Polymer*, 2010, **51**, 3377.
23. A. E. Smith, X. Xu, T. U. Abell, S. E. Kirkland, R. M. Hensarling and C. L. McCormick, *Macromolecules*, 2009, **42**, 2958.
24. *US Pat.*, 4867894, 1989.
25. *US Pat.*, 20120135902A1, 2012.
26. F. Zeng, Y. Shen, S. Zhu, and R. Pelton, *J. Polym. Sci. Part A Polym.Chem.*, 2000, **38**, 3821.
27. S. B. Lee, A. J. Russell and K. Matyjaszewski, *Biomacromolecules*, 2003, **4**, 1386.
28. B. Mao, L.-H. Gan, Y.-Y. Gan, X. Li, P. Ravi, and K.-C. Tam, *J. Polym. Sci. Part A Polym. Chem.*, 2004, **42**, 5161.
29. A. Grice, PhD Thesis, University of Warwick, 2011.
30. V. Coessens, T. Pintauer and K. Matyjaszewski, *Prog. Polym. Sci.*, 2001, **26**, 337.

31. V. Percec, T. Guliashvili, J. S. Ladislaw, A. Wistrand, A. Stjerndahl, M. J. Sienkowska, M. J. Monteiro and S. Sahoo, *J. Am. Chem. Soc.*, 2006, **128**, 14156.

32. C. Fidge, PhD Thesis, University of Warwick, 2009.

33. A. Anastasaki, C. Waldron, P. Wilson, R. McHale and D. M. Haddleton, *Polym. Chem.*, 2013, **4**, 2672.

34. B. Ivan, J. P. Kennedy and V. S. C. Chang, *J. Polym. Sci. Part A Polym. Chem.*,1980, **18**, 3177.

35. S. V. Kostjuk, *RSC Adv.*, 2015, **5**, 13125.

36. N. H. Nguyen, B. M. Rosen, X. Jiang, S. Fleischmann and V. Percec, *J. Polym. Sci. Part A Polym. Chem.*, 2009, **47**, 5577.

37. X. Jiang, S. Fleischmann, N. H. Nguyen, B. M. Rosen and V. Percec, *J. Polym. Sci. Part A Polym. Chem.*, 2009, **47**, 5591.

38. B. M. Rosen, X. Jiang, C. J. Wilson, N. H. Nguyen, M. J. Monteiro and V. Percec, *J. Polym. Sci. Part A Polym. Chem.*, 2009, **47**, 5606.

39. M. E. Levere, I. Willoughby, S. O'Donohue, P. M. Wright, A. J. Grice, C. Fidge, C. R. Becer and D. M. Haddleton, *J. Polym. Sci. Part A Polym. Chem.*, 2011, **49**, 1753.

40. P. M. Wright, G. Mantovani and D. M. Haddleton, *J. Polym. Sci. Part A Polym. Chem.*, 2008, **46**, 7376.

41. C. A. Orr, J. J. Cernohous, P. Guegan, A. Hirao, H. K. Jeon and C. W. Macosko, *Polymer*, 2001, **42**, 8171.

42. G. V. S. Reddy, G. V. Rao, R. V. K. Subramanyam and D. S. Iyengar, *Synth. Comm.*, 2000, **30**, 2233.

43. X. Jiang, M. C. Lok and W. E. Hennink, *Bioconjugate Chem.*, 2007, **18**, 2077.

44. M. Zhang, P. A. Rupar, C. Feng, K. Lin, D. J. Lunn, A. Oliver, A. Nunns, G. R. Whittell, I. Manners and M. A. Winnik, *Macromolecules*, 2013, **46**, 1296.

45. G.-Y. Shi, X.-Z. Tang and C.-Y. Pan, *J. Polym. Sci. Part A Polym. Chem.*, 2008, **46**, 2390.

46. S. Sun, Y. Cao, J. Feng and P. Wu, *J. Mater. Chem.*, 2010, **20**, 5605.

47. K. Matyjaszewski, Y. Nakagawa and S. G. Gaynor, *Macromol. Rapid Commun.*, 1997, **18**, 1057.

48. V. Coessens, Y. Nakagawa and K. Matyjaszewski, *Polym. Bull.*, 1998, **40**, 135.

49. F. L. Lin, H. M. Hoyt, H. van Halbeek, R. G. Bergman and C. R. Bertozzi, *J. Am. Chem. Soc.*, 2005, **127**, 2686.

50. M. Ciampolini and N. Nardi, *Inorg. Chem.*, 1966, **5**, 41.

3. Synthesis and Polymerisation of a Novel Polyisobutylene Acrylate

3.1. Introduction

Polyisobutylene (PIB) macromonomers continue to attract much interest both academically and industrially.[1-3] This is because PIB macromonomers can be copolymerised with other small molecule monomers such as methyl methacrylate and styrene to synthesise statistical graft copolymers.[4-6] Furthermore, bifunctionalised PIB macromonomers have been synthesised by post-polymerisation modification of telechelic PIB. Copolymerisation of these difunctionalised PIB macromonomers with other small molecule monomers leads to the formation of polymer networks and amphiphilic copolymer networks (APCNs).[7-11] These materials have been shown to be effective for a number of applications such as; sealants, coatings, adhesives and drug delivery vehicles.[1-3]

Preparation of PIB graft copolymers or APCNs that incorporate PIB rely on the synthesis of well-defined mono/multi functionalised PIB macromonomers. To date, PIB macromonomers of many monomer classes have been synthesised by multiple synthetic pathways. α-Olefin terminated PIB has been transformed to hydroxyl terminated PIB following hydroboration and oxidation. Hydroxyl terminated PIB has been subsequently esterified to the corresponding (meth)acrylate by addition of (meth)acryloyl chloride under basic conditions.[12-14] Similarly, hydroxyl terminated PIB has been reacted with anthracene protected 2-cyano acryloyl chloride or anthracene protected 2-cyano acrylic acid to yield PIB cyanoacrylates.[15,16] PIB cyanoacrylates have also been synthesised by reacting anthracene protected 2-cyano acrylic acid with bromine terminated PIB.[17] Moreover, allyl terminated PIB has been successfully converted to an epoxide to synthesise PIB epoxy.[18] Allyl halide

terminated PIBs, synthesised by capping living cationic polymerisation of IB with 1,3-butadiene,[19] have also been exploited for synthesising PIBs with functional end groups. Quantitative nucleophilic substitution, facilitated by a phase transfer catalyst, of the PIB terminal allyl halide has allowed for many potential end group modifications including; (meth)acrylate, vinyl and epoxy.[20,21] Recently, Storey and co-workers have demonstrated an elegant one-step method of synthesising PIB macromonomer (meth)acrylates.[22] This was achieved by direct quenching of a living PIB homopolymer, synthesised by living cationic polymerisation, with a phenoxyalkyl (meth)acrylate.[22]

PIB macromonomer synthesis represents a significant synthetic challenge as initial living cationic polymerisation of IB requires stringent conditions and subsequent end group modification may be time consuming requiring multiple steps. Therefore, less demanding synthetic routes to PIB macromonomers are required and a trend of simplification is represented by the examples detailed above. However, even these simplified synthetic routes require specific capping reagents or another reactive molecule which are not commercially available.

Therefore, synthesis of PIB macromonomers could be broadened further by utilising a commercial source of end functionalised PIB that can be converted to a PIB macromonomer using commercially available reagents. Such a source of commercial PIB does exist and is commonly known as “highly reactive” PIB. This material is deemed “highly reactive” as the PIB is primarily capped with a terminal *exo*-olefin.[23,24] Detailed in Section 1.4.3.1, “highly reactive” PIB is commonly utilised in the fuel additives industry to be reacted with MalA to yield PIBSAs, which are imidised with primary amines to the corresponding PIBSIs.[25] Furthermore, “highly reactive” PIB is used to alkylate phenol via a Friedel-Crafts alkylation to synthesise

PIBPs that are precursors for the so called "Mannich type dispersants".[26-28] Utilising these commercially available reagents to synthesise a PIB macromonomer is the primary objective of this chapter. It is also worthy of note that "highly reactive" PIB itself is a PIB macromonomer and has been successfully copolymerised with *N*-substituted maleimides by free radical copolymerisation initiated by dimethyl 2,2′-azobis(isobutyrate) (V601).[29]

The second part of this chapter will focus on the controlled radical polymerisation (CRP) of the newly synthesised PIB macromonomer with other small molecule monomers to synthesise novel copolymer compositions. This aim can be expressed schematically in general terms for the eventual system devised (Scheme 3.01). Where R^1 represents an acrylate or acrylamide, R^2 is the linking chemistry used to synthesise the PIB acrylate, I is the initiating group and X is a reactive end group from the chosen CRP technique. This approach will synthesise statistical copolymers of varying composition and chain length dependant on the initial monomer to initiator/mediator ratio (Scheme 3.01).

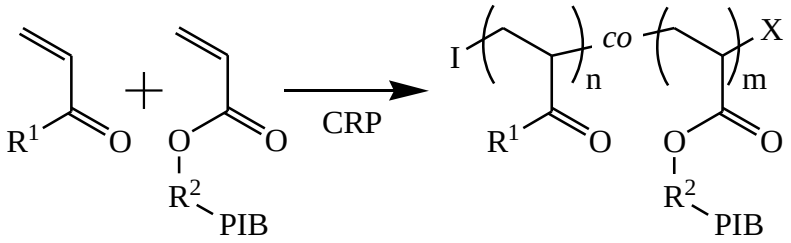

Scheme 3.01. General reaction scheme to synthesise statistical copolymers of acrylates/acrylamides and a PIB acrylate. R^1 = acrylate/acrylamide, R^2 = linker unit, I = initiator, X = reactive end group.

Another potential advantage of utilising CRP to synthesise these copolymers is the ability to synthesise block copolymers by chain extension of a chosen homopolymer synthesised by CRP, which contains a reactive end group (X), with PIB acrylate. This aim is also expressed schematically in general terms (Scheme 3.02). These

block copolymers could be potentially tuneable by block length as well as total chain length.

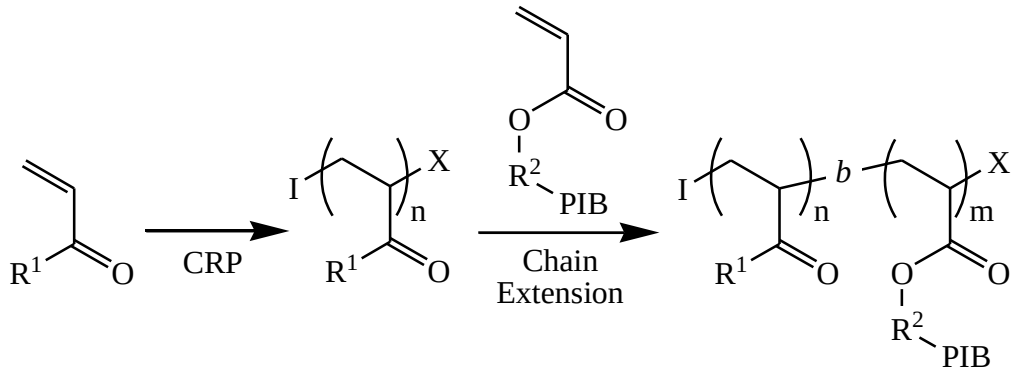

Scheme 3.02. General reaction scheme to synthesise block copolymers of acrylates/acrylamides and a PIB acrylate. R^1 = acrylate/acrylamide, R^2 = linker unit, I = initiator, X = reactive end group.

These synthetic strategies could have potential drawbacks as there are currently many variables unknown. Chosen CRP technique of all monomers may require optimisation; CTA, temperature, solvent, initiator, etc. However, there are many potential tuneable properties to the proposed copolymer structures which could lead to a novel and versatile copolymer system. Furthermore, previous DVM synthesis has been achieved by one step copolymerisation of *n*-alkyl methacrylates and dispersancy-imparting monomers.[30-33] Typical comonomers used to synthesise *n*-alkyl methacrylate based DVMs are 2-(dimethylamino)ethyl methacrylate, 2-(dimethylamino)propyl methacrylamide, *C* and *N*-vinylpyridine. Therefore, copolymerising similar dispersancy-imparting monomers is vital but substituting *n*-alkyl methacrylates for a PIB macromonomer may prove a novel alternative for providing the copolymer's solubility in a very hydrophobic medium such as fuel or other engine oils. Moreover, solubility of the PIB macromonomer copolymers will be dependent on the ratio of PIB macromonomer to comonomer. Varying the feed ratio of PIB macromonomer to comonomer will allow for copolymers of tuneable solubility to be synthesised. Therefore, it is suspected that copolymers with enhanced solubility in aliphatic hydrocarbon solvents will be synthesisable using this

alternative approach. Potentially addressing the suspected cause of the failure for PIB-*b*-PDMAEMA samples (Chapter 2, samples P2.15-17) during performance testing.

3.2. Synthesis of PIB macromonomer

The initial aim of this Chapter was the synthesis of a PIB macromonomer starting from a commercial source of PIB. As outlined earlier there are two common synthetic routes for functionalising PIB terminal olefins. These are an ene-reaction with MalA to synthesise PIBSA and subsequently PIBSIs or synthesis of PIBP by Friedel-Crafts alkylation of phenol.

PIBSA was originally envisioned as a starting material for a PIB macromonomer by imidisation of the cyclic anhydride to a cyclic imide with ethanolamine to form a PIB bearing an aliphatic primary hydroxyl.[34] This hydroxyl was then esterified with methacryloyl chloride to synthesise the corresponding PIB methacrylate. However, as a portion of the PIBSA is likely to be the doubly functionalised PIBBSA (Section 1.4.3.2), a monomer derived from this material would contain two monomer units and as such be a cross linker. This is unsuitable for the proposed synthetic strategies in Scheme 3.01 and 3.02. Therefore, PIBP derived from olefin terminate PIB was solely investigated as a reagent for the synthesis of a PIB macromonomer.

3.2.1. Synthesis of polyisobutylene phenol (PIBP)

Friedel-Crafts alkylation of phenol with PIB has been shown to be highly efficient at transforming the PIB terminal olefin end group to a phenol.[26] Both the terminal *exo*-olefin (PIB_{exo}) and *endo*-olefin (PIB_{endo}) are converted to the same *para* functionalised phenol (PIBP) resulting in the highest possible end group fidelity from the PIB supplied.[26] Furthermore, reaction conditions are non-stringent and

reaction achieves very high functionalisation utilising a strong acid catalyst at room temperature.[26] The straight forward synthesis and the potential functionalisation reactions possible with the phenolic end group is why PIBP is used extensively to synthesise the so-called Mannich fuel dispersants (Section 1.4.3.3). PIBP was synthesised according to a literature procedure by Friedel-Crafts alkylation of phenol using concentrated sulfuric acid as catalyst in DCM (Scheme 3.03).[26]

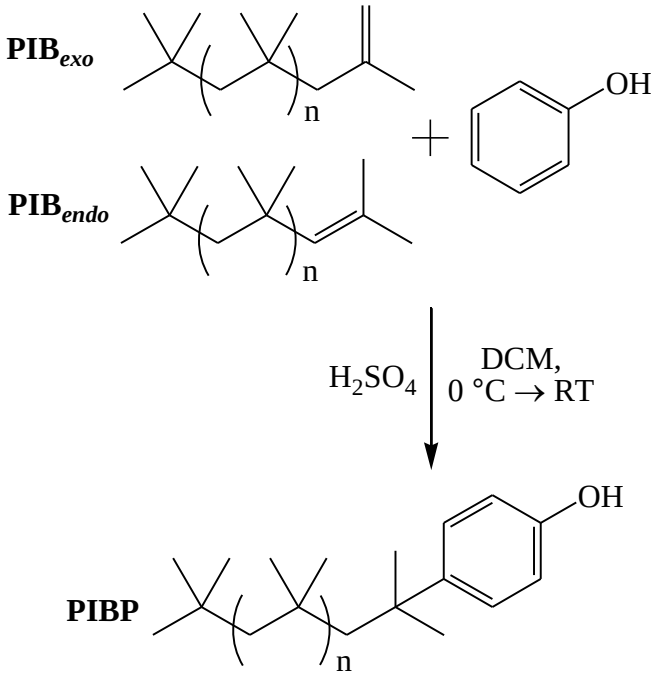

Scheme 3.03. Synthesis of PIBP via Friedel-Crafts alkylation of phenol with PIB_{exo} and PIB_{endo}.

Friedel-Crafts alkylation of phenol using the selected conditions was shown to be successful by ^{1}H-NMR spectroscopy; disappearance of all peaks corresponding to the *exo*- and *endo*-olefin present was observed as expected, confirming that both varieties of olefin end group are transformed into a phenol of which the presence is confirmed by two new doublets at 6.68 ppm and 7.16 ppm (Figure 3.01). This result agrees very strongly with the literature procedure used to prepare PIBP.[26] Relative integration of the -$C(CH_3)_3$ (H^a) PIB α-terminus at 0.97 ppm to ω-terminal *exo*- and *endo*-olefin protons ($H^{f,g,h}$) indicates that 80% of the PIB chains bear a terminal

olefin. Following Friedel-Crafts alkylation of phenol, integration of the -C(CH_3)$_3$ (H^a) PIB α-terminus at 0.97 ppm to ω-terminal phenol protons ($H^{g,e}$) estimates that 81% of PIB chains now bear the desired phenolic end group functionality.

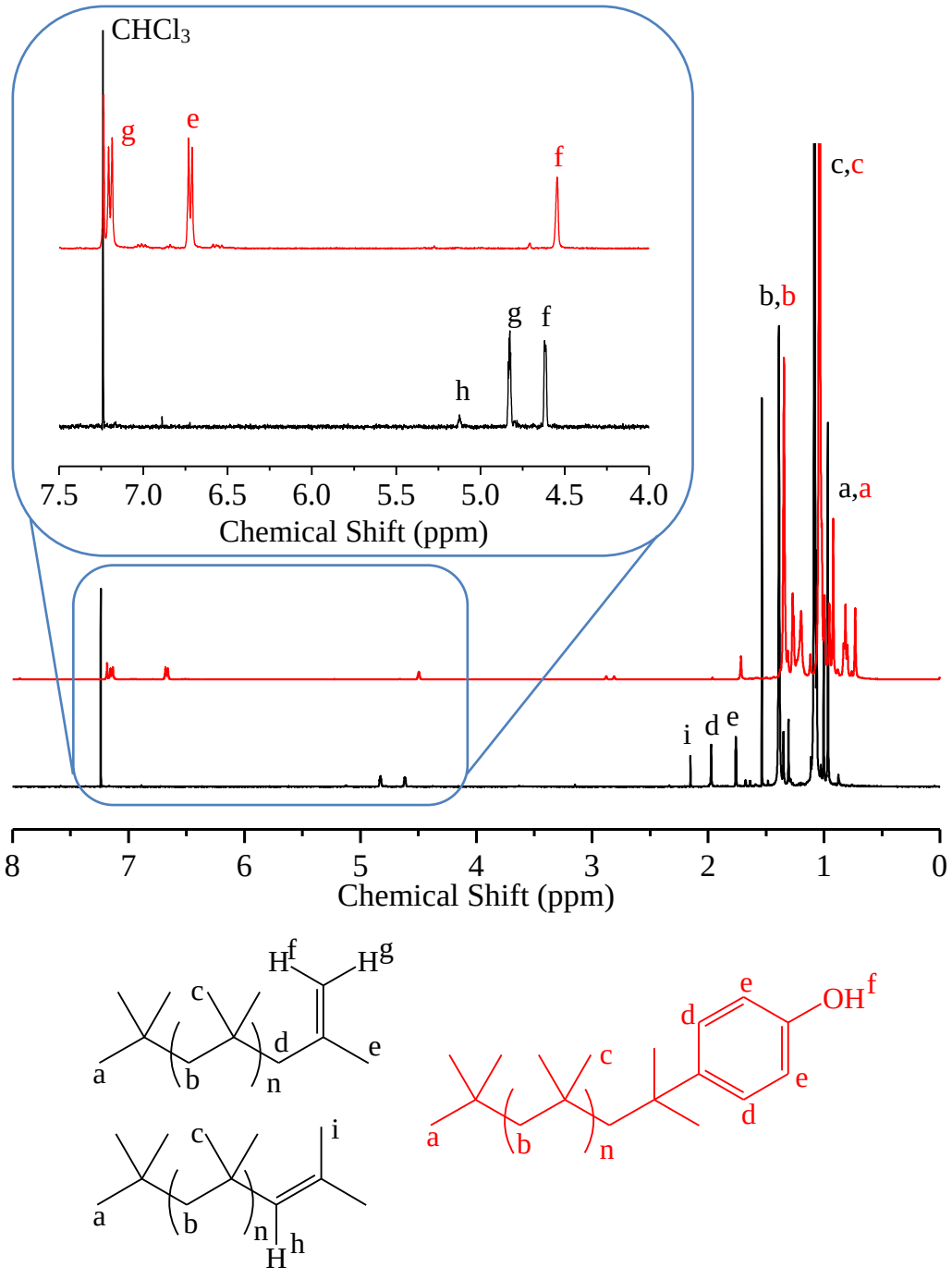

Figure 3.01. ^{1}H-NMR spectrum ($CDCl_3$, 400 MHz, 303 K) of PIB_{exo} and PIB_{endo} (black) and PIBP (red).

^{13}C-NMR spectroscopy was also utilised to support the Friedel-Crafts alkylation of phenol with PIB was successful. Resonances at 114.38 ppm and 143.86 ppm corresponding to the vinylidene carbon atoms disappeared and were replaced by four new resonances at; 114.54, 127.25, 142.64 and 153.09 ppm which correspond to the carbon atoms of the new phenol end group (Figure 3.02).

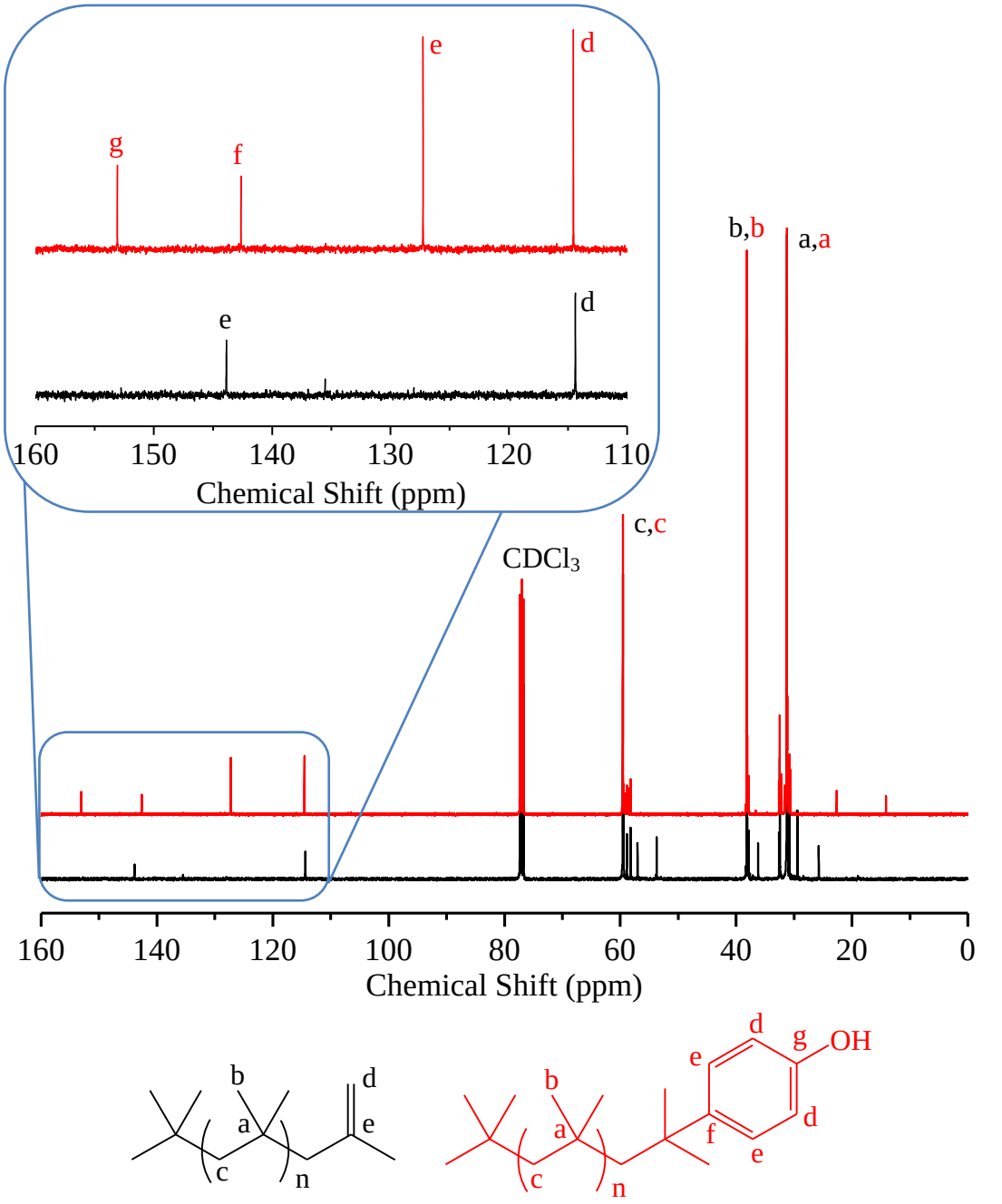

Figure 3.02. ^{13}C-NMR spectrum ($CDCl_3$, 400 MHz, 303 K) of PIB_{exo} (black) and PIBP (red).

Furthermore, addition of phenol to the PIB end group is shown by GPC equipped with a variable wavelength detector (VWD) measuring at 270 nm. Unfunctionalised PIB does not absorb UV light at 270 nm and as such shows no signal on the GPC trace (Figure 3.03 – black trace). After PIB is functionalised with phenol to PIBP it is now capable of absorbing at 270 nm and this absorbance is detectable by performing GPC with a VWD set to 270 nm (Figure 3.03 – red trace). GPC was also used to measure the M_n of PIBP by RID. M_n was found to decrease slightly after the Friedel-Crafts alkylation, from 1250 to 1200 g·mol^{-1} and the dispersity remain unchanged at 1.60. This slight reduction in M_n for PIBP from PIB is not significantly different and demonstrates well that the sulfuric acid catalyst utilised for the Friedel-Crafts alkylation is not having any significant negative effects on the PIB backbone.

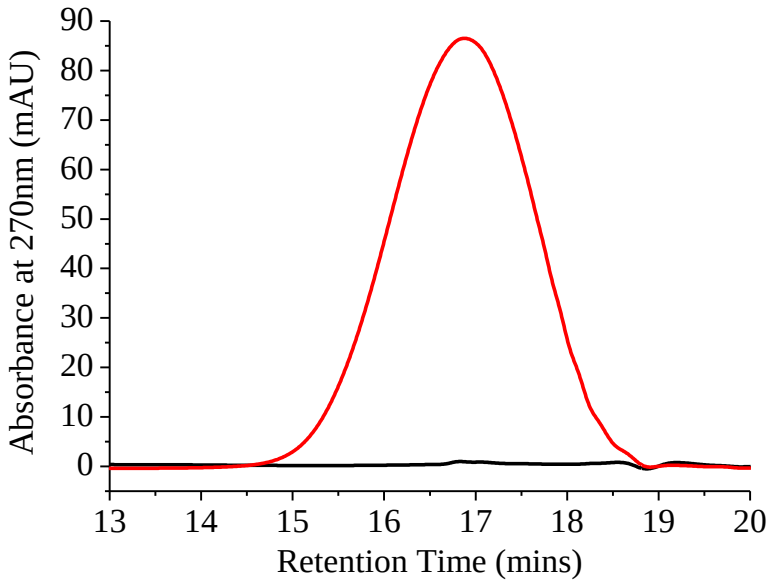

Figure 3.03. GPC traces (VWD measuring at 270 nm) of PIB$_{exo}$ and PIB$_{endo}$ (black) and PIBP (red).

3.2.2. Synthesis of polyisobutylene acrylate (PIBA)

Following the synthesis of PIBP it is now desired to transform the phenolic end group into a monomeric functionality and as such synthesise a PIB macromonomer. Phenols react slowly with carboxylic acids but react readily with acyl halides in the

presence of base to form esters. Therefore PIBP was esterified with acryloyl chloride in the presence of triethylamine (TEA) to synthesise polyisobutylene acrylate (PIBA) (Scheme 3.04). This synthetic approach to synthesise PIBPs with acrylate functionality has only been employed previously to synthesise telechelic PIB acrylates.[35] An acrylate PIB macromonomer synthesis was initially chosen as there has been impressive recent literature that documents the control of homopolymerisation and copolymerisation, with acrylamides, of acrylates to synthesise highly sequence controlled multi block copolymers as well as sequence controlled oligomers.[36,37] This is a strong demonstration of the high end group fidelity that can be achieved during RAFT polymerisation, which is essential to synthesise block copolymers such as the desired structures in Scheme 3.02.

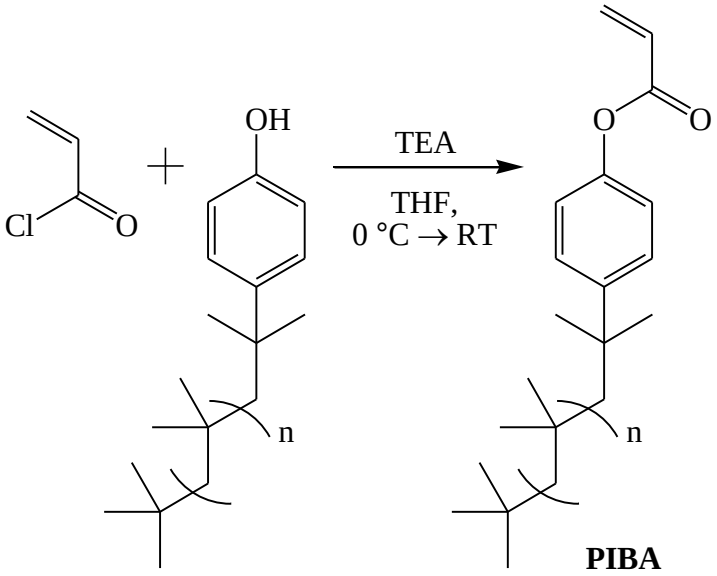

Scheme 3.04. Synthesis of PIBA by esterification of PIBP with acryloyl chloride.

Esterification of PIBP with acryloyl chloride to PIBA was confirmed by ^{1}H-NMR spectroscopy (Figure 3.04). Doublets corresponding to the four phenolic protons at 6.68 and 7.16 ppm shift down field following esterification to 6.96 and 7.29 ppm respectively. Furthermore, vinyl protons are observable at 5.90, 6.21 and 6.50 ppm which match the expected relative integrations (Figure 3.04). By relative integration

of PIBA's phenolic proton resonances to the residual PIBP phenolic proton resonances it is calculated that 98% of the PIBP was esterified to PIBA. Furthermore, relative integration of the -C(CH_3)$_3$ (H^a) PIB α-terminus at 0.97 ppm to ω-terminus acrylate protons estimates 77% of the PIB chains are acrylate functionalised. End group fidelity of PIBA is lower than other examples of PIB acrylates in the literature, but synthesis of PIBA represents a PIB macromonomer synthesis from readily available PIB that utilises the majority of terminal olefin functionality that was present on the starting PIB.

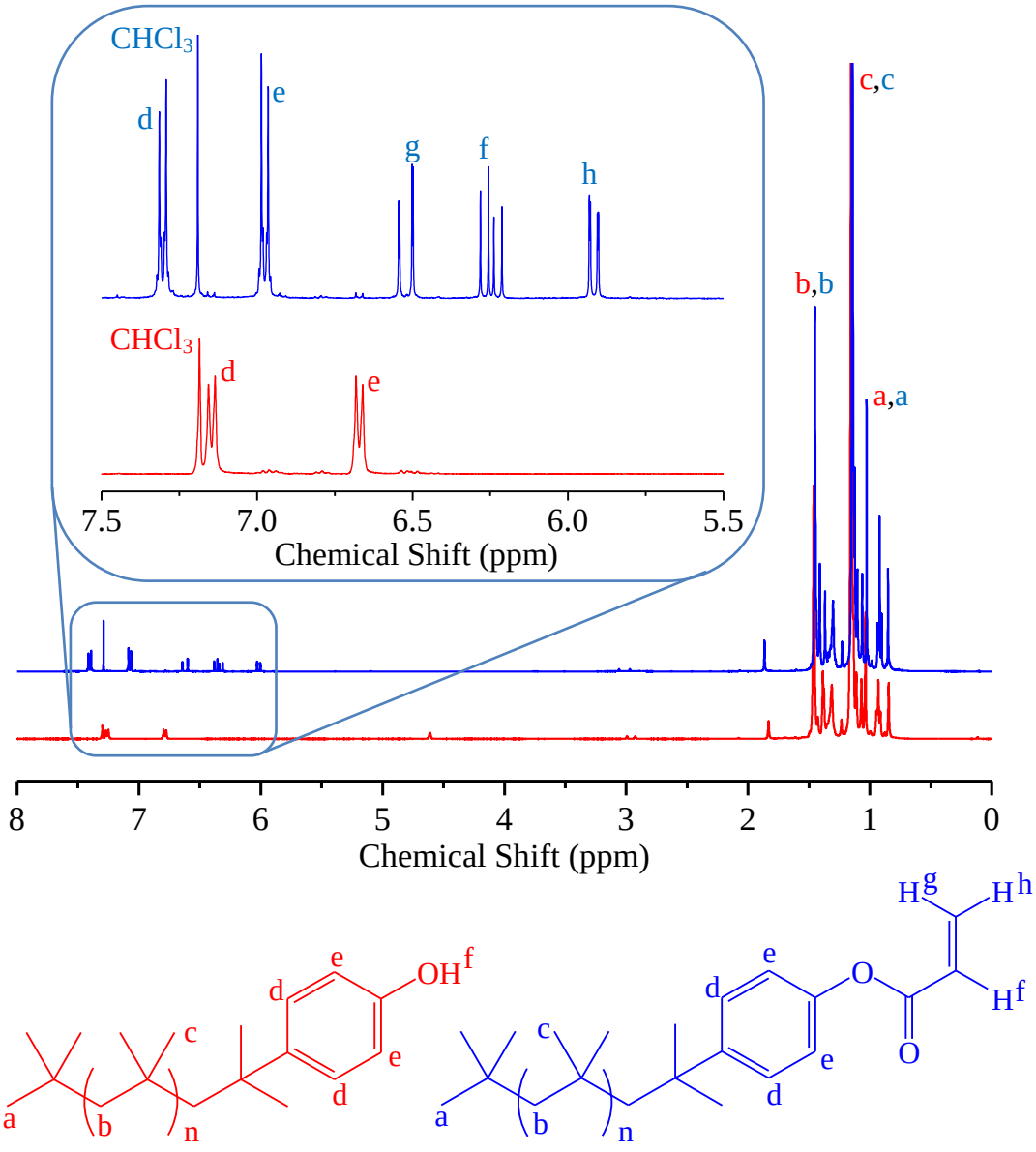

Figure 3.04. ^{1}H-NMR spectrum ($CDCl_3$, 400 MHz, 303 K) of PIBP (red) and PIBA (blue).

^{13}C-NMR spectroscopy is also utilised to confirm the esterification of PIBP to PIBA by the appearance of three new resonances at 128.19 ppm, 132.13 ppm and 164.55 ppm that correspond to the three carbon atoms of the new acrylate functionality; C^f, C^g and C^j respectively (Figure 3.05). Furthermore, all four of the phenolic carbon resonances are shifted after esterification to an acrylate (Figure 3.05).

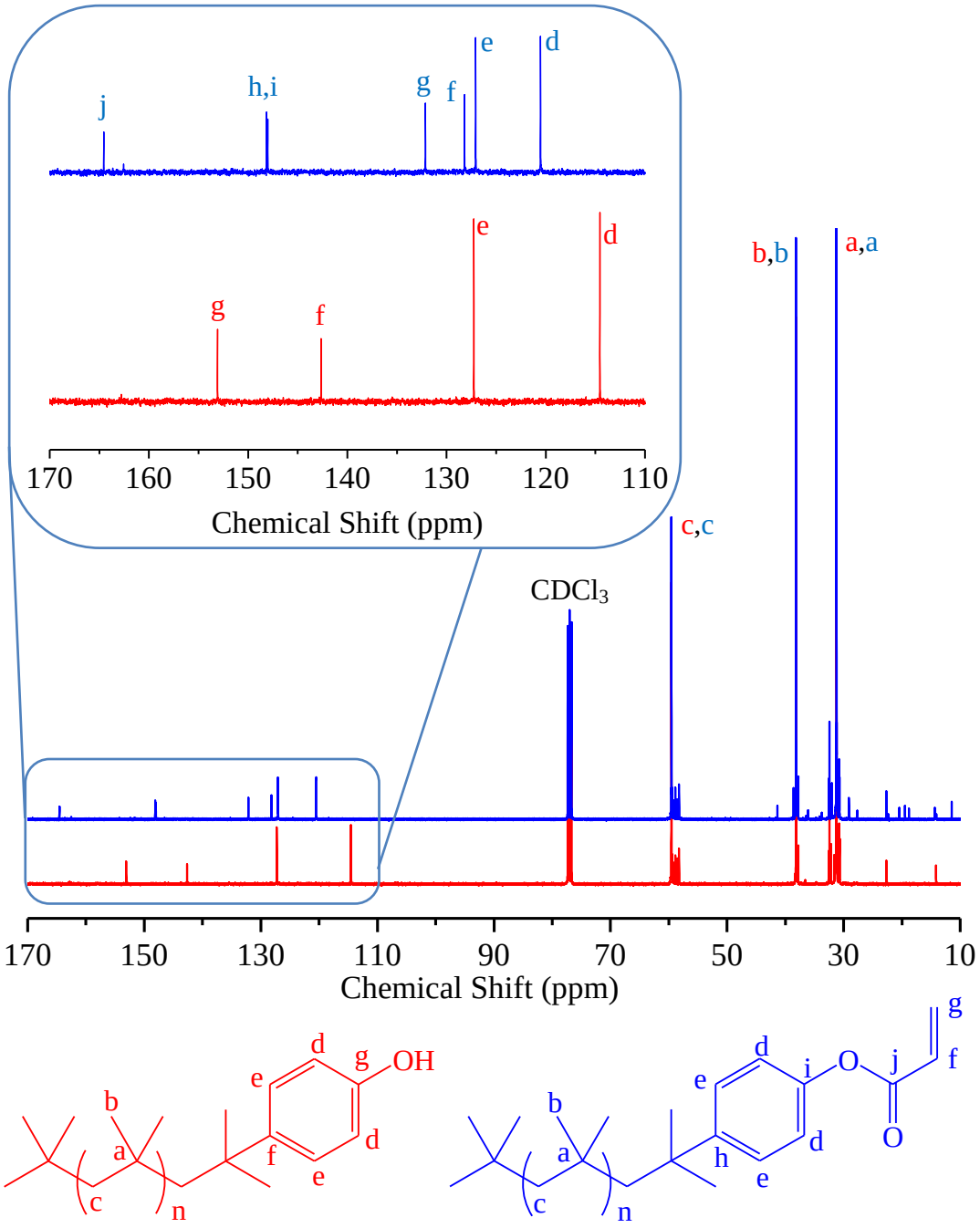

Figure 3.05. ^{13}C-NMR spectrum ($CDCl_3$, 400 MHz, 303 K) of PIBP (red) and PIBA (blue).

GPC measures an increase in M_n after esterification of PIBP to PIBA; M_n increases from 1200 to 1400 g·mol^{-1} and dispersity remains consistent only decreasing from 1.60 to 1.57. GPC traces demonstrate this increase in M_n by a slight shift to the right but perhaps more importantly is that there is no evidence of autopolymerisation occurring throughout the esterification or purification which would have manifested as a high molecular weight shoulder (Figure 3.06).

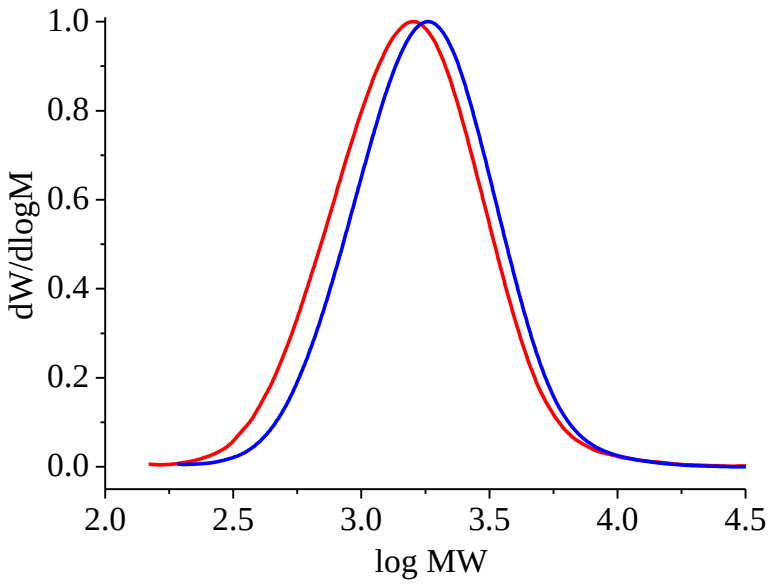

Figure 3.06. GPC traces (RID) of PIBP (red) and PIBA (blue).

PIBA was also analysed by MALDI-TOF MS (Figure 3.07). The MALDI-TOF spectrum shows one predominant distribution and another minor distribution that is separated from the former by ~20 Da. Both of these distributions have a difference of ~56.04 Da between consecutive peaks which corresponds well to the theoretical monoisotopic mass of the PIB repeat unit of 56.06 Da (Figure 3.07). Therefore, each peak is expected to correspond to a single PIBA molecule consisting of an integer number of isobutylene repeat units and the desired end groups, *tert*-butyl and phenolic acrylate.

Theoretical monoisotopic mass of PIBA molecules with DP of 1 (424.1 Da) through to 40 (2610.64 Da) were calculated. Theoretical mass was found to correspond poorly with the observed mass of both distributions on the MALDI-TOF spectrum. The theoretical mass was on average 6 Da greater than the measured mass, as shown by the theoretical/measured mass of PIBA with DP of 6 and 7 (Figure 3.07).

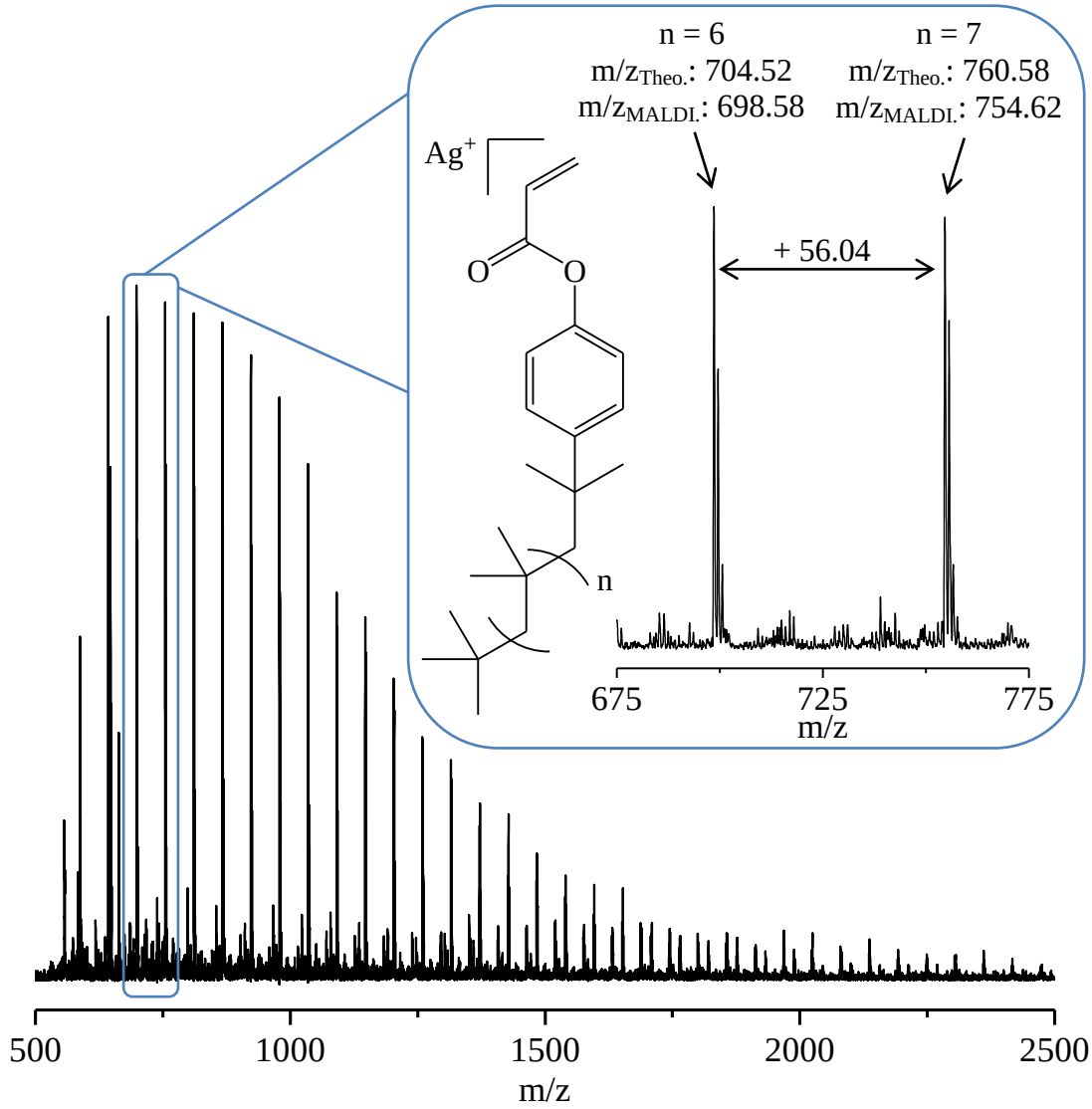

Figure 3.07. MALDI-TOF spectrum of PIBA with a zoomed region between 675 and 775.

This difference of 6 Da between theoretical and measured mass is significantly greater than any difference between theoretical and measured mass for other polymer samples measured by MALDI-TOF MS. Therefore, this may imply that the expected structure of PIBA's end groups is slightly different from the actual structure. The

ω-end group transformation of vinylidene to phenol to acrylate was confirmed by ^{1}H-NMR/^{13}C-NMR spectroscopy and GPC so is expected to be correct. The α-end group structure however is determined by the polymerisation conditions employed. PIB utilised for the synthesis of PIBA was commercially sourced PIB and as such the exact polymerisation conditions for its synthesis, in particular the initiating system, are unknown. This makes the exact identity of the α-end group less certain and as such a more likely cause of the mass difference observed by MALDI-TOF MS of PIBA. The commercial PIB provided was "highly reactive" PIB. "Highly reactive" PIB is synthesised by using initiator systems of BF_3 complexes with water/alcohols and ethers.[24] These systems synthesise PIBs with a *tert*-butyl α-end group, presence of this end group is supported by the ^{1}H-NMR spectrum of PIB which has a singlet at 1.00 ppm (Figure 3.01). Alternatively IB polymerisation can be initiated with tertiary alkyl halide – Lewis acid complexes to generate a carbocation to initiate the polymerisation.[24,38] Therefore, the α-end group and by extension the exact mass of the PIB synthesised would depend on the alkyl halide utilised to initiate polymerisation, therefore this could be a potential cause of the mass difference observed for PIBA.

Unfortunately MALDI-TOF spectra of PIB and PIBP could not be obtained, presumably because ionisation of PIB and PIBP was not achieved with the cationising agent/matrix combinations utilised. Therefore, confirmation of the PIB initiating group could not be identified with MALDI-TOF MS. Despite some uncertainty of PIBA's exact end group structure, it was demonstrated that PIBA does contain high levels of acrylate functionality, thus satisfying the first requirement of synthesising the desired copolymers described in Schemes 3.01 and 3.02.

3.3. Synthesis of statistical copolymers of DMA/DMAEA and PIBA

The synthesised PIBA was copolymerised with small molecule acrylates/acrylamides via RAFT copolymerisation to synthesis statistical copolymers bearing PIB grafts.

3.3.1. RAFT homopolymerisation of DMA

It is vital to confirm that the chosen small molecule monomer polymerises in a controlled manner before incorporation of any PIBA. *N*,*N*-dimethylacrylamide (DMA) homopolymerisation was first attempted using 3-butyl-2-(dodecylthiocarbonothioylthio)-2-methylpropionate (BDTMP) as RAFT agent and V601 as initiator in toluene at 70 °C (Scheme 3.05). These conditions were chosen as there are previous reports that utilise a trithiocarbonate RAFT agent and azo-initiator to polymerise DMA in a highly controlled manner.[39,40]

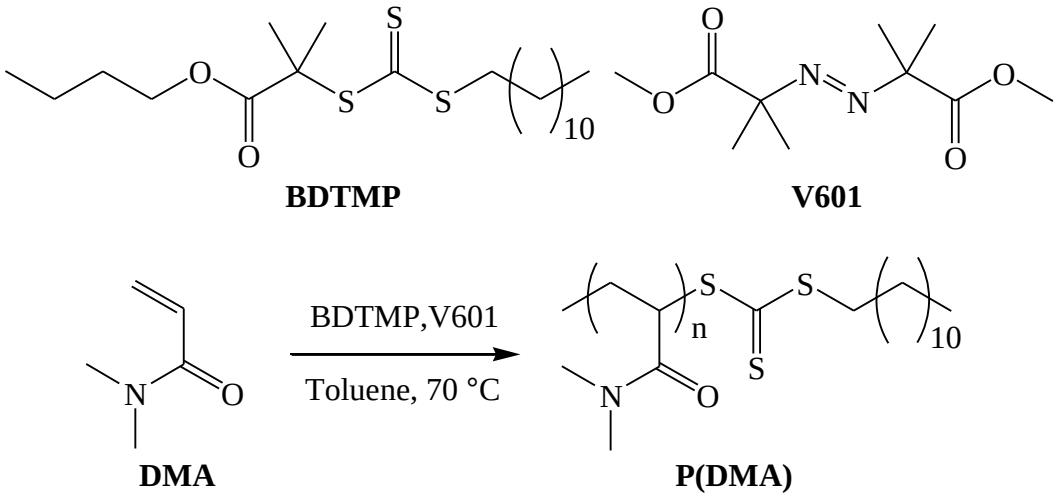

Scheme 3.05. Structure of BDTMP and V601 (top). RAFT homopolymerisation of DMA, initiated by V601 and mediated by BDTMP in toluene at 70 °C (bottom).

Samples were taken from the polymerisation at regular intervals to determine if DMA could be homopolymerised in a controlled manner using the above conditions and if the polymerisation displays pseudo first order kinetics. Producing a semi-logarithmic plot of the natural logarithm of DMA concentration against time displays a linear correlation and as such first order kinetics (Figure 3.08). An induction period

is observed for the first 15 minutes of polymerisation, this phenomenon has been observed in other RAFT agent/monomer pairs as well as DMA homopolymerisation mediated by a dithiobenzoate.[41-43] Davis and co-workers report the origin of an induction period such as this likely occurs because of slow fragmentation of the initial intermediate macroRAFT radical as the stability of the initial RAFT agent after addition of a radical is different to that of the macroRAFT radical.[43] Despite the induction period; pseudo first order kinetics are observed for the remainder of DMA homopolymerisation up to 99% DMA conversion when the last sample was taken.

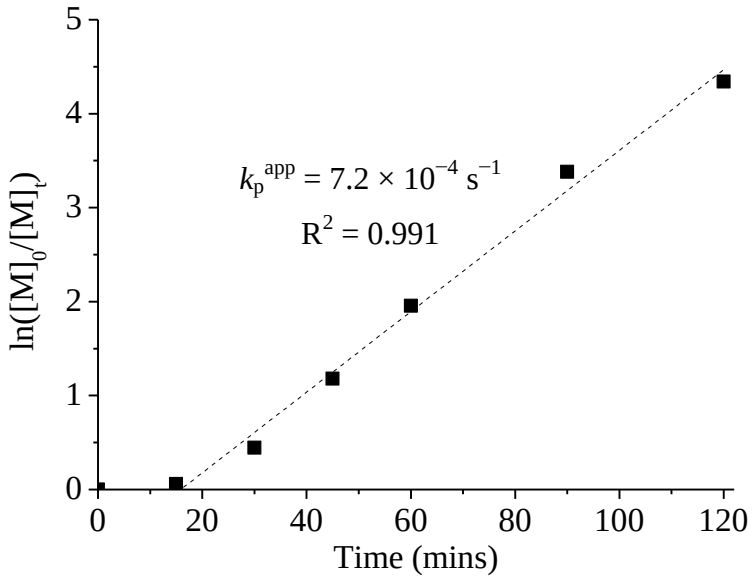

Figure 3.08. Semi-logarithmic kinetic plot for RAFT homopolymerisation of DMA (P3.01) in toluene at 70 °C, mediated by BDTMP and initiated by V601.

Evolution of M_n was also measured for the RAFT homopolymerisation of DMA. Very good agreement between the theoretical M_n and M_n measured by GPC was observed, indicating that M_n of the P(DMA) is increasing proportionally with total monomer conversion as is expected of a controlled radical polymerisation (Figure 3.09). Furthermore, P(DMA) dispersity remains consistently narrow (~1.1) throughout the entirety of the polymerisation, another expectation of controlled

radical polymerisation. Evolution of P(DMA) molecular weight is also demonstrated by the shift to higher molecular weight of overlaid GPC traces (Figure 3.10).

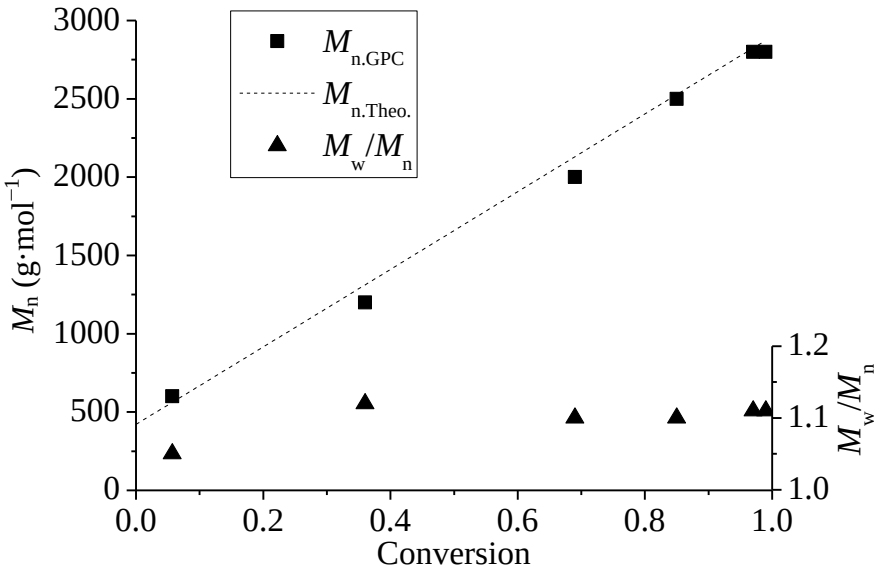

Figure 3.09. Measured M_n, theoretical M_n and M_w/M_n versus DMA conversion for RAFT homopolymerisation of DMA (P3.01) in toluene at 70 °C, mediated by BDTMP and initiated by V601.

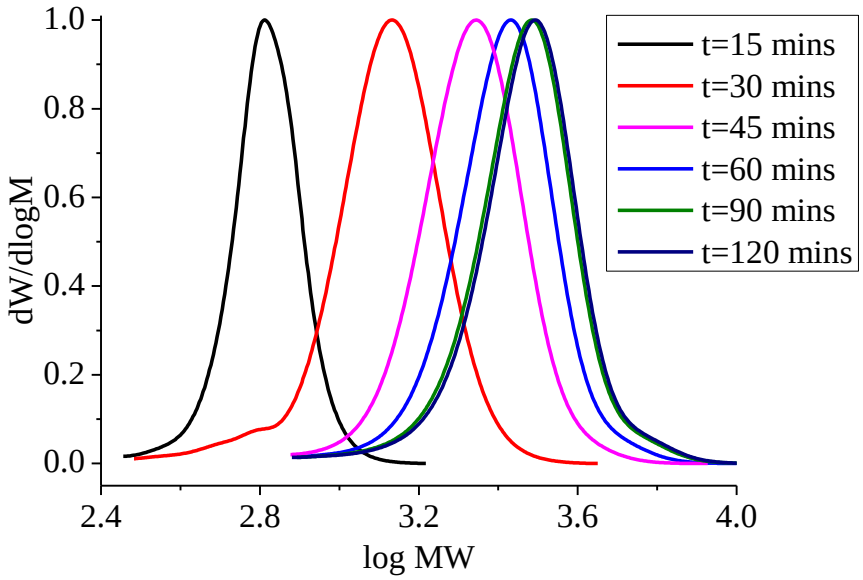

Figure 3.10. Evolution of GPC traces (RID) of P(DMA) during the RAFT homopolymerisation of DMA (P3.01) in toluene at 70 °C, mediated by BDTMP and initiated by V601.

RAFT homopolymerisation of DMA was subsequently scaled up (~10g) to synthesise P(DMA) that will be chain extended with PIBA (Table 3.01). After

obtaining kinetic measurements for RAFT homopolymerisation of DMA the intention was to stop the polymerisation at ~80% which occurred after 60 minutes. There is evidence that terminating RAFT polymerisations at lower monomer conversion improves the end group fidelity of the final polymer,[44,45] despite terminating the polymerisations after 60 minutes the final DMA conversion was found to be significantly higher at >95% (Table 3.01). This may be because these polymerisations were not sampled and as such were less disturbed and proceeded to polymerise faster to an overall greater conversion of DMA.

Table 3.01. GPC characterisation and DMA conversion for RAFT homopolymerisation of DMA in toluene at 70 °C, mediated by BDTMP and initiated by V601.

Sample	[DMA]:[BDTMP]: [V601]	DMA Conversion$^{\alpha}$ (%)	$M_{n.GPC}{}^{\beta}$ (g·mol^{-1})	$M_{n.Theo}{}^{\gamma}$ (g·mol^{-1})	$Đ^{\beta}$
P3.02	25:1:0.1	95	2600	2800	1.14
P3.03	15:1:0.1	99	1700	1900	1.14

$^{\alpha}$Calculated from GC-FID. $^{\beta}$THF + 2% TEA eluent, calibrated with PS standards. $^{\gamma}$Calculated from Equation 1.

End group fidelity is of paramount importance during and after RAFT polymerisation as the trithiocarbonate end group must be preserved if the synthesised polymer is to be used as a macroRAFT agent and chain extended with one or more monomers to synthesise diblock or multiblock copolymers. ^{1}H-NMR spectroscopy is an effective technique for determining the end group fidelity of polymers synthesised by RAFT or any other CRP technique. The ^{1}H-NMR spectrum of P3.02 is shown in Figure 3.11. Integration of the P(DMA) repeat unit resonances (H^{e-f}) against the -CH_2- (H^{d}) resonance immediately adjacent to the trithiocarbonate end group, indicates a DP of 23. This agrees well with the expected DP of 24; calculated from the initial DMA to BDTMP ratio multiplied by DMA conversion. This DP is further

supported by a relative integration of 1.9 for the resonance centred at 4 ppm, corresponding to the $–CH_2COO-$ (H^i) of BDTMP's R group. Expected relative integration of H^d to H^i should be 2:2. It is also worthy of note that the radical initiator utilised (V601) is a methyl ester as opposed to the butyl ester of BDTMP's R group. This slight difference in structure of potential initiating species is observed and quantified by ^{1}H-NMR. Integration of the resonance centred at 3.6 ppm, corresponding to the V601 methyl ester, reveals 13% of the P(DMA) chains were initiated by the radical generate from V601 decomposition (Figure 3.11).

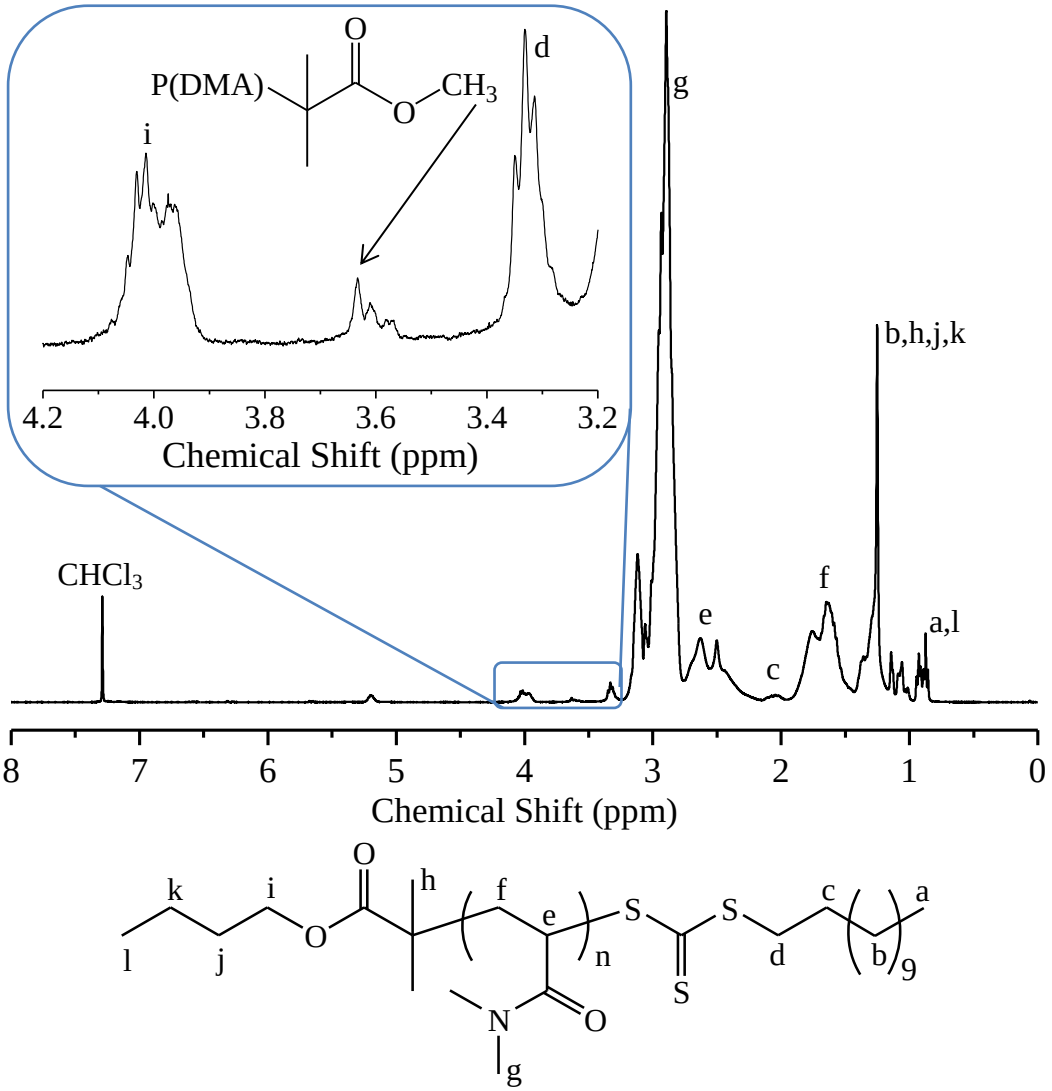

Figure 3.11. ^{1}H-NMR spectrum ($CDCl_3$, 400 MHz, 303 K) of P(DMA) (P3.02).

UV-vis spectroscopy of BDTMP in THF with 2% TEA by volume was found to have a maximum absorbance at 308 nm. This solvent mixture was selected as this was the eluent mixture for all GPC measurements. GPC measurements of P3.02 using the RID and VWD set to 308 nm gives two GPC traces which overlap well, indicating that the entire polymer distribution observed by the RID has a functional group (trithiocarbonate end group) which absorbs at 308 nm (Figure 3.12).

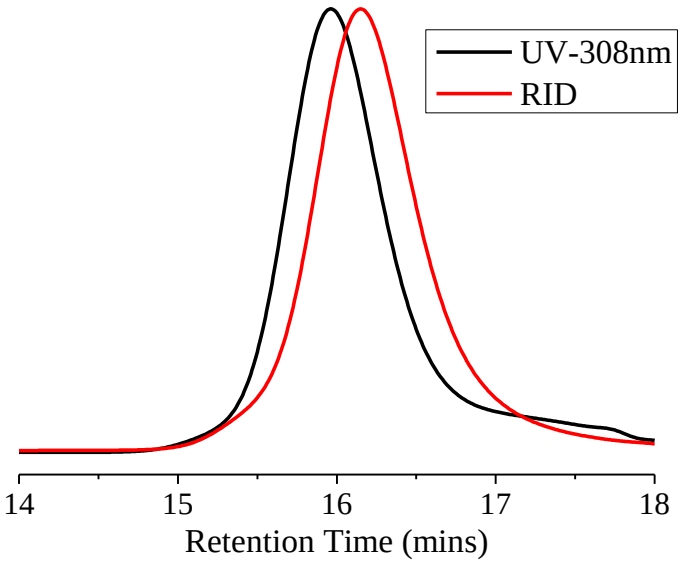

Figure 3.12. GPC traces of P3.02 measured by VWD set to 308 nm (black) and RID (red).

3.3.2. RAFT homopolymerisation of DMAEA

Copolymerisation of acrylates with PIBA was also investigated and the acrylate monomer first chosen to copolymerise with PIBA was 2-(dimethylamino)ethyl acrylate (DMAEA). This monomer was chosen in particular because it has been previously shown to be polymerised in a controlled way by RAFT with a trithiocarbonate RAFT agent,[46,47] furthermore the methacrylate (DMAEMA) analogue of DMAEA has been utilised in DVMs.[32,33]

DMAEA was homopolymerised by RAFT polymerisation using the same conditions developed earlier for DMA; polymerisation is initiated by V601 and mediated by

BDTMP in toluene at 70 °C (Scheme 3.06). Samples were taken from the polymerisation at regular intervals to measure the DMAEA conversion, P(DMAEA) M_n and dispersity over time.

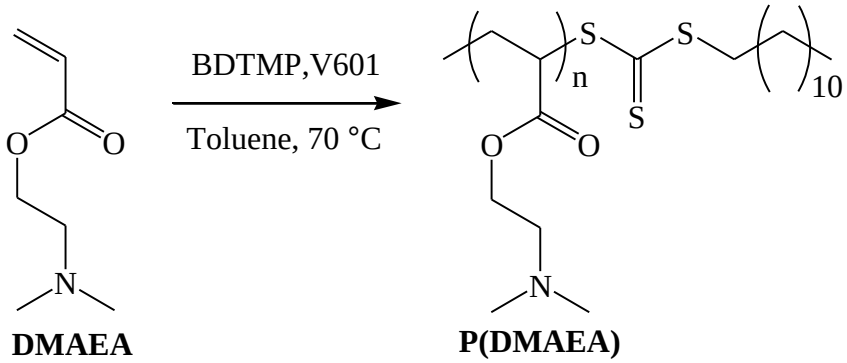

DMAEA **P(DMAEA)**

Scheme 3.06. RAFT homopolymerisation of DMAEA, initiated by V601 and mediated by BDTMP in toluene at 70 °C.

A semi-logarithmic kinetic plot for DMAEA RAFT homopolymerisation shows a linear relationship and as such pseudo first order kinetics, final DMAEA conversion was 76% after 3 hours when polymerisation was terminated (Figure 3.13).

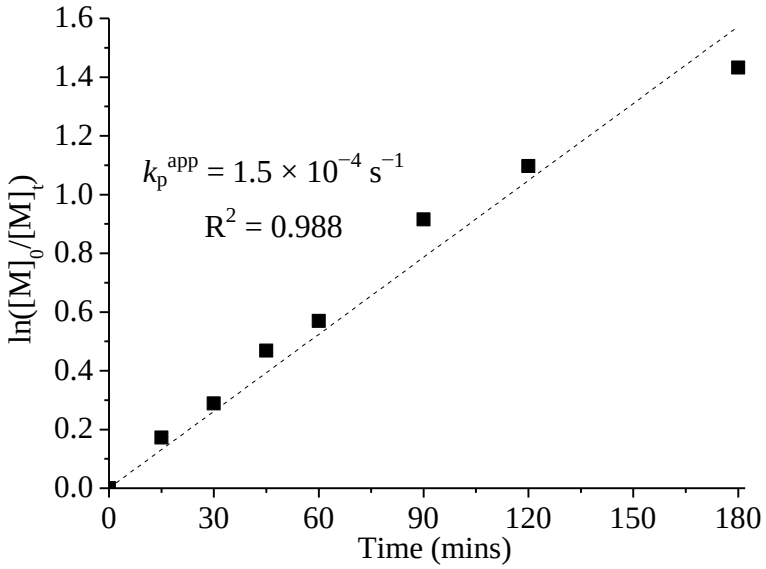

Figure 3.13. Semi-logarithmic kinetic plot for RAFT homopolymerisation of DMAEA (P3.04) in toluene at 70 °C, mediated by BDTMP and initiated by V601.

M_n of the growing P(DMAEA) chain was measured by GPC for each sample taken throughout the polymerisation. M_n of P(DMAEA) was shown to increase linearly

with DMAEA conversion and closely matched the P(DMAEA) theoretical M_n (Figure 3.14). P(DMAEA) dispersity also remained controlled throughout the polymerisation at ~1.2. Evolution of molecular weight is also demonstrated by the shift to higher molecular weight of overlaid GPC traces of each subsequent sample taken (Figure 3.15). Tailing towards lower MW is apparent for the GPC traces of P(DMAEA), this may be a consequence of non-reversible termination occurring throughout the polymerisation or a result of P(DMAEA) interacting with column material during a GPC measurement. As the kinetic plot (Figure 3.13) showed a linear relationship throughout the time measured, non-reversible termination is unlikely to be the significant factor of the GPC tailing. Therefore, non-specific interactions between P(DMAEA) and column material is expected to be the significant cause of the GPC tailing and agrees with tailing encountered in Chapter 2 when measuring GPC of P(DMAEMA) samples.

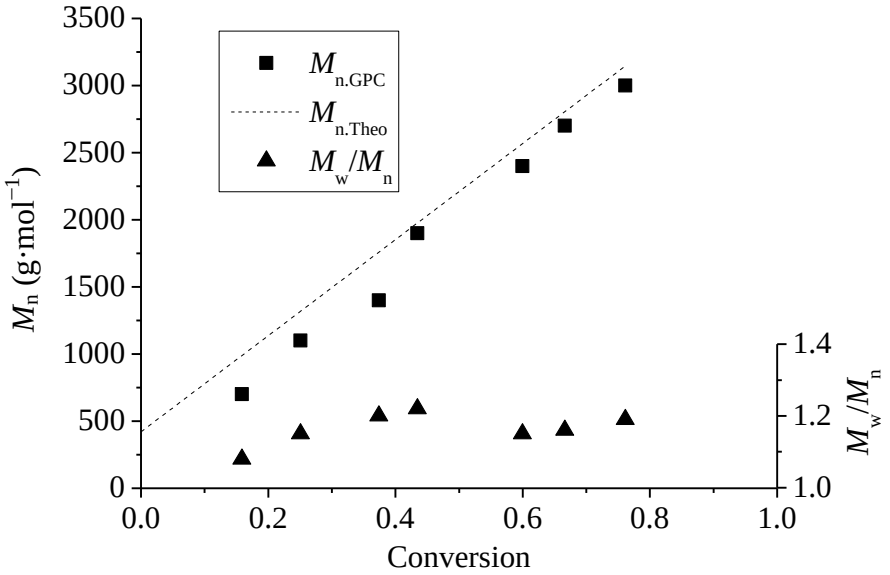

Figure 3.14. Measured M_n, theoretical M_n and M_w/M_n versus DMAEA conversion for RAFT homopolymerisation of DMAEA (P3.04) in toluene at 70 °C, mediated by BDTMP and initiated by V601.

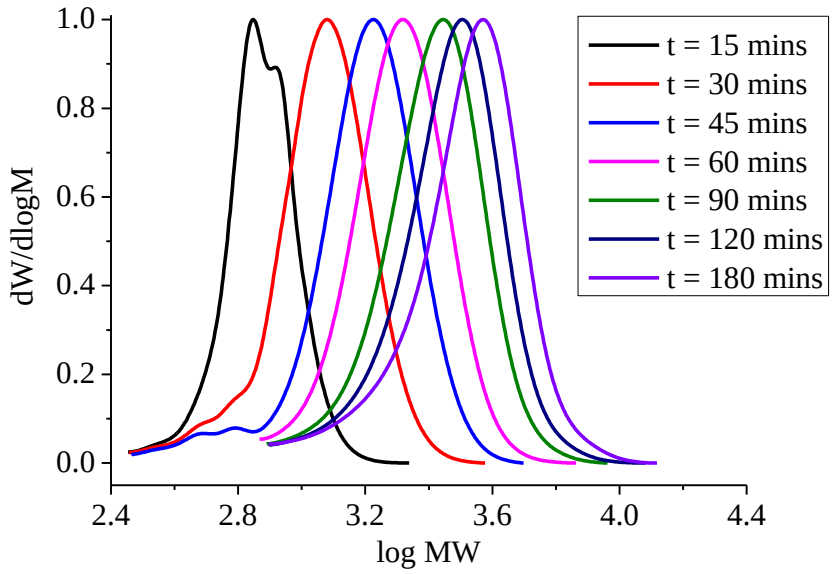

Figure 3.15. Evolution of GPC traces (RID) of P(DMAEA) during the RAFT homopolymerisation of DMAEA (P3.04) in toluene at 70 °C, mediated by BDTMP and initiated by V601.

RAFT homopolymerisation of DMAEA was subsequently scaled up to synthesise P(DMAEA) that will be chain extended with PIBA (Table 3.02). After obtaining kinetic measurements for RAFT homopolymerisation of DMAEA the intention was to stop the polymerisation at ~75%, which occurred after 180 minutes. This was for the same reasons as for DMA homopolymerisation, to preserve the end group fidelity by limiting monomer conversion. Despite terminating the polymerisations after 180 minutes the DMAEA conversion was significantly higher than expected at 92%. This behaviour also occurred when polymerising DMA and was expected to be a consequence of not sampling the polymerisation. As such polymerisation was disturbed less and proceeded to polymerise faster to a higher conversion of DMAEA (Table 3.02)

.

Table 3.02. GPC characterisation and DMAEA conversion for RAFT homopolymerisation of DMAEA in toluene at 70 °C, mediated by BDTMP and initiated by V601.

Sample	[DMAEA]: [BDTMP]:[V601]	DMAEMA Conversion$^{\alpha}$ (%)	$M_{n.GPC}{}^{\beta}$ (g·mol^{-1})	$M_{n.Theo}{}^{\gamma}$ (g·mol^{-1})	$Đ^{\beta}$
P3.05	25:1:0.1	92	3700	3800	1.20

$^{\alpha}$Calculated from GC-FID. $^{\beta}$THF + 2% TEA eluent, calibrated with PS standards. $^{\gamma}$Calculated from Equation 1.

^{1}H-NMR spectroscopy was utilised to determine the end group fidelity of the precipitated P(DMAEA) sample P3.05 (Figure 3.16). Integration of the P(DMAEA) repeat unit resonances ($H^{f/g}$) against the -CH_2- (H^{c}) resonance immediately adjacent to the trithiocarbonate end group, indicates a DP of 57. 57 is much greater than the expected DP of 23; calculated from the initial DMAEA to BDTMP ratio multiplied by DMAEA conversion. Moreover, DP of 57 does not agree with the M_n measured by GPC which closely matches the theoretical M_n, implying a lack of end group fidelity. This poor end group fidelity is further supported by the relative integration of 7.5 for the resonance centred at 4 ppm, corresponding to the –CH_2– (H^{j}) of BDTMP's R group. Expected relative integration of H^{c} to H^{j} should be 2:2. Integrating H^{j} against the repeat unit resonances ($H^{f/g}$) indicates a DP of 15 which is below the aforementioned expected DP of 23 but because of H^{j} and H^{f} being merged the calculated DP will not be as reliable. Furthermore, if relative integrations of H^{c} and H^{j} are combined to a total of 4 and then compared to the repeat unit resonances ($H^{f/g}$), a DP of 24 is calculated. This is a very close match to the expected DP of 23 and may imply that BDTMP's R group is at both the α- and ω-terminus. Therefore, a major mechanism of termination occurring throughout the homopolymerisation of DMAEA could be combination of BDTMP R group radicals and propagating P(DMAEA) radicals. A lack of end group fidelity means P3.05 will likely chain

extend poorly and further optimisation of DMAEA homopolymerisation will need to be performed to maximise the end group fidelity.

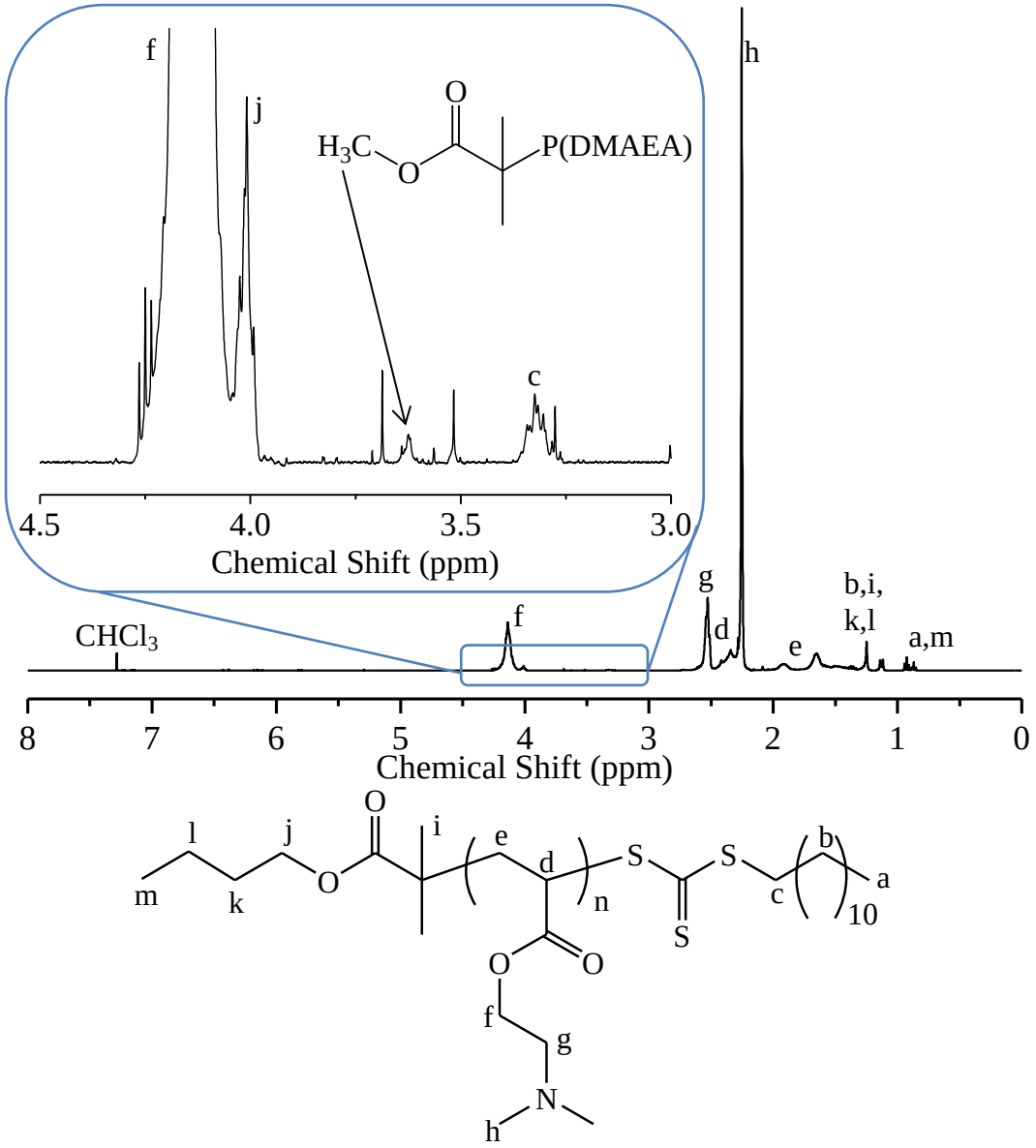

Figure 3.16. ^{1}H-NMR spectrum ($CDCl_3$, 400 MHz, 303 K) of P(DMAEA) (P3.05).

End group fidelity was shown to be diminished for the scaled up P(DMAEA) (P3.05) by ^{1}H-NMR spectroscopy. Overlaying the RID and VWD (308 nm) traces of P3.05 may reveal if any particular section of the P(DMAEA) distribution had a notable lack of trithiocarbonate end group. Overlaid RID and VWD traces show that the trithiocarbonate end group is reasonably well distributed throughout the whole distribution (Figure 3.17). A notably deviation from overlapping occurs from the

peak maximum continuing down until the base line for the entire lower molecular weight portion of the trace (Figure 3.17). This could indicate that non-reversible termination was occurring throughout the entire duration of the polymerisation.

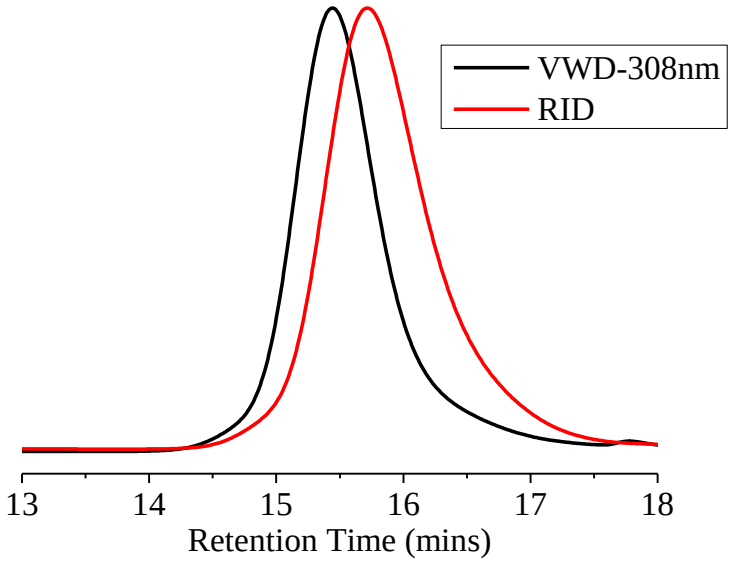

Figure 3.17. GPC traces of P3.05 measured by VWD set to 308 nm (black) and RID (red).

3.3.3. RAFT homopolymerisation of PIBA

After selecting two suitable monomers (DMA and DMAEA) to copolymerise with PIBA and confirming they can be homopolymerised with reasonable control by the selected RAFT polymerisation system; initiated by V601 and mediated by BDTMP in toluene at 70 °C. This system was utilised for the homopolymerisation of PIBA to poly(polyisobutylene acrylate) (P(PIBA)) (Scheme 3.07). This will ensure the RAFT system is suitable for each monomer before copolymerising PIBA with either DMA or DMAEA.

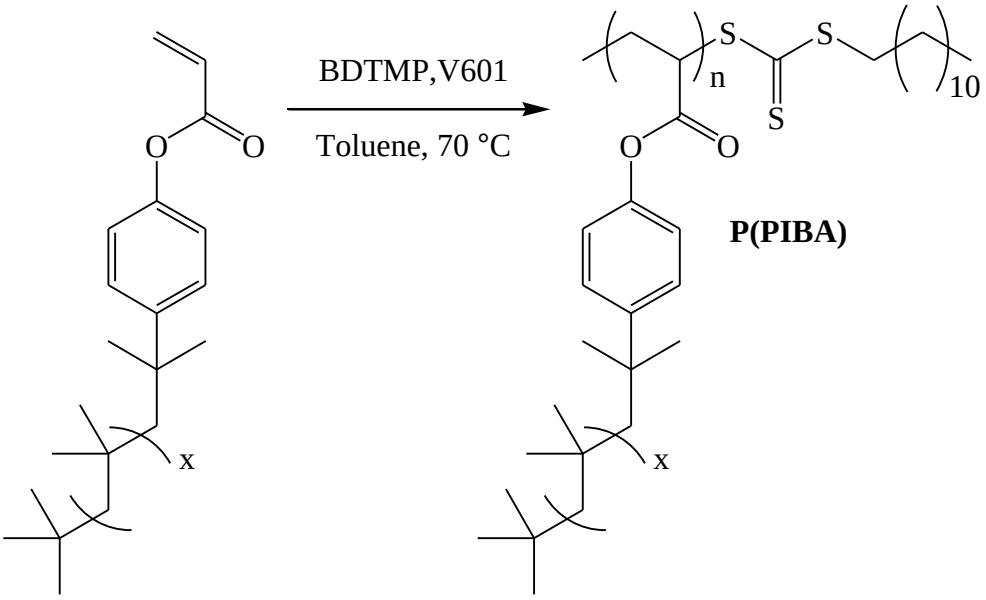

Scheme 3.07. RAFT homopolymerisation of PIBA; initiated by V601 and mediated by BDTMP in toluene at 70 °C.

Initial attempts at homopolymerising PIBA at a monomer to RAFT agent ratio of 25:1 were unsuccessful as very low conversions (~10%) of PIBA to P(PIBA) were obtained. Potential causes for low conversion of PIBA are; phenyl acrylates are incompatible with the BDTMP/V601 system, acrylate is too sterically hindered and unable to initiate/propagate fast enough, chain entanglement of the PIB chains is high and hinders mobility or an impurity is inhibiting/retarding the polymerisation, such as the residual 2% PIBP which has a *para*-substituted phenol as an end group. Substituted phenols are commonly used as radical inhibitors/retarders.[38]

A number of these potential problems could be addressed or at least minimalised by increasing the concentration of initiator. Increasing initiator concentration would increase rate of initiation and propagation as well as overpowering the PIBP which is present and may be inhibiting/retarding the polymerisation. RAFT homopolymerisation of PIBA was attempted again after reducing the monomer to initiator ratio from 25:0.1 to 10:0.1, following this initiator concentration was increased further to a new monomer to initiator ratio of 10:0.25 (Table 3.03).

Table 3.03. GPC characterisation and PIBA conversion for free radical and RAFT homopolymerisation of PIBA in toluene at 70 °C, mediated by BDTMP and initiated by V601.

Sample	[PIBA]:[BDTMP]:[V601]	PIBA Conversion$^{\alpha}$ (%)	$M_{n.GPC}{}^{\beta}$ (g·mol^{-1})	$M_{w.GPC}{}^{\beta}$ (g·mol^{-1})	$Đ^{\beta}$
P3.06	10:1:0.10	65	3000	7000	2.36
P3.07	10:1:0.25	97	4600	8800	1.93
P3.08	10:0:0.10	85	4400	55500	12.52
P3.09	10:0:0.25	95	5800	57000	9.84
P3.10	10:0:0.50	>99	5900	57800	9.83
P3.11	10:0:1.0	>99	6000	60200	9.92

$^{\alpha}$Calculated from ^{1}H-NMR spectroscopy. $^{\beta}$THF + 2% TEA eluent, calibrated with PS standards.

Increasing the initiator concentration in the RAFT homopolymerisation of PIBA had the expected result; PIBA conversion was increased significantly to 65% when using 0.1 equivalents of V601 to 10 equivalents of PIBA. Furthermore, PIBA conversion could be further increased to 97% when increasing the equivalents of V601 to 0.25. GPC measures an increase in M_n for both homopolymerisations of PIBA attempted and polymer dispersity is much higher than what is normally expected of controlled polymerisation (Table 3.03). However, high dispersity was expected as the initial monomer itself is a polymer with a broad dispersity (1.57) and polymerisation will only exaggerate this dispersity. Increase to higher molecular weight can be clearly seen when comparing the GPC traces of polymerisation after 0 hours, essentially the GPC trace of PIBA, and after ~20 hours when the polymerisation was terminated (Figure 3.18).

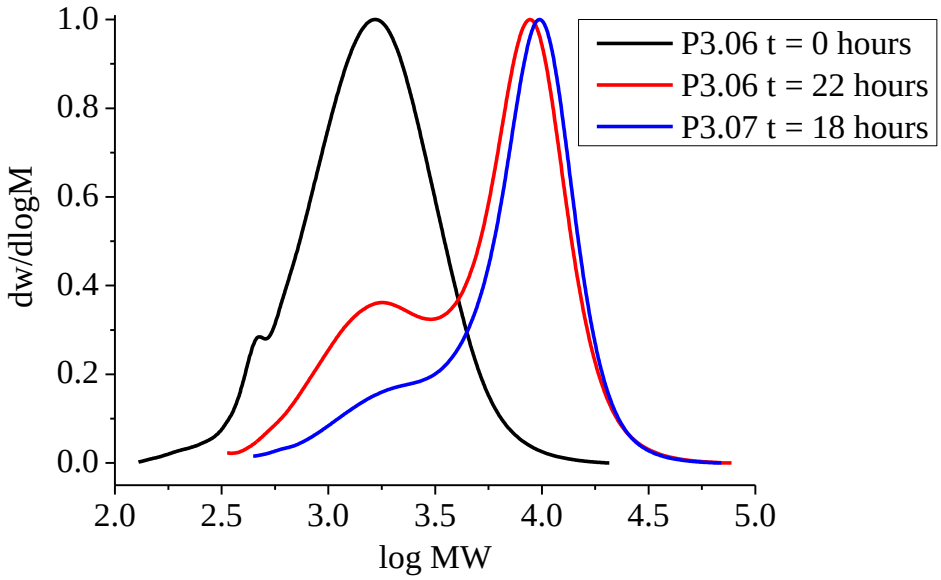

Figure 3.18. GPC traces (RID) of P(PIBA) (P3.06 and P3.07) after RAFT homopolymerisation of PIBA in toluene at 70 °C, mediated by BDTMP and initiated by V601.

Increasing the concentration of the radical initiator V601 enabled the RAFT polymerisation of PIBA to achieve high conversions (97%). However, increasing the concentration of radicals could lead to higher rates of termination, create a non-living polymerisation system and be a cause for the high dispersity of P(PIBA) samples (P3.06 and P3.07). Therefore, a short series of PIBA free radical polymerisations (P3.08-P3.11) were performed to investigate the effectiveness of BDTMP as a RAFT agent for PIBA homopolymerisation (Table 3.03). All concentrations of V601 utilised in free radical polymerisations of PIBA achieved high PIBA conversion (≥85%) but synthesised P(PIBA) with extremely high dispersity (>9.8) (Table 3.03). Furthermore, GPC traces of P(PIBA) synthesised by free radical polymerisation are very ill-defined; traces are multi modal and proceed to very high molecular weight (>1 × 10^6 g·mol^{-1}) (Figure 3.19). This indicates that BDTMP is essential for synthesising P(PIBA) with a lower dispersity and that free radical polymerisation is not occurring when BDTMP is utilised to mediate the polymerisation of PIBA.

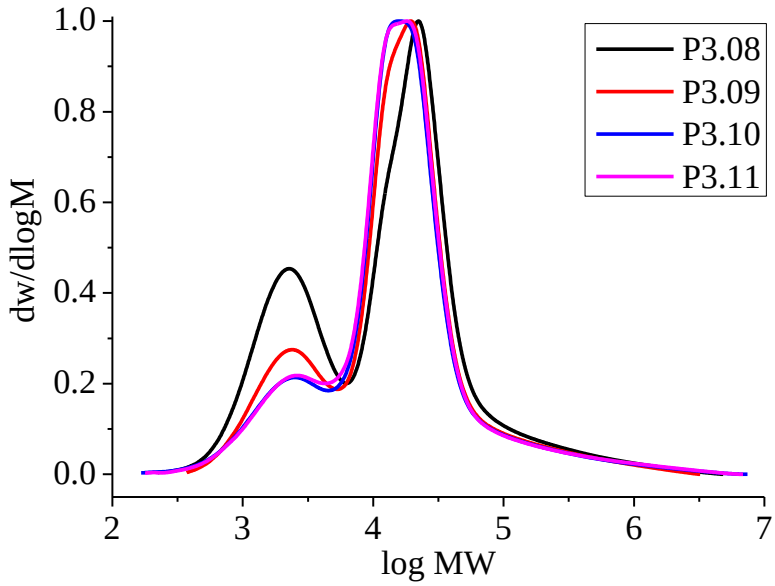

Figure 3.19. GPC traces (RID) of P(PIBA) (P3.08-P3.11) after 20 hours of free radical homopolymerisation of PIBA in toluene at 70 °C, initiated by V601.

Measured M_n of the P(PIBA) is significantly lower than the theoretical M_n calculated from the PIBA conversion; P3.06 measured M_n was 3000 g·mol^{-1} and theoretical M_n is 9200 g·mol^{-1}, P3.07 measured M_n was 4600 g·mol^{-1} and theoretical M_n is 13500 g·mol^{-1}. These discrepancies between measured and theoretical M_n will be partially caused by the lower molecular weight impurities (unfunctionalised PIB and unconverted PIBA) coeluting with the P(PIBA) distribution and being included in the final integration to measure the M_n. Furthermore, polymerising PIBA will synthesise a graft shaped polymer and these polymers as with star shaped polymers have a lower hydrodynamic volume compared to their linear homologs of the same molecular weight. This leads to an increase in retention time and thus a lower apparent M_n found by GPC when measuring with a RID and calibrating with linear polymer standards.[48,49] Universal calibration GPC utilising viscometry and light scattering detectors can be used to measure M_n of graft and star shaped polymers to attain better estimates of molecular weight averages as well as the number of branches.[48,49]

3.3.4. RAFT copolymerisation of DMA and PIBA

After confirming that the current RAFT polymerisation system was suitable for the controlled homopolymerisation of DMA and can also be used to homopolymerise PIBA to high conversions, RAFT copolymerisation of DMA and PIBA was performed to synthesise the statistical copolymer P[(DMA)-*co*-(PIBA)] (Scheme 3.08). This afforded the desired structure described at the beginning of this chapter (Scheme 3.01).

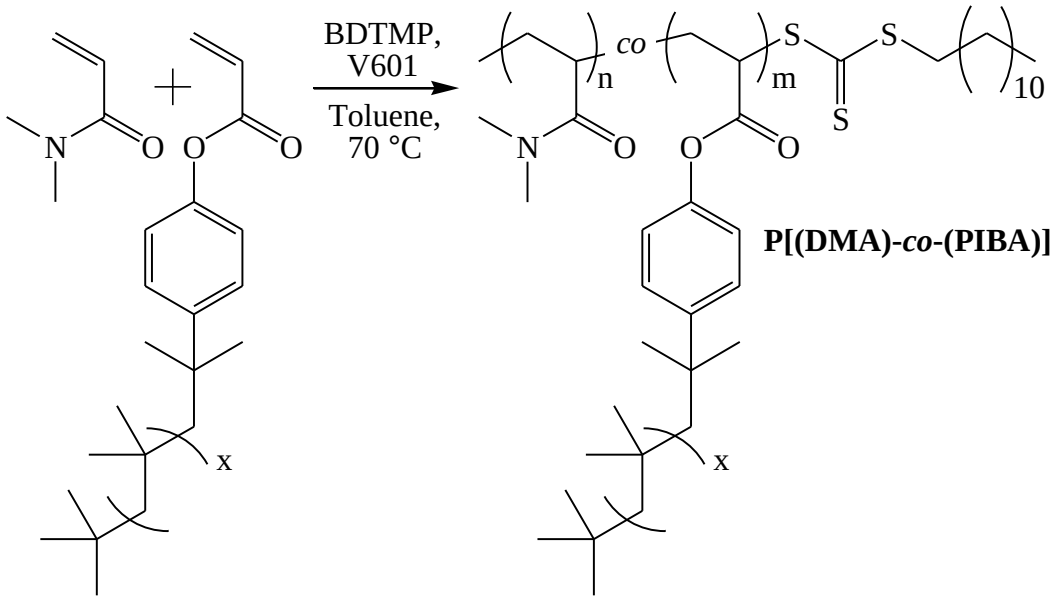

Scheme 3.08. RAFT copolymerisation of DMA and PIBA, initiated by V601 and mediated by BDTMP in toluene at 70 °C.

Kinetic measurements were performed for the RAFT copolymerisation of DMA and PIBA. DMA and PIBA conversions could be measured independently by ^{1}H-NMR spectroscopy and this revealed that the two monomers polymerised at a similar rate, at this given monomer ratio of DMA:PIBA = 22.5:2.5, showing pseudo first order kinetics after an induction period (Figure 3.20). The induction period occurred for both DMA and PIBA and lasted the same length of time. Furthermore, the induction period persisted longer than the induction period observed throughout DMA homopolymerisation, 60 minutes compared to 20 minutes. Final conversions for both

DMA and PIBA were >99%, and this is in good agreement with the conversions obtained for the RAFT homopolymerisation of DMA and PIBA performed earlier in this chapter.

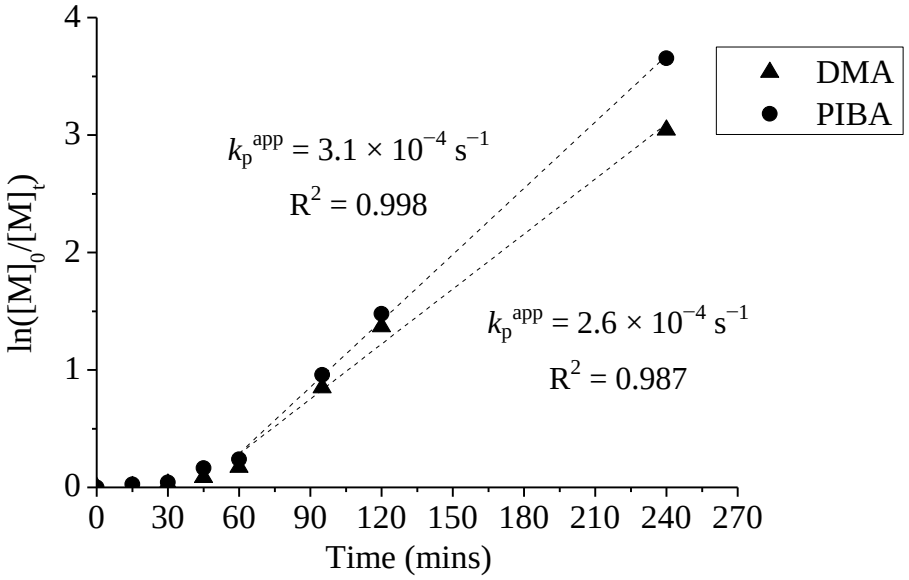

Figure 3.20. Semi-logarithmic kinetic plot for RAFT copolymerisation of DMA and PIBA (P3.12) in toluene at 70 °C, mediated by BDTMP and initiated by V601.

Measuring M_n of the growing P[(DMA)-*co*-(PIBA)] throughout copolymerisation revealed that the M_n increases with monomer conversion, however the relationship between M_n and total monomer conversion is non-linear (Figure 3.21). Moreover, M_n measured by GPC at low total conversion (<20%) is greater than the calculated theoretical M_n but as total monomer conversion increases above 20% the measured M_n becomes significantly lower than the theoretical value. This difference in measured and theoretical M_n was also observed for the RAFT homopolymerisation of PIBA and was explained as a limitation of using GPC with linear narrow molecular standards which underestimates M_n of star/graft polymers, such as this copolymer P[(DMA)-*co*-(PIBA)], as they have a lower hydrodynamic volume compared to a linear polymer of the same molecular weight.

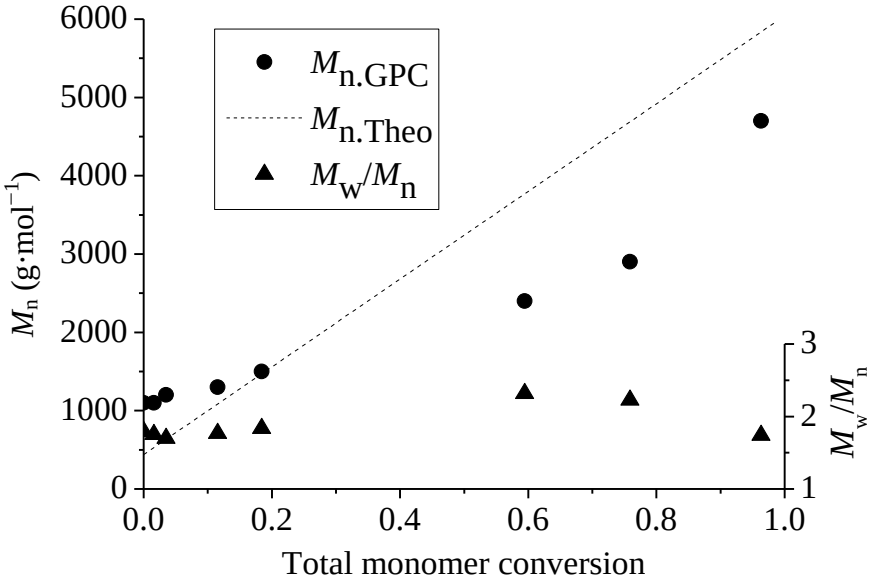

Figure 3.21. Measured M_n, theoretical M_n and M_w/M_n versus total monomer conversion for RAFT copolymerisation of DMA and PIBA (P3.12) in toluene at 70 °C, mediated by BDTMP and initiated by V601.

Overlaying GPC traces of P[(DMA)-*co*-(PIBA)] throughout copolymerisation also demonstrates the evolution of molecular weight throughout polymerisation (Figure 3.22).

RAFT copolymerisation of DMA and PIBA was then attempted with different equivalents of DMA and PIBA to synthesise P[(DMA)-*co*-(PIBA)] with a greater composition of PIBA and thus contain more hydrophobic groups relative to polar monomers.

Additional copolymerisations were performed at 20:5 (P3.13) and 15:10 (P3.14) monomer equivalents (DMA:PIBA) and were polymerised for 8 hours instead of 4 hours given the higher proportion of PIBA used in the copolymerisation (Table 3.04). P3.13 copolymerisation performed as expected and achieved >99% conversion of both DMA and PIBA; final M_n and M_w were also higher compared to P3.12 as the copolymer now contained more of the macromonomer PIBA however this did also result in an increased polymer dispersity.

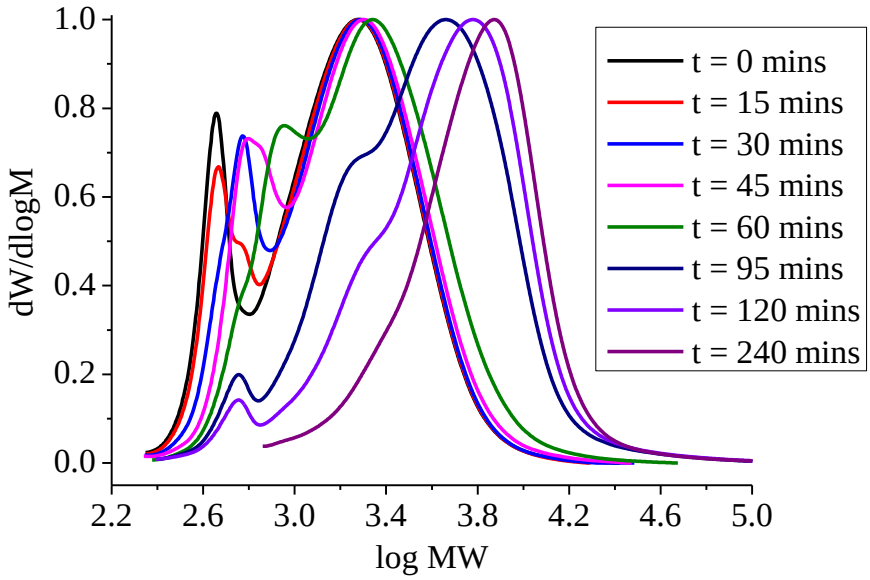

Figure 3.22. Evolution of GPC traces (RID) of P[(DMA)-*co*-(PIBA)] during the RAFT copolymerisation of DMA and PIBA (P3.12) in toluene at 70 °C, mediated by BDTMP and initiated by V601.

Copolymerisation with the highest equivalents of PIBA (P3.14) also achieved high conversion of DMA and PIBA; 95% and 85% respectively, however this was a deviation from the near-quantitative conversions obtained previously. Lower conversion of PIBA is also responsible for lowering the M_n of the final copolymer and is clearly visible on the GPC as the lower molecular weight distribution of a bimodal distribution (Figure 3.23). Regarding the asymmetry of the GPC trace for P3.14, M_w may be a more reasonable mass average to consider as it is less skewed by the low molecular weight distribution impurity and as expected P3.14 does have the highest M_w. Overlaying GPC traces of the three synthesised P[(DMA)-*co*-(PIBA)] samples also demonstrates the shift towards higher molecular weight (Figure 3.23).

Table 3.04. GPC characterisation and monomer conversions for RAFT copolymerisation of DMA and PIBA in toluene at 70 °C, mediated by BDTMP and initiated by V601.

Sample	[DMA]:[PIBA]:[BDTMP]	DMA;PIBA Conversion$^{\alpha}$ (%)	$M_{n.GPC}{}^{\beta}$ (g·mol^{-1})	$M_{w.GPC}{}^{\beta}$ (g·mol^{-1})	$Đ^{\beta}$
P3.12	22.5:2.5:1	>99;>99	5000	8500	1.70
P3.13	20:5:1	99;>99	5300	11600	2.21
P3.14	15:10:1	95;85	4800	17000	3.50

$^{\alpha}$Calculated from ^{1}H-NMR spectroscopy. $^{\beta}$THF + 2% TEA eluent, calibrated with PS standards.

These copolymerisations were performed with 0.1 equivalents of initiator relative to BDTMP, it was shown in Section 3.3.3 that increasing initiator equivalents from 0.1 to 0.25 increased PIBA conversion from 65% to 97%. This may be required as well as longer reaction times if higher proportions of PIBA are too be incorporated into a P[(DMA)-*co*-(PIBA)] copolymer.

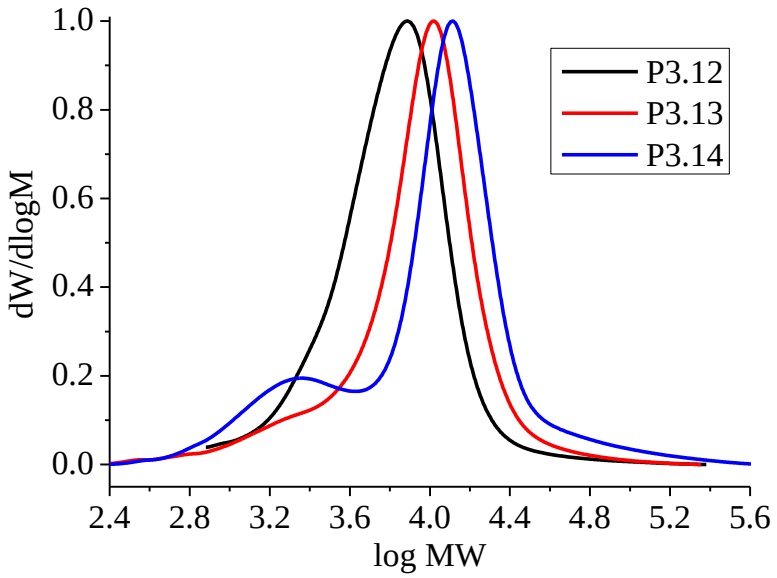

Figure 3.23. GPC traces (RID) of P[(DMA)-*co*-(PIBA)] synthesised by RAFT copolymerisation of DMA and PIBA in toluene at 70 °C, mediated by BDTMP and initiated by V601.

3.3.5. RAFT copolymerisation of DMAEA and PIBA

An analogous RAFT copolymerisation of DMAEA and PIBA was also attempted using the same conditions shown to be effective for the RAFT copolymerisation of DMA and PIBA (Scheme 3.09). Reaction time was extended to 24 hours owing to the slower polymerisation of DMAEA measured in Section 3.3.2.

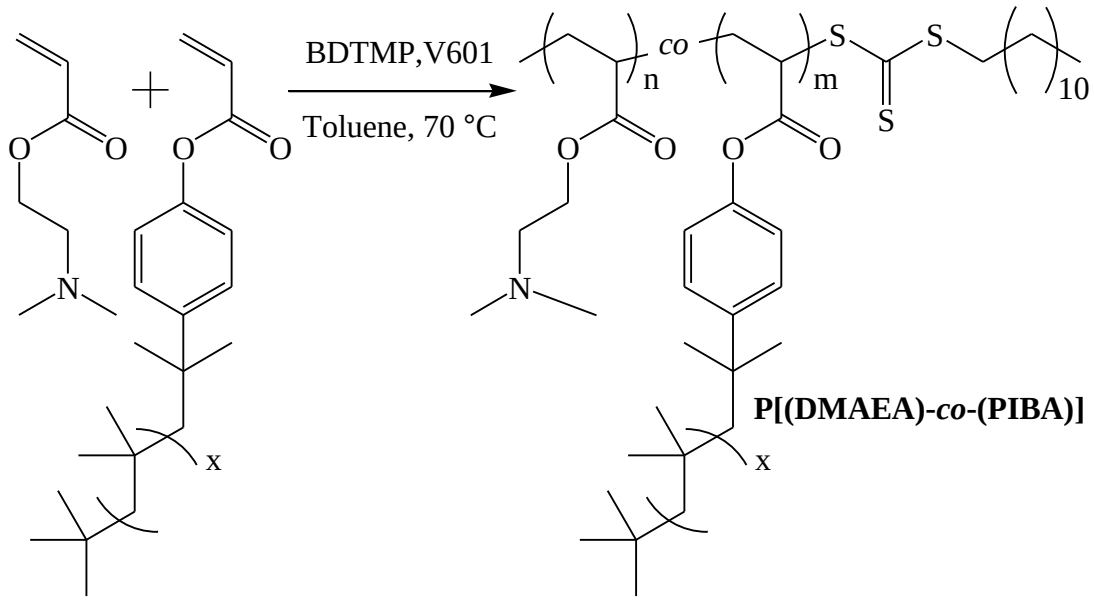

Scheme 3.09. RAFT copolymerisation of DMAEA and PIBA, initiated by V601 and mediated by BDTMP in toluene at 70 °C.

Copolymerisation was attempted at a 20:5 monomer equivalents of DMAEA to PIBA. After 24 hours at 70 °C the final conversion of DMAEA was 46% and PIBA was 58%, this is considerably lower than the analogous copolymerisation performed with DMA instead of DMAEA which reached 99% conversion for both the DMA and PIBA in only 8 hours. GPC did measure an increase in both M_n and M_w, 2800 and 6200 g·mol^{-1}, respectively, as well as an increase in polymer dispersity to 2.20. This increase in molecular weight is apparent when overlaying the GPC traces of the 0 and 24 hour time samples but it is also apparent that there is unconverted PIBA still present (Figure 3.24).

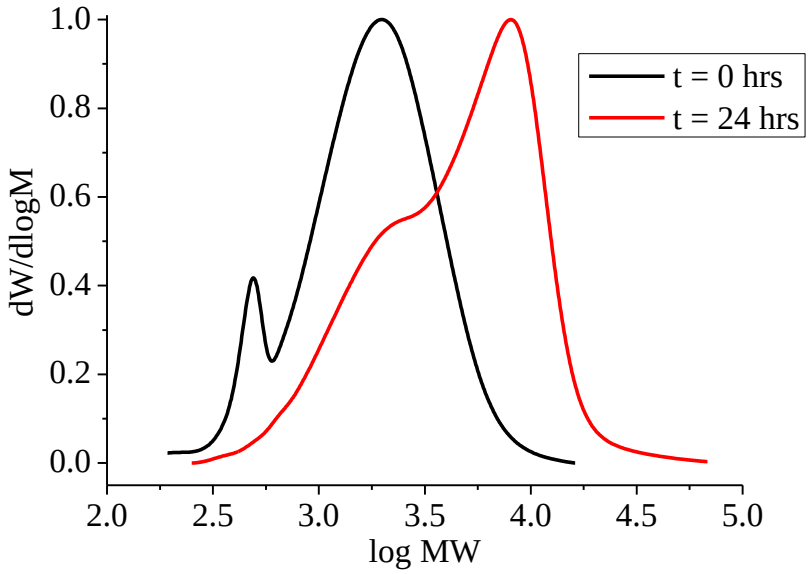

Figure 3.24. GPC traces (RID) of P[(DMAEA)-*co*-(PIBA)] (P3.15) synthesised by RAFT copolymerisation of DMAEA and PIBA in toluene at 70 °C, mediated by BDTMP and initiated by V601.

It is currently unclear why such a slow polymerisation was observed when copolymerising DMAEA with PIBA. A potential cause could be related to the loss of end group fidelity by non-reversible termination as P(DMAEA) synthesised in Section 3.3.2 was shown to have reduced end group fidelity. A reduction in rate of polymerisation was expected when copolymerising PIBA with DMAEA and this may have resulted in rates of termination now being relatively faster compared to the rate of DMAEA/PIBA propagation. This would therefore lead to the lower conversions obtained when copolymerising DMAEA and PIBA. Further optimisation is required if more copolymerisations of DMAEA and PIBA are to be attempted.

3.4. Synthesis of block copolymers of DMA and PIBA

Statistical copolymers of DMA and DMAEA with PIBA were successfully synthesised by RAFT polymerisation. A block copolymer of PIBA and P(DMA) was attempted next by exploiting the trithiocarbonate end group present on P(DMA)

homopolymer synthesised by RAFT earlier in the chapter and using those polymers as macroRAFT agents in place of BDTMP.

3.4.1. Chain extension of P(DMA) with PIBA

Chain extension of P(DMA) (P3.02) with PIBA was performed at increasingly higher equivalents of PIBA to P(DMA) whilst maintaining 0.25 equivalents of V601 to P(DMA), a ratio found earlier to be adequate at homopolymerising PIBA to very high conversion (97%) (Scheme 3.10). This synthesised a range of P[(DMA)-*b*-(PIBA)] block copolymers with a fixed chain length of the P(DMA) block whilst increasing length of the P(PIBA) block.

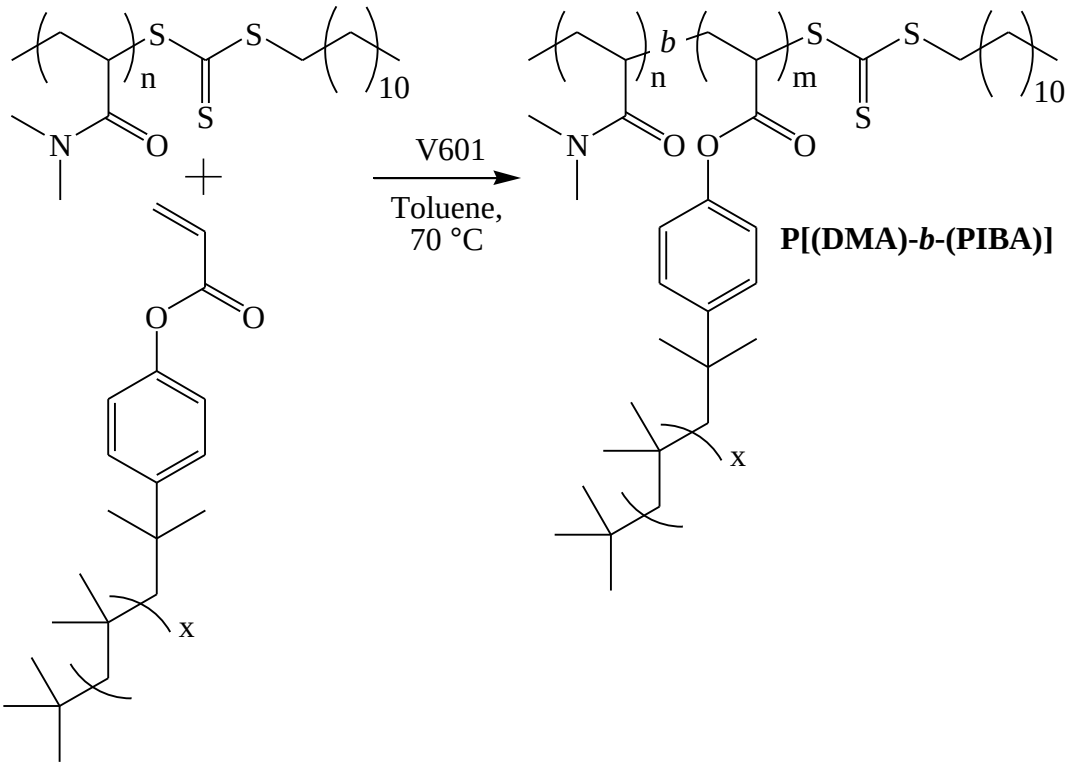

Scheme 3.10. Chain extension of P(DMA) (P3.02) with PIBA in toluene at 70 °C, initiated by V601.

Chain extension of P(DMA) with PIBA was performed at three different ratios of P(DMA) to PIBA; 1:4, 1:7 and 1:10. Conversion of PIBA was very high (≥97%) for all three chain extensions (Table 3.05). Furthermore, a notable increase of M_n and M_w, 2600 and 3000 g·mol^{-1}, respectively, of the original P(DMA) (P3.02) was

measured by GPC after 24 hours of polymerisation at 70 °C (Table 3.05). M_n and especially M_w increased to a greater extent as the equivalents of PIBA increased from 4 to 7 to 10. This is expected as each P(DMA) is now on average chain extended with more PIBA repeat units.

Table 3.05. GPC characterisation and PIBA conversion for the chain extension of P(DMA) (P3.02) with PIBA in toluene at 70 °C, initiated by V601.

Sample	[P(DMA)]: [PIBA]	PIBA Conversion$^{\alpha}$ (%)	$M_{n.GPC}{}^{\beta}$ (g·mol^{-1})	$M_{w.GPC}{}^{\beta}$ (g·mol^{-1})	$Đ^{\beta}$
P3.16	1:4	>99	6600	13000	1.96
P3.17	1:7	>99	8500	17000	2.02
P3.18	1:10	97	8800	21000	2.44

$^{\alpha}$Calculated from ^{1}H-NMR spectroscopy. $^{\beta}$THF + 2% TEA eluent, calibrated with PS standards.

However, upon inspection of the crude GPC traces of the chain extensions it was visible that all three chain extensions were bimodal and the lower molecular weight distribution corresponded to the P(DMA) macroRAFT agent (Figure 3.25). This indicates that some of the P(DMA) failed to reinitiate and was not chain extended with PIBA. Fortunately the solubility of the initial P(DMA) and newly synthesised P[(DMA)-*b*-(PIBA)] are sufficiently different so the P(DMA) can be removed by precipitation into acetone in which the P[(DMA)-*b*-(PIBA)] is insoluble. Purification of the P[(DMA)-*b*-(PIBA)] samples is shown by GPC through the disappearance of the distribution which corresponded to the P(DMA) (Figure 3.26). However, there is still a low molecular weight shoulder on the P[(DMA)-*b*-(PIBA)] distributions which is caused by the presence of unfunctionalised PIB which contains no terminal olefin and as such was not possible to be modified to PIBA via Friedel-Crafts alkylation of

phenol and subsequent esterification. Precipitated molecular weight averages and dispersity is reported in Table 3.05.

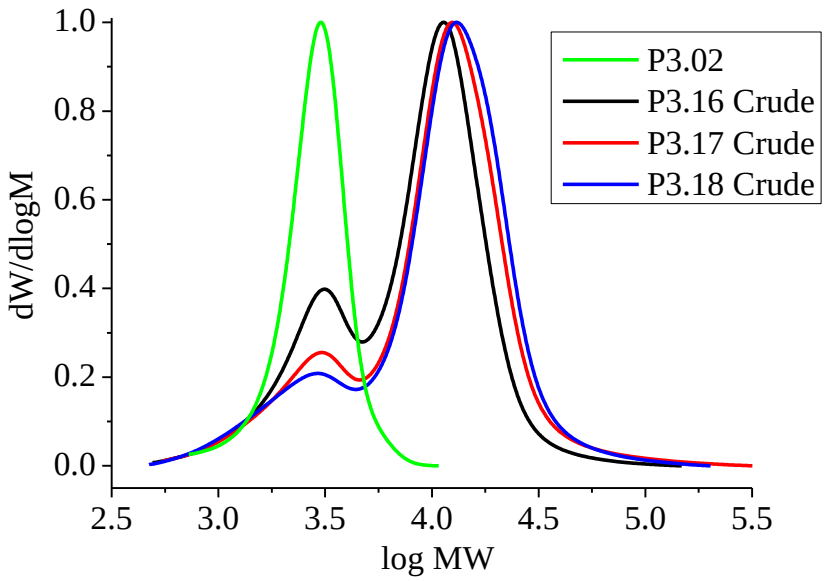

Figure 3.25. GPC traces (RID) of P(DMA) (P3.02) and P[(DMA)-*b*-(PIBA)]s (P3.16-P3.18) synthesised by chain extension of P(DMA) (P3.02) with PIBA in toluene at 70 °C, initiated by V601.

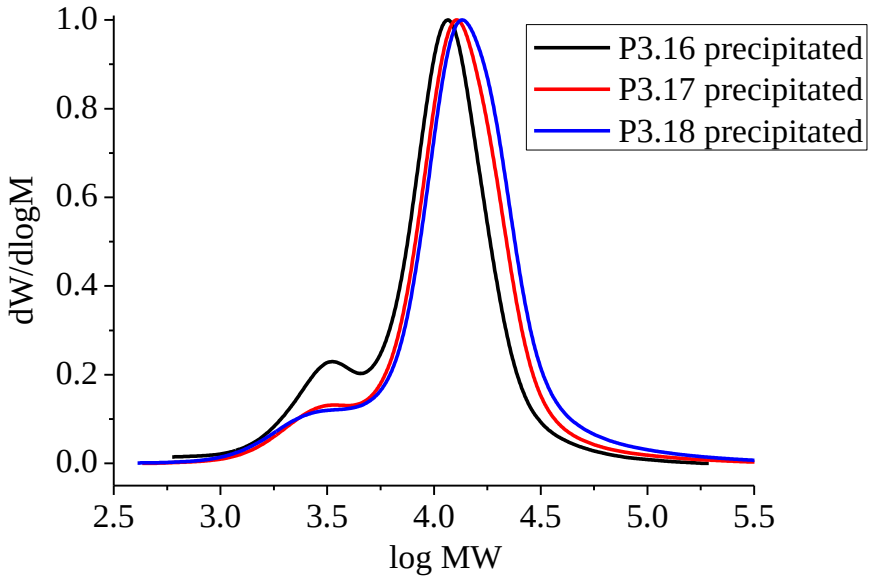

Figure 3.26. GPC traces (RID) of precipitated P[(DMA)-*b*-(PIBA)] synthesised by chain extension of P(DMA) (P3.02) with PIBA in toluene at 70 °C, initiated by V601.

Chain extension of P(DMA) with PIBA was non-quantitative as evidenced by the residual distribution of P(DMA) in the GPC traces (Figure 3.25). This may have

occurred because of multiple reasons but a likely cause is that the end group fidelity of the P(DMA) was not as high as initially assumed by the ^{1}H-NMR spectroscopy measurements (Figure 3.11). MALDI-TOF MS is an effective technique for determining the exact end group structure of polymeric samples. Therefore MALDI-TOF MS was measured for P(DMA) P3.02 (Figure 3.27). The MALDI-TOF spectrum of P3.02 shows multiple distributions with a difference of ~99.05 Da between consecutive peaks which corresponds well with the theoretical monoisotopic mass of the P(DMA) repeat unit of 99.07 Da. These multiple distributions imply that many potential variations of α- and ω-end group are present.

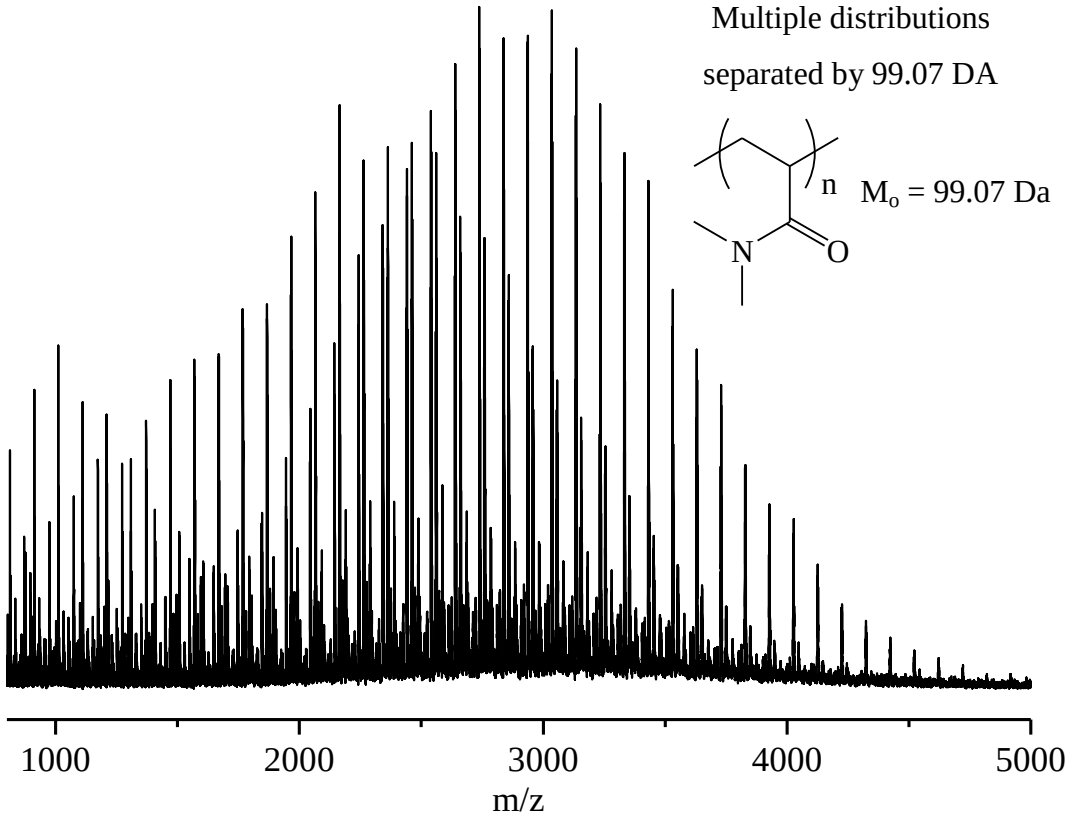

Figure 3.27. MALDI-TOF spectrum of P(DMA) (P3.02).

Two distributions correspond to the two expected P(DMA) structures; α-terminus is either a methyl ester (initiated by radicals produced from V601 decomposition) ($C_1P(DMA)_nC_{12}$) or a butyl ester (initiated by radicals produced from BDTMP fragmentation) ($C_4P(DMA)_nC_{12}$). The ω-terminus for both of these species is the

desired trithiocarbonate (Figure 3.28). $C_1P(DMA)_nC_{12}$ is observed at the lower m/z range (<2000 Da) whilst $C_4P(DMA)_nC_{12}$ is observe throughout the entire spectrum (Figure 3.29 and 3.30).

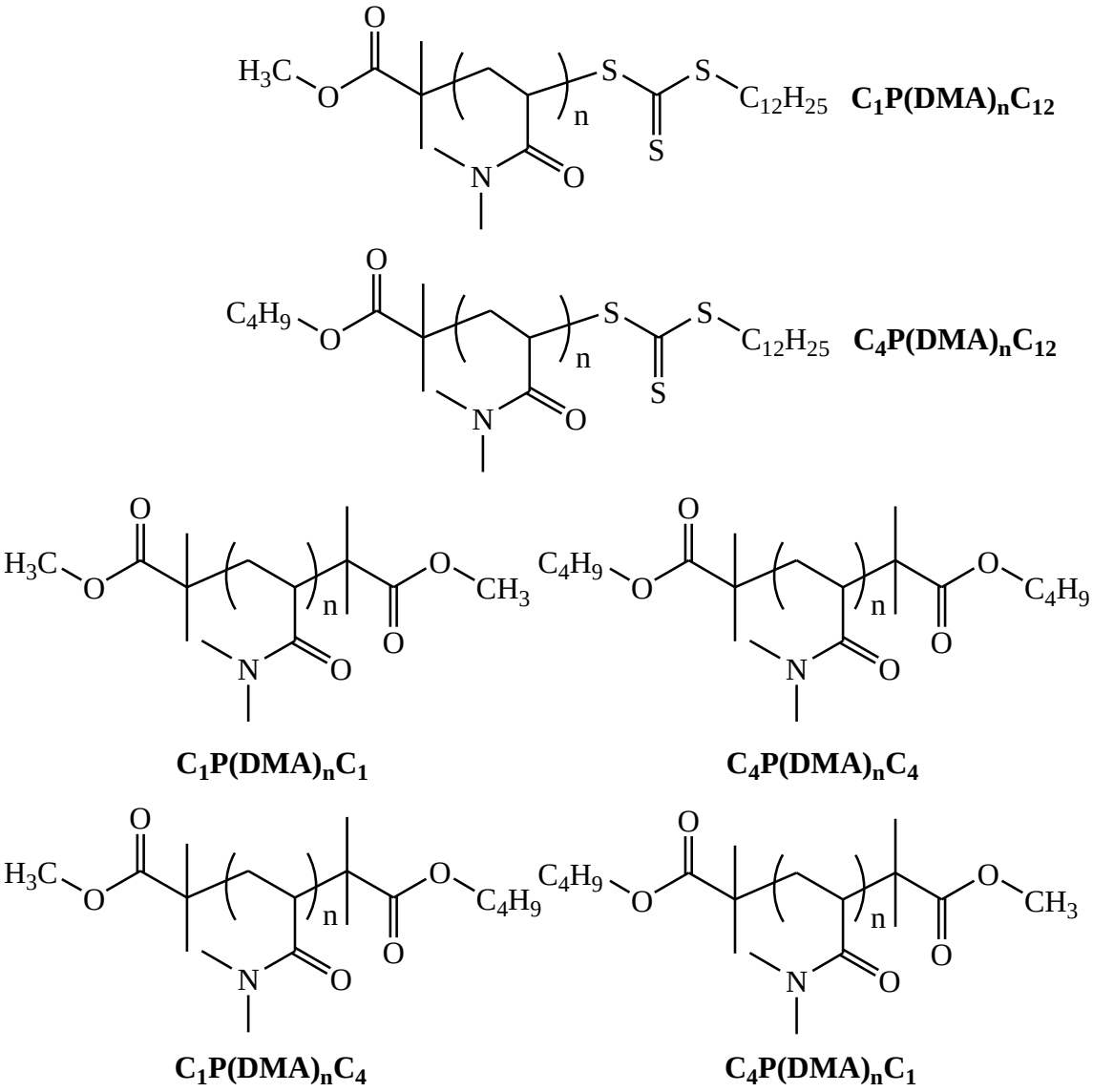

Figure 3.28. Potential α- and ω-end groups of P(DMA) (P3.02) synthesised by RAFT polymerisation, mediated by BDTMP and initiated by V601 in toluene at 70 °C.

However, there is also evidence for a number of potentially terminated P(DMA) chains. Termination may have occurred by combination of propagating polymeric radicals and initiating radicals. As the RAFT polymerisation system has two initiating species there is potentially two different radical species for the polymeric radical to combine with. This leads to the possibility of four different end group

combinations and three alternative mass distributions as two of the end group combinations give the same expected mass (Figure 3.28). All of these combinations, except for $C_4P(DMA)_nC_4$, are observed throughout the MALDI-TOF spectrum of P3.02 (Figure 3.29 and 3.30). It should also be noted that termination by recombination of propagating polymer radicals is also possible. Termination by recombination of polymer radicals would have the same mass distribution as the P(DMA) terminated by recombination of initiating species detailed above, e.g. two C_1 initiated P(DMA) radicals combining would have the same mass distribution as $C_1P(DMA)_nC_1$. However, recombination of polymer radicals is not expected to be the major cause of termination as earlier kinetic measurements of DMA homopolymerisation showed no formation of a high molecular weight shoulder which would have appeared if polymer radicals were combining (Figure 3.10).

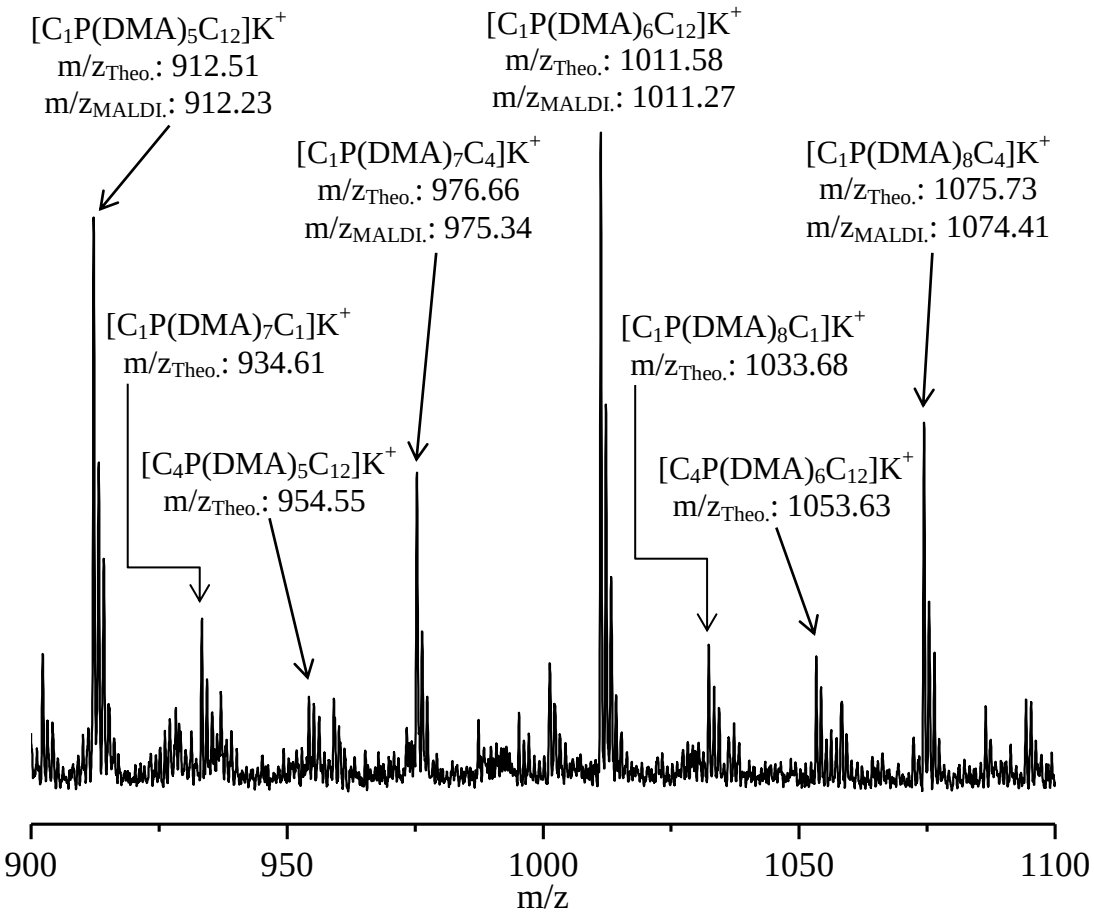

Figure 3.29. MALDI-TOF mass spectrum of P(DMA) (P3.02) between 900 and 1100 Da.

As m/z increases the predominant trithiocarbonate end capped species is initiated by the butyl ester from BDTMP fragmentation (Figure 3.28). Furthermore, the second most intense polymer distribution potentially corresponds to $C_1P(DMA)_nC_4$/ $C_4P(DMA)_nC_1$ species as well as a P(DMA) that has been terminated via disproportionation ($C_4P(DMA)_n$=CH), as the theoretical masses for these species would overlap (Figure 3.30). Moreover, another P(DMA) distribution can be identified that may have occurred as a result of combination between the intermediate RAFT adduct radical and a initiator/polymer radical (Figure 3.30). Many potential combinations of this species could exist; DP of the P(DMA) chains centred around the RAFT adduct as well as the initiating group that initiated each P(DMA) chain. Of these combinations, a terminated P(DMA) RAFT adduct bearing two butyl ester initiating groups and one methyl ester initiating group closely matches the observed m/z. Termination of intermediate RAFT adduct radical with a cyanoisopropyl radical has been observed by MALDI-TOF MS previously.[50] There is also evidence of one other unknown distribution which exhibits a separation of 99.0 Da between peaks so therefore has differing end groups from those stated already and does not correlate to any other salt adducts of P(DMA).

Confirmation by MALDI-TOF MS that part of the P(DMA) (P3.02) sample is not end capped by the desired trithiocarbonate end group but rather a methy/butyl ester explains why chain extension with PIBA was non-quantitative and residual P(DMA) was observed. Future optimisation will focus on obtaining perfect end fidelity and thus a greater block efficiency when chain extended with PIBA.

Despite the non-quantitative chain extension of P(DMA) to P[(DMA)-*b*-(PIBA)] these chain extensions are very promising and demonstrate that such a block copolymer can be synthesised and has many potential tuneable properties; P(DMA)

block length, PIBA block length, length of PIB graft and potentially the use of a different acrylamide to form the initial block can provide an alternative functionality.

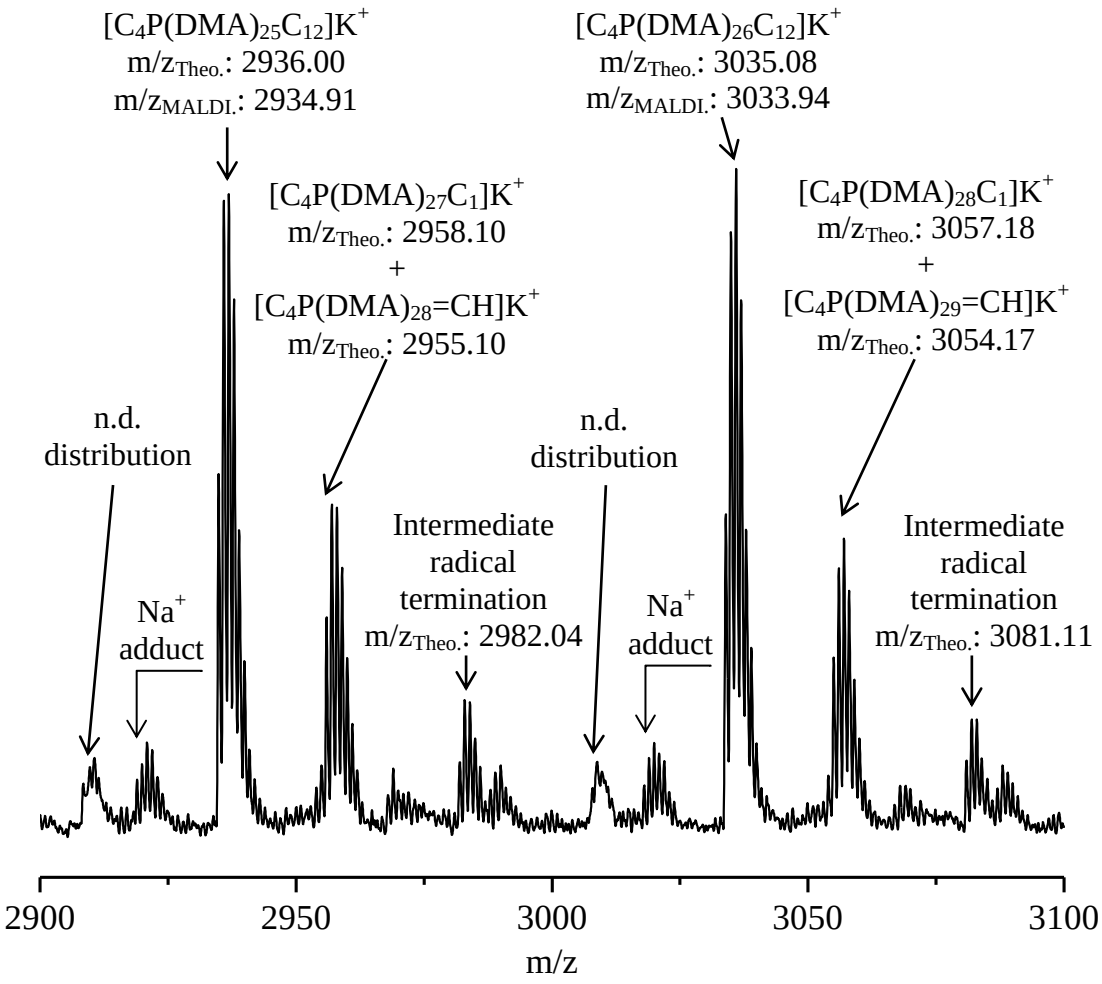

Figure 3.30. MALDI-TOF mass spectrum of P(DMA) (P3.02) between 2900 and 3100 Da.

3.5. Conclusions

PIB terminal olefins have been successfully converted to a phenol end group by Friedel-Crafts alkylation of phenol with said PIB to synthesise PIBP. PIBP was modified into a PIB macromonomer by esterification of PIBP with acryloyl chloride to synthesise a PIBA. Both of these transformations were supported by; ^{1}H-NMR and ^{13}C-NMR spectroscopy, GPC and MALDI-TOF MS.

RAFT polymerisation; mediated by BDTMP, initiated by V601 in toluene at 70 °C, was utilised to homopolymerise two monomers, DMA and DMAEA, in a controlled

process to synthesise homopolymers of controlled molecular weight with low dispersities at high monomer conversion. These same conditions for RAFT polymerisation were optimised slightly to successfully homopolymerise the newly synthesised PIBA to very high conversion (97%).

RAFT polymerisation was utilised to synthesise copolymers of PIBA; firstly PIBA was copolymerised with either DMA or DMAEA to synthesise P[(DMA)-*co*-(PIBA)] or P[(DMAEA)-*co*-(PIBA)] respectively. DMA copolymerisations were highly effective; conversion of both monomers were all above 85% even at increasing molar equivalents of PIBA and M_w increased predictably as more PIBA was incorporated into the copolymer. DMAEA was less successful and resulted in lower monomer conversions but was still successful at synthesising the desired statistical copolymer.

Finally, chain extensions of P(DMA) synthesised by RAFT polymerisation with PIBA to synthesise P[(DMA)-*b*-(PIBA)] was achieved. P(DMA) chain extensions were performed and >97% conversion of PIBA was obtained at all molar equivalents of PIBA and M_w increased expectedly as more PIBA was polymerised. There was evidence of P(DMA) that was not chain extended by a residual peak observed by GPC. P(DMA) was reanalysed by MALDI-TOF MS and this confirmed the presence of P(DMA) that was not terminated by the desired trithiocarbonate functionality and could not be chain extended. However it was possible to remove this P(DMA) by selective precipitation to obtain the desired P[(DMA)-*b*-(PIBA)] block copolymers. P[(DMA)-*b*-(PIBA)] and P[(DMA)-*co*-(PIBA)] samples were not submitted for fuel dispersant performance testing. This was partially due to the presence of a trithiocarbonate end group which may degrade upon testing to release

malodours/harmful small molecules. Therefore, a future aspect of this work will concern the end group removal of the trithiocarbonate end groups before testing.

Moreover, this methodology of copolymerising/homopolymerising a PIB macromonomer by RAFT polymerisation with a chosen acrylamide/acrylate can be utilised to synthesise new graft copolymers which have multiple properties that could be tuned for the demand. Firstly, copolymer architecture can be either a statistical copolymer, block copolymer or potentially a star if a multifunctional RAFT agent is utilised. Secondly, the chosen acrylamide/acrylate could vary beyond the two investigated in this chapter. Statistical copolymers could vary in composition of PIBA to acrylamide/acrylate. Block copolymers could vary in block length of acrylamide/acrylate as well as the PIBA block length. Finally, the chain length of the PIBA could be tuned by functionalising a different molecular weight PIB as "highly reactive" PIB is available with a greater M_n such as 2300 g·mol^{-1}.

3.6. Experimental

3.6.1. Instrumentation

3.6.1.1. Gel permeation chromatography

Molecular weight averages and polymer dispersity were determined by GPC. GPC samples were prepared to a concentration of 1 mg·mL^{-1} and passed through 0.4 µm PTFE filters before injection. GPC measurements were performed on an Agilent 1260 infinity system equipped with 2 PLgel 5 µm mixed-D columns (300 × 7.5 mm), a PLgel 5 mm guard column (50 × 7.5 mm), a refractive index detector (RID) and variable wavelength detector (VWD). Columns and RID were maintained at 40 °C. The system was eluted with THF and 2% v/v TEA at a flow rate of 1 mL·min^{-1} and the RID was calibrated with linear narrow polystyrene standards.

3.6.1.2. Nuclear magnetic resonance spectroscopy

^{1}H-NMR and ^{13}C-NMR spectra were measured using a Bruker AV-400. Chemical shifts are reported in parts per million (ppm) and all spectra are referenced against the residual solvent peak found in the deuterated NMR solvent. Abbreviations used for peak multiplicity are as follows; s = singlet, d = doublet, t = triplet, q = quartet and m = multiplet.

3.6.1.3. Gas chromatography – flame ionisation detection

GC-FID was used to measure monomer conversions (DMA and DMAEA). GC-FID analysis was performed using an Agilent Technologies 7820A. An Agilent J&W HP-5 capillary column of 30 m × 0.320 mm, film thickness 0.25 µm was used. The oven temperature was programmed as follows: 40 °C (hold for 1 minute) increase at 30 °C min^{-1} to 300 °C (hold for 2.5 minutes). The injector was operated at 250 °C and the FID was operated at 320 °C. Nitrogen was used as carrier gas at flow rate of 6.5 mL min^{-1} and a split ratio of 1:1 was applied. Chromatographic data was processed using OpenLab CDS ChemStation Edition, version C.01.05.

3.6.1.4. Ultraviolet – visible spectroscopy

UV measurements were performed on a PerkinElmer UV/Vis Spectrometer Lambda 35 using a quartz crystal cuvette measuring between 100-700 nm.

3.6.1.5. Matrix-assisted laser desorption/ionisation time-of-flight mass spectrometry

MALDI-TOF MS was performed using a Bruker Daltonics Autoflex MALDI-ToF mass spectrometer, equipped with a nitrogen laser at 337 nm with positive ion ToF detection. PIB samples were measured as follows; solutions in THF of dithranol as matrix (30 mg·mL^{-1}), silver trifluoroacetate as cationisation agent (10 mg·mL^{-1}) and

sample (10 mg·mL^{-1}) were mixed together in a 15:1:5 volume ratio for a total volume of 105 μL. 1 μL of the mixture was applied to the target plate. P(DMA) samples were measured as follows; solutions in THF of *trans*-2-[3-(4-tertbutylphenyl)-2-methyl-2-propylidene]malonitrile (DCTB) as matrix (30 mg·mL^{-1}), potassium trifluoroacetate as cationisation agent (10 mg·mL^{-1}) and sample (10 mg·mL^{-1}) were mixed together in a 3:1:1 volume ratio for a total volume of 75 μL. 1 μL of the mixture was applied to the target plate. Spectra were recorded in reflectron mode and the mass spectrometer was calibrated with a peptide mixture up to 6000 Da.

3.6.2. Materials

Phenol (Fisher Scientific, >98%), sulfuric acid (BDH laboratories, 98%), magnesium sulfate (Fisher Scientific), 35% HCl solution (VWR), triethylamine (Aldrich, ≥99%), acryloyl chloride (Aldrich, 97%) were all used as received. Dimethyl 2,2′-azobis(isobutyrate) and 3-butyl-2-(dodecylthiocarbonothioylthio)-2-methylpropionate were provided by University of Warwick and used as received. DCM, *n*-hexane, ethanol, DMF, THF and toluene used were all HPLC grade and used as received.

N,*N*-dimethylacrylamide (Aldrich, 99%) and 2-(dimethylamino)ethyl acrylate (Aldrich, 98%) were destabilised by passing through a short column of basic aluminium oxide prior to polymerisation. “Highly reactive” PIB was donated by Innospec LTD and used as received.

3.6.3. Procedures

3.6.3.1. Synthesis of PIBP

PIB (50.1 g, 50.1 mmol, 1 eq.) and phenol (47.0 g, 501 mmol, 10 eq.) were dissolved in DCM (300 mL) and cooled down to 0 °C. Concentrated sulfuric acid (3.2 mL, 60.1 mmol, 1.2 eq.) was added drop wise to the solution maintained at 0 °C. Mixture was allowed to reach room temperature and left stirring for 60 hours. DCM was removed in vacuo and the resulting viscous liquid was dissolved in *n*-hexane (200 mL). Organic layer was washed with 90% ethanol 10% water solution (2 × 50 mL), DMF (4 × 50 mL) and again with 90% ethanol 10% water solution (2 × 50 mL). Organic layer was dried over magnesium sulfate before filtering and removing all *n*-hexane to yield the product PIBP. ^{1}H-NMR ($CDCl_3$, 400 MHz, 303 K): δ (ppm) 0.97-1.03 ((-C$\underline{H}_3$)$_3$, PIB *α*-terminus), 1.05-1.16 ((-C$\underline{H}_3$)$_2$, PIB repeat unit), 1.39-1.46 (s, -C$\underline{H}_2$-, PIB repeat unit), 1.80 (s, -C$\underline{H}_2$C(CH$_3$)$_2$(C$_6$H$_5$OH)), 6.75 (d, C$_6\underline{H}_{5ortho}$OH), 7.22 (d, C$_6\underline{H}_{5meta}$OH). ^{13}C-NMR ($CDCl_3$, 400 MHz, 303 K): δ (ppm) 31.24 (s, -CH$_2\underline{C}$(CH$_3$)$_2$-, PIB repeat unit), 38.16 (s, -CH$_2$C($\underline{C}$H$_3$)$_2$-, PIB repeat unit), 59.55 (s, -$\underline{C}$H$_2$C(CH$_3$)$_2$-, PIB repeat unit), 114.54 (s, -($\underline{C}_{6ortho}$H$_5$)OH), 127.24 (s, -($\underline{C}_{6meta}$H$_5$)OH), 142.63 (s, -($\underline{C}_{6para}$H$_5$)OH), 153.08 (s, -($\underline{C}_6$H$_5$)OH). GPC: M_n 1200 g·mol^{-1}, M_w 1900 g·mol^{-1}, $Đ$ 1.60.

3.6.3.2. Synthesis of PIBA

PIBP (30.13 g, 30.13 mmol, 1 eq.) was dissolved in THF (150 mL) and cooled down to 0 °C. TEA (5.3 mL, 37.03 mmol, 1.25 eq.) was added to the solution followed by drop wise addition of acryloyl chloride (3.1 mL, 38.15 mmol, 1.25 eq.) to the solution maintained at 0 °C and left to stir at 0 °C for 4 hours before allowing to reach room temperature and left to stir for a further 18 hours. THF was removed in vacuo and the resulting viscous liquid was dissolved in *n*-hexane (150 mL). The

organic layer was washed with 1 M HCl solution (3 × 40 mL), 90% ethanol 10% water solution (2 × 40 mL), DMF (4 × 40 mL) and again with 90% ethanol 10% water solution (2 × 40 mL). The organic layer was dried over magnesium sulfate before filtering and removing all *n*-hexane to yield the product PIBA. ^{1}H-NMR ($CDCl_3$, 400 MHz, 303 K): δ (ppm) 0.97-1.03 ((-C$\underline{H}_3)_3$, PIB α-terminus), 1.05-1.16 ((-C$\underline{H}_3)_2$, PIB repeat unit), 1.39-1.46 (s, -C$\underline{H}_2$-, PIB repeat unit), 1.84 (s, -C$\underline{H}_2$C$(CH_3)_2(C_6H_5O$-)), 5.98 (d, -CH=C$H_{cis}\underline{H}_{trans}$), 6.29 (q, -C$\underline{H}$=C$H_{cis}H_{trans}$), 6.58 (d, -CH=C$\underline{H}_{cis}H_{trans}$), 7.04 (d, $C_6\underline{H}_{5ortho}$O-), 7.37 (d, $C_6\underline{H}_{5meta}$O-).^{13}C-NMR ($CDCl_3$, 400 MHz, 303 K): δ (ppm) 31.24 (-CH_2C(C$\underline{H}_3)_2$-, PIB repeat unit), 38.16 (-CH_2C$\underline{C}(CH_3)_2$-, PIB repeat unit), 59.55 (-C$\underline{H}_2$C$(CH_3)_2$-, PIB repeat unit), 120.52 (-(C$\underline{C}_{6ortho}H_5$)-O-), 127.06 (-(C$\underline{C}_{6meta}H_5$)-O-), 128.18 (-C$\underline{C}$=C), 132.13 (-C=C$\underline{C}$), 148.01 (-(C$\underline{C}_6H_5$)-O-), 148.14 (-(C$\underline{C}_6H_5$)-O-), 164.55 (-C$\underline{C}$OO-). GPC: M_n 1400 g·mol^{-1}, M_w 2100 g·mol^{-1}, $Đ$ 1.56.

3.6.3.3. RAFT homopolymerisation of DMA

DMA, BDTMP, V601 and toluene were charged into a Schlenk tube and degassed by gentle bubbling of N_2 gas for 30 minutes. Schlenk tube was submerged into an oil bath at 70 °C. Samples taken via degassed syringe at desired time points. Schlenk tube removed after 1 hour and placed into liquid N_2 to quickly reduce the temperature and terminate polymerisation. Reaction mixture was diluted with acetone and P(DMA) was precipitated into a large volume of *n*-hexane, filtered and dried overnight under vacuum. Product was a yellow solid.

Table 3.11 shows the quantities of all individual substances (DMA, BDTMP, V601 and toluene) used to synthesise P(DMA)s (P3.01-P3.03) prepared by the procedure detailed above.

^{1}H-NMR ($CDCl_3$, 400 MHz, 303 K): δ (ppm) 1.40-1.93 (m, -C$\underline{H}_2$-), 2.14-2.74 (m, -C$\underline{H}$-), 2.74-3.23 (m, -N(C$\underline{H}_3$)$_2$).

Table 3.06. GPC characterisation and DMA conversion for P(DMA)s (P3.01-P3.03) prepared by RAFT polymerisation.

Sample	DMA Conversion$^{\alpha}$ (%)	$M_{n.GPC}{}^{\beta}$ (g·mol^{-1})	$M_{n.Theo}{}^{\gamma}$ (g·mol^{-1})	$Đ^{\beta}$
P3.01	99	2800	2900	1.11
P3.02	95	2600	2800	1.14
P3.03	99	1700	1900	1.14

$^{\alpha}$Calculated from GC-FID. $^{\beta}$THF + 2% TEA eluent, calibrated with PS standards. $^{\gamma}$Calculated from Equation 1.

3.6.3.4. RAFT homopolymerisation of DMAEA

DMAEA, BDTMP, V601 and toluene were charged into a Schlenk tube and degassed by gentle bubbling of N_2 gas for 30 minutes. Schlenk tube was submerged into an oil bath at 70 °C. Samples taken via degassed syringe at desired time points. Schlenk tube removed after 3 hours and placed into liquid N_2 to quickly reduce the temperature and terminate polymerisation. Reaction mixture was diluted with acetone and P(DMAEA) was precipitated into a large volume of cold *n*-hexane. P(DMAEA) was allowed to settle before carefully decanting off the excess *n*-hexane, P(DMAEA) dissolved in acetone and precipitated again in *n*-hexane before removing excess solvent under vacuum. Product collected was viscous yellow liquid.

Table 3.12 shows the quantities of all individual substances (DMAEA, BDTMP, V601 and toluene) used to synthesise P(DMAEA)s (P3.04 and P3.05) prepared by the procedure detailed above.

^{1}H-NMR ($CDCl_3$, 400 MHz, 303 K): δ (ppm) 1.54-2.01 (m, -C$\underline{H}_2$-), 2.17-2.45 (m, -N(C$\underline{H}_3$)$_2$ and -C$\underline{H}$-), 2.45-2.63 (m, -$CH_2C\underline{H}_2N(CH_3)_2$), 4.03-4.24 (m, -$C\underline{H}_2CH_2N(CH_3)_2$).

Table 3.07. GPC characterisation and DMAEA conversion for P(DMAEA)s (P3.04 and P3.05) prepared by RAFT polymerisation.

Sample	DMAEA Conversion$^{\alpha}$ (%)	$M_{n.GPC}{}^{\beta}$ (g·mol^{-1})	$M_{n.Theo}{}^{\gamma}$ (g·mol^{-1})	$Đ^{\beta}$
P3.04	76	3000	3100	1.19
P3.05	92	3700	3800	1.14

$^{\alpha}$Calculated from GC-FID. $^{\beta}$THF + 2% TEA eluent, calibrated with PS standards. $^{\gamma}$Calculated from Equation 1.

3.6.3.5. RAFT/free radical homopolymerisation of PIBA

PIBA, BDTMP, V601 and toluene were charged into a Schlenk tube and degassed by gentle bubbling of N_2 gas for 30 minutes. Schlenk tube was submerged into an oil bath at 70 °C. Schlenk tube removed after ~20 hours and placed into liquid N_2 to quickly reduce the temperature and terminate polymerisation.

Table 3.13 shows the quantities of all individual substances (PIBA, BDTMP, V601 and toluene) used to synthesise P(PIBA)s (P3.06-P3.11) prepared by the procedure detailed above.

^{1}H-NMR ($CDCl_3$, 400 MHz, 303 K): δ (ppm) 0.97-1.02 (s, (-C$\underline{H}_3$)$_3$, PIB *α*-terminus), 1.05-1.19 (m, (-C$\underline{H}_3$)$_2$, PIB repeat unit), 1.38-1.45 (m, -C$\underline{H}_2$-, PIB repeat unit), 1.75-1.90 (s, -C$\underline{H}_2$-, P(PIBA) repeat unit), 2.25-2.38 (m, -C$\underline{H}$-, P(PIBA) repeat unit), 6.88-7.39 (m, -(C$_6\underline{H}_4$)-, P(PIBA) repeat unit).

Table 3.08. GPC characterisation and PIBA conversion for P(PIBA)s (P3.06-P3.11) prepared by RAFT/free radical polymerisation.

Sample	PIBA Conversion$^{\alpha}$ (%)	$M_{n.GPC}{}^{\beta}$ (g·mol^{-1})	$M_{w.GPC}{}^{\beta}$ (g·mol^{-1})	$Đ^{\beta}$
P3.06	65	3000	7000	2.36
P3.07	97	4600	8800	1.93
P3.08	85	4400	55500	12.52
P3.09	95	5800	57000	9.84
P3.10	>99	5900	57800	9.83
P3.11	>99	6000	60200	9.92

$^{\alpha}$Calculated from ^{1}H-NMR spectroscopy. $^{\beta}$THF + 2% TEA eluent, calibrated with PS standards.

3.6.3.6. RAFT comopolymerisation of DMA and PIBA

DMA, PIBA, BDTMP, V601 and toluene were charged into a Schlenk tube and degassed by gentle bubbling of N_2 gas for 30 minutes. Schlenk tube was submerged into an oil bath at 70 °C. Samples taken via degassed syringe at desired time points. Schlenk tube removed after 8 hours and placed into liquid N_2 to quickly reduce the temperature and terminate polymerisation. Reaction mixture was diluted with THF and P[(DMA)-*co*-(PIBA)] was precipitated into a large volume of acetone. P[(DMA)-*co*-(PIBA)] was allowed to settle before decanting off the excess acetone, P[(DMA)-*co*-(PIBA)] dissolved in THF and precipitated again in acetone before removing excess solvent under vacuum. Product collected was a very viscous pale yellow liquid.

Table 3.14 shows the quantities of all individual substances (DMA, PIBA, BDTMP, V601 and toluene) used to synthesise P[(DMA)-*co*-(PIBA)]s (P3.12-P3.14) prepared by the procedure detailed above.

^{1}H-NMR ($CDCl_3$, 400 MHz, 303 K): δ (ppm) 0.98-1.02 (s, (-C$\underline{H}_3$)$_3$, PIB *α*-terminus), 1.06-1.18 (m, (-C$\underline{H}_3$)$_2$, PIB repeat unit), 1.40-1.49 (m, -C$\underline{H}_2$-, PIB repeat unit), 1.52-1.96 (m, -C$\underline{H}_2$-, P(DMA) and P(PIBA) repeat unit), 2.33-2.75 (m, -C$\underline{H}$-, P(DMA) and P(PIBA) repeat unit), 2.75-3.21 (m, -N(C$\underline{H}_3$)$_2$, P(DMA) repeat unit), 6.88-7.39 (m, -(C$_6\underline{H}_4$)-, P(PIBA) repeat unit).

Table 3.09. GPC characterisation and monomer conversions for P[(DMA)-*co*-(PIBA)]s (P3.12-P3.14) prepared by RAFT polymerisation.

Sample	DMA;PIBA Conversion$^{\alpha}$ (%)	$M_{n.GPC}{}^{\beta}$ (g·mol^{-1})	$M_{w.GPC}{}^{\beta}$ (g·mol^{-1})	$Đ^{\beta}$
P3.12	>99;>99	5000	8500	1.70
P3.13	99;>99	5300	11600	2.21
P3.14	95;85	4800	17000	3.50

$^{\alpha}$Calculated from ^{1}H-NMR spectroscopy. $^{\beta}$THF + 2% TEA eluent, calibrated with PS standards.

3.6.3.7. RAFT comopolymerisation of DMAEA and PIBA

DMAEA (0.7 mL, 4.61 mmol, 20 eq.), PIBA (1.56 g, 1.16 mmol, 5 eq.), BDTMP (0.098 g, 0.233 mmol, 1 eq.), V601 (0.005 g, 0.0217 mmol, 0.1 eq.) and toluene (3.8 mL) were charged into a Schlenk tube and degassed by gentle bubbling of N_2 gas for 30 minutes. Schlenk tube was submerged into an oil bath at 70 °C. Schlenk tube removed after 24 hours and placed into liquid N_2 to quickly reduce the temperature and terminate polymerisation. ^{1}H-NMR ($CDCl_3$, 400 MHz, 303 K): δ (ppm) 0.98-1.02 (s, (-C$\underline{H}_3$)$_3$, PIB *α*-terminus), 1.06-1.18 (m, (-C$\underline{H}_3$)$_2$, PIB repeat unit), 1.40-1.49 (m, -C$\underline{H}_2$-, PIB repeat unit), 1.52-2.01 (m, -C$\underline{H}_2$-, P(DMAEA) and P(PIBA) repeat unit), 2.17-2.63 (m, -C$\underline{H}$-, P(DMAEA) and P(PIBA) repeat unit, -N(C$\underline{H}_3$)$_2$ and CH$_2$C$\underline{H}_2$N(CH$_3$)$_2$, P(DMAEA) repeat unit), 4.03-4.24 (m,

-C<u>H</u>$_2$CH$_2$N(CH$_3$)$_2$, P(DMAEA) repeat unit), 6.89-7.41 (m, -(C$_6$<u>H</u>$_4$)-, P(PIBA) repeat unit). GPC: M_n 2800 g·mol^{-1}, M_w 6200 g·mol^{-1}, $Đ$ 2.20.

3.6.3.8. Chain extension of P(DMA) with PIBA

P(DMA) (P3.02), PIBA, V601 and toluene were charged into a Schlenk tube and degassed by gentle bubbling of N_2 gas for 30 minutes. Schlenk tube was submerged into an oil bath at 70 °C. Schlenk tube removed after 24 hours and placed into liquid N_2 to quickly reduce the temperature and terminate polymerisation. Reaction mixture was diluted with THF and P[(DMA)-*b*-(PIBA)] was precipitated into a large volume of acetone. P[(DMA)-*b*-(PIBA)] was allowed to settle before carefully decanting off the excess acetone, P[(DMA)-*b*-(PIBA)] dissolved in THF and precipitated again in acetone before removing excess solvent under vacuum. Product collected was a very viscous pale yellow liquid.

Table 3.15 shows the quantities of all individual substances (P(DMA), PIBA, V601 and toluene) used to synthesise P[(DMA)-*b*-(PIBA)]s (P3.16-P3.18) prepared by the procedure detailed above.

^{1}H-NMR ($CDCl_3$, 400 MHz, 303 K): δ (ppm) 0.98-1.02 (s, (-C<u>H</u>$_3$)$_3$, PIB *α*-terminus), 1.06-1.18 (m, (-C<u>H</u>$_3$)$_2$, PIB repeat unit), 1.40-1.49 (m, -C<u>H</u>$_2$-, PIB repeat unit), 1.52-1.96 (m, -C<u>H</u>$_2$-, P(DMA) and P(PIBA) repeat unit), 2.33-2.75 (m, -C<u>H</u>-, P(DMA) and P(PIBA) repeat unit), 2.75-3.21 (m, -N(C<u>H</u>$_3$)$_2$, P(DMA) repeat unit), 6.88-7.39 (m, -(C$_6$<u>H</u>$_4$)-, P(PIBA) repeat unit).

Table 3.10. GPC characterisation and PIBA conversion for P[(DMA)-*b*-(PIBA)]s (P3.16-P3.18) prepared by chain extension of P(DMA) with PIBA (P3.02).

Sample	PIBA Conversion$^{\alpha}$ (%)	$M_{n.GPC}{}^{\beta}$ (g·mol^{-1})	$M_{w.GPC}{}^{\beta}$ (g·mol^{-1})	$Đ^{\beta}$
P3.16	>99	6600	13000	1.96
P3.17	>99	8500	17000	2.02
P3.18	97	8800	21000	2.44

$^{\alpha}$Calculated from ^{1}H-NMR spectroscopy. $^{\beta}$THF + 2% TEA eluent, calibrated with PS standards.

Table 3.11. Quantities of DMA, BDTMP, V601 and toluene used to synthesise P(DMA)s (P3.01-P3.03).

Sample	DMA			BDTMP			V601			Toluene
	(mL)	(mmol)	(eq.)	(g)	(mmol)	(eq.)	(mg)	(mmol)	(eq.)	(mL)
P3.01	2	19.4	25	0.324	0.770	1	18	0.0782	0.1	2
P3.02	15	146	25	2.44	5.80	1	133	0.578	0.1	15
P3.03	15	146	15	4.08	9.70	1	224	0.973	0.1	15

Table 3.12. Quantities of DMAEA, BDTMP, V601 and toluene used to synthesise P(DMAEA)s (P3.04 and P3.05).

Sample	DMAEA			BDTMP			V601			Toluene
	(mL)	(mmol)	(eq.)	(g)	(mmol)	(eq.)	(mg)	(mmol)	(eq.)	(mL)
P3.04	2.5	16.5	25	0.278	0.661	1	15	0.0651	0.1	2.5
P3.05	6	39.5	25	0.665	1.58	1	36	0.148	0.1	6

Table 3.13. Quantities of PIBA, BDTMP, V601 and toluene used to synthesise P(PIBA)s (P3.06-P3.11).

Sample	PIBA			BDTMP			V601			Toluene
	(g)	(mmol)	(eq.)	(g)	(mmol)	(eq.)	(mg)	(mmol)	(eq.)	(mL)
P3.06	1.5	1.11	10	0.048	0.114	1	2.6	0.0113	0.1	3
P3.07	1.5	1.11	10	0.049	0.116	1	6.5	0.0282	0.25	3
P3.08	1	0.741	10	0	0	0	17.0	0.0738	0.1	2
P3.09	1	0.741	10	0	0	0	8.6	0.0373	0.25	2
P3.10	1	0.741	10	0	0	0	4.2	0.0182	0.5	2
P3.11	1	0.741	10	0	0	0	1.7	0.00738	1	2

Table 3.14. Quantities of DMA, PIBA, BDTMP, V601 and toluene used to synthesise P[(DMA)-*co*-(PIBA)]s (P3.12-P3.14).

Sample	DMA			PIBA			BDTMP			V601			Toluene
	(mL)	(mmol)	(eq.)	(g)	(mmol)	(eq.)	(g)	(mmol)	(eq.)	(mg)	(mmol)	(eq.)	(mL)
P3.12	0.5	4.85	22.5	0.73	0.541	2.5	0.091	0.216	1	5	0.0217	0.1	2
P3.13	0.45	4.37	20	1.46	1.08	5	0.093	0.221	1	5	0.0217	0.1	3.5
P3.14	0.11	1.07	15	1.02	0.756	10	0.031	0.0737	1	1.7	0.00738	0.1	2.2

Table 3.15. Quantities of P(DMA) (P3.02), PIBA, V601 and toluene used to synthesise P[(DMA)-*b*-(PIBA)]s (P3.16-P3.18).

Sample	P(DMA)			PIBA			V601			Toluene
	(g)	(mmol)	(eq.)	(g)	(mmol)	(eq.)	(mg)	(mmol)	(eq.)	(mL)
P3.16	0.48	0.185	1	1.02	0.756	4	11	0.0478	0.25	3
P3.17	0.28	0.108	1	1.01	0.748	7	6	0.0261	0.25	2.6
P3.18	0.19	0.0731	1	1.00	0.741	10	4	0.0174	0.25	2.4

3.7. References

1. J. E. Puskas, Y. Chen, Y. Dahman and D. Padavan, *J. Polym. Sci. Part A Polym. Chem.*, 2004, **42**, 3091.
2. R. Tripathy, J. V. Crivello and R. Faust, *J. Polym. Sci. Part A Polym. Chem.*, 2013, **51**, 305.
3. J. P. Kennedy, S. C. Guhaniyogi and V. Percec, *Polym. Bull.*, 1982, **8**, 571.
4. J. P. Kennedy and M. Hiza, *J. Polym. Sci., Polym. Chem. Ed.*, 1983, **21**, 1033.
5. A. Takacs and R. Faust, *J. Macromol. Sci. Chem.*, 1996, **A33**, 177.
6. W. Ma, Y. Wu, L. Feng and R. Xu, *Polymer*, 2012, **53**, 3185.
7. J. P. Kennedy, S. Midha and A. Gadkari, *J. Macromol. Sci. Chem.*, 1991, **A28**, 209.
8. T. K. Georgiou, C. S. Patrickios, P. W. Groh and B. Iván, *Macromolecules*, 2007, **40**, 2335.
9. G. Kali, S. Vavra, K. László and B. Iván, *Macromolecules*, 2013, **46**, 5337.
10. S. K. Jewrajka and J. P. Kennedy, *J. Polym. Sci. Part A Polym. Chem.*, 2008, **46**, 2612.
11. J. Scherble, R. Thomann, B. Iván and R. Mulhaupt, *J. Polym. Sci. Part B Polym. Phys.*, 2001, **39**, 1429.
12. T. P. Liao and J. P. Kennedy, *Polym. Bull.*, 1981, **6**, 135.
13. M. Haraszti, E. Toth and B. Ivan, *Chem. Mater.*, 2006, **18**, 4952.
14. G. Kali and B. Iván, *Macromol. Chem. Phys.*, 2015, **216**, 605.
15. J. P. Kennedy, S. Midha and A. Gadkari, *J. Macromol. Sci. Chem.*, 1991, **A28**, 209-224.
16. I. Szanka, A. Szanka, S. Sen, N. Nugay and J. P. Kennedy, *J. Polym. Sci. Part A Polym. Chem.*, 2015, **53**, 1640.

17. Y. Kwon and J. P. Kennedy, *Polym. Adv. Technol.*, 2007, **18**, 800.
18. B. Ivan and J. P. Kennedy, *J. Polym. Sci., Polym. Chem. Ed.*, 1990, **28**, 89.
19. P. De and R. Faust, *Macromolecules*, 2006, **39**, 6861.
20. U. Ojha, R. Rajkhowa, S. R. Agnihotra and R. Faust, *Macromolecules*, 2008, **41**, 3832.
21. R. Tripathy, U. Ojha and R. Faust, *Macromolecules*, 2009, **42**, 3958.
22. C. P. Roche, M. R. Brei, B. Yang and R. F. Storey, *ACS Macro Lett.*, 2014, **3**, 1230.
23. A. Guerrero, K. Kulbaba and M. Bochmann, *Macromolecules*, 2007, **40**, 4124.
24. S. V. Kostjuk, *RSC Adv.*, 2015, **5**, 13125.
25. S. P. Srivastava and J. Hancsók, *Fuels and Fuel-Additives*, John Wiley & Sons, 1st edn. 2014, ch. 5, pp. 177-208.
26. C. Hongfa, J. Tian, H. S. Bazzi and D. E. Bergbreiter, *Org. Lett.*, 2007, **9**, 3259.
27. D. E. Bergbreiter, C. Hobbs, J. Tian, H. Koizumi, H.-L. Su and C. Hongfa, *Pure Appl. Chem.*, 2009, **11**, 1981.
28. L. R. Rudnick, *Lubricant Additives: Chemistry and Applications,* CRC Press, 2nd edn., 2009, ch. 5, pp. 143-166.
29. M. Hisano, K. Takeda, T. Takashima, Z. Jin, A. Shiibashi and A. Matsumoto, *Macromolecules*, 2013, **46**, 7733.
30. *US Pat.*, 6124249, 2000.
31. *US Pat.*, 6331603B1, 2001.
32. *US Pat.*, 4867894, 1989.
33. *US Pat.*, 20120135902A1, 2012.
34. *US Pat.*, 5993497, 1999.

35. A. Lange, S. Csihony and M. Kleiner, *Pat. Application*, WO2014090672A1, 2014.
36. G. Gody, T. Maschmeyer, P. B. Zetterlund and S. Perrier, *Nat. Commun.*, 2013, **4**, 2505.
37. J. Vandenbergh, G. Reekmans. P. Adriaensens and T. Junkers, *Chem. Commun.*, 2013, **49**, 10358.
38. G. Odian, *Principles of Polymerization*, John Wiley & Sons, 4th edn. 2004.
39. A. J. Convertine, B. S. Lokitz, Y. Vasileva, L. J. Myrick, C. W. Scales, A. B. Lowe and C. L. McCormick, *Macromolecules*, 2006, **39**, 1724.
40. G. Gody, T. Maschmeyer, P. B. Zetterlund and S. Perrier, *Macromolecules*, 2014, **47**, 3451.
41. C. Schilli, M. G. Lanzendörfer and A. H. E. Müller, *Macromolecules*, 2002, **35**, 6819.
42. P. Relógio, M.-T. Charreyre, J. P. S. Farinha, J. M. G. Martinho and C. Pichot, *Polymer*, 2004, **45**, 8639.
43. S. Perrier, C. Barner-Kowollik, J. F. Quinn, P. Vana and T. P. Davis, *Macromolecules*, 2002, **35**, 8300.
44. M. Mertoglu, S. Garnier, A. Laschewsky, K. Skrabania and J. Storsberg, *Polymer*, 2005, **46**, 7726.
45. J. Vandenbergh, T. D. Ogawa and T. Junkers, *J. Polym. Sci. Part A Polym. Chem.*, 2013, **51**, 2366.
46. N. Suchao-in, S. Chirachanchai and S. Perrier, *Polymer*, 2009, **50**, 4151.
47. W. Zhao, P. Fonsny, P. FitzGerald, G. G. Warr and S. Perrier, *Polym. Chem.*, 2013, **4**, 2140.

48. K. L. Beers, S. G. Gaynor and K. Matyjaszewski, *Macromolecules*, 1998, **31**, 9413.

49. K. Ohno, B. Wong and D. M. Haddleton, *J. Polym. Sci. Part A Polym. Chem.*, 2001, **39**, 2206.

50. M. Bathfield, F. D'Agosto, R. Spitz, C. Ladaviere, M.T. Charreyre and T. Delair, *Macromol. Rapid Commun.*, 2007, **28**, 856.

4. Copolymerisation of Functionalised α-Methyl Styrenes and Maleic Anhydride

4.1. Introduction

Styrene-maleic anhydride copolymers (P(SMalA)) have been of considerable interest both academically and industrially for many decades. This is because P(SMalA) copolymers have many desirable properties such as high temperature resistance and reactivity of the anhydride moiety.[1] P(SMalA) copolymers have been applied in many applications from polymer-protein conjugates as drug delivery vehicles,[1] emulsifiers for the formation of microcapsules[2,3] and as a reactive copolymer for the one-pot formation of shell cross-linked nanostructures.[4]

Within the fuel additive industry P(SMalA) copolymers have been utilised since 1967 to improve detergency and dispersency, as well as other properties, of fuel oil as well as mineral oil based lubricants.[5,6] This was achieved by part functionalisation (30 to 95%) of the maleic anhydride (MalA) repeat units with long chain aliphatic alcohols to provide solubility within oil.[5,6] Dispersency was then provided by further functionalisation of the remaining carboxyl groups with diamines, with 5 to 40% functionalisation found to be most effective for P(SMalA) copolymers.[5,6] Typical diamines utilised were aliphatic primary amines bearing a tertiary amine with aliphatic substituents, such as 3-(dimethylamino)-1-propylamine.[5,6] Other similar fuel additives have been synthesised by using styrene-maleic anhydride-methyl methacrylate terpolymers in place of P(SMalA) copolymers.[7] Reactive MalA repeat units are again esterified with aliphatic alcohols before the addition of nitrogen containing moieties such as 3-morpholinopropylamine.[7] More recently, Lubrizol have designed novel dispersant viscosity modifiers (DVM) based on P(SMalA)

copolymers that have been partly modified with long chain alcohol mixtures and an aromatic amine such as 4-aminodiphenylamine, 2-aminobenzimidazole or 3-nitroaniline.[8]

P(SMalA) properties and applications are undoubtedly linked to the alternating monomer microstructure of styrene (Sy) and MalA during copolymerisation, which is well-documented.[9] Although there remains debate regarding the exact mechanism of why this monomer alternation may occur.[9] MalA is a strongly-electron accepting monomer and is unable to homopolymerise radically, but when copolymerised in the presence of an electron-donating monomer, such as Sy, a highly reactive system is created that heavily favours cross-propagation instead of homopolymerisation.[9,10] However, it is of worthy of note that Sy can still homopolymerise within this system and this would cause misinsertions within the final alternating copolymer microstructure. These misinsertions could be further minimised or eliminated altogether by utilising α-methyl styrene (AMS) in place of Sy during Sy-MalA copolymerisations. AMS has a low ceiling temperature (61 °C), so polymerisation at or above this temperature results in a rate of homopolymerisation that is slower than the rate of depolymerisation.[11] Therefore, this reduces the probability of AMS homopolymerisation and as such the likeliness of any misinsertions in the final alternating copolymer.

Given that AMS-MalA copolymerisations have the potential to synthesise perfectly alternating copolymers, it may be expected that functional derivatives of AMS will also exhibit the same cross-propagation behaviour with MalA and thus synthesise alternating copolymers bearing a chosen functionality. Considering this, 3-isopropenyl-α,α-dimethylbenzyl isocyanate (TMI) may be an ideal commercially available monomer to utilise. TMI features an α-unsaturation as well as a reactive

isocyanate functionality. Via the α-unsaturation TMI has been radically copolymerised with a variety of monomers; Sy, methyl methacrylate, *n*-butyl acrylate, ethyl acrylate and chlorotrifluoroethylene.[12-18] Cationic polymerisation has also been utilised to homopolymerise[19] and copolymerise TMI.[20-22] Moreover, the isocyanate present on TMI makes it an ideal compound for new monomer synthesis or post-polymerisation modification. TMI has been demonstrated to be effective for both; primary amines and hydroxyls have been coupled with TMI's isocyanate to synthesise new monomers,[23] functionalise polymer end groups,[24] as well as modify copolymers post-polymerisation.[17,18,20-22,25]

Considering the potential versatility of TMI modification, its copolymerisation behaviour with MalA and the previously demonstrated application of P(SMalA) copolymers within the fuel additive industry, the following synthetic pathway was designed (Scheme 4.01). Firstly, TMI will be reactively coupled with a linear long chain aliphatic primary amine, to synthesise a new hydrophobic monomer that can be copolymerised with MalA to synthesise alternating copolymers. Finally, this newly synthesised alternating copolymer will be modified post-polymerisation with primary amines, via the MalA repeat unit, bearing a tertiary amine moiety to furnish a bifunctionalised alternating copolymer.

This pathway is believed to be an efficient and robust way of synthesising a novel class of copolymers that incorporate all of the necessary components to function as a fuel additive, particularly a DVM like the example discussed in Section 1.4.4. Furthermore, it is expected that having a more versatile system could be another means of addressing the most significant problem of the synthesis from Chapter 2; PIB-*b*-PDMAEMA block copolymers were insoluble in non-polar solvents such as *n*-hexane and petroleum ether. This issue arose as the PDMAEMA block had a

higher molecular weight than the PIB block for all prepared samples. This deviates from typical fuel dispersants which have one small polar head group to one or more very large hydrophobic groups to keep the additive soluble in fuel. By utilising the proposed alternating copolymer in Scheme 4.01 and grafting polar groups to an existing hydrophobic polymer the resulting copolymers solubility could be better controlled as grafting density of polar moieties can be controlled. Furthermore, this synthetic approach will also allow scope for screening different polar groups on the same polymer backbone, maintaining consistent DP of copolymer backbone, as well as potentially including multiple functionalities on one polymer backbone.

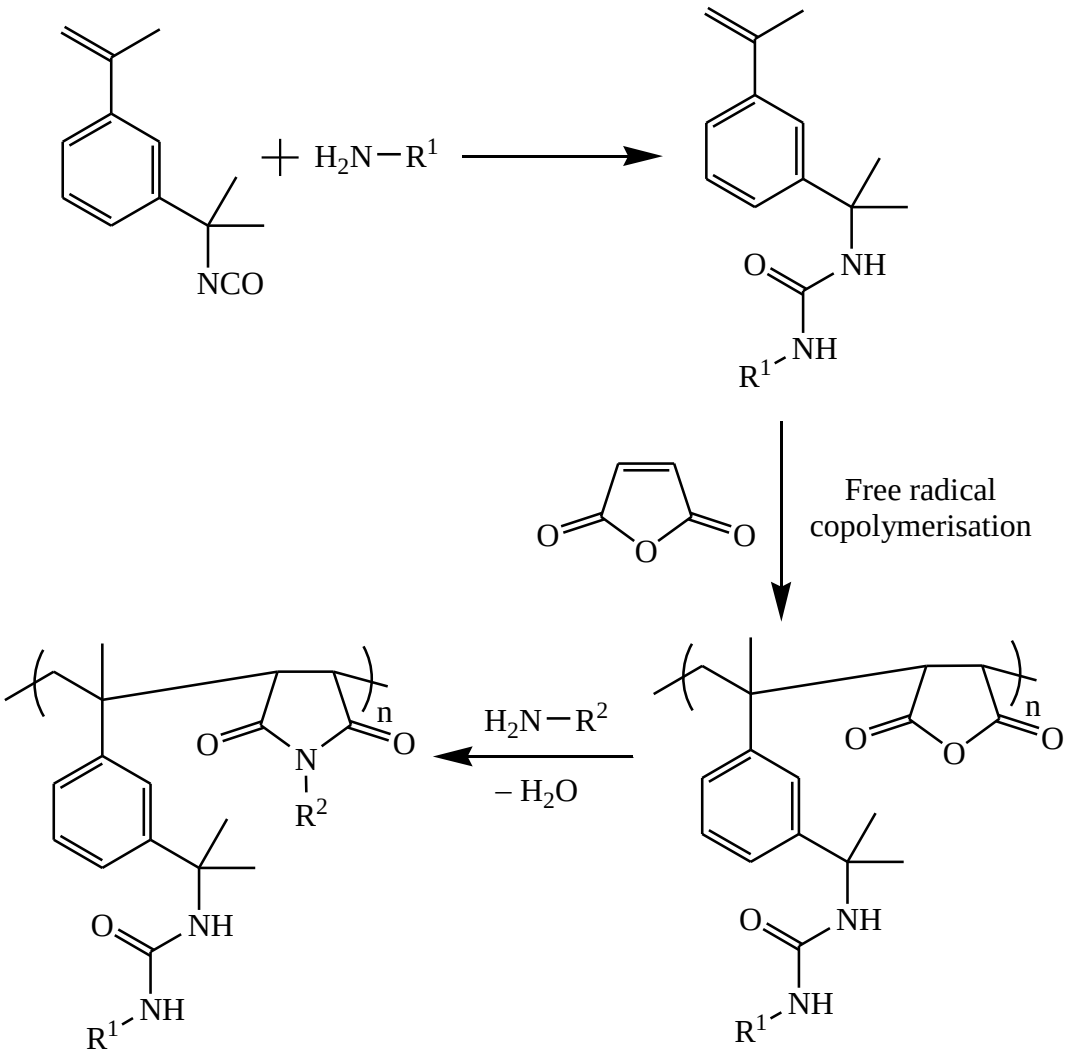

Scheme 4.01. Proposed synthetic pathway to synthesise bifunctionalised alternating copolymers utilising TMI and MalA. R^1 = linear aliphatic chain. R^2 = tertiary amine.

4.2. Free radical copolymerisation of AMS and MalA

P[(AMS)-*a*-(MalA)] was prepared via free radical copolymerisation of AMS and MalA, initiated by 2,2′-azobis(2-methylpropionitrile) (AIBN), in 2-butanone (MEK) at 80 °C for four hours (Scheme 4.02). Free radical polymerisation was chosen as other controlled radical techniques have been shown to be ineffective at controlling AMS-MalA copolymerisations. MalA is suspected to interact with the transition metal complexes used to mediate ATRP[9] and RAFT AMS-MalA copolymerisations have given poor control with little evidence of the RAFT agent mediating the copolymerisation, potentially caused by a low chain transfer constant to RAFT agent.[26] This is a potential drawback when utilising AMS in place of Sy, as Sy-MalA copolymerisations have adapted very readily to controlled radical polymerisation techniques, namely NMP and RAFT, to synthesise well-defined alternating and block copolymers.[4,26-32] Catalytic chain transfer polymerisation is a potentially viable technique and has been utilised to copolymerise Sy/AMS mixtures with MalA, giving control over which monomer is present as the copolymer end group.[33] Furthermore, free radical polymerisation can be performed in the absence of halides, metals or sulfur, all of which are controlled substances within the fuel industry.

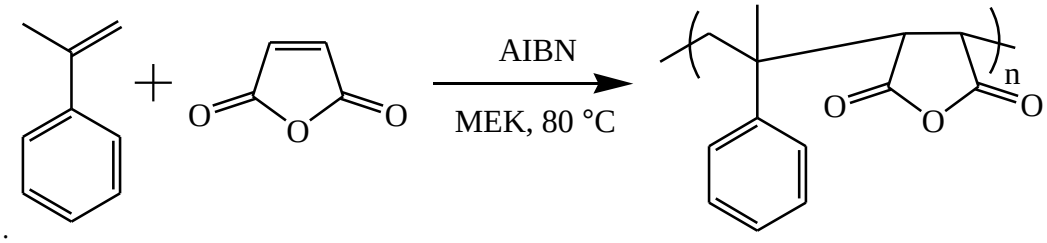

Scheme 4.02. Free radical copolymerisation of AMS and MalA, initiated by AIBN in MEK at 80 °C.

Copolymerisation of AMS and MalA is expected to give an alternating monomer sequence, as both AMS and MalA are incapable of homopolymerisation under selected conditions. Therefore, free radical homopolymerisations of AMS and MalA

were attempted to assure no significant homopolymerisation of either monomer can occur. AMS (C1) and MalA (C2) conversion was 0% by GC-FID after 4 hours of attempted homopolymerisation (Table 4.01). Furthermore, GPC was utilised to identify any higher molecular weight species. MalA control (C2) showed no higher molecular weight species. AMS control (C1) did show a very low molecular weight species, M_n 330 g·mol^{-1}, which may indicate the formation of dimer/trimer species or the species formed after initiation by a 2-cyanoprop-2-yl radical. With confidence that each monomer was not significantly homopolymerising under the selected conditions, AMS and MalA were copolymerised at a variety of monomer to initiator ratios to determine how much of an influence this may have on the final molecular weight and monomer conversions.

Increasing the concentration of initiator lowered the M_n of P[(AMS)-*a*-(MalA)] obtained and had no significant effects on dispersity, which was approximately 1.8 for each sample, or the monomer conversions which remained consistently high above 70% (Table 4.01, samples P4.01-P4.03).

Table 4.01. GPC characterisation and monomer conversions for the attempted free radical homopolymerisation of AMS/MalA (C1/2) and AMS-MalA copolymerisations (P4.01-P4.03).

Sample	[AMS]:[MalA] :[AIBN]	AMS;MalA Conversion$^{\alpha}$ (%)	$M_{n.GPC}{}^{\beta}$ (g·mol^{-1})	$M_{w.GPC}{}^{\beta}$ (g·mol^{-1})	$Đ^{\beta}$
C1	25:0:1	0;-	330	380	1.15
C2	0:25:1	-;0	-	-	-
P4.01	10:10:1	74;86	6500	11800	1.81
P4.02	25:25:1	76;83	10700	19600	1.83
P4.03	50:50:1	78;84	14500	26100	1.80

$^{\alpha}$Calculated from GC-FID. $^{\beta}$THF eluent, calibrated with PS standards.

GPC chromatograms of P[(AMS)-*a*-(MalA)] samples P4.01-P4.03 show slightly asymmetrical peaks (Figure 4.01). This may be a result of the free radical polymerisation, which is known to undergo uncontrolled polymerisation and yield polymers with higher dispersity (>1.5). However, it is has been reported that the MalA repeat unit, of P(SMalA) copolymers, interacts with the GPC column packing material (styrene-divinylbenzene) by adsorbing to the surface of said packing material which increases the polymer retention time and as a result reduces the measured M_n.[34] This may also explain the tailing observed on the GPC traces.[34] Furthermore, MalA repeat units are easily hydrolysed to the corresponding dicarboxylic acid, maleic acid (MalAc), which also interacts with the GPC column.[34] Therefore, all precipitated copolymer samples were thoroughly dehydrated in an oven at 80 °C before measuring to help ensure the copolymer has the desired ring closed structure. Throughout Chapter 2/3 all GPC measurements were performed in THF, with 2% triethylamine (TEA) added to reduce the interaction between PDMAEMA and GPC column packing material. However, all GPC measurements of MalA containing copolymers in this chapter were measured using neat THF as eluent. This is because P[(AMS)-*a*-(MalA)] samples measured by THF eluent containing 2% TEA did not display a signal on the RID, this may occur as some tertiary amines can degrade P(SMalA) copolymers.[35] Certain tertiary amines may also catalyse the decarboxylation of MalA to carbon dioxide, carbon monoxide and acetylene, potentially eliminating tertiary amine containing monomers from future copolymerisations.[35] Acetic acid is often utilised as a GPC eluent additive to suppress MalA containing copolymer's column interactions but could not be tested due to equipment usage constraints.[34] Therefore, a lack of suitable eluent additive to suppress the interactions between P[(AMS)-*a*-(MalA)] samples and column packing

material may result in further observed tailing as well as an underestimation of the final copolymers M_n.

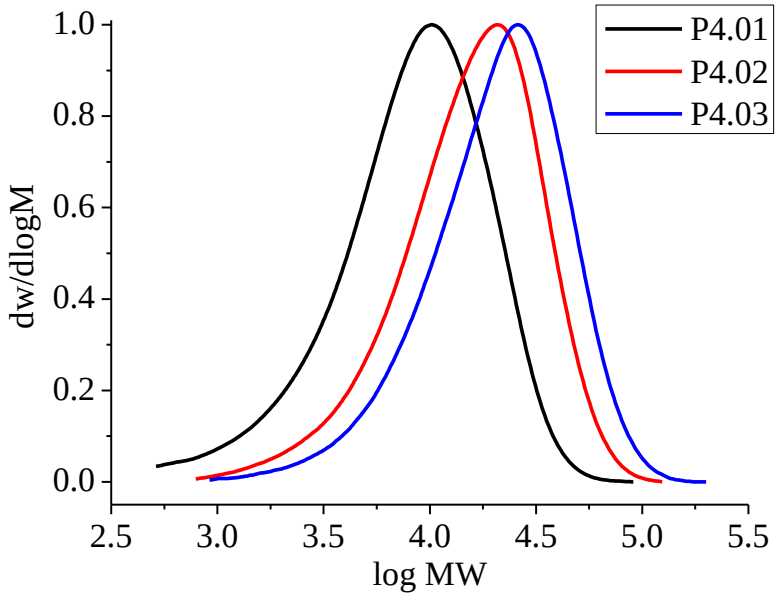

Figure 4.01. GPC traces of P[(AMS)-*a*-(MalA)] samples (P4.01-P4.03) synthesised by AMS-MalA free radical copolymerisation.

4.3. Synthesis of $AMSC_6$

An aim of this chapter is to copolymerise functionalised AMS monomers with MalA (Scheme 4.01). The functionalised AMS monomers to be synthesised within this chapter will contain a urea linkage, formed after coupling a primary amine with an isocyanate. MalA can be ring opened by primary and secondary amines as well as decarboxylated or homopolymerised by tertiary amines.[35] It was essential to determine if the nitrogen present in a urea linkage would lead to any of these negative consequences during copolymerisation, therefore hexylamine was coupled with TMI to synthesise 3-hexyl-1-[1-(*m*-isopropenylphenyl)-1-methylethyl]urea ($AMSC_6$) (Scheme 4.03). $AMSC_6$ was subsequently copolymerised with MalA to ensure the urea linkage did not negatively impact copolymerisation.

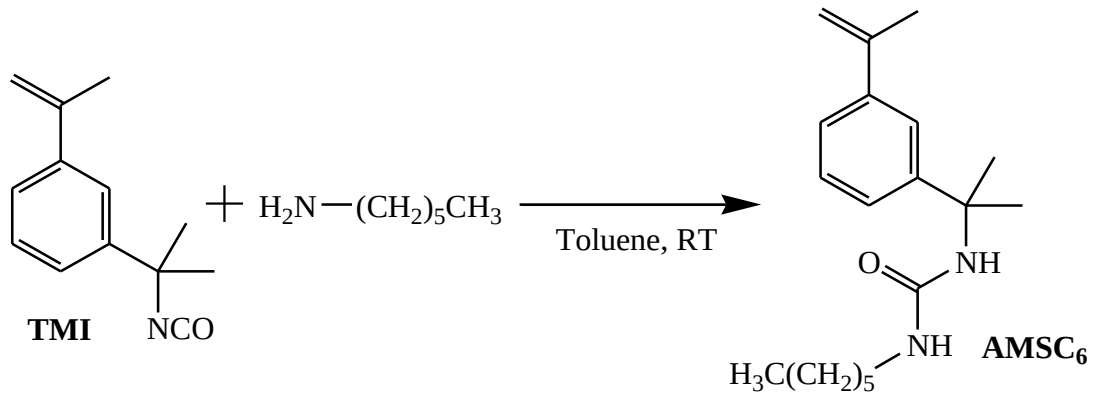

Scheme 4.03. Synthesis of $AMSC_6$ by coupling TMI with hexylamine.

$AMSC_6$ was synthesised according to Scheme 4.03. After 3 hours of stirring at room temperature the product precipitates from the toluene and can simply be filtered and dried in vacuo to obtain the product (yield = 86%). The structure is confirmed by ^{1}H-NMR and ^{13}C-NMR spectroscopy (Figure 4.02 and 4.03, respectively).

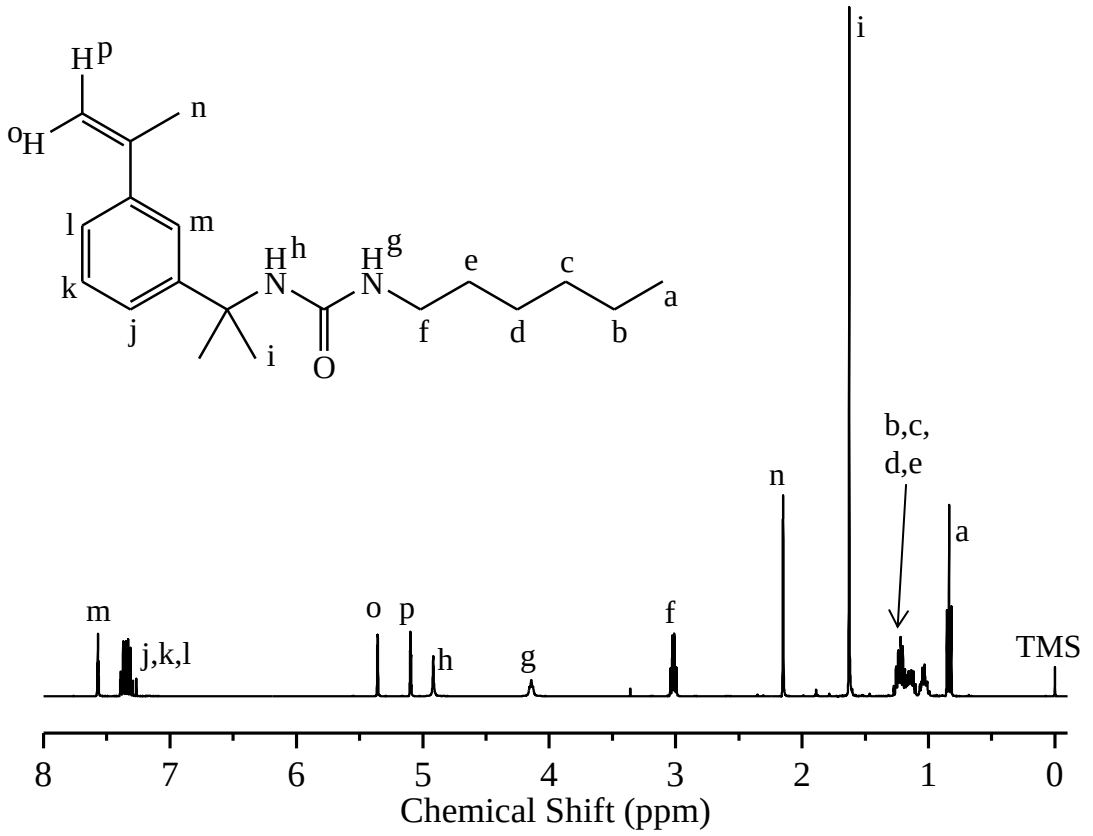

Figure 4.02. ^{1}H-NMR spectrum ($CDCl_3$, 400 MHz, 298 K) of $AMSC_6$.

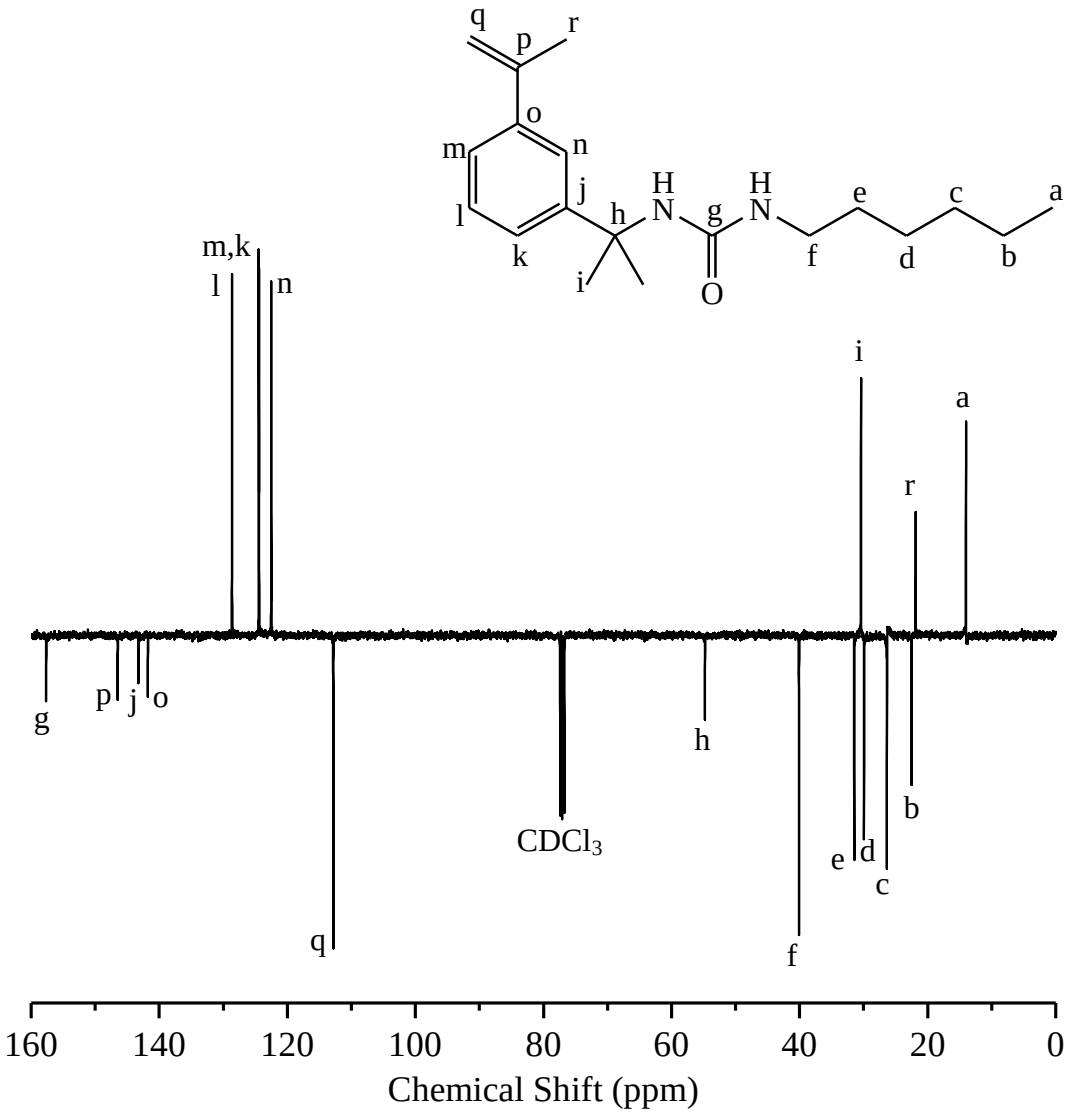

Figure 4.03. ^{13}C-NMR spectrum ($CDCl_3$, 400 MHz, 298 K) of $AMSC_6$.

FT-IR spectroscopy showed no transmittance at 2259 cm^{-1} which corresponds to the isocyanate group on TMI, thereby confirming all of the isocyanate had been consumed. Synthesis of $AMSC_6$ was shown to be a highly efficient reaction with minimal work up required to obtain high yields of very pure product. Furthermore, $AMSC_6$ contains the required urea linkage to test if it may have any negative or positive implications throughout copolymerisation with MalA.

4.3.1. Free radical copolymerisation of $AMSC_6$ and MalA

Before copolymerisation of $AMSC_6$ and MalA, a free radical homopolymerisation of $AMSC_6$ was attempted. This was to determine if $AMSC_6$ is capable of homopolymerisation. After 4 hours GC-FID measured 0% conversion of $AMSC_6$ (Table 4.02, sample C3). GPC was again used to confirm if any higher molecular weight species had formed, and indeed a higher molecular weight species with M_n of 450 g·mol^{-1} and $Đ$ of 1.02 was observed. However, this species is only 2.7% of the total integration area when integrated with the $AMSC_6$ distribution (M_n 220 g·mol^{-1}, $Đ$ = 1.01). Therefore, this species is expected to be either a dimer of $AMSC_6$ or potentially an $AMSC_6$ that has been initiated by a 2-cyanoprop-2-yl radical and unable to propagate further (Figure 4.09). A low ceiling temperature, similar to that of AMS, is expected to be the reason why $AMSC_6$ is unable to homopolymerise radically. Therefore, copolymerisation of $AMSC_6$ and MalA will result in alternating copolymers as only cross propagation is possible. Free radical copolymerisation of $AMSC_6$ and MalA was performed to synthesise P[($AMSC_6$)-*a*-(MalA)] using the same conditions found earlier to be effective for AMS and MalA (Scheme 4.04). Monomer to initiator ratio was varied to determine if this would have any influence on copolymer M_n or monomer conversions.

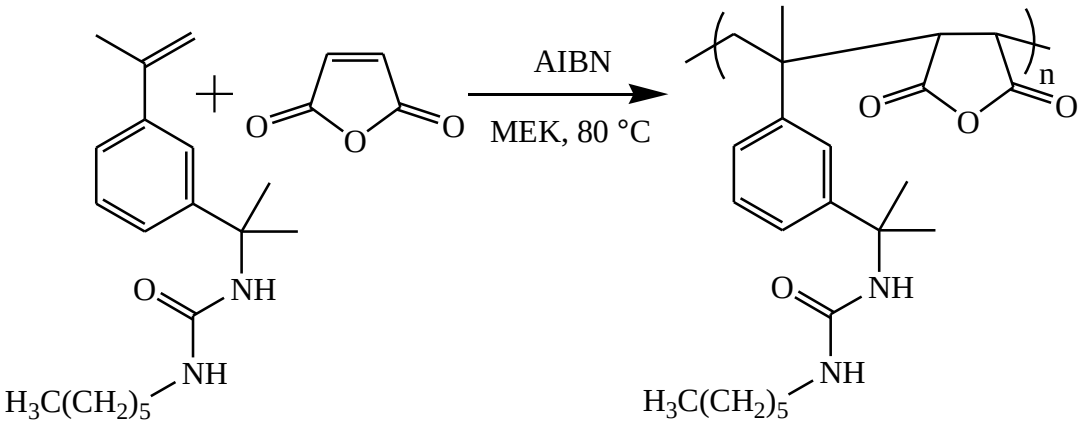

Scheme 4.04. Free radical copolymerisation of $AMSC_6$ and MalA, initiated by AIBN in MEK at 80 °C.

Copolymerisation of $AMSC_6$ and MalA was found to be possible. Similar trends are observed for that of the AMS and MalA copolymerisation; increasing the monomer to initiator ratio leads to a higher M_n and dispersity remains consistently between 1.8-1.9 (Table 4.02). However, increasing the concentration of initiator in this system led to a higher overall monomer conversion compared to AMS and MalA conversions, which were largely unaffected by the monomer to initiator ratios attempted. This may become a complication if higher molecular weight P[($AMSC_6$)-*a*-(MalA)] was desired but of the monomer to initiator ratios tested the monomer conversions are adequately high (>80%) (Table 4.02).

Table 4.02. GPC characterisation and monomer conversions for $AMSC_6$ free radical homopolymerisation (C3) and $AMSC_6$-MalA free radical copolymerisations (P4.04-P4.06).

Sample	[$AMSC_6$]:[MalA]:[AIBN]	$AMSC_6$;MalA Conversion$^{\alpha}$ (%)	$M_{n.GPC}{}^{\beta}$ (g·mol^{-1})	$M_{w.GPC}{}^{\beta}$ (g·mol^{-1})	$Đ^{\beta}$
C3	25:0:1	0;-	450	460	1.02
P4.04	10:10:1	95;91	8700	15700	1.81
P4.05	25:25:1	92;93	10400	19000	1.90
P4.06	50:50:1	81;85	17200	32500	1.89

$^{\alpha}$Calculated from GC-FID. $^{\beta}$THF eluent, calibrated with PS standards.

GPC chromatograms show that different M_n P[($AMSC_6$)-*a*-(MalA)] are synthesisable and the curves are reasonably symmetrical with some low molecular weight tailing observed again (Figure 4.04). Tailing is expected to be occurring for the same reasons explained earlier; adsorption of the MalA repeat units to the GPC column packing material (styrene-divinylbenzene).[34]

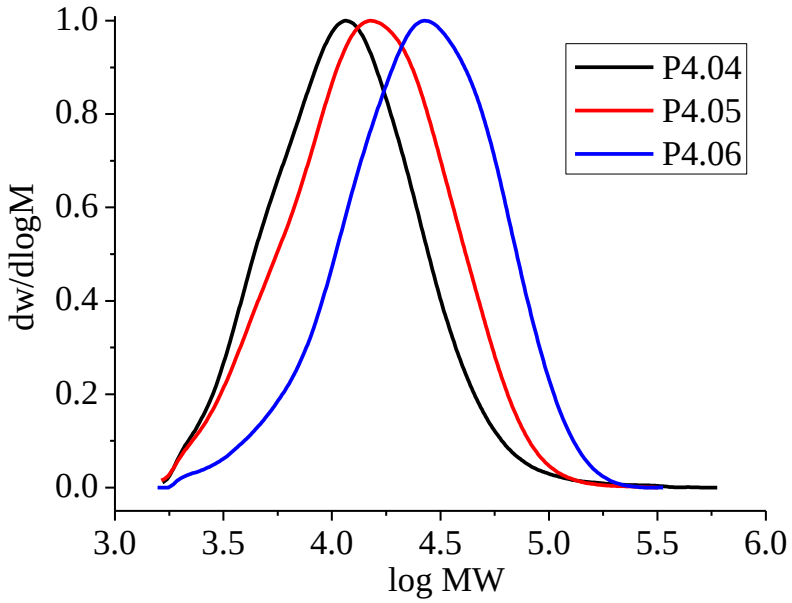

Figure 4.04. GPC traces of P[(AMSC$_6$)-*a*-(MalA)] samples (P4.04-P4.06) synthesised by AMSC$_6$-MalA free radical copolymerisation.

Furthermore, MALDI-TOF MS can be utilised to confirm the alternating nature of P[(AMSC$_6$)-*a*-(MalA)] copolymers. As these copolymers are expected to be perfectly alternating the MALDI-TOF spectrum should show a single distribution which has peaks separated by the combined mass of AMSC$_6$ and MalA (400.26 Da). The repeat unit masses are combined under the assumption that no homopolymerisation of either monomer and therefore a difference of 302.24 or 98.01 Da (for AMSC$_6$ and MalA respectively) should not be observed. This expectation is observed on the MALDI-TOF spectrum (Figure 4.05). However, two significant distributions are observed, these two distributions are caused by different mechanisms of termination throughout the free radical copolymerisation. The most intense distribution has expected masses that correspond to copolymers that are both initiated and terminated by 2-cyanoprop-2-yl radicals generated from AIBN decomposition, (Figure 4.05, blue triangles). The second most intense distribution is also initiated by 2-cyanoprop-2-yl radicals but has expected masses that correspond

to copolymers terminated by disproportionation (Figure 4.05, red diamonds). Therefore, the difference between the two distributions is 69.06 Da, the combined mass of the cyanoisopropyl and one less hydrogen when P[(AMSC$_6$)-*a*-(MalA)] is terminated by unsaturation.

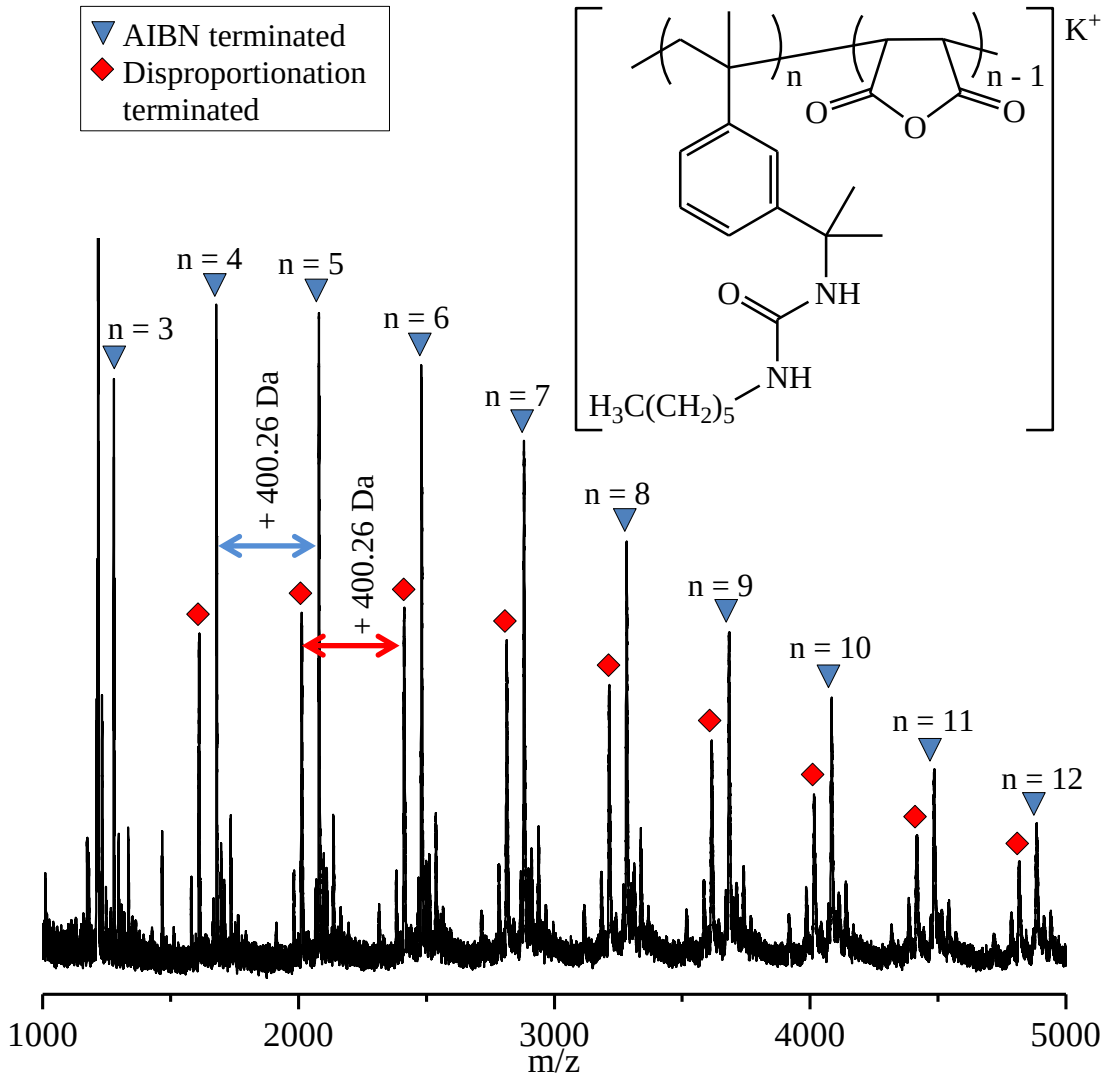

Figure 4.05. MALDI-TOF spectrum of P[(AMSC$_6$)-*a*-(MalA)] (P4.04).

On further examination of the distribution masses only copolymers with the general formula P[(AMSC$_6$)$_n$(MalA)$_{n-1}$]K$^+$ could be identified. As copolymers are expected to be alternating this implies that all copolymer chains may initiate and terminate with an AMSC$_6$ monomer. As other arrangements of copolymer chains which are initiated/terminated with a MalA would require homopolymerisation of AMSC$_6$ to total the measured mass. Research performed by Klumperman supports this

observation.[36] Klumperman and co-workers investigated the initialisation behaviour of a RAFT mediated Sy-MalA copolymerisation and found different RAFT agent leaving groups, cyanoisopropyl or cumyl, showed different preference for the first monomer addition.[36] Cyanoisopropyl was shown to predominantly add a Sy whilst cumyl leaving groups selectively added a MalA.[36] This behaviour is likely to continue into an AMS-MalA copolymerisation as AMS is an electron rich monomer and would act as electron donor for the electrophilic 2-cyanoprop-2-yl radical.

MALDI-TOF also reveals the presence of copolymers which contain one ring opened MalA repeat unit to a MalAc repeat unit, +18.02 Da. There is an additional distribution approximately +30 Da from the AIBN terminated distribution. Unfortunately, spectrum resolution is insufficient to be confident the monoisotopic pattern has been identified but it is suspected the peak at +30 Da is caused by a MalA repeat unit that has been ring opened by methanol to the corresponding half ester (MalMe). This presumably occurred during purification as the copolymer was precipitated into methanol (Figure 4.06). These side reactions could be suppressed by increasing the time spent drying the copolymer as well as precipitating into an alternative non-solvent instead of methanol.[9] After close inspection of the MALDI-TOF spectrum there is evidence of one distribution, which is still separated by 400.3 Da, that requires homopolymerisation of $AMSC_6$ to have occurred. This distribution contains 2 fewer MalA repeat units than $AMSC_6$ and therefore $AMSC_6$ has likely homopolymerised once to create this distribution (Figure 4.06). There is one final side product which shows a separation of 56.2 Da from the main distributions. This side product has not been formally identified yet but is not expected to be caused by misinsertions of monomer units as the distribution peaks are separated by 400.3 Da, therefore the alternating monomer microstructure is likely preserved.

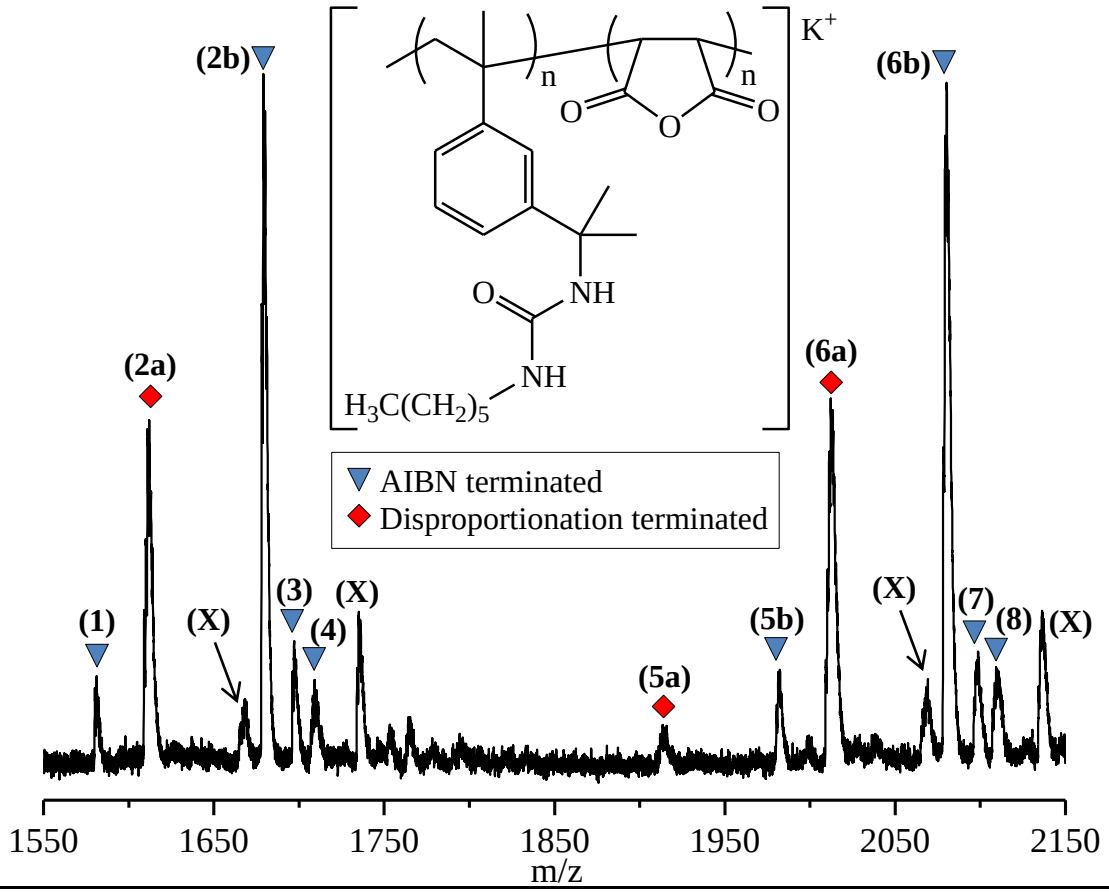

Name	Expected structure	Termination	m/z_{Theo}	m/z_{MALDI}	Δ
(1)	$P[(AMSC_6)_4(MalA)_2]K^+$	AIBN	1580.21	1580.06	0.15
(2a)	$P[(AMSC_6)_4(MalA)_3]K^+$	Dispro	1609.16	1609.11	0.05
(2b)	$P[(AMSC_6)_4(MalA)_3]K^+$	AIBN	1678.22	1678.10	0.12
(3)	$P[(AMSC_6)_4(MalA)_2(MalAc)_1]K^+$	AIBN	1696.24	1696.11	0.13
(4)	$P[(AMSC_6)_4(MalA)_2(MalMe)_1]K^+$	AIBN	1710.24	n.d.	n.d.
(5a)	$P[(AMSC_6)_5(MalA)_3]K^+$	Dispro	1911.40	n.d	n.d.
(5b)	$P[(AMSC_6)_5(MalA)_3]K^+$	AIBN	1980.46	1980.50	0.04
(6a)	$P[(AMSC_6)_5(MalA)_4]K^+$	Dispro	2009.42	2009.33	0.09
(6b)	$P[(AMSC_6)_5(MalA)_4]K^+$	AIBN	2078.48	2078.42	0.06
(7)	$P[(AMSC_6)_5(MalA)_3(MalAc)_1]K^+$	AIBN	2096.02	2096.42	0.40
(8)	$P[(AMSC_6)_5(MalA)_3(MalMe)_1]K^+$	AIBN	2110.50	n.d	n.d.

Figure 4.06. MALDI-TOF spectrum of P[($AMSC_6$)-*a*-(MalA)] (P4.04) between 1550-2150 Da, (X) = n.d. side product, Dispro. = disproportionation.

This is good evidence that the urea linkage found on $AMSC_6$ is having no detrimental effects on the MalA throughout copolymerisation, as such it is expected a urea linkage on future AMS monomers will also have no negative effects on MalA during free radical copolymerisations.

4.4. Synthesis of $AMSC_{18}$

Synthesis of $AMSC_6$ and subsequent copolymerisation with MalA was demonstrated to be a simple and effective method of incorporating alkyl grafts onto a P[(AMS)-*a*-(MalA)] backbone. Considering the original application of these alternating copolymers were novel DVMs, alkyl grafts were added to increase the solubility of the copolymers in hydrophobic media. Hexyl groups are unlikely to be sufficiently long enough to fully solubilise the potentially very polar side groups after functionalisation of the MalA repeat groups with primary amines (Scheme 4.01). Therefore, octadecylamine was reacted with TMI to synthesise a new monomer, 3-Octadecyl-1-[1-(*m*-isopropenylphenyl)-1-methylethyl]urea ($AMSC_{18}$), that contains a much larger alkyl side group that will impart more hydrophobic character onto the final copolymer (Scheme 4.05).

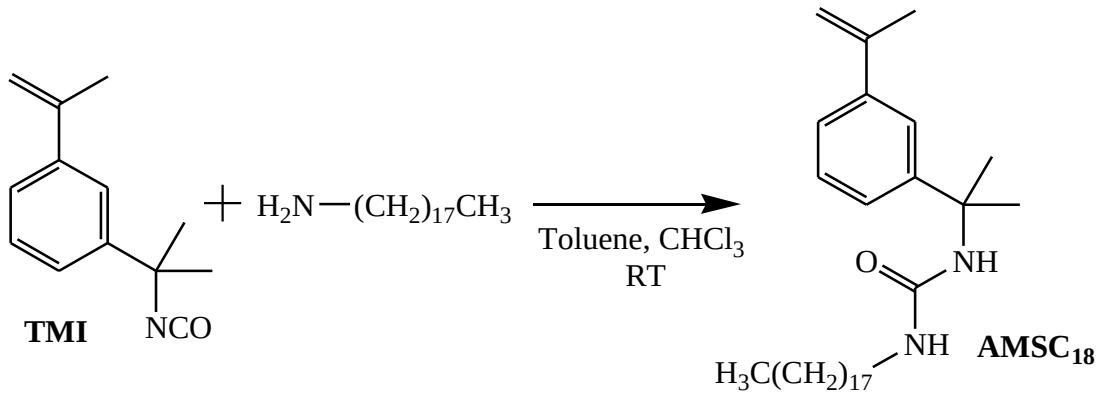

Scheme 4.05. Synthesis of $AMSC_{18}$ by coupling TMI with octadecylamine.

Synthesis of $AMSC_{18}$ was also very successful and the reaction behaved very similarly to that of $AMSC_6$, after 3 hours of stirring at room temperature the desired

product precipitated out of solution and was purified simply by filtration and drying under vacuum. The expected structure was confirmed by ^{1}H-NMR and ^{13}C-NMR spectroscopy (Figure 4.07 and Figure 4.08, respectively).

FT-IR spectroscopy measured no transmittance at 2259 cm^{-1} which corresponds to the isocyanate group on TMI, thereby confirming all of the isocyanate had been consumed. $AMSC_{18}$ synthesis was found to be as efficient and straight forward as the synthesis of $AMSC_6$, achieving high yield and purity with short reaction times at room temperature and minimal purification. Furthermore, this compound has been successfully scaled up to ~100 g scale, yield = 89%.

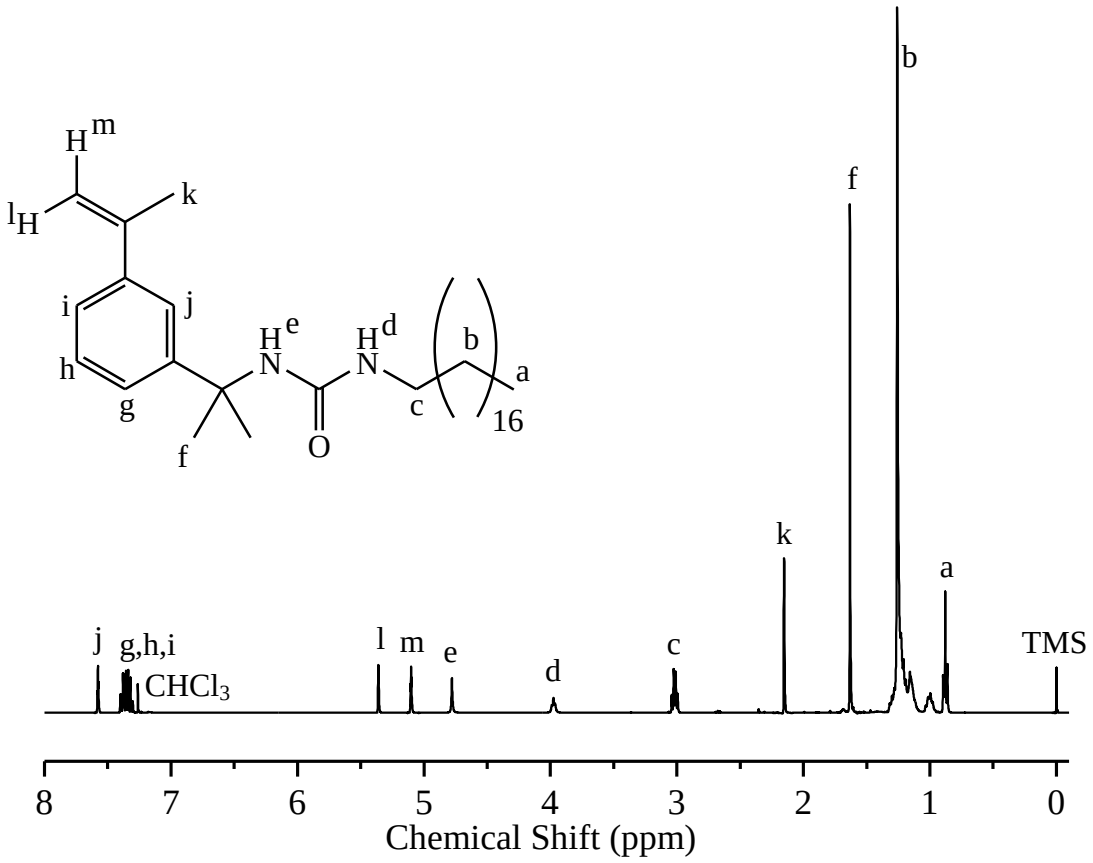

Figure 4.07. ^{1}H-NMR spectrum ($CDCl_3$, 400 MHz, 298 K) of $AMSC_{18}$.

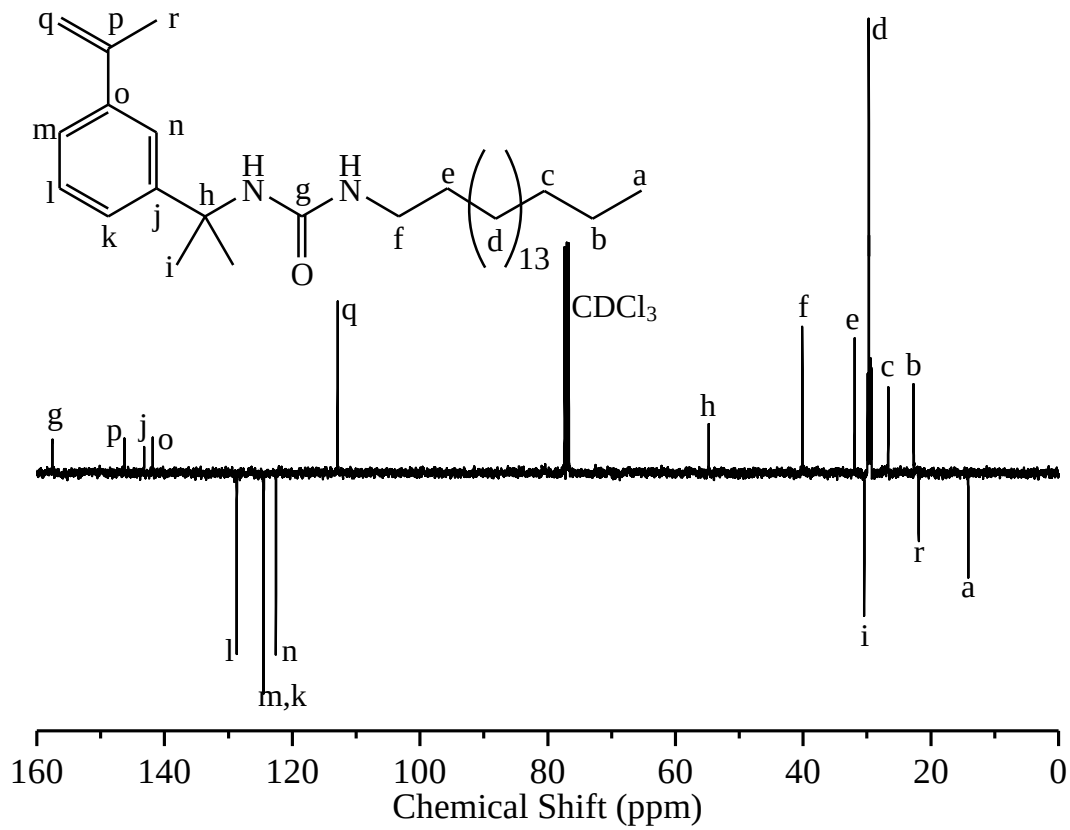

Figure 4.08. ^{13}C-NMR spectrum ($CDCl_3$, 400 MHz, 298 K) of $AMSC_{18}$.

4.4.1. Free radical copolymerisation of $AMSC_{18}$ and MalA

Copolymerisation of $AMSC_{18}$ and MalA can now be attempted to synthesise an alternating copolymer (P[($AMSC_{18}$)-*a*-(MalA)]), which will bear longer alkyl grafts then previously synthesised. Before said copolymerisation was conducted, a free radical homopolymerisation of $AMSC_{18}$ was attempted to be certain no homopolymerisation occurs. Results obtained for the control homopolymerisation of $AMSC_{18}$ (C4) were very similar to that of AMS and $AMSC_6$. Conversion of $AMSC_{18}$ was measured to be 0% by GC-FID (Table 4.03). Furthermore, GPC did measure a low molecular weight species had formed with a M_n of 1200 g·mol^{-1} and a $Đ$ of 1.02, however this species is only 3% of the total integration when the $AMSC_{18}$ distribution is also integrated (M_n 570 g·mol^{-1} and $Đ$ = 1.01, Figure 4.09).

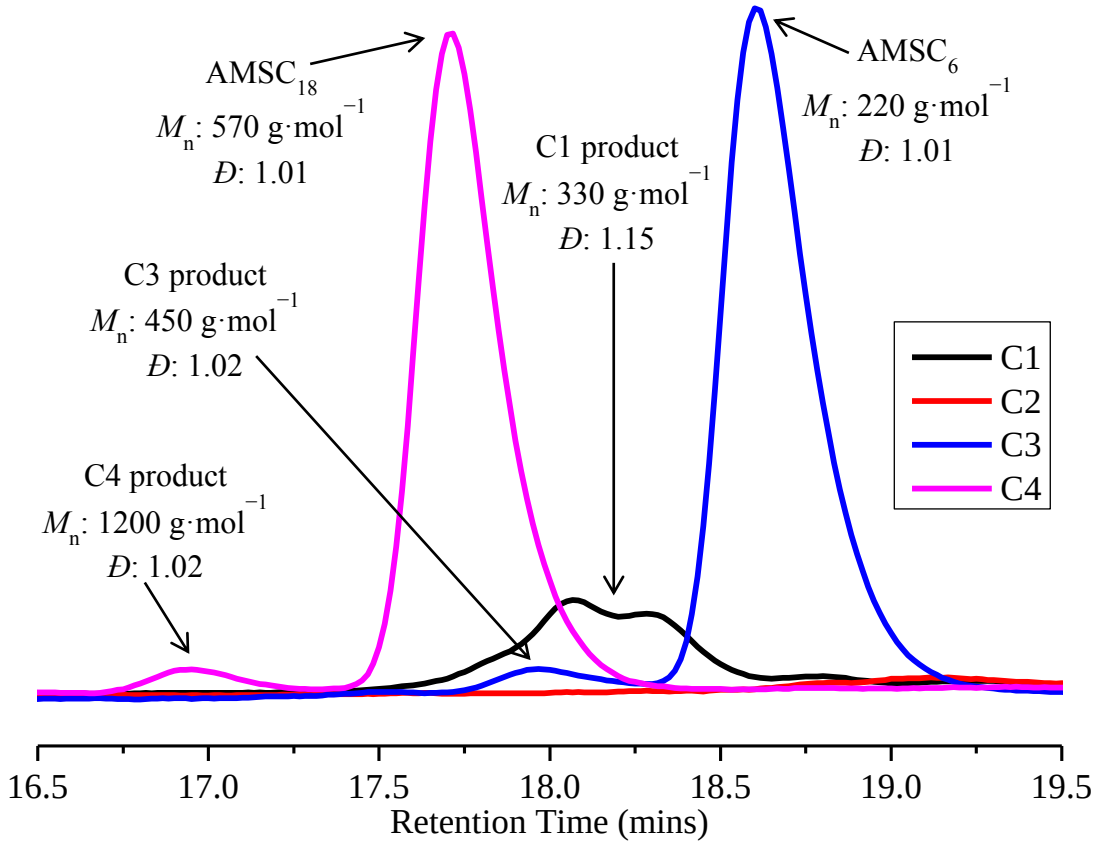

Figure 4.09. Final GPC traces for the free radical homopolymerisation controls of AMS (C1), MalA (C2), $AMSC_6$ (C3) and $AMSC_{18}$ (C4).

Therefore, the C4 product is expected to be either an $AMSC_{18}$ dimer or an $AMSC_{18}$ that has been initiated by a 2-cyanoprop-2-yl radical and unable to propagate further. As $AMSC_{18}$ did not homopolymerise significantly, it is expected to alternate when copolymerised with MalA. Free radical copolymerisation conditions utilised were the same as those for copolymerisation of AMS/$AMSC_6$ and MalA (Scheme 4.06).

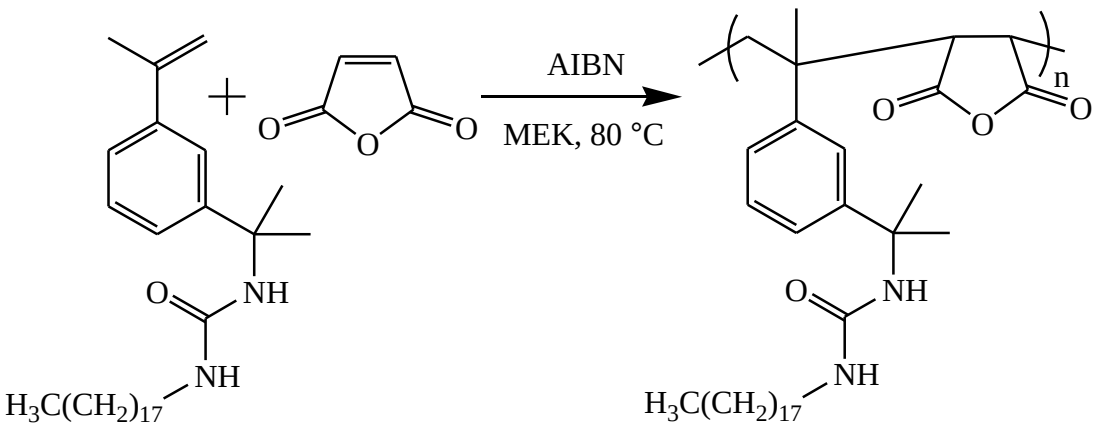

Scheme 4.06. Free radical copolymerisation of $AMSC_{18}$ and MalA, initiated by AIBN in MEK at 80 °C.

Copolymerisation of $AMSC_{18}$ with MalA was successful and continued to show the same trends observed for AMS and MalA copolymerisations. Lowering the monomer to initiator ratio led to a decrease in M_n and monomer conversions remained consistent for all three initiator concentrations tested, ~75 % (Table 4.03).

Table 4.03. GPC characterisation and monomer conversions for $AMSC_{18}$ free radical homopolymerisation (C4) and $AMSC_6$-MalA free radical copolymerisations (P4.07-P4.09).

Sample	[$AMSC_{18}$]: [MalA]:[AIBN]	$AMSC_{18}$;MalA Conversion$^{\alpha}$ (%)	$M_{n.GPC}{}^{\beta}$ (g·mol^{-1})	$M_{w.GPC}{}^{\beta}$ (g·mol^{-1})	$Đ^{\beta}$
C4	25:0:1	0;N/A	1200	1300	1.02
P4.07	5:5:1	72;74	4000	6800	1.70
P4.08	15:15:1	74;76	6000	11000	1.84
P4.09	25:25:1	72;77	7500	14300	1.91

$^{\alpha}$Calculated from GC-FID. $^{\beta}$THF eluent, calibrated with PS standards.

Polymer dispersity gives the appearance of decreasing as initiator concentration is increased. However, this is a consequence when determining the molecular weight by GPC as lower molecular weight P[($AMSC_{18}$)-*a*-(MalA)] coelutes with $AMSC_{18}$. As such this issue is most apparent for P4.07 and can be seen on the GPC traces by the trace not returning to the base line at 3.0 log MW (Figure 4.10). Furthermore, removal of $AMSC_{18}$ from P[($AMSC_{18}$)-*a*-(MalA)] proved to be very challenging and could not be achieved by precipitation without removing a significant portion of the lower molecular weight P[($AMSC_{18}$)-*a*-(MalA)].

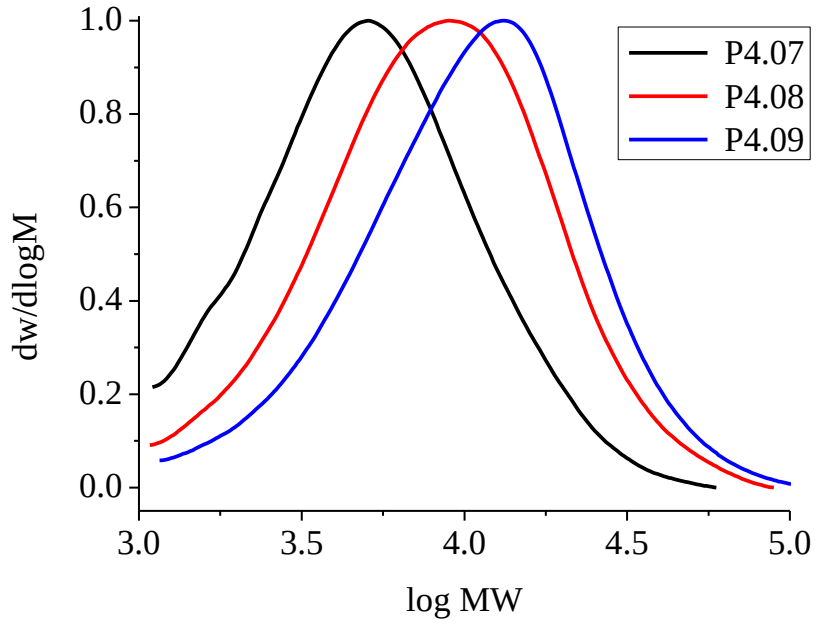

Figure 4.10. GPC traces of P[(AMSC$_{18}$)-*a*-(MalA)] samples (P4.07-P4.09) synthesised by AMSC$_{18}$-MalA free radical copolymerisation.

MALDI-TOF MS was utilised to confirm the alternating nature of the synthesised P[(AMSC$_{18}$)-*a*-(MalA)]. Similar characteristics to the P[(AMSC$_6$)-*a*-(MalA)] are observed. Alternating behaviour is again supported by the distributions showing a mass difference between repeat units that is the combined mass of AMSC$_{18}$ and MalA, 568.45 Da. As peaks are separated by the combined mass of AMSC$_{18}$ and MalA it indicates that no homopolymerisation of AMSC$_{18}$ or MalA occurred throughout copolymerisation. There is again two main distributions; the more intense distribution corresponding to copolymers initiated and terminated by 2-cyanoprop-2-yl radicals (Figure 4.11, blue triangles). The second distribution corresponds to copolymers terminated by disproportionation (Figure 4.11, red diamonds). Furthermore, a general formula for observable copolymers could be identified; P[(AMSC$_{18}$)$_n$(MalA)$_{n-1}$]K$^+$, this implies the consequence that all copolymer chains are initiated and terminated by an AMSC$_{18}$ unit. This is in good agreement with the MALDI-TOF MS measurement for P[(AMSC$_6$)-*a*-(MalA)] copolymers and is likely

caused by the same reason, 2-cyanoprop-2-yl radicals preferentially add an electron donating monomer ($AMSC_{18}$) instead of the electron accepting MalA.

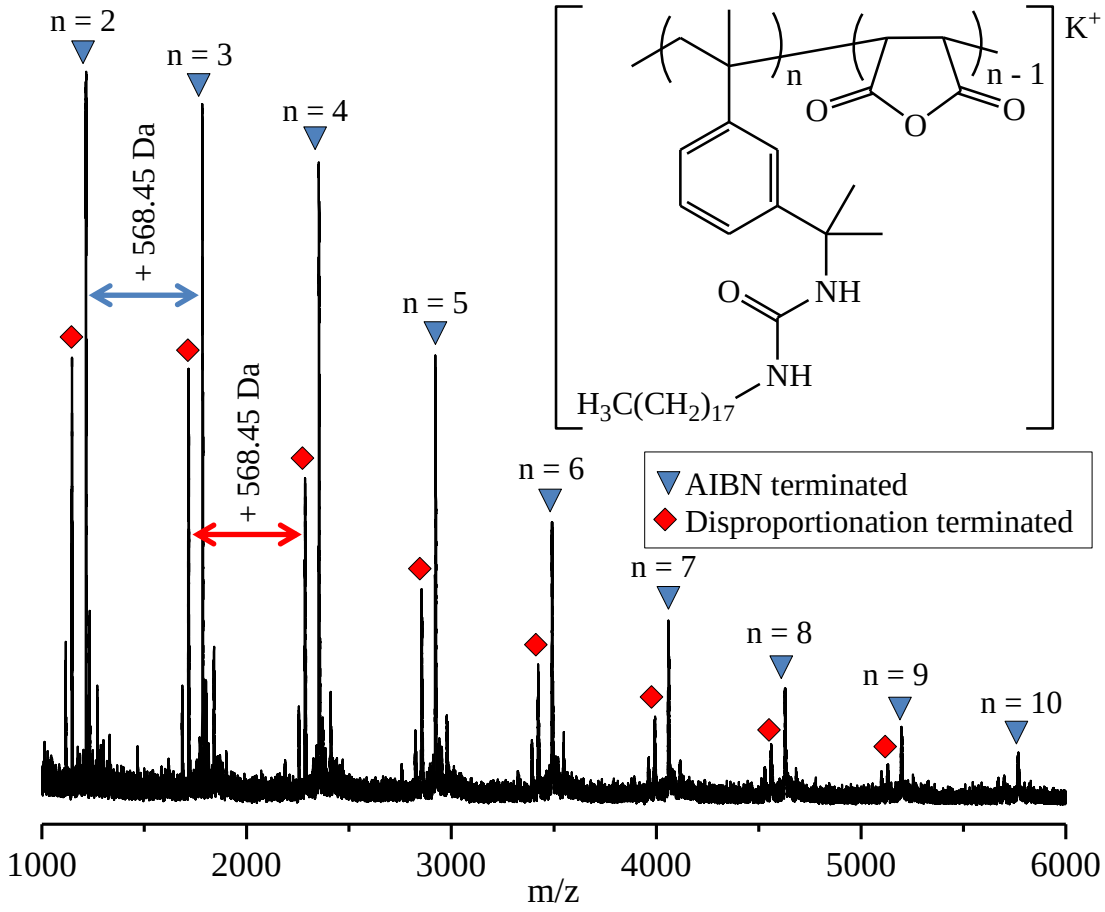

Figure 4.11. MALDI-TOF spectrum of P[($AMSC_{18}$)-*a*-(MalA)] (P4.07).

There is again evidence of MalA repeat units being ring opened to MalAc repeat units by water (Figure 4.12). There is potentially a doubly ring opened product (P[$(AMSC_{18})_3(MalAc)_2$]) as well but the resolution is too low to be certain of the mass. Species containing a MalMe repeat unit should not occur as methanol was not used during purification. $AMSC_{18}$ homopolymerisation is observable by MALDI-TOF MS by the distribution containing (1), (5a) and (5b) (Figure 4.12). As this distribution contains 2 fewer MalA repeat units than $AMSC_{18}$ it would have required $AMSC_{18}$ homopolymerisation to have occurred once. This distribution continues to show peak separation of 568.5 Da, implying some alternating micro structure of the copolymer despite one homopolymerisation of $AMSC_{18}$.

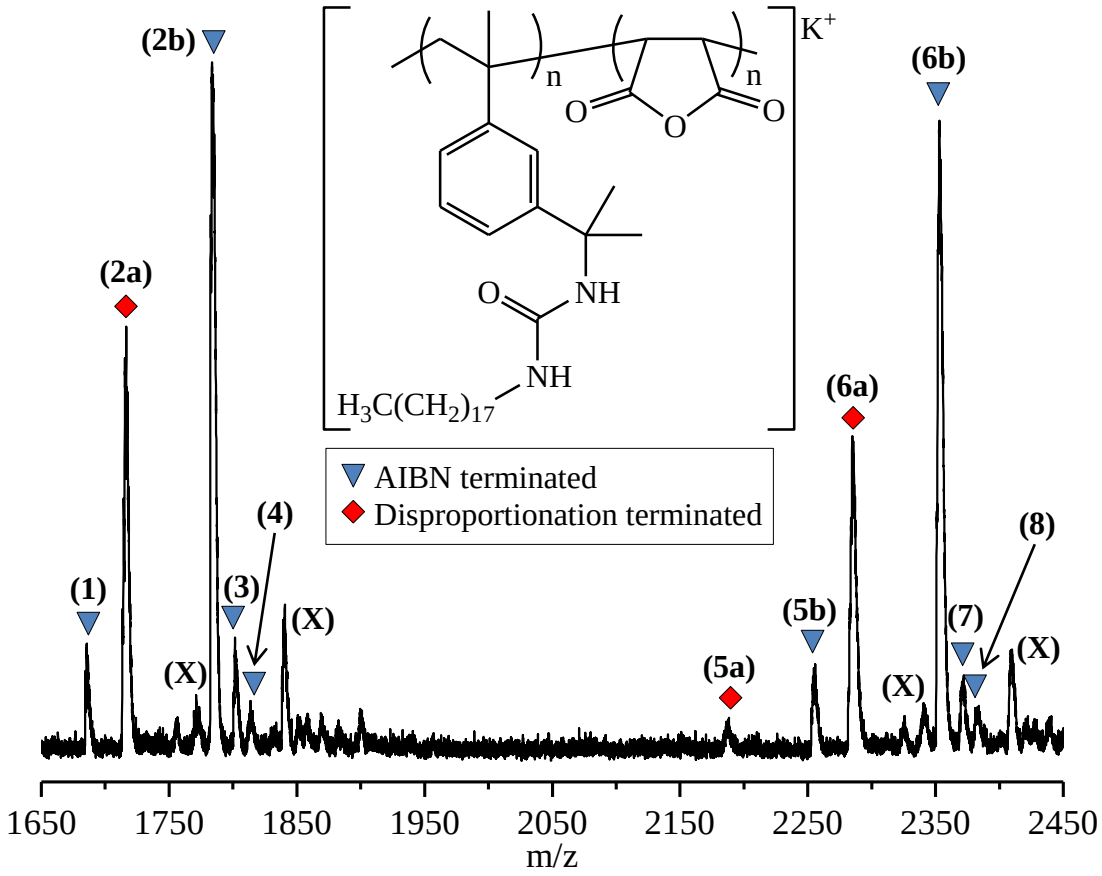

Name	Expected structure	Termination	m/z_{Theo}	m/z_{MALDI}	Δ
(1)	$P[(AMSC_{18})_3(MalA)_1]K^+$	AIBN	1684.52	1684.51	0.01
(2a)	$P[(AMSC_{18})_3(MalA)_2]K^+$	Dispro	1713.40	1713.48	0.08
(2b)	$P[(AMSC_{18})_3(MalA)_2]K^+$	AIBN	1782.54	1782.58	0.04
(3)	$P[(AMSC_{18})_3(MalA)_1(MalAc)_1]K^+$	AIBN	1800.49	1800.56	0.07
(4)	$P[(AMSC_{18})_3(MalAc)_2]K^+$	AIBN	1818.51	n.d.	n.d.
(5a)	$P[(AMSC_{18})_4(MalA)_2]K^+$	Dispro	2183.91	n.d	n.d.
(5b)	$P[(AMSC_{18})_4(MalA)_2]K^+$	AIBN	2252.97	2253.01	0.04
(6a)	$P[(AMSC_{18})_4(MalA)_3]K^+$	Dispro	2281.92	2281.70	0.22
(6b)	$P[(AMSC_{18})_4(MalA)_3]K^+$	AIBN	2350.97	2351.19	0.22
(7)	$P[(AMSC_{18})_4(MalA)_2(MalAc)_1]K^+$	AIBN	2368.99	2368.92	0.07
(8)	$P[(AMSC_{18})_5(MalA)_3(MalMe)_1]K^+$	AIBN	2382.99	n.d	n.d.

Figure 4.12. MALDI-TOF spectrum of $P[(AMSC_{18})$-*a*-(MalA)] (P4.07) between 1650 and 2450 Da. (X) = n.d. side product, Dispro. = disproportionation.

An unknown side product appearing +56.2 Da from the main distributions is again present (Figure 4.12). This unknown distribution again shows a peak separation of 568.5 Da, the combined mass of $AMSC_{18}$ and MalA, which implies an alternating microstructure is still present.

This characterisation again confirms the urea linkage present in $AMSC_{18}$ does not cause any significant negative effects on the MalA throughout copolymerisation and an alternating monomer micro structure is present for the majority of the copolymer distribution. $AMSC_{18}$ was further studied to be utilised as a hydrophobic comonomer to copolymerise with MalA.

4.4.2. Free radical copolymerisation of $AMSC_{18}$ and MalA using AMSD as CTA

Monomer to initiator concentration was capable of influencing the final molecular weight of P[($AMSC_{18}$)-*a*-(MalA)] synthesised. However, large quantities of AIBN (5.3 wt%) were required to achieve the lowest molecular weight copolymer synthesised (P4.07). This is a potential problem when considering scaling up the synthesis as free radical initiators, such as AIBN, are explosive compounds when heated and heating large quantities during polymerisation can lead to excessive nitrogen gas generation and thermal runaway. Therefore, chain transfer was considered as a means of limiting the molecular weight by adding a chain transfer agent (CTA) rather than using higher concentrations of initiator. Various thiols and halogens were considered as possible CTAs but as the fuel additive industry has very strict guidelines for sulfur and halogen-containing species an alternative was found to avoid these compounds. One compound that has been previously utilised as a CTA for AMS-MalA copolymerisation is the α-methylstyrene dimer (AMSD).[37] AMSD has been shown to be a powerful CTA with a mechanism of chain transfer based on a reversible addition fragmentation chain transfer, a mechanism which has

been capable of displaying living polymerisations.[38,39] Therefore, AMSD was added as a CTA to the free radical copolymerisation of $AMSC_{18}$ and MalA to see if any reduction in molecular weight could be achieved (Scheme 4.07).

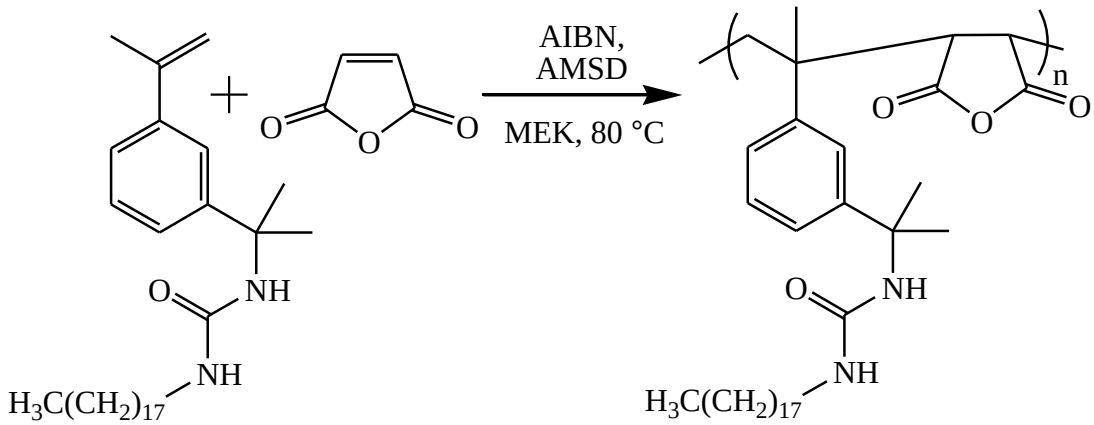

Scheme 4.07. Free radical copolymerisation of $AMSC_{18}$ and MalA, initiated by AIBN and mediated by AMSD in MEK at 80 °C.

AMSD was capable of decreasing the M_n of P[($AMSC_{18}$)-*a*-(MalA)] obtained (Table 4.04). Five equivalents of AMSD relative to initiator was enough to reduce the molecular weight by over half whilst maintaining AMS and MalA conversions above 70%. As a result, low molecular weight P[($AMSC_{18}$)-*a*-(MalA)] can now be synthesised by addition of AMSD rather than utilising large quantities of AIBN, reducing the wt% from 5.3% to 1.5%.

Table 4.04. GPC characterisation and monomer conversions for $AMSC_{18}$-MalA free radical copolymerisation mediated with AMSD.

Sample	[$AMSC_{18}$]:[MalA]:[AMSD]:[AIBN]	$AMSC_{18}$;MalA Conversion$^{\alpha}$ (%)	$M_{n.GPC}{}^{\beta}$ (g·mol^{-1})	$M_{w.GPC}{}^{\beta}$ (g·mol^{-1})	$Đ^{\beta}$
P4.11	25:25:5:1	72;73	3300	6600	2.00
P4.10	25:25:1:1	72;76	7000	23100	3.30
P4.07	25:25:0:1	72;77	7500	14300	1.91

$^{\alpha}$Calculated from GC-FID. $^{\beta}$THF eluent, calibrated with PS standards.

GPC traces of the purified P[(AMSC$_{18}$)-*a*-(MalA)] samples synthesised with the presence of AMSD as CTA show the same issue regarding coelution of the obtained copolymer and AMSC$_{18}$ (Figure 4.13), thus GPC traces do not return to baseline.

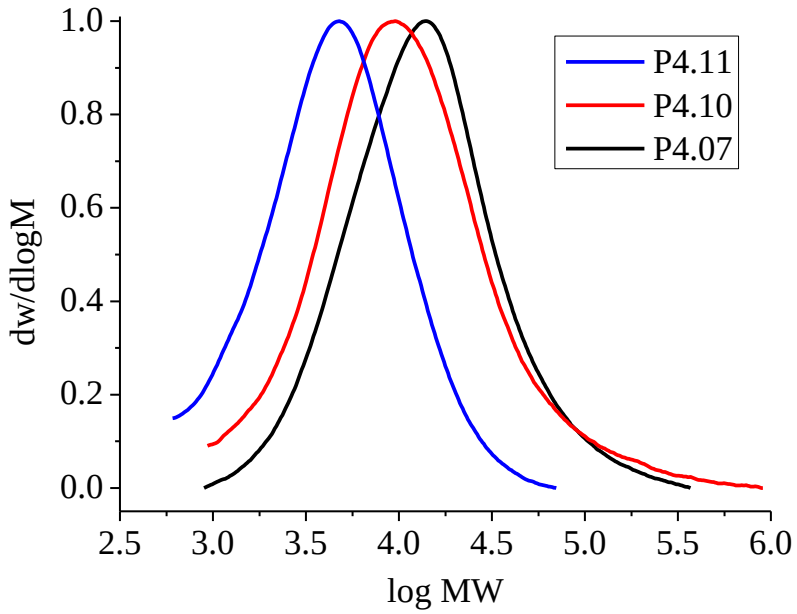

Figure 4.13. GPC traces of P[(AMSC$_{18}$)-*a*-(MalA)] samples (P4.07, P4.10/P4.11) synthesised by AMSC$_{18}$-MalA free radical copolymerisation using AMSD as a CTA.

4.5. Synthesis of AMSDMA

The previous functionalised AMS monomers (AMSC$_6$ and AMSC$_{18}$) were designed to bear an alkyl moiety. Once copolymerised with MalA the resulting alternating copolymer could then be functionalised via ring opening of the MalA repeat unit with a primary amine bearing a tertiary amine (Scheme 4.01). An alternative route to achieve similar alternating copolymer architecture would be to synthesise an AMS monomer bearing a tertiary amine, copolymerise said monomer with MalA and finally functionalise the MalA repeat units with linear aliphatic primary amines. A tertiary amine bearing AMS monomer was synthesised by reactive coupling of *N*,*N*-dimethylethylenediamine and TMI to synthesise 3-[2-(dimethylamino)ethyl]-1-[1-(*m*-isopropenylphenyl)-1-methylethyl]urea (AMSDMA) (Scheme 4.08).

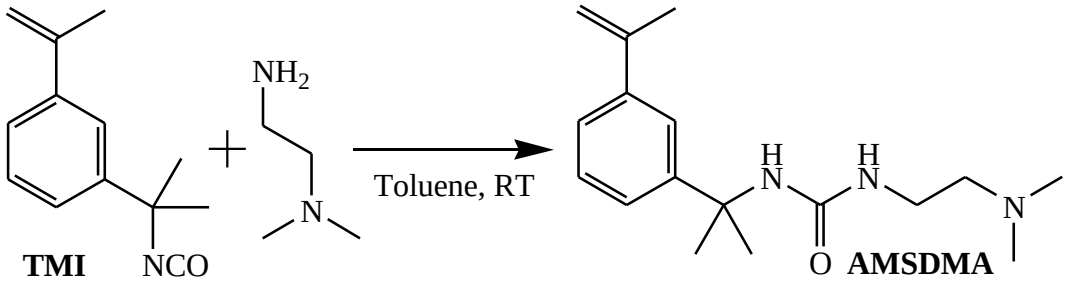

Scheme 4.08. Synthesis of AMSDMA by reacting TMI with *N*,*N*-dimethylethylenediamine.

Synthesis of AMSDMA proceeded in a similar fashion to that of $AMSC_6$, after 3 hours of reacting at room temperature the product (AMSDMA) precipitated out of solution and was purified by filtration and washing with acetone before drying in vacuo. The expected structure was confirmed by ^{1}H-NMR and ^{13}C-NMR spectroscopy (Figure 4.14 and 4.15, respectively).

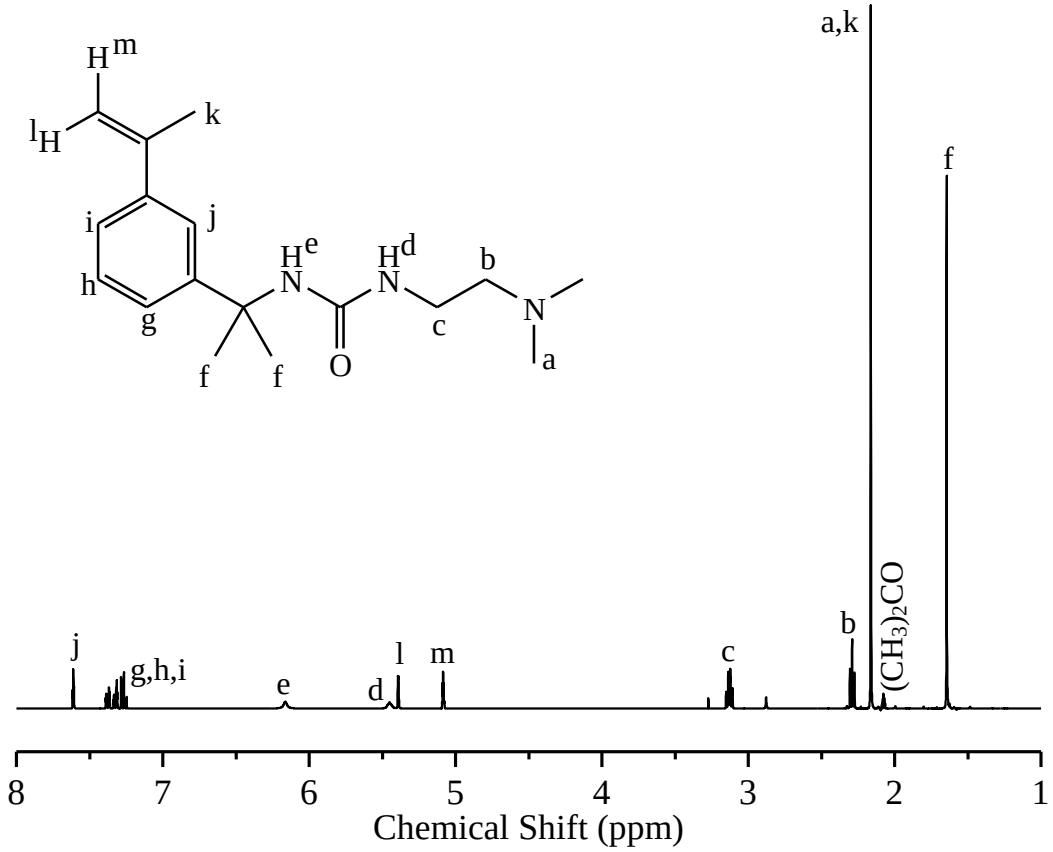

Figure 4.14. ^{1}H-NMR spectrum ($(CD_3)_2CO$, 400 MHz, 298 K) of AMSDMA.

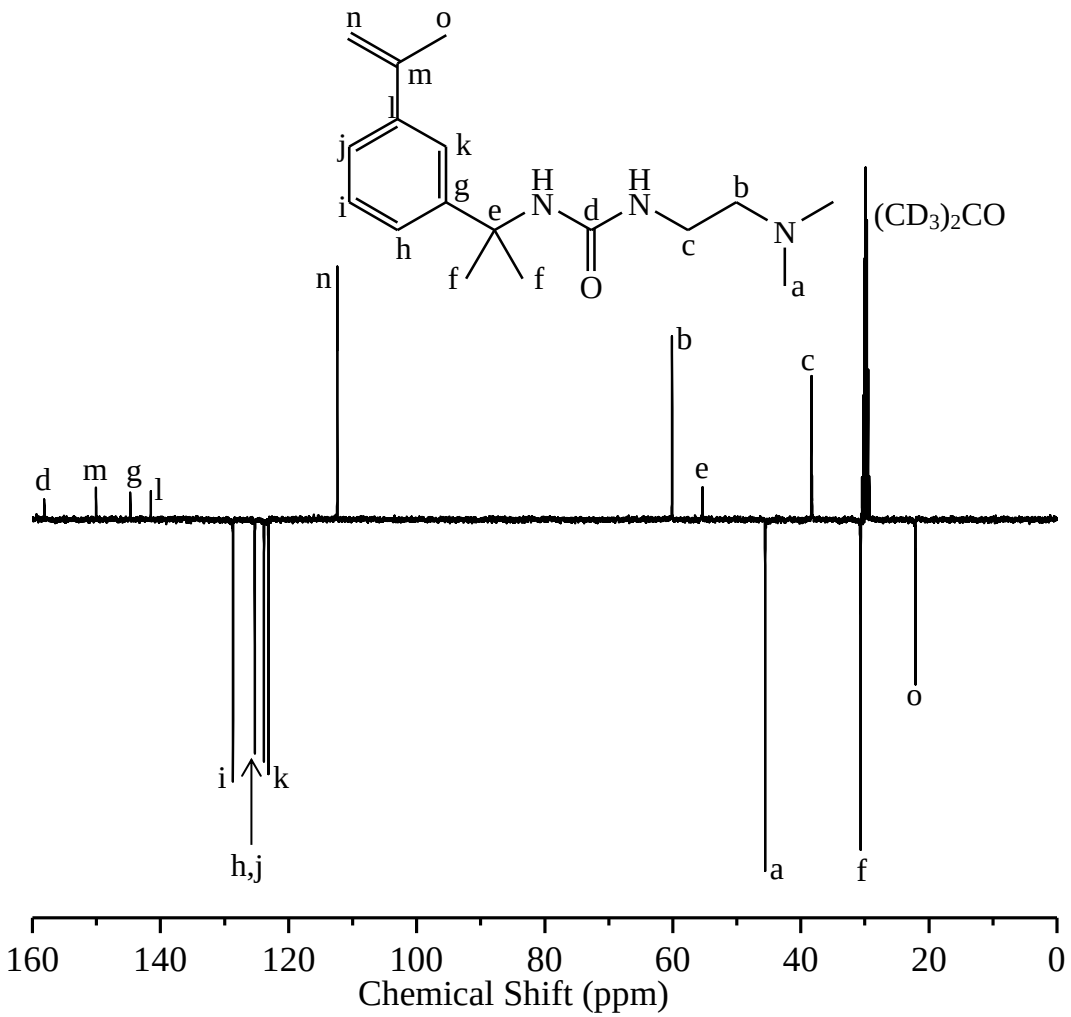

Figure 4.15. ^{13}C-NMR spectrum ($(CD_3)_2CO$, 400 MHz, 298 K) of AMSDMA.

4.5.1. Attempted free radical copolymerisation of AMSDMA and MalA

Free radical copolymerisation of AMSDMA and MalA was performed using conditions that have been previously effective; AIBN initiated in MEK at 80 °C. However, AMSDMA-MalA copolymerisation was unsuccessful. The reaction mixture quickly turned brown after heating to 80 °C and after four hours the mixture was completely opaque with black precipitate. Said precipitate was insoluble in all available GPC (THF, $CHCl_3$, DMF and H_2O) and NMR ($CDCl_3$, $(CD_3)_2CO$, DMF-d_7 and D_2O) solvents at room temperature. It is expected the dimethylamino moiety present on AMSDMA may have decarboxylated and homopolymerised MalA to the insoluble black precipitate. This represents a potential limitation to this synthetic

approach as many tertiary amine bearing monomers will not undergo free radical copolymerisation with MalA without significant side reactions.

4.6. Imidisation of P[(AMSC$_{18}$)-*a*-(MalA)]

Continuing from the synthesis of P[(AMSC$_{18}$)-*a*-(MalA)], the final stage of the planned synthesis is to modify the MalA repeat units with functional primary amines to form the corresponding functional succinic imide repeat unit. 4-(Aminomethyl)pyridine was utilised to functionalise the MalA repeat unit of P[(AMSC$_{18}$)-*a*-(MalA)] to a new repeat unit; *N*-(4-methylpyridine)maleimide (PyMI) (Scheme 4.09). This functionalisation was performed at high temperature (160 °C) to encourage ring close of the amine modified MalA repeat units by loss of water. Therefore, a high-boiling hydrophobic solvent was required to effectively remove the water in conjunction with Dean-Stark apparatus. Caromax 20 is a mixture of hydrophobic C10-20 aromatic compounds with a boiling range of 160-230 °C, therefore a suitable solvent for the modification of P[(AMSC$_{18}$)-*a*-(MalA)].

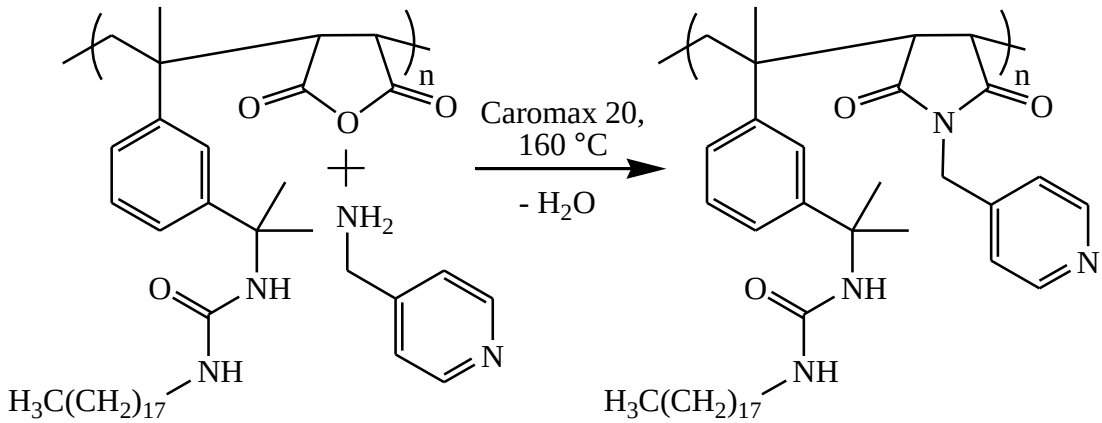

Scheme 4.09. Functionalisation of P[(AMSC$_{18}$)-*a*-(MalA)] (P4.11) by imidisation of MalA repeat units with 4-(aminomethyl)pyridine to synthesise P[(AMSC$_{18}$)-*a*-(PyMI)].

Imidisation of cyclic anhydrides to cyclic imides is a two-step reaction. Firstly the primary amine ring opens the cyclic anhydride to form a new amide bond and a carboxylic acid. Given sufficiently high temperature (160-200 °C) and continual

removal of water (Dean-Stark apparatus), the carboxylic acid and amine bond will cyclise with loss of water to from a cyclic imide retaining the functionality present on the original primary amine. Imidisation of P[(AMSC$_{18}$)-*a*-(MalA)] with 4-(aminomethyl)pyridine was shown to be successful by FT-IR spectroscopy (Figure 4.16). There is loss of cyclic anhydride peaks at 1858 cm^{-1} and 1777 cm^{-1} replaced by new peaks at 1771 cm^{-1} and 1698 cm^{-1}.

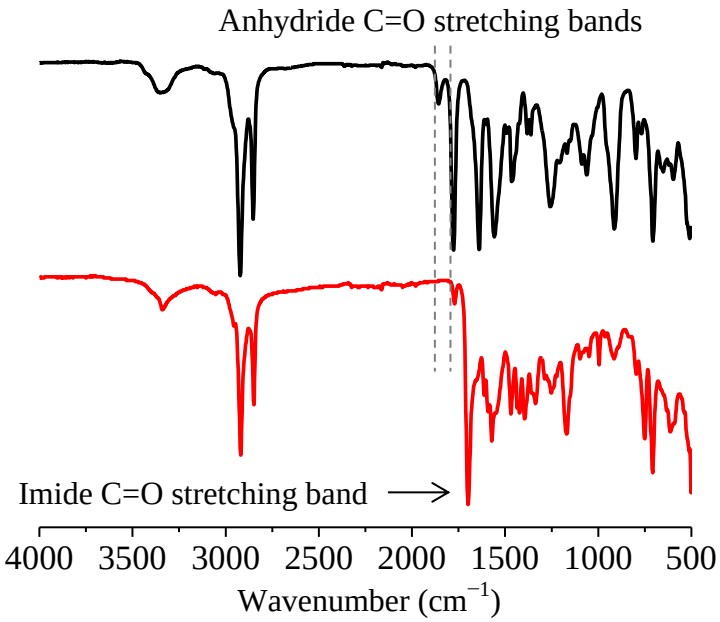

Figure 4.16. FT-IR spectra of P[(AMSC$_{18}$)-*a*-(MalA)] (P4.11) (black) and P[(AMSC$_{18}$)-*a*-(PyMI)] (red).

^{1}H-NMR spectroscopy also supports the addition of pyridine functionality by the appearance of two broad signals centred at 7.55 ppm and 8.43 ppm, corresponding to the *ortho* and *meta* protons of the pyridine group (Figure 4.17). Furthermore, following modification of the MalA repeat units to PyMI repeat units the copolymer is rendered insoluble in *n*-hexane. Therefore, it is now possible to remove the excess AMSC$_{18}$ monomer present in P[(AMSC$_{18}$)-*a*-(MalA)] by precipitation in *n*-hexane. This is confirmed by, the disappearance of vinylidene protons seen at 5.37 ppm and

5.12 ppm as well as other proton resonances in the ^{1}H-NMR spectrum of P[(AMSC$_{18}$)-*a*-(MalA)] but not P[(AMSC$_{18}$)-*a*-(PyMI)] (Figure 4.17).

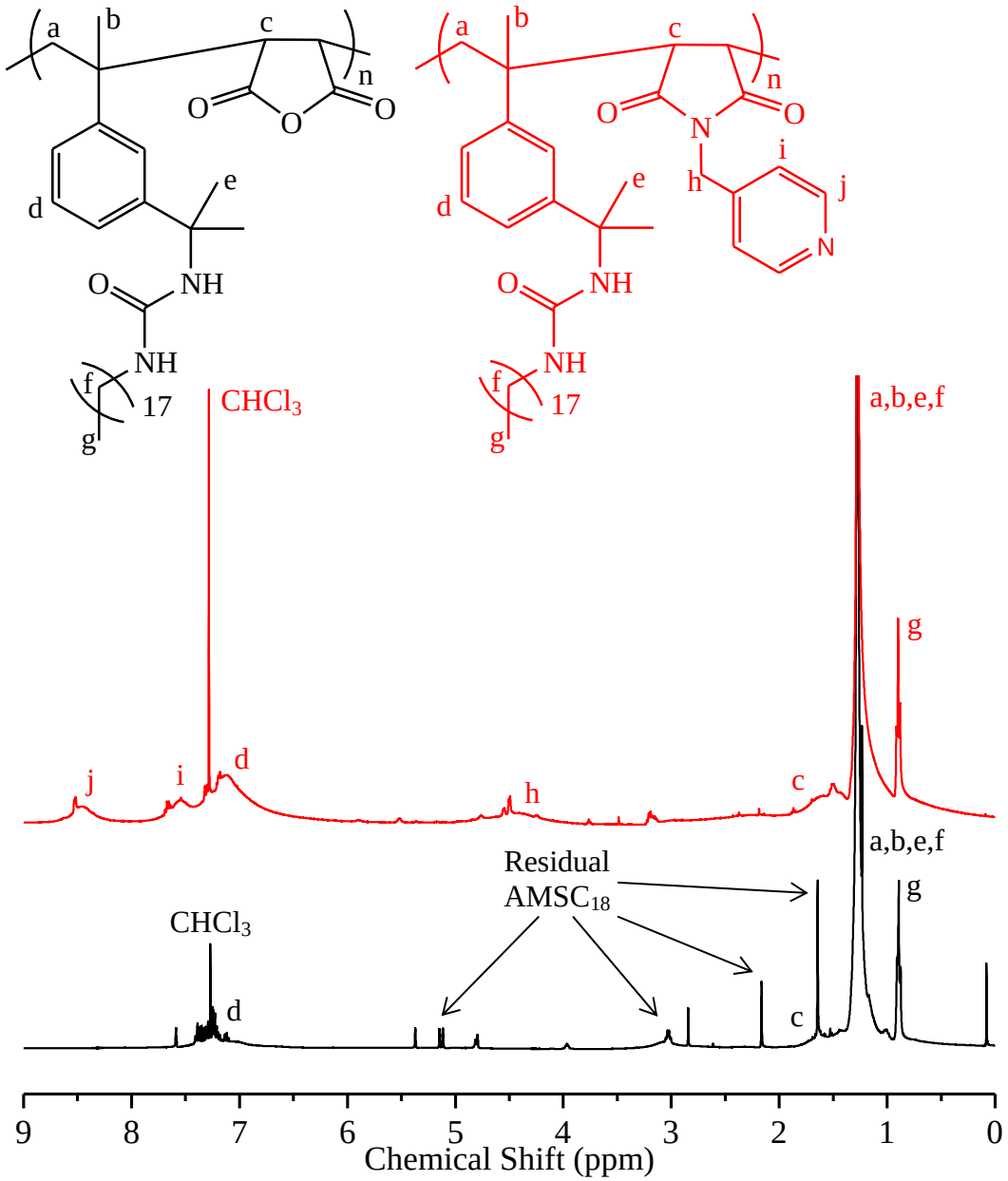

Figure 4.17. ^{1}H-NMR spectra ($CDCl_3$, 400 MHz, 298 K) of P[(AMSC$_{18}$)-*a*-(MalA)] (P4.11) (black) and P[(AMSC$_{18}$)-*a*-(PyMI)] (red).

Furthermore, tertiary amines have been shown to degrade Sy-MalA copolymers, therefore GPC was used to confirm that P[(AMSC$_{18}$)-*a*-(MalA)] was not degraded throughout the reaction with 4-(aminomethyl)pyridine. P[(AMSC$_{18}$)-*a*-(MalA)] was rendered insoluble in THF after modification to P[(AMSC$_{18}$)-*a*-(PyMI)] and as such

had to be measured by GPC eluted with DMF containing 5mM ammonium tetrafluoroborate instead of THF. GPC measured a very significant increase in M_n following imidisation; 3300 g·mol^{-1} to 23700 g·mol^{-1} (Figure 4.18). An increase in molecular weight was expected as mass was added to every MalA repeat unit, however this alone may not explain the large mass increase. It was discussed earlier that P(SMalA) copolymers are known to adsorb to GPC columns when neat THF is used as an eluent; this increases the copolymer's retention time and thus underestimates the M_n. It may be possible that the functionalised copolymer P[(AMSC$_{18}$)-*a*-(PyMI)] does not adsorb to the GPC column as strongly or at all, thus lowering the copolymers retention time and increasing the calculated M_n.

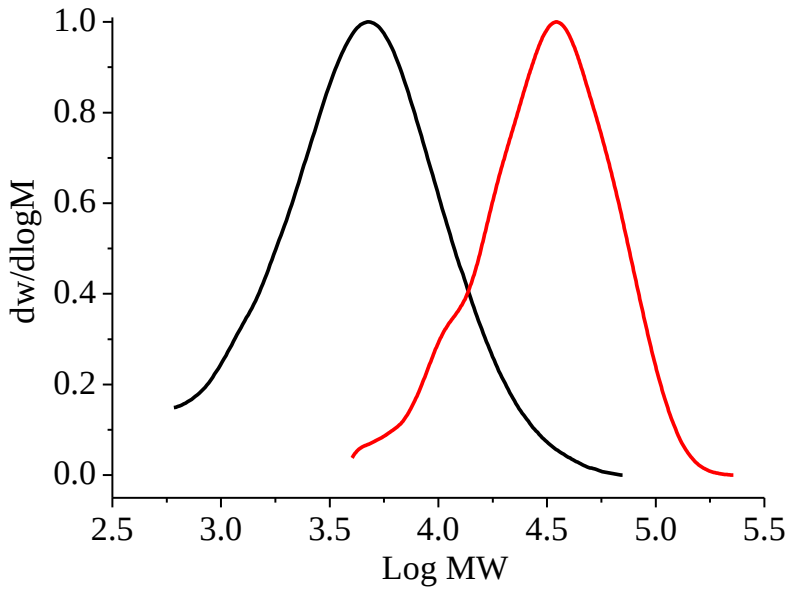

Figure 4.18. GPC traces of P[(AMSC$_{18}$)-*a*-(MalA)] (P4.11) (black) and P[(AMSC$_{18}$)-*a*-(PyMI)] (red).

The newly synthesised P[(AMSC$_{18}$)-*a*-(PyMI)] now has alternating functionalities of pyridine and alkyl grafts. Synthesis of P[(AMSC$_{18}$)-*a*-(PyMI)] represents an example of how functionality can be incorporated onto a P[(AMSC$_{18}$)-*a*-(MalA)] precursor to synthesise a copolymer with alternating functionalities. An analogous methodology could potentially be achieved with primary hydroxyls in place of the primary amine.

4.7. Conclusions

Coupling TMI and primary amines has been shown to be a simple and efficient method for synthesising AMS monomers functionalised with linear alkyl chains, hexyl and octadecyl, as well as a dimethylamino group. Alkyl functionalised monomers ($AMSC_6$ and $AMSC_{18}$) were than successfully copolymerised with MalA by free radical copolymerisation to synthesise alternating copolymers. Alternating microstructure of the copolymers was supported by attempted homopolymerisations of the individual monomers (AMS, MalA, $AMSC_6$ and $AMSC_{18}$), which do not homopolymerise. Furthermore, MALDI-TOF MS characterisation also demonstrates how the distributions of repeat units are separated by mass that corresponds to the combined mass of AMS monomers and MalA, indicating an alternating structure. additionally MALDI-TOF MS demonstrates that all copolymer chains begin and end with AMS monomers. Alternating copolymer's molecular weights could be influenced by the initiator concentration, as evidenced by higher concentrations of initiator giving lower molecular weight copolymers, whilst retaining high monomer conversions >70% and dispersities of ~2. Furthermore, no adverse effects on the MalA were observed by the presence of a urea linkage during copolymerisation, such as homopolymerisation or decarboxylation of the MalA. However, when TMI was functionalised with a dimethylamino group (AMSDMA), copolymerisation with MalA was not possible.

An example of post-polymerisation modification of P[($AMSC_{18}$)-*a*-(MalA)] was demonstrated by imidisation of the MalA repeat unit with 4-(aminomethyl)pyridine at 160 °C to synthesise P[($AMSC_{18}$)-*a*-(PyMI)]. This modification highlights the potential versatility of P[($AMSC_{18}$)-*a*-(MalA)], using alternative primary amines in place of 4-(Aminomethyl)pyridine would impart different functionality onto the final

copolymer. Other primary amines that were utilised to functionalise P[(AMSC$_{18}$)-*a*-(MalA)] include 3-(dimethylamino)-1-propylamine, 1-(2-aminoethyl)piperazine and 4-(2-aminoethyl)morpholine. Functionalisation with these amines was demonstrated by FT-IR spectroscopy but other characterisation techniques (^{1}H-NMR spectroscopy, GPC etc.) were less effective as the resulting copolymers were poorly soluble at room temperature in the available solvents. P[(AMSC$_{18}$)-*a*-(PyMI)] and other functionalised [(AMSC$_{18}$)-*a*-(MalA)] derivatives were submitted to Innospec for performance testing as fuel dispersants. However, the copolymers did not exhibit sufficient solubility (10 wt%) in testing solvents (aliphatic hydrocarbons) at room temperature and as a consequence they were not advanced to next stage of testing. Solubility of the functionalised P[(AMSC$_{18}$)-*a*-(MalA)] in testing solvents may have been insufficient as too many polar functional groups were grafted to the copolymer backbone. This could be addressed by reducing the grafting density of polar side groups in exchange for non-polar groups such as linear aliphatic chains. Furthermore, presence of a urea linkage on the AMSC$_{18}$ repeat units may reduce the solubility as this is another polar functional group.

Despite the negative application testing, this chapter demonstrates a versatile new class of alternating copolymers that are capable of being independently functionalised on both the AMS and MalA repeat units whilst maintaining a near-perfect alternating microstructure.

4.8. Experimental

4.8.1. Instrumentation

4.8.1.1. Gel permeation chromatography

Molecular weight averages and polymer dispersity were determined on one of two GPC systems. System 1; GPC samples were prepared to a concentration of 1 mg·mL^{-1} and passed through 0.4 µm PTFE filters before injection. GPC measurements were performed an Agilent 390-LC system equipped with a PL-AS RT autosampler, 2 PLgel 5 µm mixed-C columns (300 × 7.5 mm), a PLgel 5 mm guard column (50 × 7.5 mm), a refractive index detector (RID). Columns and RID were maintained at 50 °C. The system was eluted with THF at a flow rate of 1 mL·min^{-1} and the RID was calibrated with linear narrow polystyrene standards. System 2; GPC samples were prepared to a concentration of 1mg·mL^{-1} and passed through 0.2 µm nylon filters before injection. GPC measurements were performed on an Agilent 1260 infinity system equipped with 2 PLgel 5 µm mixed-D columns (300 × 7.5 mm), a PLgel 5 mm guard column (50 × 7.5 mm), a RID and variable wavelength detector (VWD). Columns and RID were maintained at 50 °C. The system was eluted with DMF containing 5 mM ammonium tetrafluoroborate at a flow rate of 1 mL·min^{-1} and the RID was calibrated with linear narrow polystyrene standards.

4.8.1.2. Nuclear magnetic resonance spectroscopy

^{1}H-NMR and ^{13}C-NMR spectra were measured using a Bruker DPX-300 or DPX-400. Chemical shifts are reported in parts per million (ppm) and all spectra are referenced against the residual solvent peak found in the deuterated NMR solvent or

TMS. Abbreviations used for peak multiplicity are as follows; s = singlet, d = doublet, t = triplet, q = quartet and m = multiplet.

4.8.1.3. Gas chromatography – flame ionisation detection

GC-FID was used to measure monomer conversions. GC-FID analysis was performed using a Varian 450. A FactorFour^{TM} capillary column VF-1 ms, of 15 m × 0.25 mm I.D., film thickness 0.25 µm from Varian was used. The oven temperature was programmed as follows: 40 °C (hold for 1 minute) increase at 40 °C·min^{-1} to 300 °C (hold for 2.5 minutes). The injector was operated at 200 °C and the FID was operated at 220 °C. Hydrogen was used as carrier gas at flow rate of 54 µL min^{-1} and a split ratio of 1:100 was applied. Chromatographic data was processed using Galaxie Chromatography data system, version 1.9.302.530.

4.8.1.4. Fourier transform infrared spectroscopy

FT-IR spectra were recorded on a Bruker Vector-22 spectrometer using a Golden Gate diamond attenuated total reflection cell. All FT-IR spectra are plotted transmittance against wavenumber (cm^{-1}).

4.8.1.5. Matrix-assisted laser desorption/ionisation time-of-flight mass spectrometry

MALDI-TOF MS was performed using a Bruker Daltonics Autoflex MALDI-ToF mass spectrometer, equipped with a nitrogen laser at 337 nm with positive ion ToF detection. Solutions in THF of *trans*-2-[3-(4-tertbutylphenyl)-2-methyl-2-propylidene]malonitrile (DCTB) as matrix (30 mg·mL^{-1}), potassium trifluoroacetate as cationisation agent (10 mg·mL^{-1}) and sample (10 mg·mL^{-1}) were mixed together in a 3:1:1 volume ratio for a total volume of 75 µL. 1 µL of the mixture was applied

to the target plate. Spectra were recorded in reflectron mode and the mass spectrometer was calibrated with a peptide mixture up to 6000 Da.

4.8.2. Materials

Maleic anhydride (Aldrich, 99%), 3-Isopropenyl-α,α-dimethylbenzyl isocyanate (Aldrich, 95%), hexylamine (Aldrich, 99%), octadecylamine (Aldrich, 97%), α-methylstyrene dimer (Aldrich, 97%), 4-(aminomethyl)pyridine (Aldrich, 98%) were all used as received.

α-Methylstyrene (Aldrich, 99%) was destabilised before use by passing through a short column of basic aluminium oxide. 2,2′-Azobis(2-methylpropionitrile) (Aldrich, 98%) was recrystallized from methanol.

Butanone, and toluene were all HPLC grade and used as received. Caromax 20 was provided by Innospec LTD and used as received. All other solvents were of general lab quality and used as received.

4.8.3. Procedures

4.8.3.1. Free radical copolymerisation of AMS and MalA

AMS, MalA, AIBN and MEK were charged into a Schlenk tube and degassed by gentle bubbling of N_2 gas for 20 minutes. Schlenk tube was submerged into an oil bath at 80 °C and removed after 4 hours. Product was precipitated into a large volume of methanol, filtered and placed into a vacuum oven at 80 °C overnight to remove all residual solvent.

Table 4.09 shows the quantities of all individual substances (AMS, MalA, AIBN and MEK) used to synthesise alternating copolymers (P4.01-P4.03) prepared by the procedure detailed above.

^{1}H-NMR (400 MHz, 298 K, $(CD_3)_2CO$): δ (ppm) 0.31 – 1.97 (m, -C<u>H</u>$_2$- and -(C<u>H</u>$_3$), P(AMS) repeat unit), 2.12 – 3.55 (m, -C<u>H</u>-, P(MalA) repeat unit), 6.80 – 7.90 (m, -(C$_6$<u>H</u>$_5$), P(AMS) repeat unit). FT-IR (neat): (cm^{-1}) 2981 (w), 2361 (w), 2341 (w), 1856 (m), 1772 (s), 1498 (w), 1479 (w), 1446 (w), 1393 (w), 1252 (w), 1058 (m), 1001 (w), 909 (s), 757 (m), 700 (s), 611 (m).

Table 4.05. GPC characterisation and monomer conversions for P[(AMS)-*a*-(MalA)] samples (P4.01-P4.03) prepared by free radical copolymerisation of AMS and MalA.

Sample	AMS;MalA Conversion$^{\alpha}$ (%)	$M_{n.GPC}{}^{\beta}$ (g·mol^{-1})	$M_{w.GPC}{}^{\beta}$ (g·mol^{-1})	$Đ^{\beta}$
P4.01	74;86	6500	11800	1.81
P4.02	76;83	10700	19600	1.83
P4.03	78;84	14500	26100	1.80

$^{\alpha}$Calculated from GC-FID. $^{\beta}$THF eluent, calibrated with PS standards.

4.8.3.2. Synthesis of AMSC$_6$

Hexylamine (4 mL, 30.3 mmol, 1.2 eq.) was added drop wise to a solution of TMI (5 mL, 25.3 mmol, 1 eq.) in toluene (20 mL) and left stirring at room temperature for 3 hours. Product precipitated out of solution. Reaction mixture cooled to 0 °C, product collected by filtration and dried overnight in vacuo.

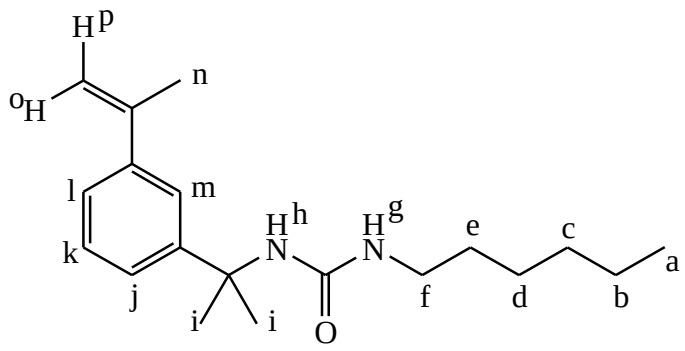

^{1}H-NMR (400 MHz, 298 K, $CDCl_3$): δ (ppm) 0.84 (t, *J* = 7.3 Hz, H_a, 3 H), 0.99 – 1.28 (m, $H_{b\text{-}e}$, 8 H), 1.63 (s, H_i, 6 H), 2.15 (s, H_n, 3 H), 3.02 (q, *J* = 5.5, 7.0 Hz, H_f, 2H), 4.14 (t, *J* = 5.0 Hz, H_g, 1 H), 4.92 (s, H_h, 1 H), 5.10 (t, *J* = 1.5 Hz, H_p, 1 H), 5.36 (s, H_o, 1 H), 7.27 – 7.39 (m, $H_{j\text{-}l}$, 3 H), 7.57 (t, *J* = 1.8 Hz, H_m, 1 H).

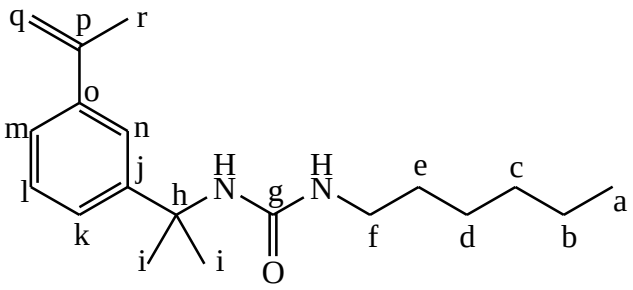

^{13}C-NMR (400 MHz, 298 K, $CDCl_3$): δ (ppm) 13.96 (s, C_a), 21.83 (s, C_r), 22.46 (s, C_b), 26.29 (s, C_c), 29.87 (s, C_d), 30.35 (s, C_i), 31.41 (s, C_e), 40.04 (s, C_f), 54.76 (s, C_h), 112.75 (s, C_q), 122.44 (s, C_n), 124.34 (s, C_m), 124.41 (s, C_k), 128.58 (s, C_l), 141.71 (s, C_o), 143.19 (s, C_j), 146.43 (s, C_p), 157.60 (s, C_g). FT-IR (neat): (cm^{-1}) 3364 (m), 3299 (m), 2966 (m), 2931 (m), 2856 (m), 2361 (w), 1632 (s), 1560 (s), 1485 (m), 1457 (m), 1439 (w), 1378 (w), 1359 (w), 1270 (s), 1240 (w), 1218 (w), 1149 (m), 887 (m), 800 (m), 723 (w), 655 (m), 530 (m).

4.8.3.3. Free radical copolymerisation of $AMSC_6$ and MalA

$AMSC_6$, MalA, AIBN and MEK were charged into a Schlenk tube and degassed by gentle bubbling of N_2 gas for 20 minutes. Schlenk tube was submerged into an oil

bath at 80 °C and removed after 4 hours. Product was precipitated into approximately 50 mL of methanol, filtered and placed into a vacuum oven at 80 °C overnight to remove all residual solvent.

Table 4.10 shows the quantities of all individual substances ($AMSC_6$, MalA, AIBN and MEK) used to synthesise alternating copolymers (P4.04-P4.06) prepared by the procedure detailed above.

^{1}H-NMR (400 MHz, 298 K, $(CD_3)_2CO$): δ (ppm) 0.56 – 1.03 (m, -$CH_2(CH_2)_4C\underline{H}_3$, P($AMSC_6$) repeat unit), 1.04 – 1.93 (m, -$C\underline{H}_2$-, -($C\underline{H}_3$), -$CH_2(C\underline{H}_2)_4CH_3$, -NH-$C(C\underline{H}_3)_2$-, P($AMSC_6$) repeat unit), 2.18 – 2.65 (m, -$C\underline{H}_2(CH_2)_4CH_3$, P($AMSC_6$) repeat unit), 2.65 – 3.56 (m, -C<u>H</u>-, P(MalA) repeat unit), 5.41 – 6.52 (m, -N<u>H</u>CON<u>H</u>-, P($AMSC_6$) repeat unit), 6.52 – 7.82 (m, -($C_6\underline{H}_4$)-, P($AMSC_6$) repeat unit). FT-IR (neat): (cm^{-1}) 3380 (br, w), 2928 (w), 2857 (w), 2361 (m), 2341 (m), 1857 (w), 1775 (s), 1641 (w), 1560 (m), 1487 (m), 1381 (w), 1361 (w), 1265 (m), 1167 (w), 1088 (m), 912 (s), 796 (w), 768 (m), 651 (w), 500 (w).

Table 4.06. GPC characterisation and monomer conversions for P[($AMSC_6$)-*a*-(MalA)] samples (P4.04-P4.06) prepared by free radical copolymerisation of $AMSC_6$ and MalA.

Sample	$AMSC_6$;MalA Conversion$^{\alpha}$ (%)	$M_{n.GPC}{}^{\beta}$ ($g \cdot mol^{-1}$)	$M_{w.GPC}{}^{\beta}$ ($g \cdot mol^{-1}$)	$Đ^{\beta}$
P4.04	95;91	8700	15700	1.81
P4.05	92;93	10400	19000	1.90
P4.06	81;85	17200	32500	1.89

$^{\alpha}$Calculated from GC-FID. $^{\beta}$THF eluent, calibrated with PS standards.

4.8.3.4. Synthesis of $AMSC_{18}$

Octadecylamine (4.2 g, 15.6 mmol, 1.2 eq.) was dissolved in a mixture of chloroform (5 mL) and toluene (15 mL) and added drop wise to a solution of TMI

(2.5 mL, 12.6 mmol, 1 eq.) in toluene (5 mL) and chloroform (1.5 mL) and left stirring at room temperature for 3 hours. Product precipitated out of solution. Reaction mixture cooled to 0 °C, product collected by filtration and dried overnight in vacuo.

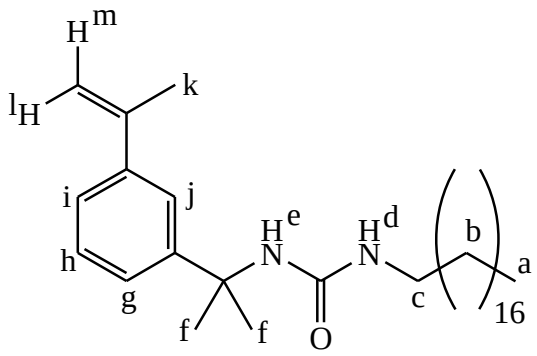

^{1}H-NMR (400 MHz, 298 K, $CDCl_3$): δ (ppm) 0.88 (t, *J* = 7.0 Hz, $\underline{H}_a$, 3 H), 1.00 – 1.32 (m, $\underline{H}_b$, 32 H), 1.63 (s, $\underline{H}_f$, 6 H), 2.15 (s, $\underline{H}_k$, 3 H), 3.03 (q, *J* = 6.0, 6.5 Hz, $\underline{H}_c$, 2 H), 3.98 (t, *J* = 5.3 Hz, $\underline{H}_d$, 1 H), 4.78 (s, $\underline{H}_e$, 1 H), 5.10 (m, $\underline{H}_m$, 1 H), 5.36 (s, $\underline{H}_l$, 1 H), 7.30 – 7.40 (m, $\underline{H}_{g\text{-}i}$, 3 H), 7.58 (m, $\underline{H}_j$, 1 H).

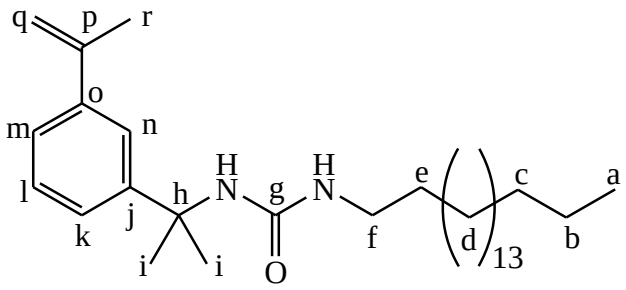

^{13}C-NMR (400 MHz, 298 K, $CDCl_3$): δ (ppm) 14.10 (s, $\underline{C}_a$), 21.87 (s, $\underline{C}_r$), 22.67 (s, $\underline{C}_b$), 26.62 (s, $\underline{C}_c$), 29.68 (m, $\underline{C}_d$), 30.39 (s, $\underline{C}_i$), 31.91 (s, $\underline{C}_e$), 40.09 (s, $\underline{C}_f$), 54.74 (s, $\underline{C}_h$), 112.86 (s, $\underline{C}_q$), 122.52 (s, $\underline{C}_n$), 124.46 (s, $\underline{C}_{m,k}$), 128.67 (s, $\underline{C}_l$), 141.83 (s, $\underline{C}_o$), 143.16 (s, $\underline{C}_j$), 146.23 (s, $\underline{C}_i$), 157.53 (s, $\underline{C}_g$). FT-IR (neat): (cm^{-1}) 3364 (w), 3301 (w), 2967 (m), 2919 (m), 2851 (m), 2361 (w), 1631 (s), 1560 (s), 1485 (m), 1379 (w), 1270 (m), 1147 (m), 887 (m), 801 (m), 723 (m), 653 (m), 505 (m).

4.8.3.5. Free radical copolymerisation of $AMSC_{18}$ and MalA

$AMSC_{18}$, MalA, and MEK were charged into a Schlenk tube and heated to 35 °C to fully homogenise the mixture. Degassed by gentle bubbling of N_2 gas for 10 minutes. Schlenk tube was submerged into an oil bath at 80 °C before the addition of a degassed solution of AIBN in MEK. Schlenk tube was removed from the oil bath after 4 hours. Mixture was allowed to cool before diluting with *n*-hexane. Organic phase was extracted with distilled water twice to remove the unconverted MalA. All remaining solvent was evaporated and product was placed into a vacuum oven at 80 °C overnight to remove all residual solvent.

Table 4.11 shows the quantities of all individual substances ($AMSC_{18}$, MalA, AIBN and MEK) used to synthesise alternating copolymers (P4.07-P4.09) prepared by the procedure detailed above.

^{1}H-NMR (400 MHz, 298 K, $CDCl_3$): δ (ppm) 0.83 – 0.95 (m, -$CH_2(CH_2)_{16}C\underline{H}_3$, P($AMSC_{18}$) repeat unit), 0.96 – 1.85 (m, -$C\underline{H}_2$-, -($C\underline{H}_3$), -$C\underline{H}_2(C\underline{H}_2)_{16}CH_3$, -NH-$C(C\underline{H}_3)_2$-, P($AMSC_{18}$) repeat unit), 2.80 – 3.26 (m, -C<u>H</u>-, P(MalA) repeat unit), 6.35 – 7.45 (m, -N<u>H</u>CON<u>H</u>-, -($C_6\underline{H}_4$)-, P($AMSC_{18}$) repeat unit). FT-IR (neat): (cm^{-1}) 3371 (w), 2922 (s), 2852 (m), 2361 (m), 2341 (m), 1857 (w), 1776 (s), 1639 (w), 1562 (m), 1464 (w), 1381 (w), 1361 (w), 1261 (m), 1167 (w), 1060 (m), 914 (s), 797 (w), 709 (m), 506 (m).

Table 4.07. GPC characterisation and monomer conversions for P[($AMSC_{18}$)-*a*-(MalA)] samples (P4.07-P4.09) prepared by free radical copolymerisation of $AMSC_{18}$ and MalA.

Sample	$AMSC_{18}$;MalA Conversion$^{\alpha}$ (%)	$M_{n.GPC}{}^{\beta}$ ($g \cdot mol^{-1}$)	$M_{w.GPC}{}^{\beta}$ ($g \cdot mol^{-1}$)	$Đ^{\beta}$
P4.07	72;74	4000	6800	1.70
P4.08	74;76	6000	11000	1.84
P4.09	72;77	7500	14300	1.91

$^{\alpha}$Calculated from GC-FID. $^{\beta}$THF eluent, calibrated with PS standards.

4.8.3.6. Free radical copolymerisation of $AMSC_{18}$ and MalA using AMSD as a CTA.

$AMSC_{18}$, MalA, and MEK were charged into a Schlenk tube and heated to 35 °C to fully homogenise the mixture. Degassed by gentle bubbling of N_2 gas for 10 minutes. Schlenk tube was submerged into an oil bath at 80 °C before the addition of a degassed solution of AIBN and AMSD in MEK. Schlenk tube was removed from the oil bath after 4 hours. Mixture was allowed to cool before diluting with *n*-hexane. Organic phase was extracted with distilled water twice to remove the unconverted MalA. All remaining solvent was evaporated and product was placed into a vacuum oven at 80 °C overnight to remove all residual solvent.

Table 4.12 shows the quantities of all individual substances ($AMSC_{18}$, MalA, AIBN, AMSD and MEK) used to synthesise alternating copolymers (P4.07 and P4.10-P4.11) prepared by the procedure detailed above.

^{1}H-NMR (400 MHz, 298 K, $CDCl_3$): δ (ppm) 0.83 – 0.95 (m, -$CH_2(CH_2)_{16}C\underline{H}_3$, P($AMSC_{18}$) repeat unit), 0.96 – 1.88 (m, -$C\underline{H}_2$-, -($C\underline{H}_3$), -$C\underline{H}_2(C\underline{H}_2)_{16}CH_3$, -NH-$C(C\underline{H}_3)_2$-, P($AMSC_{18}$) repeat unit), 2.65 – 3.38 (m, -C<u>H</u>-, P(MalA) repeat unit), 4.80 (m, -$C(C_6H_4)$=$C\underline{H}_{trans}H_{cis}$, end group), 5.14 (m, -$C(C_6H_4)$=$CH_{trans}\underline{H}_{cis}$, end group),

6.35 – 7.97 (m, -NHCONH-, -(C_6H_4)-, P($AMSC_{18}$) repeat unit). FT-IR (neat): (cm^{-1}) 3350 (w), 2922 (s), 2852 (s), 1858 (w), 1777 (s), 1639 (s), 1558 (s), 1465 (w), 1381 (w), 1361 (w), 1257 (m), 1168 (w), 1061 (m), 913 (s), 797 (w), 707 (s), 509 (s).

Table 4.08. GPC characterisation and monomer conversions for P[($AMSC_{18}$)-*a*-(MalA)] samples (P4.07 and P4.10-P4.11) prepared by free radical copolymerisation of $AMSC_{18}$ and MalA.

Sample	$AMSC_{18}$;MalA Conversion$^{\alpha}$ (%)	$M_{n.GPC}{}^{\beta}$ ($g \cdot mol^{-1}$)	$M_{w.GPC}{}^{\beta}$ ($g \cdot mol^{-1}$)	$Đ^{\beta}$
P4.11	72;73	3300	6600	2.00
P4.10	72;76	7000	23100	3.30
P4.07	72;77	7500	14300	1.91

$^{\alpha}$Calculated from GC-FID. $^{\beta}$THF eluent, calibrated with PS standards.

4.8.3.7. Synthesis of AMSDMA

N,*N*-dimethylethylenediamine (4.15 mL, 38.0 mmol, 1.5 eq.) was added drop wise to a solution of TMI (5 mL, 25.3 mmol, 1 eq.) in toluene (40 mL) and left stirring at room temperature for 3 hours. Product precipitated out of solution. Reaction mixture cooled to 0 °C, product collected by filtration, washed with cold toluene and dried overnight under vacuum.

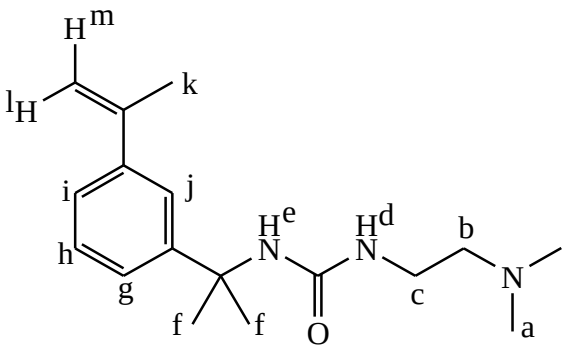

^{1}H-NMR (400 MHz, 298 K, $(CD_3)_2CO$): δ (ppm) 1.62 (s, $\underline{H}_f$, 6 H), 2.14 (s, $\underline{H}_{a/k}$, 9 H), 2.26 (t, *J* = 6.0 Hz, $\underline{H}_b$, 2 H), 3.11 (q, *J* = 5.5, 6.0 Hz, $\underline{H}_c$, 2 H), 5.06 (m, $\underline{H}_m$, 1 H), 5.37 (m, $\underline{H}_l$, 1 H), 5.42 (m, $\underline{H}_d$, 1 H), 6.14 (s, $\underline{H}_e$, 1 H), 7.21 – 7.37 (m, $\underline{H}_{g\text{-}i}$, 3 H), 7.59 (t, *J* = 1.8 Hz, $\underline{H}_j$, 1 H).

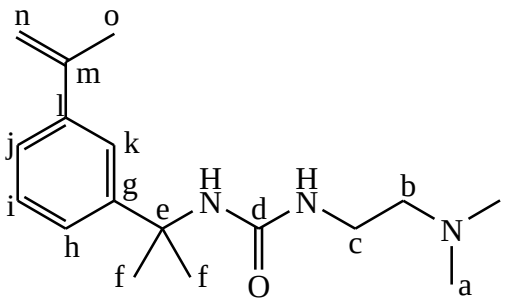

^{13}C-NMR (400 MHz, 298 K, $(CD_3)_2CO$): δ (ppm) 22.14 (s, $\underline{C}_o$), 30.72 (s, $\underline{C}_f$), 38.39 (s, $\underline{C}_c$), 45.62 (s, $\underline{C}_a$), 55.39 (m, $\underline{C}_e$), 60.15 (s, $\underline{C}_b$), 112.42 (s, $\underline{C}_n$), 123.16 (s, $\underline{C}_j$), 123.89 (s, $\underline{C}_k$), 125.32 (s, $\underline{C}_h$), 128.72 (s, $\underline{C}_i$), 141.56 (s, $\underline{C}_l$), 144.76 (s, $\underline{C}_g$), 150.11 (s, $\underline{C}_m$), 158.19 (s, $\underline{C}_d$).

4.8.3.8. Imidisation of P[(AMSC$_{18}$)-*a*-(MalA)]

P[(AMSC$_{18}$)-*a*-(MalA)] (P4.11, 0.10 g, 0.176 mmol, 1 eq.) was dissolved in Caromax 20 (2 mL) at 60 °C. 4-(aminomethyl)pyridine (36 µL, 0.352 mmol, 2 eq.) was added drop wise to the reaction mixture before equipping the round bottom flask with a Dean-Stark condenser and increasing the temperature to 160 °C. After 4 hours the reaction was cooled to room temperature and the polymer was precipitated into

n-hexane twice from chloroform and dried overnight under vacuum. ^{1}H-NMR (400 MHz, 298 K, ($CDCl_3$): δ (ppm) 0.71 – 0.96 (m, -$CH_2(CH_2)_{16}C\underline{H}_3$, P($AMSC_{18}$) repeat unit), 0.96 – 1.95 (m, -$C\underline{H}_2$-, -($C\underline{H}_3$), -$C\underline{H}_2(C\underline{H}_2)_{16}CH_3$, -NH-$C(C\underline{H}_3)_2$-, P($AMSC_{18}$) repeat unit), 1.99 – 3.05 (m, -C<u>H</u>-, P(MalA) repeat unit), 4.00 – 5.03 (m, -$C\underline{H}_2(C_5H_4N)$, P(PyMI) repeat unit), 6.16 – 7.93 (m, -N<u>H</u>CON<u>H</u>-, -($C_6\underline{H}_4$)-, P($AMSC_{18}$) repeat unit, -$CH_2(C_5\underline{H}_4N)$, P(PyMI) repeat unit), 8.04 – 8.96 (m, -$CH_2(C_5\underline{H}_4N)$, P(PyMI) repeat unit. FT-IR (neat): (cm^{-1}) 3399 (br, w), 2954 (w), 2919 (m), 2849 (m), 1771 (w), 1698 (s), 1613 (w), 1592 (m), 1571 (m), 1469 (m), 1435 (w), 1395 (w), 1336 (w), 1287 (m), 1252 (s), 1170 (s), 1048 (w), 995 (w), 914 (m), 795 (m), 751 (s), 708 (s), 511(m). GPC (DMF, 5 mM NH_4BF_4): M_n 23700 $g \cdot mol^{-1}$, M_w 38400 $g \cdot mol^{-1}$, $Đ$ 1.62.

Table 4.09. Quantities of AMS, MalA, AIBN and MEK used to synthesise samples P4.01-P4.03.

Polymer	AMS			MalA			AIBN			MEK
Sample	**(mL)**	**(mmol)**	**(eq.)**	**(g)**	**(mmol)**	**(eq.)**	**(mg)**	**(mmol)**	**(eq.)**	**(mL)**
P4.01	1	7.69	10	0.748	7.65	10	126	0.767	1	2
P4.02	1	7.69	25	0.759	7.65	25	51	0.311	1	2
P4.03	1	7.69	50	0.746	7.65	50	25	0.152	1	2

Table 4.10. Quantities of $AMSC_6$, MalA, AIBN and MEK used to synthesise samples P4.04-P4.06.

Polymer	$AMSC_6$			MalA			AIBN			MEK
Sample	**(g)**	**(mmol)**	**(eq.)**	**(g)**	**(mmol)**	**(eq.)**	**(mg)**	**(mmol)**	**(eq.)**	**(mL)**
P4.04	0.250	0.827	10	0.082	0.836	10	13.6	0.0828	1	3
P4.05	0.247	0.817	25	0.081	0.836	25	5.4	0.0328	1	3
P4.06	0.255	0.843	50	0.081	0.836	50	2.7	0.0164	1	3

Table 4.11. Quantities of $AMSC_{18}$, MalA, AIBN and MEK used to synthesise samples P4.07-P4.09.

Polymer	$AMSC_{18}$			MalA			AIBN			MEK
Sample	**(g)**	**(mmol)**	**(eq.)**	**(g)**	**(mmol)**	**(eq.)**	**(mg)**	**(mmol)**	**(eq.)**	**(mL)**
P4.07	0.248	0.527	5	0.052	0.530	5	17.0	0.104	1	3
P4.08	0.251	0.533	15	0.052	0.530	15	5.8	0.0353	1	3
P4.09	0.253	0.537	25	0.052	0.530	25	3.5	0.0213	1	3

Table 4.12. Quantities of $AMSC_{18}$, MalA, AIBN, AMSD and MEK used to synthesise samples P4.07 and P4.10-P4.11.

Polymer	$AMSC_{18}$			MalA			AIBN			AMSD			MEK
Name	**(g)**	**(mmol)**	**(eq.)**	**(g)**	**(mmol)**	**(eq.)**	**(mg)**	**(mmol)**	**(eq.)**	**(μL)**	**(mmol)**	**(eq.)**	**(mL)**
P4.11	0.249	0.529	5	0.052	0.530	25	3.5	0.0213	1	25	0.105	5	3
P4.10	0.252	0.535	15	0.052	0.530	25	3.5	0.0213	1	5	0.0209	1	3
P4.07	0.253	0.537	25	0.052	0.530	25	3.5	0.0213	1	0	0	0	3

4.9. References

1. H. Maeda, *Adv. Drug Delivery Rev.*, 2001, **46**, 169.
2. J.-F. Su, L.-X. Wang, L. Ren, Z. Huang and X.-W. Meng, *J. Appl. Polym. Sci.*, 2006, **102**, 4996.
3. F. Yu, Z.-H. Chen and X.-R. Zeng, *Colloid Polym. Sci.*, 2009, **287**, 549.
4. S. Harrisson and K. L. Wooley, *Chem. Commun.*, 2005, 3259.
5. *US Pat.*, 3329658, 1967.
6. *US Pat.*, 3449250, 1969.
7. *US Pat.*, 6544935B1, 2003.
8. *US Pat.*, 8168574B2, 2012.
9. B. Klumperman, *Polym. Chem.*, 2010, **1**, 558.
10. S. Srichan, D. Chang-Seng and J.-F. Lutz, *ACS Macro Lett.*, 2012, **1**, 589.
11. H. W. McCormick, *J. Polym. Sci.*, 1957, **25**, 488.
12. S. Mohammed, E. S. Daniels, A. Klein and M. S. El-Aasser, *J. Appl. Polym. Sci.*, 1998, **67**, 685.
13. V. Alexanian, R. G. Lees and D. E. Fiori, *Eur. Pat. Appl.*, 0336129 A2, 1989.
14. R. W. Dexter, P. S. Forgione and S. Balwant, *Eur. Pat. Appl.*, 0130323 A2, 1985.
15. L. Barner, C. Barner-Kowollik and T. P. Davis, *J. Polym. Sci. Part A Polym. Chem.*, 2002, **40**, 1064.
16. J. Moraes, T. Maschmeyer and S. Perrier, *J. Polym. Sci. Part A Polym. Chem.*, 2011, **49**, 2771.
17. J. Moraes, T. Maschmeyer and S. Perrier, *Aust. J. Chem.*, 2011, **64**, 1047.
18. M. Kyulavska, G. Kostov, B. Ameduri and R. Mateva, *J. Polym. Sci. Part A Polym. Chem.*, 2010, **48**, 2681.

19. *Eur. Pat. Appl.*, 0130313 A2, 1985.
20. L. Toman, M. Janata, J. Spěváček, B. Dvořánková, P. Látalová, P. Vlček, A. Sikora, J. Michálek and M. Pekárek, *J. Polym. Sci. Part A Polym. Chem.*, 2006, **44**, 2891.
21. L. Toman, M. Janata, J. Spěváček, J. Brus, A. Sikora, P. Látalová, P. Holler, P. Vlček, and B. Dvořánková, *J. Polym. Sci. Part A Polym. Chem.*, 2006, **44**, 6378.
22. L. Toman, M. Janata, J. Spěváček, J. Brus, A. Sikora, J. Horský, P. Vlček and P. Látalová, *J. Polym. Sci. Part A Polym. Chem.*, 2009, **47**, 1284.
23. C. S. Lee, W. W. Y. Lau, S. Y. Lee and S. H. Goh, *J. Polym. Sci. Part A Polym. Chem.*, 1991, **29**, 1889.
24. G. Boutevin, B. Ameduri, J. J. Robin, B. Boutevin and J. P. Joubert, *Polym. Bull.*, 2000, **44**, 239.
25. Z. Yin, C. Koulic, C. Pagnoulle and R. Jérôme, *Macromol. Chem. Phys.*, 2002, **203**, 2021.
26. M. C. Davies, J. V. Dawkins and D. J. Hourston, *Polymer*, 2005, **46**, 1739.
27. B. Lessard and M. Maric, *Macromolecules*, 2010, **43**, 879.
28. D. Benoit, C. J. Hawker, E. E. Huang, Z. Lin and T. P. Russell, *Macromolecules*, 2000, **33**, 1505.
29. E.-S. Park, M.-N. Kim, I.-M. Lee, H. S. Lee and J.-S. Yoon, *J. Polym. Sci. Part A Polym. Chem.*, 2000, **38**, 2239.
30. E. Chernikova, P. Terpugova, C. Bui and B. Charleux, *Polymer*, 2003, **44**, 4101.
31. M.-Q. Zhu, L.-H. Wei, M. Li, L. Jiang, F.-S. Du, Z.-C. Li and F.-M. Li, *Chem. Commun.*, 2001, 365.
32. H. De Brouwer, M. A. J. Schellekens, B. Klumperman, M. J. Monteiro and A. L. German, *J. Polym. Sci. Part A Polym. Chem.*, 2000, **38**, 3596.

33. G. C. Sanders, R. Duchateau, C. Y. Lin, M. L. Coote and J. P. A. Heuts, *Macromolecules*, 2012, **45**, 5923.

34. J. C. J. F. Tacx, N. L. J. Meijerink and K. Suen, *Polymer*, 1996, **37**, 4307.

35. J. Rocks, L. Rintoul, F. Vohwinkel and G. George, *Polymer*, 2004, **45**, 6799.

36. E. T. A. van den Dungen, R. Rinquest, N. O. Pretorius, J. M. McKenzie, J. B. McLeary, R. D. Sanderson and B. Klumperman, *Aust. J. Chem.*, 2006, **59**, 742.

37. M. A. Shenoy and K. S. Joshi, *J. Appl. Polym. Sci.*, 2000, **75**, 424.

38. A. A. Gridnev, *J. Polym. Sci. Part A Polym. Chem.*, 2002, **40**, 1366.

39. J. Kristina, G. Moad, E. Rizzardo, C. L. Winzor, C. T. Berge and M. Fryd, *Macromolecules*, 1995, **28**, 5381.

5. Polymerisation and Modification of 2,3,4,5,6-Pentafluorostyrene

5.1. Introduction

Highlighted throughout Chapter 1, CRP techniques (Section 1.2) in tandem with post-polymerisation modification (Section 1.3) ignited new and persisting interest for polymer synthesis. As a consequence, increasingly specialised polymeric materials are being synthesised for a vast number of applications.

One monomer which has been effortlessly integrated within CRP as well as pre/post-polymerisation modification is 2,3,4,5,6-pentafluorostyrene (PFS). PFS has been homopolymerised to well-defined poly(2,3,4,5,6-pentafluorostyrene) (P(PFS)) by multiple CRP techniques, such as ATRP,[1-3] NMP,[4-6] and RAFT.[7-10] Well-defined random copolymers of PFS and various comonomers; PEGMA,[11] styrene,[12] fluorinated (meth)acrylates,[10] as well as alternating copolymers of PFS with styrene[13] or 4-azidostyrene[3] have been synthesised. Furthermore, CRP techniques have been utilised to synthesise copolymers of PFS with higher order architecture. Block copolymers of PFS and many comonomers have been prepared; GMA,[2,7] glyceryl methacrylate,[7] DMAEMA,[8] 4-hydroxystyrene,[9] 4-vinylpyridine,[9] *tert*-butyl acrylate,[12] acrylic acid,[12] styrene,[14] DMA,[14] and PEG.[15] These block copolymers have been demonstrated to display various properties such as; pH responsive self-assemby,[8] forming films with strong phase-segregation behaviour.[9] 4 and 6-arm star (co)polymers of PFS and styrene have also been synthesised by utilising a multifunctional ATRP initiator.[15]

PFS has been utilised as a feedstock for the synthesis of *para*-functionalised styrenic monomers via substitution of the labile *para*-fluorine (*p*-fluoro) with various nucleophiles. For example, PFS has been functionalised with fluorinated alcohols,

such as 2,2,3,3,3-pentafluoropropan-1-ol, and subsequently (co)polymerised to synthesise highly fluorinated polymers with low energy surfaces or that are superhydrophobic.[16,17] Similarly, PFS *p*-fluoro has been substituted for 3-buten-1-ol to synthesise an alkene bearing monomer.[18] Selective RAFT polymerisation of the styrenyl group furnished a styrenic backbone with pendent alkene groups.[18] PFS *p*-fluoro substitution with (6-methylcyclohex-3-enyl)methanol has been reported to synthesise a cycloalkenyl functionalised monomer.[19] This monomer was also selectively RAFT polymerised, via the styrenyl group, to prepare a polymer bearing pendant cycloalkenyl groups that could undergo further post-polymerisation modifications; epoxidation, osmylation and thiol-ene addition.[19] Furthermore, substitution of the *p*-fluoro with thiols is another facile method of preparing functionalised monomers from PFS. Acetylated thiosugars (glucose) in the presence of TEA have been shown to quickly and efficiently substitute the *p*-fluoro to synthesise an acetylated glycomonomer.[20] Following removal of the acetyl groups and subsequent polymerisation via NMP, this has been demonstrated as an effective methodology of synthesising well-defined glycopolymers.[20]

P(PFS) is commonly utilised as a polymer/comonomer that can be functionalised by post-polymerisation. P(PFS) is most often functionalised via substitution of the *p*-fluoro with a thiol, commonly referred to as the thiol-*para* fluoro "click" reaction. Numerous thiols have been reported to date for the modification of P(PFS); 4-methoxybenzyl thiol,[9] thiolphenol,[11] thiosugars,[4,21] 2-mercaptoethanol,[22] 3-mercapto-1,2-propanediol,[22,23] 6-mercaptohexan-1-ol,[24] PEG thiol.[25] Substitution of P(PFS) *p*-fluoro has also been reported with primary amines. Substitution with primary amines proceeds in the absence of catalyst or base but does require elevated

temperature (95 °C) and a microwave synthesiser.[6] Primary amines utilised include; 5-aminopentan-1-ol,[6] *α*-amino-PEG,[6] amino-functionalised iridium complex.[26]

Owing to the synthetic versatility of PFS and P(PFS) to synthesise well-defined and functional polymeric materials, PFS and P(PFS) have been utilised as feedstock to prepare materials for numerous possible applications. Potential applications include; organocatalysts,[3] super hydrophobic surfaces,[17] biocompatible coatings for superparamagnetic particles.[20]

The initial aim of this chapter is to contribute a novel synthetic approach of functionalising PFS and P(PFS) to the diverse range of modification techniques already applicable to PFS and P(PFS). The second aim of this chapter is to synthesise novel block copolymers of PFS and another multifunctional monomer, 2-isopropenyl-2-oxazoline (iPOx), to prepare block copolymers of well-defined architecture that can modified by multiple pathways.

5.2. Homopolymerisation and (multi)functionalisation of PFS

As mentioned in Section 5.1, PFS has been polymerised via a number of CRP techniques; ATRP, NMP and RAFT. Of these techniques available, RAFT polymerisation was selected because the second objective of this chapter is the preparation of block copolymers composed of PFS and iPOx (P[(PFS)-*b*-(iPOx)]) (Section 5.3). CRP of iPOx has been reported in the literature by RAFT polymerisation as opposed to ATRP or NMP.[27,28] Therefore, RAFT polymerisation was believed to be the best candidate for the preparation of P[(PFS)-*b*-(iPOx)] copolymers. As such all PFS was polymerised via RAFT polymerisation so it may act as macroRAFT agent for iPOx polymerisation if required.

5.2.1. RAFT homopolymerisation of PFS

RAFT (co)polymerisation of PFS has been reported in literature utilising a variety of RAFT agent classes; trithiocarbonates, dithiobenzoates and dithiocarbamates.[13] Different initiating systems have also been effectively demonstrated; azo initiators such as AIBN at higher temperatures (60-90 °C) and redox initiators at room temperature.[13] Furthermore, polar and non-polar solvents as well as bulk conditions have all been utilised for the RAFT (co)polymerisation of PFS.[13] Given the diversity of successful conditions reported, the RAFT polymerisation system utilised throughout Chapter 4 to polymerise DMA and DMAEA was expected to be a suitable system for PFS as well. PFS was homopolymerised by the following RAFT polymerisation system; initiated by V601, mediated by 3-butyl-2-(dodecylthiocarbonothioylthio)-2-methylpropionate (BDTMP), toluene as solvent (equal volume to PFS) and temperature was 70 °C (Scheme 5.01).

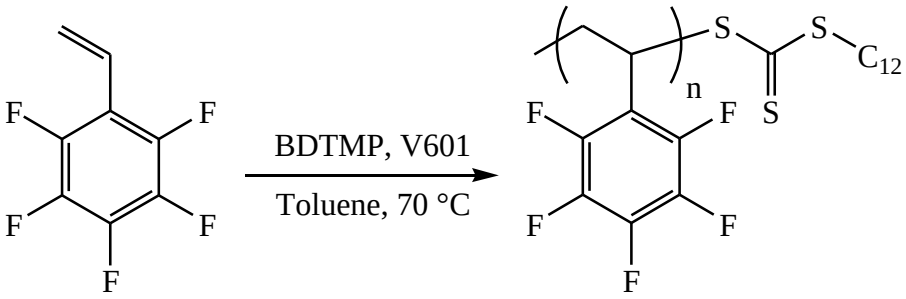

Scheme 5.01. RAFT homopolymerisation of PFS, initiated by V601 and mediated by BDTMP in toluene at 70 °C.

Conditions utilised for the RAFT polymerisation of PFS were shown to be suitable at synthesising well-defined P(PFS) (Table 5.01). P(PFS) was synthesised at two target DPs, 25 (P5.01) and 30 (P5.02), by changing the PFS to BDTMP ratio. Both polymerisations of PFS achieved suitably high conversions of PFS (≥69%), M_n measured by GPC closely matched the theoretical M_n and dispersity was very low

(≤1.10) (Table 5.01). However, these RAFT polymerisation conditions required extended reaction times (70 hours) to obtain satisfactory conversion of PFS.

Table 5.01. GPC characterisation and PFS conversion for the RAFT homopolymerisation of PFS in toluene at 70 °C, mediated by BDTMP and initiated by V601.

Sample	[PFS]: [BDTMP]:[V601]	PFS Conversion$^{\alpha}$ (%)	$M_{n.GPC}{}^{\beta}$ (g·mol^{-1})	$M_{n.Theo}{}^{\gamma}$ (g·mol^{-1})	$Đ^{\beta}$
P5.01	25:1:0.1	85	4400	4500	1.10
P5.02	30:1:0.l	69	4700	4400	1.08

$^{\alpha}$Calculated from GC-FID. $^{\beta}$DMF + 5 mM NH_4BF_4 eluent, calibrated with PS standards. $^{\gamma}$Calculated from Equation 1.

GPC traces of P(PFS) synthesised by RAFT polymerisation show well-defined symmetrical peaks with minimal formation of high molecular weight shoulders, indicating that bimolecular termination of polymeric radicals was supressed throughout polymerisation (Figure 5.01).

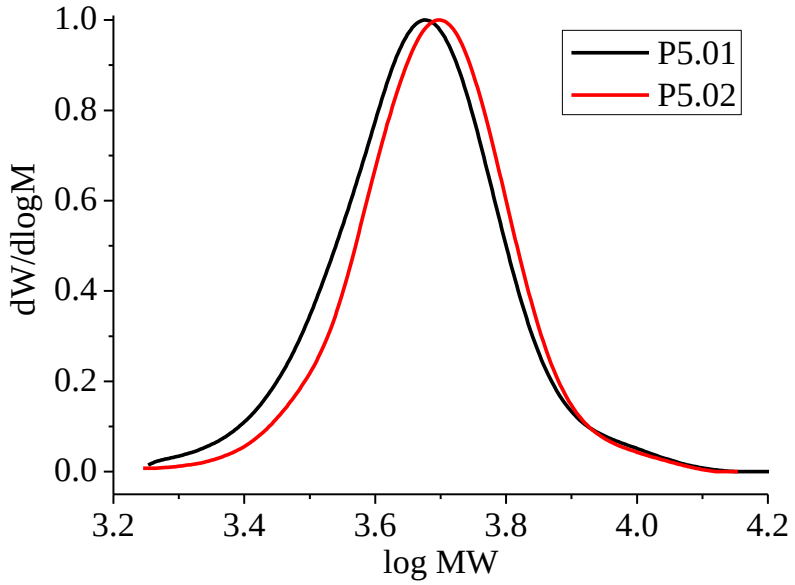

Figure 5.01. GPC traces (RID) of P(PFS) samples (P5.01/02) prepared by RAFT homopolymerisation of PFS in toluene at 70 °C, mediated by BDTMP and initiated by V601.

High end group fidelity of the P(PFS) is of great importance when the P(PFS) is to be used as a macroRAFT agent for the polymerisation of iPOx (Section 5.3). ^{1}H-NMR spectroscopy is an effective technique for determining the end group fidelity of polymers synthesised by RAFT polymerisation by identifying resonances of protons present on the trithiocarbonate end group. The ^{1}H-NMR spectrum of P5.01 is shown in Figure 5.02, high end group fidelity of P5.01 is especially crucial as this P(PFS) was utilised as a macroRAFT agent for iPOx polymerisation in Section 5.3. Relative integration of the P(PFS) repeat unit resonances (H^{e} and H^{f}) to the methylene (H^{d}) resonance immediately adjacent to the trithiocarbonate end group indicates a DP of 22. This is in very good agreement with the expected DP of 21; calculated from the initial PFS to BDTMP ratio multiplied by PFS conversion. This is good evidence that the end group fidelity of P5.01 is suitably high enough to be utilised as macroRAFT agent. Furthermore, it is possible to observe signals corresponding to the two different initiating radicals present in the polymerisation. A signal centred at 3.8 ppm corresponds to $–CH_2COO-$ (H^{h}) of BDTMP's R group and a signal centred at 3.7 ppm is the methyl protons of V601 derived radicals (Figure 5.02).

GPC measuring with a VWD set to 308 nm has been utilised in previous chapters to further support the presence of a trithiocarbonate end group. However, in this instance it is not suitable as P(PFS) absorbs at 308 nm despite the presence of a trithiocarbonate end group. Therefore, measuring GPC with a VWD at 308 nm would not necessarily prove the presence of a trithiocarbonate end group. Following this successful synthesis of well-defined P(PFS) by RAFT polymerisation, P5.01 was utilised to synthesise novel block copolymers of PFS and iPOx (Section 5.3) and P5.02 was utilised for devising a novel transformation of the P(PFS) backbone.

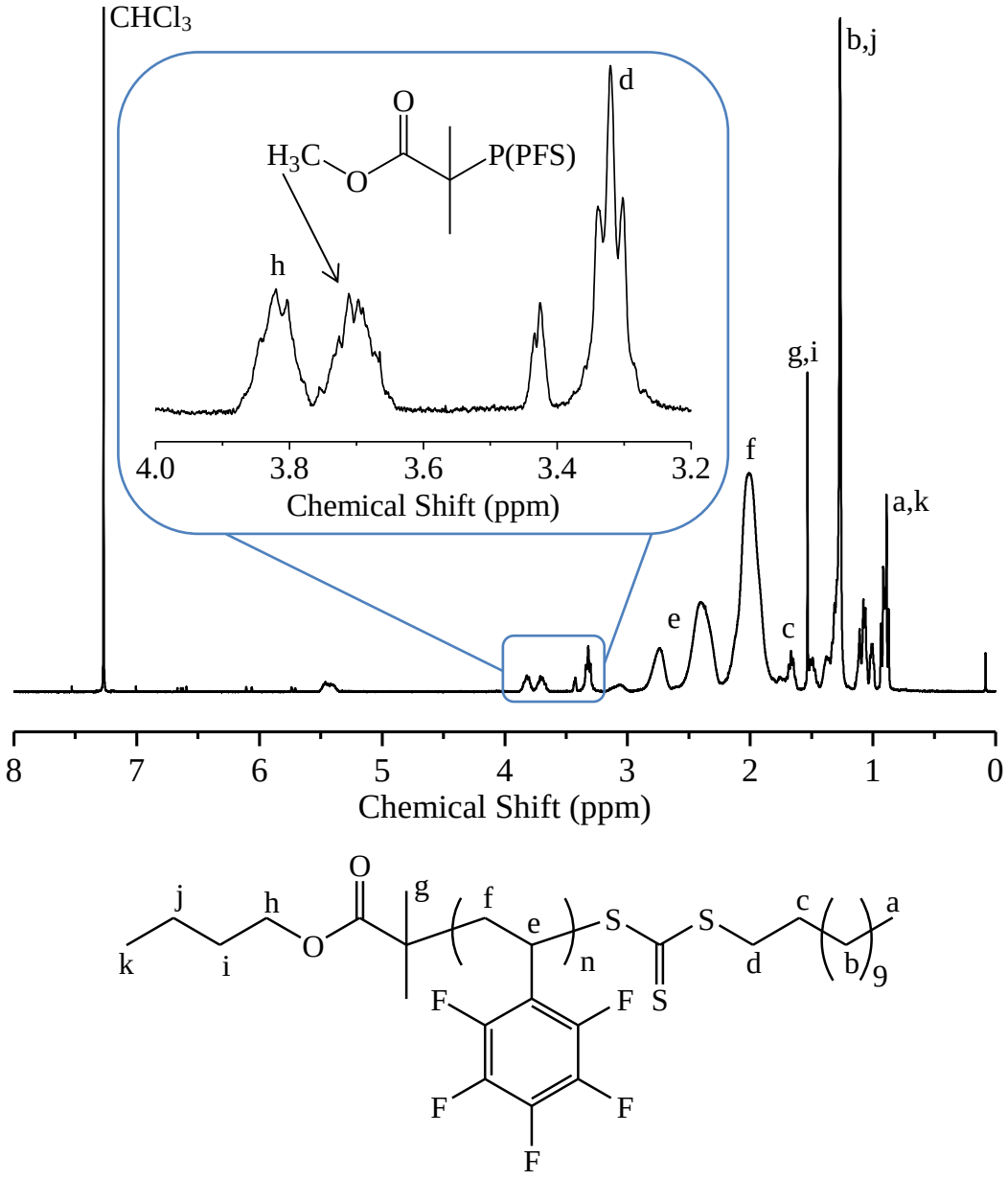

Figure 5.02. ^{1}H-NMR spectrum ($CDCl_3$, 400 MHz, 303 K) of P(PFS) (P5.01).

5.2.2. Attempted functionalisation of P(PFS) with thiols

As detailed in Section 5.1 the most common modification of P(PFS) is substitution of the *p*-fluoro with a thiol.[4,9,11,21-25] Despite multiple examples of PFS (co)polymerisation by RAFT in the literature,[7-10,12-14] there are relatively few examples of these RAFT polymerisations that subsequently modify P(PFS) repeat units by substitution of the *p*-fluoro with a thiol.[9] In this example Voit and co-workers substituted the *p*-fluoro of P(PFS) (block)copolymers with 4-methoxy

benzylthiol.[9] Voit and co-workers demonstrated that the substitution of P(PFS) with 4-methoxy benzylthiol was successful by ^{19}F-NMR and ^{1}H-NMR spectroscopy.[9] However, Voit and co-workers also reported that GPC measurements observed formation of a large high molecular weight shoulder after substitution with 4-methoxy benzylthiol which they attributed to a GPC column interaction or formation of aggregates.[9] It is important to determine if this high molecular weight shoulder formed because of the reasons stated and is specific to the polymer synthesised by Voit and co-workers or if it is a general issue of modifying P(PFS) synthesised by RAFT polymerisation. Therefore, P(PFS) (P5.02) was modified via *p*-fluoro substitution with two thiols, thiophenol (TP) and 2-mercaptoethanol (ME), to observe if any high molecular shoulders form. Substitution was performed in DMF at 60 °C and mediated by TEA for 1 hour (Scheme 5.02).

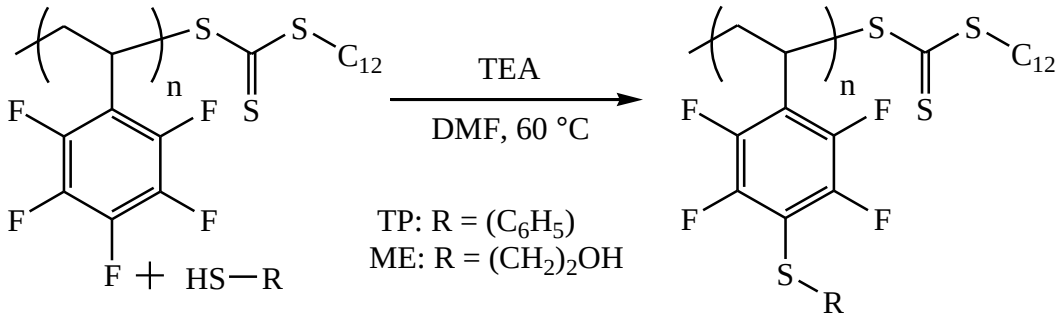

Scheme 5.02. Attempted *p*-fluoro substitution of P(PFS) (P5.02) with TP and ME.

GPC measurements following the *p*-fluoro substitution of P(PFS) with both thiols, TP and ME, displayed broad distributions that contained multiple high molecular weight shoulders (Figure 5.03). M_n increased from 4700 g·mol^{-1} to 8600 and 23500 g·mol^{-1} after substitution with TP and ME, respectively. Furthermore, dispersity increased from 1.08 to 1.36 and 1.56 after substitution with TP and ME, respectively. Planned modifications of P(PFS) in later sections will also utilise

p-fluoro substitution with thiols and therefore the underlying cause of these negative results must be resolved.

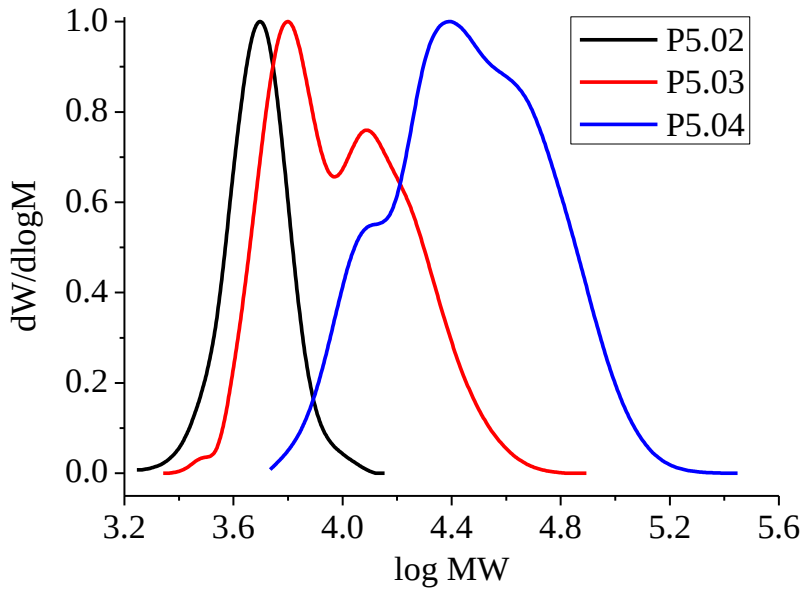

Figure 5.03. GPC traces (RID) of P(PFS) (P5.02) and attempted *p*-fluoro substitution of with TP (P5.03) and ME (P5.04).

Formation of aggregates or GPC column interactions can not be excluded currently but poor GPC traces after *p*-fluoro substitution with thiols has not been reported when the P(PFS) substituted was prepared by other CRP techniques, ATRP or NMP. Therefore, presence of a thiocarbonylthio end group, such as a trithiocarbonate, may be a cause of complications when performing *p*-fluoro substitutions with thiols.

Thiocarbonylthio end groups are routinely removed by aminolysis to generate polymeric thiols after nucleophilic substitution with primary/secondary amines as well as sodium azide (Section 1.3.2).[29-31] Aminolysis of the thiocarbonylthio end group removal is therefore not compatible with P(PFS) as generation of polymeric thiols may result in branching/crosslinking after said polymeric thiols substitute *p*-fluoros along the P(PFS) backbone. Moreover, this potential process of

branching/crosslinking prevents P(PFS) modification by *p*-fluoro substitutions with primary amines when the P(PFS) has a thiocarbonylthio end group.

Therefore, if the small molecule thiols or their thiolate anions, *p*-fluoro substitutions are performed in the presence of base (TEA), may generate a P(PFS) thiol if the small molecule thiols are suitably nucleophilic to remove trithiocarbonate end group by nucleophilic substitution. Said P(PFS) thiol could then substitute *p*-fluoros on other P(PFS) chains and form polymer branches, this would give a multimodal GPC trace that displays high molecular weight shoulders. To test this idea and potentially obtain well-defined GPC traces of modified P(PFS), the trithiocarbonate end group was removed before any further attempts at *p*-fluoro substitution with thiols.

5.2.3. End group removal and subsequent functionalisation of P(PFS)

As initial attempts to functionalise the P(PFS) backbone via substitution of the *p*-fluoro with thiols were shown to be ill-defined by GPC, it was proposed that removal of the trithiocarbonate end group may improve the results obtained by GPC. As discussed in Section 1.2.4 there are two common methods of trithiocarbonate end group removal which remove all sulfur from the polymer molecule; thermolysis and radical induced addition.[32,33] Either of these methods would be suitable for trithiocarbonate removal as no reactive polymeric thiol is generated, which is believed to have caused the multi modal GPC in Figure 5.03.

Trithiocarbonate end group removal was achieved by a radical induced addition procedure adapted from literature.[33] P(PFS) (P5.02) was heated at 80 °C in presence of a large excess (20 eq.) of V601 for 4 hours (Scheme 5.03). V601 decomposes to generate radicals which subsequently attack the P(PFS) macroRAFT agent and cause fragmentation to a new trithiocarbonate and a P(PFS) radical. As there is an absence

of monomer and a large excess of V601 derived radicals present, these radicals combine with P(PFS) radicals to synthesise a methyl ester ω-terminus.

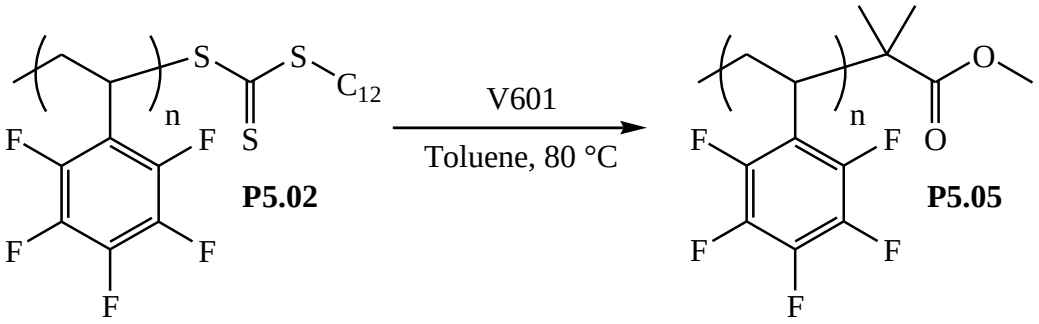

Scheme 5.03. Synthesis of trithiocarbonate end group removed P(PFS) (P5.05) by radical induced addition of V601 derived radicals.

P(PFS) trithiocarbonate end group removal is supported by ^{1}H-NMR spectroscopy (Figure 5.04). The methylene protons immediately adjacent to trithiocarbonate (H^{d}) display a triplet at 3.32 ppm and after radical induced addition this triplet is near-entirely diminished. 96% of the trithiocarbonate has been removed as measured by integration of the triplet at 3.32 ppm before and after radical induced addition. Other signals on ^{1}H-NMR spectra also support the removal of the trithiocarbonate; alkyl protons (H^{a} and H^{b}) disappear leaving a single triplet at 0.92 ppm (H^{t}), integration of the methyl ester proton at 3.70 ppm (H^{l}) increases as well as the methyl protons (H^{p} and H^{m}) at 1.55 ppm (Figure 5.04).

Following removal of the trithiocarbonate end group, GPC measured an increase in M_{n} of P(PFS) from 4700 to 5700 g·mol^{-1} and dispersity remained very low at 1.05. The GPC trace of trithiocarbonate removed P(PFS) (P5.05) displays a modal distribution with no significant appearance of high molecular shoulders, indicating that bimolecular termination did not occur throughout end group removal by radical induced addition (Figure 5.05).

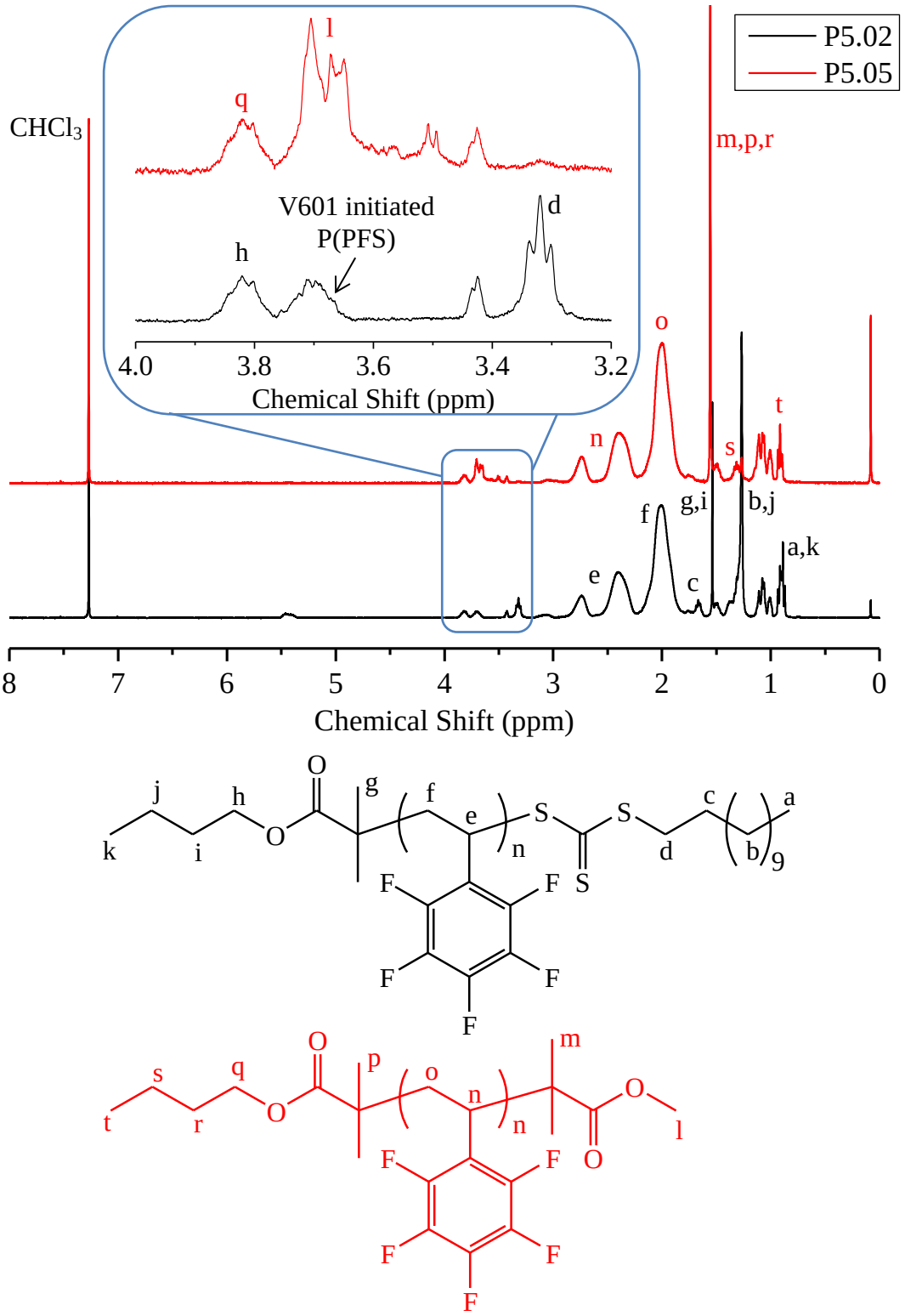

Figure 5.04. ^{1}H-NMR spectrum ($CDCl_3$, 400 MHz, 303 K) of P(PFS) with (P5.02) and without (P5.05) a trithiocarbonate end group.

Removal of the P(PFS) trithiocarbonate end group was sufficiently removed by radical induced addition. Therefore, P5.05 was utilised in *p*-fluoro substitution with

thiols and a primary amine to observe if any improvement in the GPC measurements was obtained.

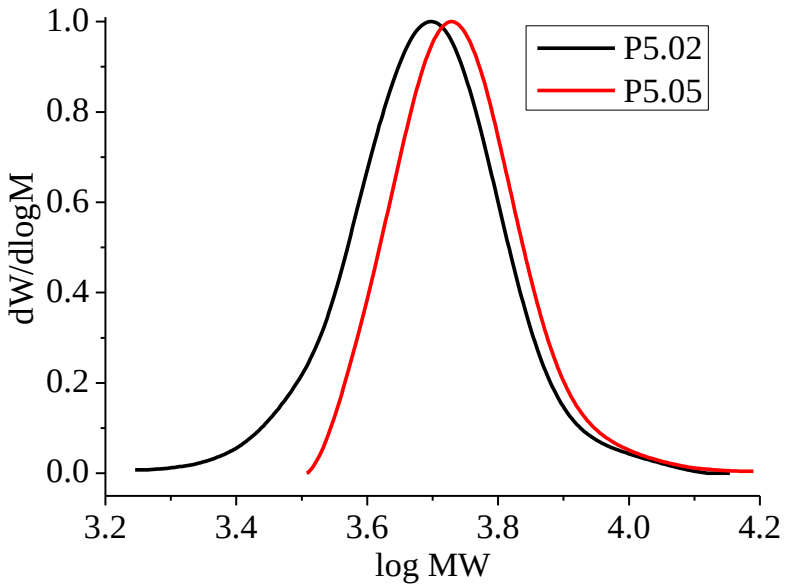

Figure 5.05. GPC traces (RID) of P(PFS) with (P5.02) and without (P5.05) a trithiocarbonate end group.

5.2.3.1. Functionalisation with thiols and primary amines

Functionalisation of P(PFS), via substitution of the *p*-fluoro, was then repeated with P(PFS) not bearing the reactive trithiocarbonate end group (P5.05). *p*-Fluoro substitutions were performed with thiols; TP and 1-butanethiol (BT) (Scheme 5.04) and a primary amine; hexylamine (Scheme 5.05). Conditions for the *p*-fluoro substitutions with thiols were unchanged from the previous section, 60 °C in DMF and mediated with TEA. *p*-fluoro substitution with hexylamine utilised effective conditions reported in the literature for functionalising P(PFS) with a variety of primary amines; heating at 95 °C by microwave in DMF.[6]

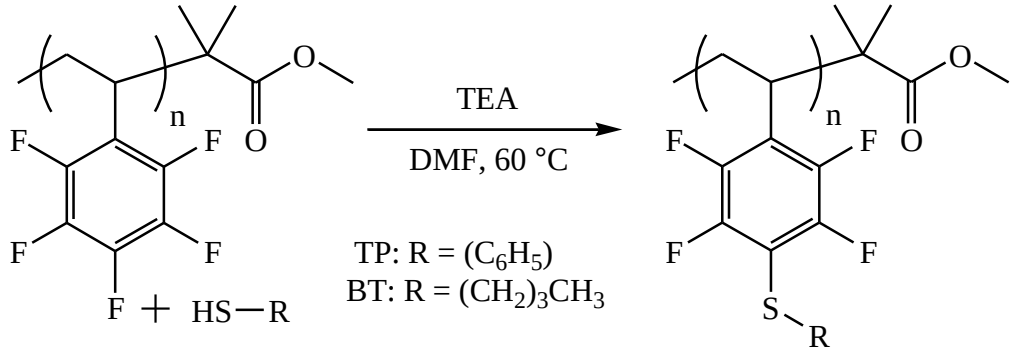

Scheme 5.04. *p*-Fluoro substitution of P(PFS) (P5.05) with thiols; TP and BT.

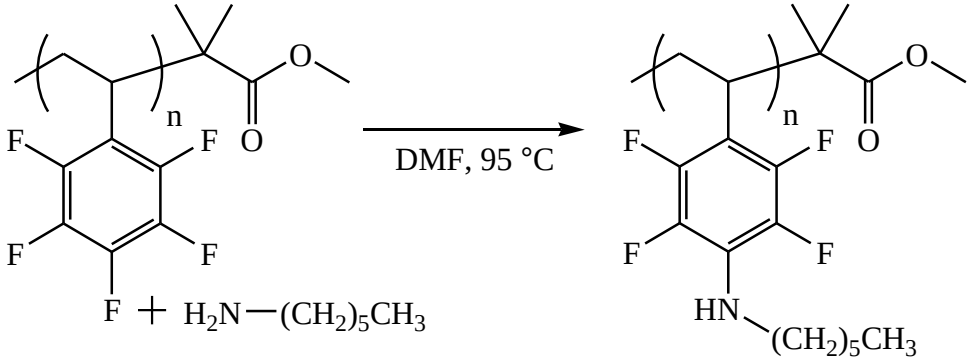

Scheme 5.05. *p*-Fluoro substitution of P(PFS) (P5.05) with hexylamine.

Functionalisation of P(PFS) with thiols (TP and BT) and hexylamine was achieved with much greater control than attempts from the previous section. Following functionalisation, GPC measured well-defined modal distributions for all three nucleophiles used to functionalise P(PFS) (Figure 5.06). Therefore supporting the assumption that trithiocarbonate end groups were being cleaved to furnish P(PFS) thiols which subsequently substituted *p*-fluoros to form branched macromolecules. However, GPC measurements of all functionalised P(PFS) products display a slight high molecular shoulder (Figure 5.06), this may have occurred as residual trithiocarbonate end group (4% by ^{1}H-NMR spectroscopy) was present and could result in low levels of branching by the process described above. Functionalisation with TP and hexylamine both lead to an increase in M_n as expected, 7000 and 7300 g·mol^{-1} respectively, whilst maintaining dispersity <1.10 (Table 5.02). However,

functionalisation with BT gave a lower M_n by GPC (4500 g·mol^{-1}) despite adding mass to the repeat unit structure, it is unclear why GPC measures a lower M_n for this functionalisation but the product remains as well-defined as the other modifications.

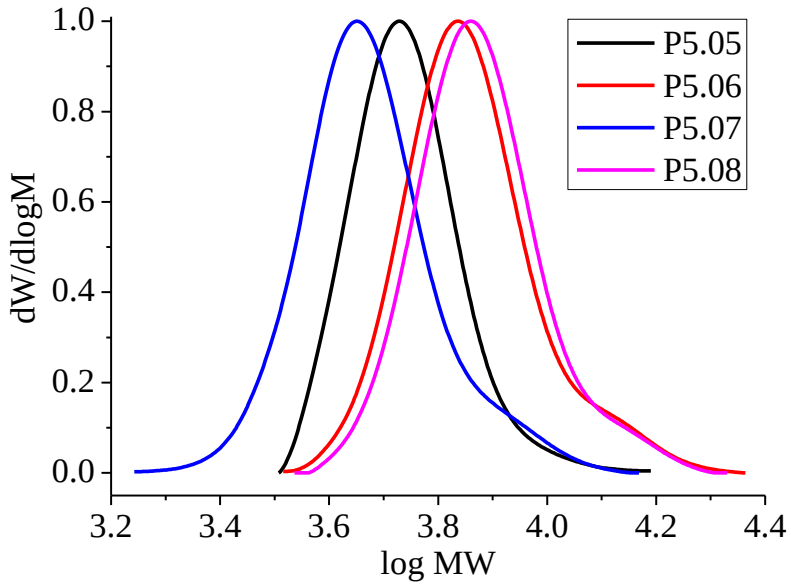

Figure 5.06. GPC traces (RID) of P(PFS) before (P5.05) and after *p*-fluoro substitution with TP (P5.06), BT (P5.07) and hexylamine (P5.08).

Table 5.02. Characterisation for P(PFS) functionalised via *p*-fluoro substitution with nucleophiles; thiols (TP and BT) and hexylamine.

Sample	Nucleophile	Degree of Substitution$^{\alpha}$ (%)	$M_{n.GPC}{}^{\beta}$ (g·mol^{-1})	$M_{w.GPC}{}^{\beta}$ (g·mol^{-1})	$Đ^{\beta}$
P5.05	-	-	5400	5700	1.05
P5.06	TP	95	7000	7600	1.09
P5.07	BT	55	4500	4900	1.09
P5.08	Hexylamine	50	7300	7800	1.07

$^{\alpha}$Estimated from ^{1}H-NMR. $^{\beta}$DMF + 5 mM NH_4BF_4 eluent, calibrated with PS standards.

^{1}H-NMR spectroscopy of the purified P(PFS) modifications (P5.06-08) was utilised to calculate the degree of substitution of P(PFS) repeat units with the various nucleophiles. Relative integrations of backbone protons and unmerged signals of the

new functionality could be acquired from fully assignable ^{1}H-NMR spectra (Figure 5.07). These relative integrations were utilised to estimate the degree of substitution after each modification of P5.05 (Table 5.02).

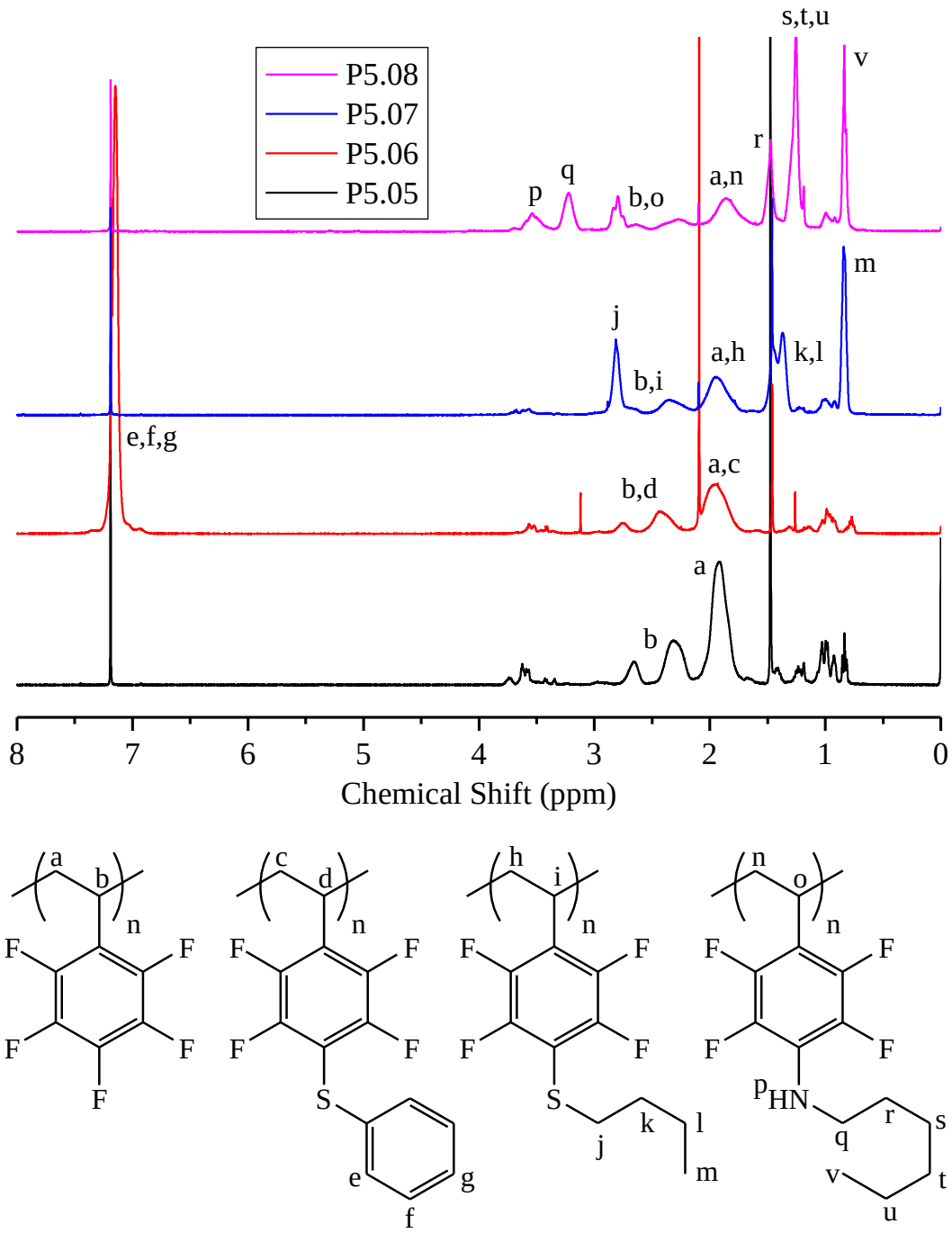

Figure 5.07. ^{1}H-NMR spectrum ($CDCl_3$, 400 MHz, 303 K) of P(PFS) before (P5.05) and after *p*-fluoro substitution with TP (P5.06), BT (P5.07) and hexylamine (P5.08).

TP was measured to be the most efficient of the nucleophiles utilised, 95% of the P(PFS) repeat units were substituted after 1 hour using only 1 eq. of TP relative to

P(PFS) repeat units. BT was less efficient, substituting 55% of the repeat units after 1 hour and hexylamine less efficient still at 50% degree of substitution. The degree of substitution for these nucleophiles and other similar species may be increased by extending the reaction duration. However, optimisation of these *p*-fluoro substitutions was not the main focus but rather confirming the detriment of not removing the trithiocarbonate end group before post-polymerisation modification.

5.2.3.2. Functionalisation with sodium azide

Modification of P(PFS) with thiols and primary amines is well known and other nucleophiles, such as hydroxyls, have been utilised to modify PFS to synthesise functional monomers (Section 5.1). Another reagent which has not been employed to modify PFS or P(PFS), but has been for other pentafluorophenyl containing compounds, is sodium azide.[34] The nucleophilic azide anion can substitute the *p*-fluoro to impart an azide functionality directly to the aromatic ring.[34] This methodology has been reported to synthesise 1-azido-2,3,5,6-tetrafluorobenzene by heating pentafluorobenzene and sodium azide in DMF at 70 °C for 2 hours.[34] Therefore, this synthetic methodology was applied to PFS and P(PFS) to synthesise a novel aromatic azide functionalised monomer and polymer, respectively. PFS and sodium azide were heated at 70 °C for 3 hours in DMF (Scheme 5.06).

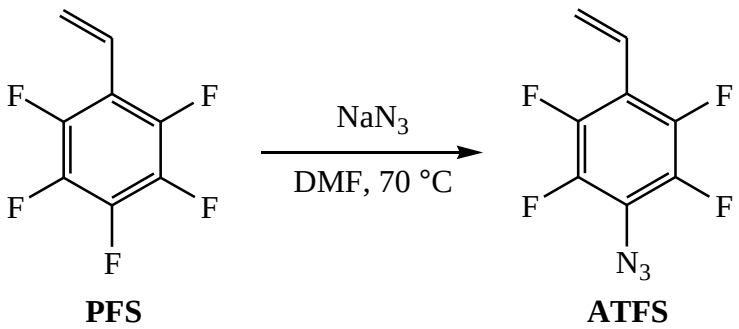

PFS **ATFS**

Scheme 5.06. *p*-Fluoro substitution of PFS with sodium azide to synthesise ATFS.

After 3 hours no PFS was detectable by GC-FID and subsequent purification by extraction furnished the desired product; 4-azido-2,3,5,6-tetrafluorostyrene (ATFS) in good yield (87%).

^{19}F-NMR spectroscopy supports the expected structure of ATFS (Figure 5.08). Firstly, there are now only two resonances of equal relative integration whereas the ^{19}F-NMR spectrum of PFS has three signals of relative integration 2:1:2, thus supporting the *p*-fluoro has been substituted. Moreover, multiplicity of the ATFS ^{19}F-NMR spectrum has been simplified; the new *meta*-fluorine (*m*-fluoro) at −153 ppm is split into a doublet of doublets as expected but the PFS *m*-fluoro displays a doublet of triplets as a result of the extra coupling with the *p*-fluoro (Figure 5.08).

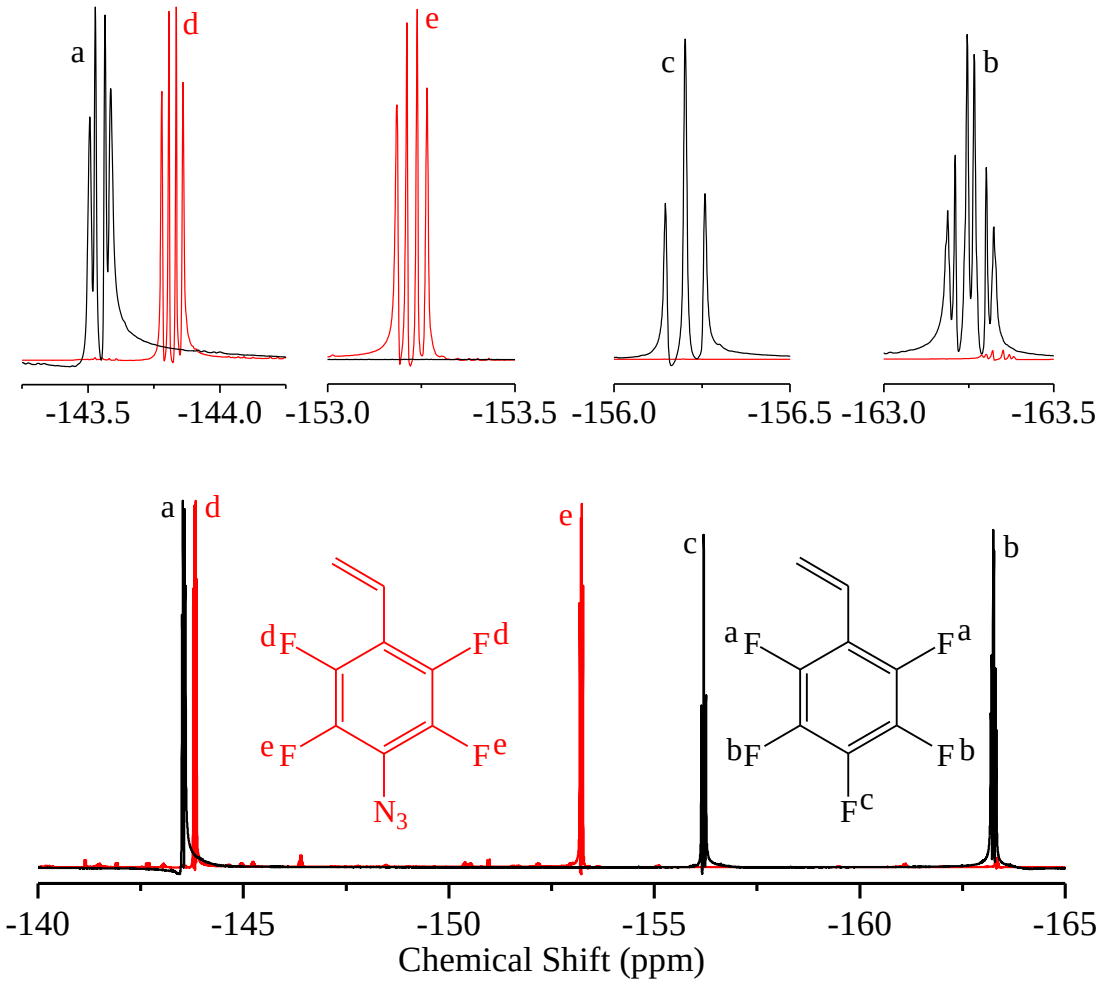

Figure 5.08. ^{19}F-NMR spectra ($CDCl_3$, 400 MHz, 303 K) of PFS (black) and ATFS (red).

^{1}H-NMR of ATFS is relatively unchanged; expected resonances and multiplicity for the vinyl protons are observed at 5.59 (doublet), 5.96 (doublet) and 6.54 ppm (doublet of doublets). Furthermore, the presence of azide functionality is supported by FT-IR spectroscopy due to its very characteristic peaks. A very strong signal at 2117 cm^{-1} appears after substituting the *p*-fluoro with sodium azide that was not previously present on PFS (Figure 5.09).

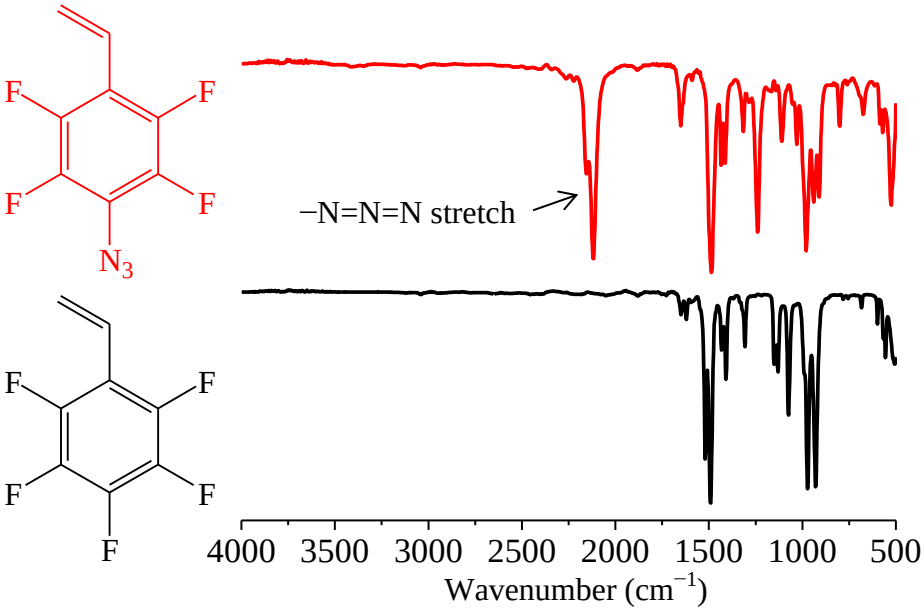

Figure 5.09. FT-IR spectra of PFS (black) and ATFS (red).

ATFS may prove to be a new versatile monomer as styrenes are compatible with a wide variety of polymerisation techniques and the azide moiety may allow for pre/post-polymerisation modification principally via CuAAC reactions. Furthermore, synthesis of ATFS provides a small molecule model reaction for the same *p*-fluoro modification of P(PFS) with sodium azide.

P(PFS) (P5.05) and sodium azide were heated at 70 °C for 4 hours in DMF to synthesise poly(4-azido-2,3,5,6-tetrafluorostyrene) (P(ATFS)) (Scheme 5.07). P(PFS) without a trithiocarbonate end group was utilised for this modification as it has been recently demonstrated that sodium azide, similarly to other nucleophiles,

can convert the trithiocarbonate to a thiol.[31] Therefore, if trithiocarbonate terminated P(PFS) was utilised, it would be converted to the polymeric thiol and potentially result in unfavourable branching as observed in Section 5.2.2.

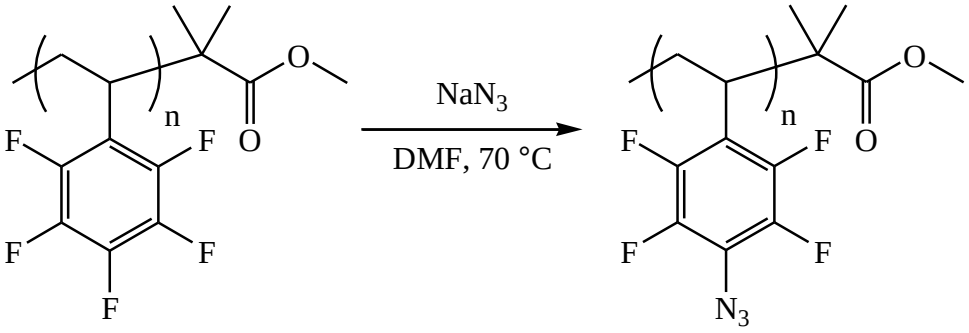

Scheme 5.07. *p*-Fluoro substitution of P(PFS) (P5.05) with sodium azide.

P(PFS) was reacted with different molar equivalents of sodium azide in an effort to part functionalise the P(PFS) and prepare a copolymer of P[(PFS)-*co*-(ATFS)] with tuneable ratios of azide to *p*-fluoro functionality. Relative molar equivalents of sodium azide to P(PFS) repeat units were 0.5 and 2. ^{19}F-NMR spectroscopy after substitution of P(PFS) with sodium azide is consistent with ^{19}F-NMR spectroscopy measured for PFS/ATFS (Figure 5.10) Resonances at −161 and −154 ppm which correspond to the P(PFS) repeat unit *m*-fluoro and *p*-fluoro, respectively, diminish and a new resonance appears at −151 ppm which corresponds to *m*-fluoro of the new P(ATFS) repeat units. *Ortho*-fluorine (*o*-fluoro) of P(PFS) and P(ATFS) repeat units have similar chemical shifts and form a merged signal at −143 ppm.

Relative integrations of the P(PFS) and P(ATFS) repeat unit signals were successfully tuned by varying the molar equivalents of sodium azide added to the reaction. Degree of substitution was estimated by the relative integration of P(PFS) and P(ATFS) *m*-fluoro signals on the ^{19}F-NMR spectra (Figure 5.10). 52% and 95%

of the P(PFS) repeat units were converted to P(ATFS) when utilising 0.5 and 2 molar equivalents of sodium azide, respectively (Table 5.03).

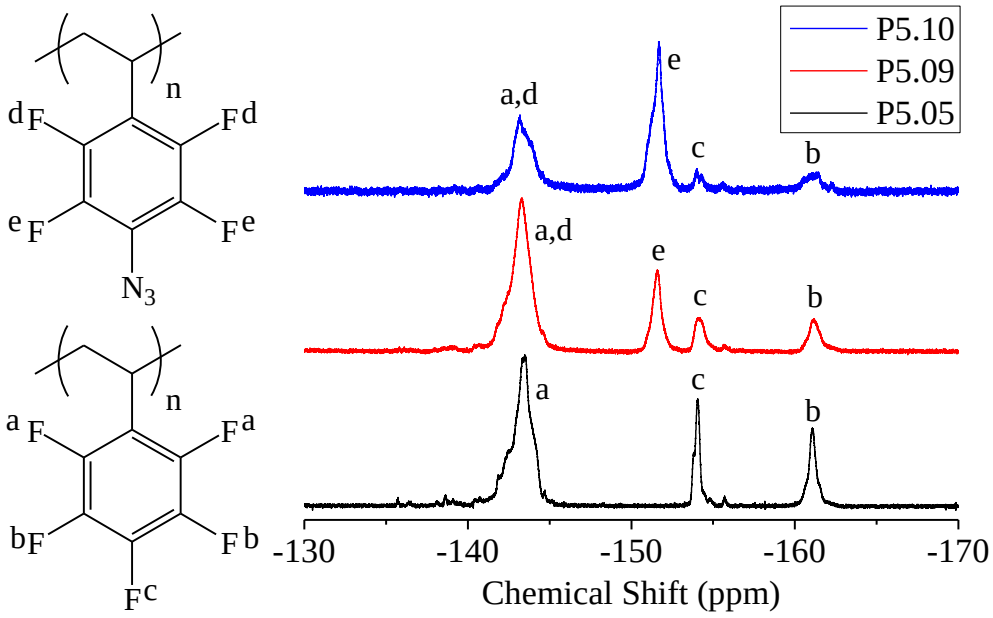

Figure 5.10. ^{19}F-NMR spectra ($CDCl_3$, 400 MHz, 303 K) of P(PFS) (P5.05) and P[(PFS)-*co*-(ATFS)] samples (P5.09/10).

Table 5.03. Characterisation for P(PFS) and P[(PFS)-*co*-(ATFS)] synthesised by *p*-fluoro substitution with sodium azide.

Sample	[P(PFS)]:[NaN_3]	Degree of Substitution$^{\alpha}$ (%)	$M_{n.GPC}^{\beta}$ (g·mol^{-1})	$M_{w.GPC}^{\beta}$ (g·mol^{-1})	$Đ^{\beta}$
P5.05	-	-	5400	5700	1.05
P5.09	1:0.5	52	5700	6200	1.10
P5.10	1:2	95	5500	6000	1.11

$^{\alpha}$Estimated from ^{19}F-NMR. $^{\beta}$DMF + 5 mM NH_4BF_4 eluent, calibrated with PS standards.

GPC measurements of the azide functionalised P(PFS) observed a slight shift towards higher M_n (<300 g·mol^{-1}) whilst retaining low dispersity (~1.1). High molecular weight shoulders appear on the GPC traces for the azide functionalised products (P5.09/10) (Figure 5.11). These shoulders are suspected to have occurred for the same reasons earlier; residual trithiocarbonate end group is being converted to

a thiol which subsequently substitutes a *p*-fluoro on the P(PFS) and leads to branching. Despite these high molecular shoulders the P[(PFS)-*co*-(ATFS)] is suitably well defined and the polymer backbone has not experienced any significant negative changes.

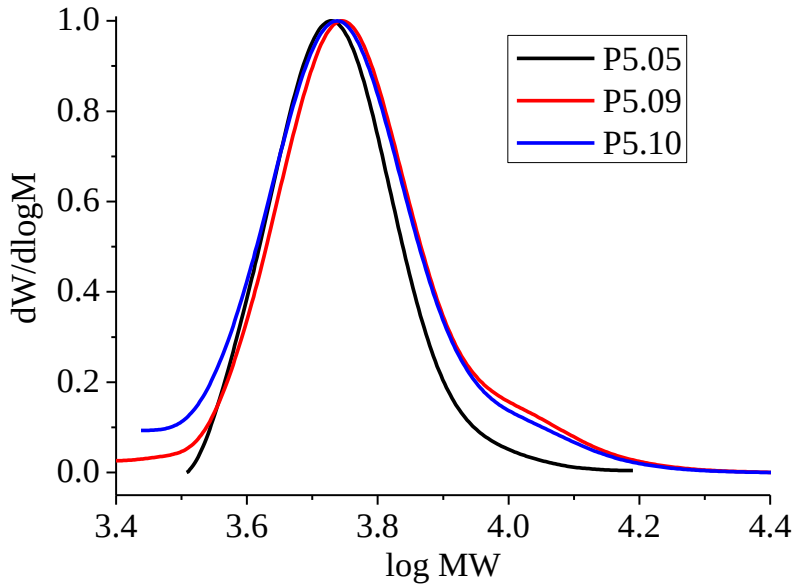

Figure 5.11. GPC traces (RID) of P(PFS) (P5.05) and P[(PFS)-*co*-(ATFS)] samples (P5.09/10).

Furthermore, FT-IR spectroscopy was again utilised to support the presence of the desired azide functionality (Figure 5.12). Following substitution of the *p*-fluoro with sodium azide there is appearance of a strong signal at 2123 cm^{-1} on the FT-IR spectrum of P5.09. This signal occurs in the expected region for azide functionality and collaborates well with the FT-IR spectra measured for ATFS.

P(PFS) synthesised by RAFT polymerisation and subsequently modified to remove the trithiocarbonate end group has been demonstrated to be a suitable backbone for post-polymerisation modification. Backbone modifications have been demonstrated by known processes such as, *p*-fluoro substitution with thiols and primary amines, as well as a novel functionalisation; *p*-fluoro substitution with sodium azide. The next

section combines these modifications in subsequent functionalisations of the same P(PFS) to prepare a multifunctional backbone.

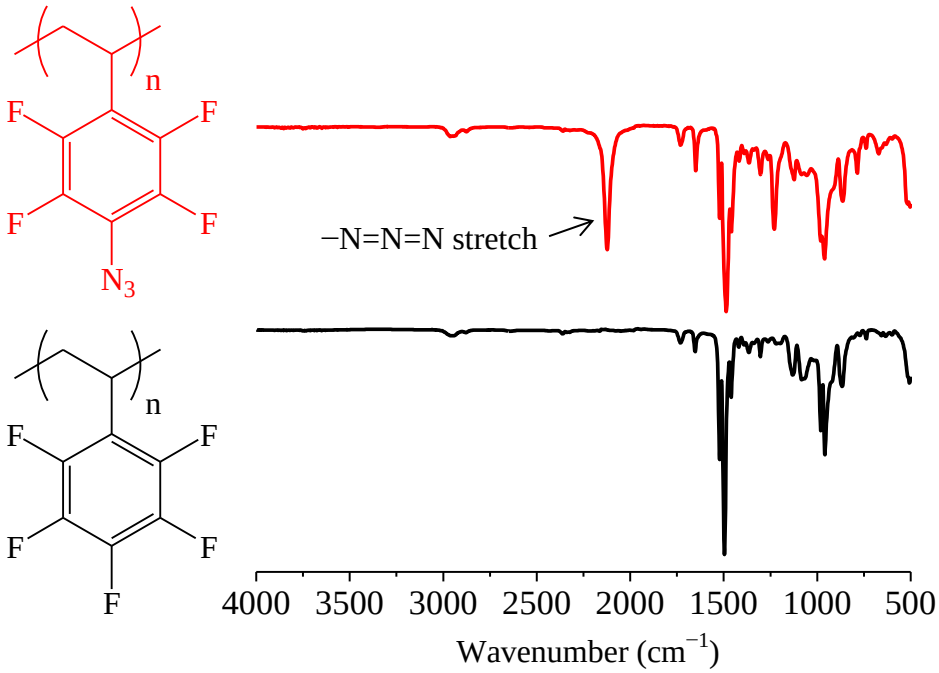

Figure 5.12. FT-IR spectra of P(PFS) (P5.05, black) and P[(PFS)-*co*-(ATFS)] (P5.09, red).

5.2.3.3. Multiple subsequent modifications of P(PFS)

Trithiocarbonate end group removed P(PFS) (P5.05) was modified by three subsequent modifications in the following order; partial substitution of the P(PFS) *p*-fluoros with TP, substitution of the remaining *p*-fluoros with sodium azide and finally a [4+2] cycloaddition between the P(ATFS) repeat units and propargyl alcohol (PA) (Scheme 5.08). The *p*-fluoro substitutions with TP and sodium azide were shown to be effective in Sections 5.2.3.1 and 5.2.3.2, respectively, and [4+2] cycloadditions between activated azides such as 4-azido-2,3,5,6-tetrafluorophenyl species have reported as effective reactions for the synthesis of copolymers by click polymerisation.[35]

The defined order for these subsequent modifications is one of three possible synthetic routes. Substitution of P(PFS) *p*-fluoros with TP was chosen to be the first

modification as it was shown to be very efficient, near quantitative conversion in 1 hour, and purification of the product was simple precipitation. Substitution of P(PFS) *p*-fluoros with sodium azide followed by TP may be ineffective as some thiols have been shown to reduce aryl azides to the corresponding aryl amines.[36] Furthermore, substitution of P(PFS) *p*-fluoros with sodium azide was performed second as it was the less efficient of the two substitutions and as such an excess of sodium azide may be required to convert remaining P(PFS) to P(ATFS) repeat units.

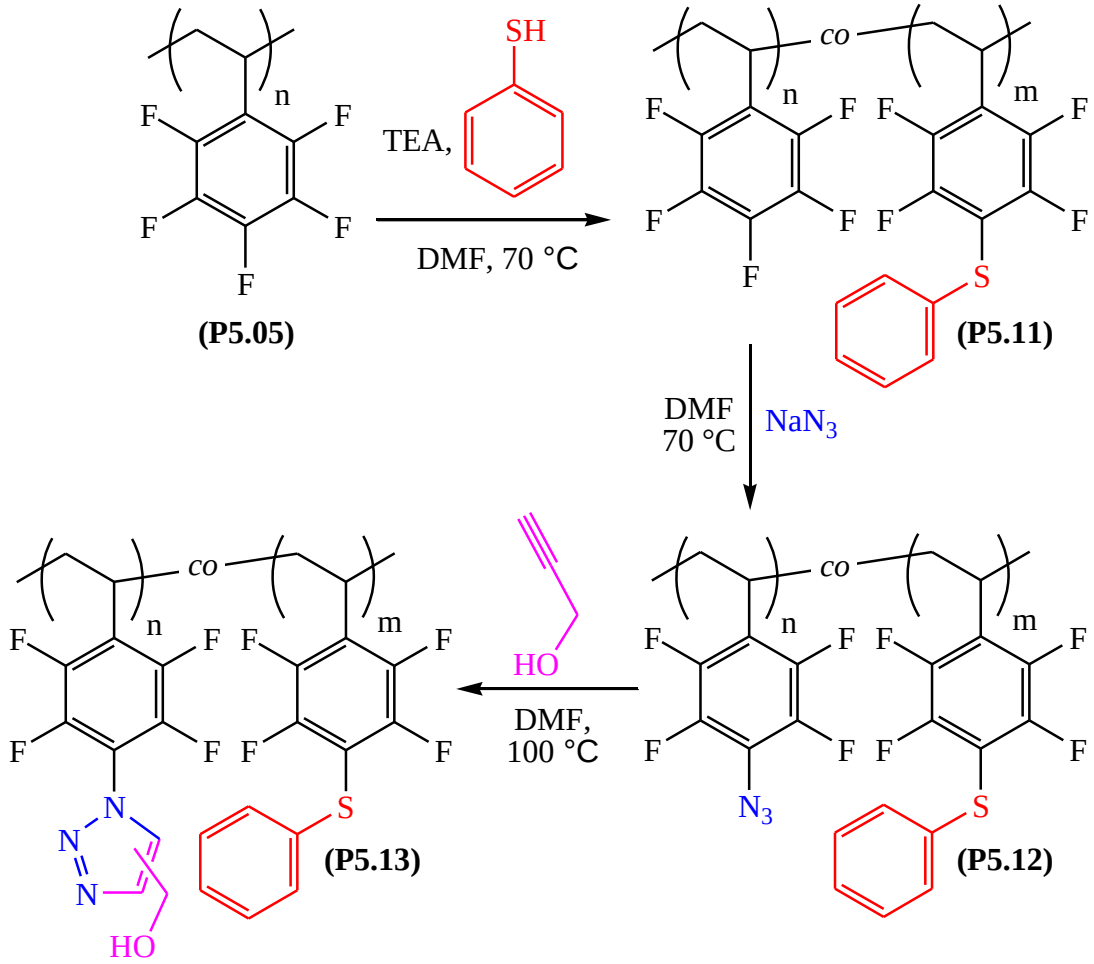

Scheme 5.08. Multiple subsequent modifications of P(PFS) (P5.05); *p*-fluoro substitution with TP (P5.11), *p*-fluoro substitution with sodium azide (P5.12) and [4+2] cycloaddition of P(ATFS) repeat units and PA (5.13).

Subsequent modifications of P(PFS) are supported by ^{19}F-NMR, ^{1}H-NMR and FT-IR spectroscopy as well as GPC measurements. ^{19}F-NMR spectroscopy demonstrates the partial *p*-fluoro substitution with TP by diminishing P(PFS) *p*-fluoro (−154 ppm)

and *m*-fluoro (−161 ppm) signals and the appearance of a *m*-fluoro (−133 ppm) for the TP substituted repeat units (Figure 5.13).

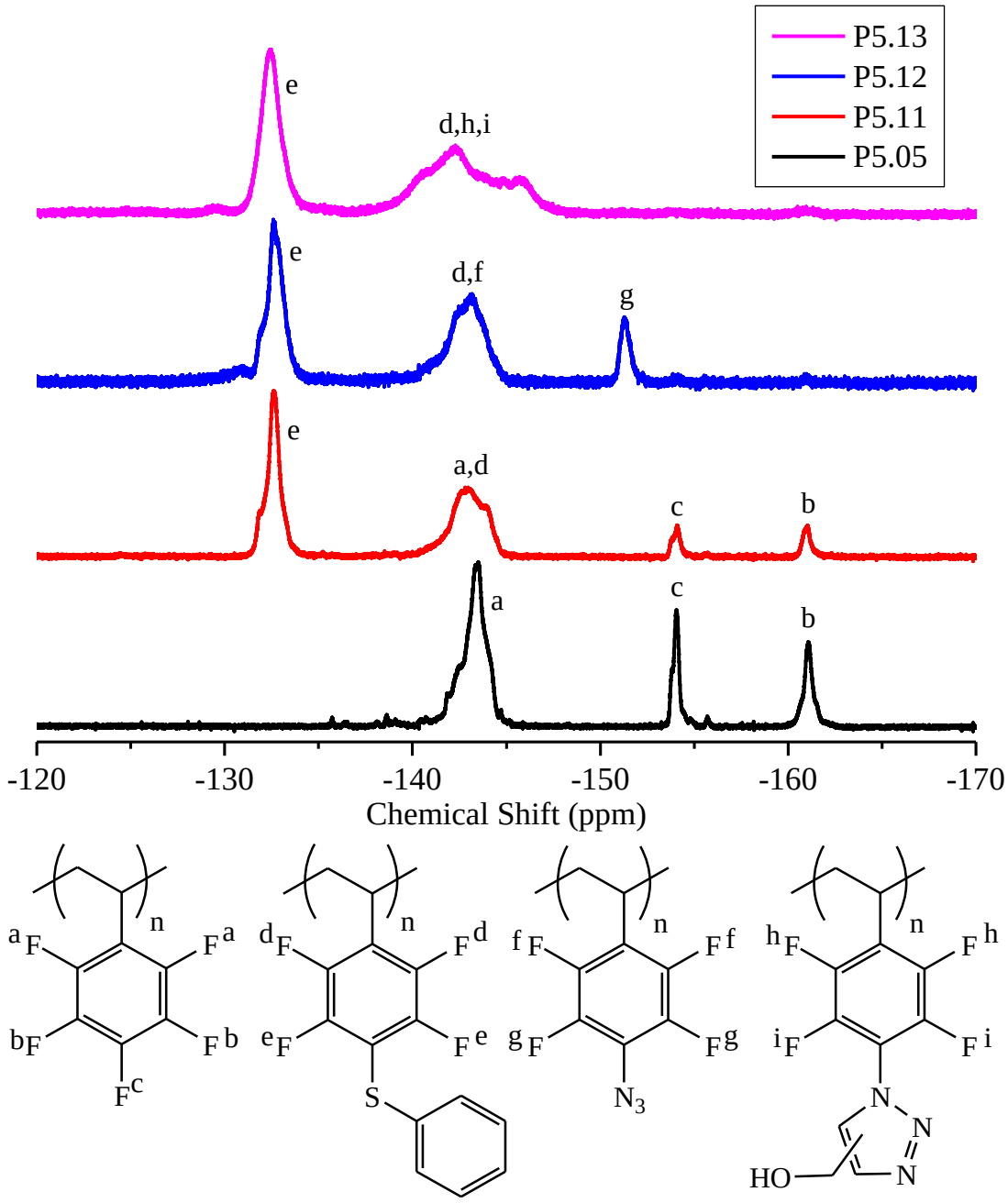

Figure 5.13. ^{19}F-NMR spectra ($CDCl_3$, 400 MHz, 303 K) of P(PFS) before (P5.05) and after each subsequent functionalisation; *p*-fluoro substitution with TP (P5.11), *p*-fluoro substitution with sodium azide (5.12) and [4+2] cycloaddition of P(ATFS) repeat units with PA (5.13).

Following *p*-fluoro substitution with sodium azide the remaining P(PFS) signals, *p*-fluoro (−154 ppm) and *m*-fluoro (−161 ppm), are replaced with a new signal (−151 ppm) corresponding to the *m*-fluoro of the P(ATFS) repeat units (Figure 5.13). This

is in good agreement with the initial sodium azide substitution experiments in Section 5.2.3.2. However, it should be noted that a larger excess of sodium azide (3 eq.) was required to fully substitute the remaining P(PFS) *p*-fluoros within 12 hours. ^{19}F-NMR spectroscopy indicates that the [4+2] cycloaddition of P(ATFS) repeat units and PA proceeded to full conversion. Disappearance of the P(ATFS) *m*-fluoro (−151 ppm) signals is observed as well as the formation of an increasingly merged signal centred at (−142 ppm) (Figure 5.13). However, ^{19}F-NMR spectroscopy does not confirm that cycloaddition has occurred as other processes, such as degradation of the azide, would also likely display a disappearance of the P(ATFS) *m*-fluoro signal at −151 ppm.

^{1}H-NMR spectroscopy was utilised to identify the appearance of relevant signals following the addition of functional groups to the P(PFS) backbone. After *p*-fluoro substitution with TP there is a large signal centred at 7.3 ppm corresponding to the aromatic protons of TP substituted repeat units (Figure 5.14). Relative integration of the aromatic signal to the backbone protons between 1.78-2.88 ppm, backbone protons signals do not vary greatly depending on the *para* substituent, estimating a 59% degree of substitution of P(PFS) with TP (Figure 5.14).

After *p*-fluoro substitution of the remaining P(PFS) repeat units with sodium azide there is no significant differences in the ^{1}H-NMR spectrum to the previous product (Figure 5.14). This is expected as the azide functionality contains no new protons and the polymeric backbone protons to not appear to change significantly with new *para* substituents (Figure 5.14).

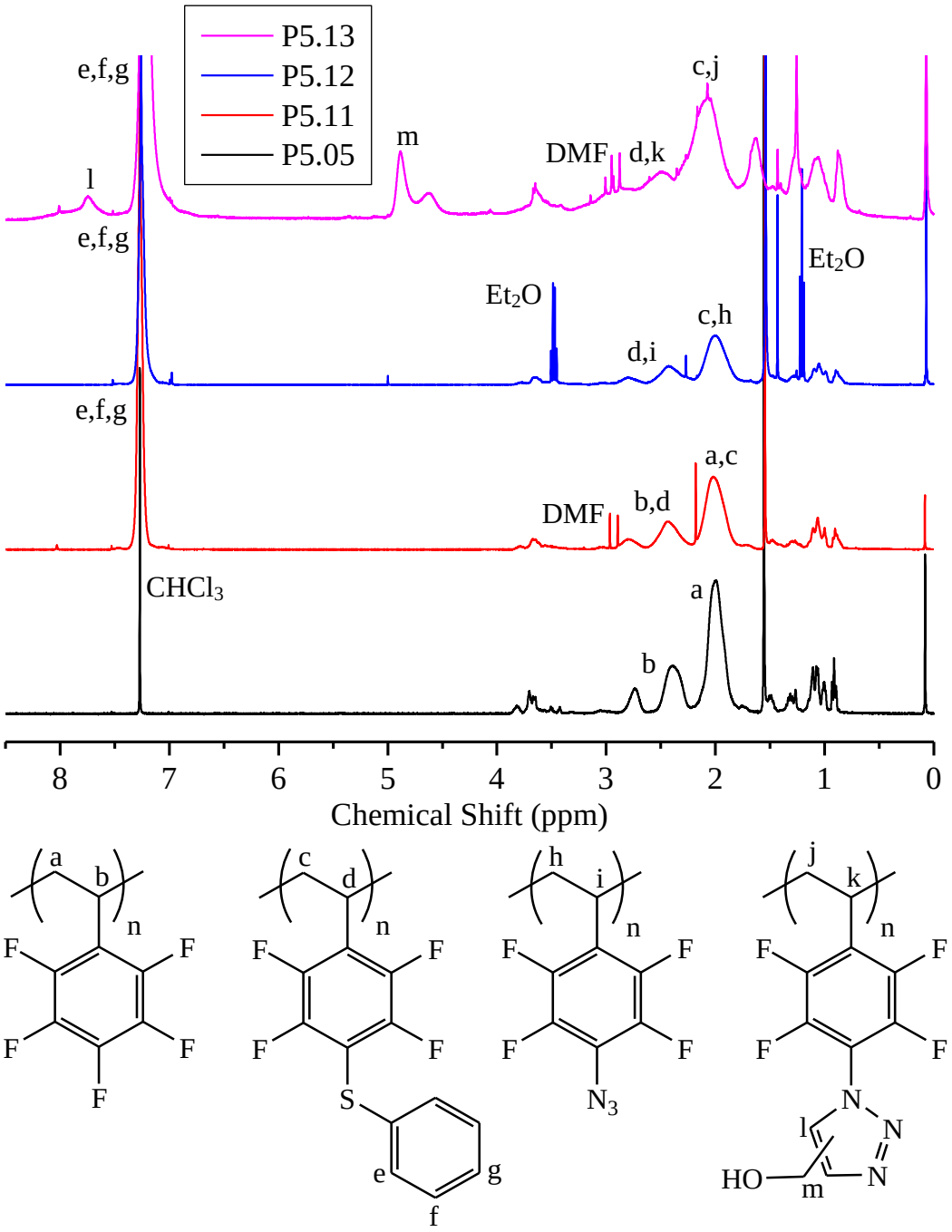

Figure 5.14. ^{1}H-NMR spectra ($CDCl_3$, 400 MHz, 303 K) of P(PFS) before (P5.05) and after each subsequent functionalisation; *p*-fluoro substitution with TP (P5.11), *p*-fluoro substitution with sodium azide (5.12) and [4+2] cycloaddition of P(ATFS) repeat units with PA (5.13).

Finally, ^{1}H-NMR spectroscopy was utilised to support the ^{19}F-NMR spectrum that [4+2] cycloaddition between P(ATFS) repeat units and PA was successful. New signals appear at 7.7 and 4.9 ppm which correspond to the triazole proton and methylene protons of PA, respectively (Figure 5.14). As cycloaddition was performed in the absence of catalyst there is no control of which regioisomer is

formed. A bimodal peak at 4.9 ppm for the PA methylene protons indicates a mixture of 1,4- and 1,5-triazole products (Figure 5.14). Relative integration of the methylene protons to triazole protons match the expected 2:1 integration well at 2:0.90. However, relative integration of methylene protons to backbone or TP aromatic protons are difficult to resolve as signals are significantly more merged from the previous ^{1}H-NMR spectrum (Figure 5.14). Relative integration of TP aromatic protons to PA methylene protons is 9.2:2 which is greater than the expected value of 7.5:2 (Figure 5.14). Measuring the ^{1}H-NMR spectrum in different solvent will assist in obtaining a more reliable integration but initial estimations are a good indication that P(ATFS) units and PA successfully underwent cycloaddition.

FT-IR spectroscopy provides further qualitative evidence for the subsequent modification steps of P(PFS) (Figure 5.15).

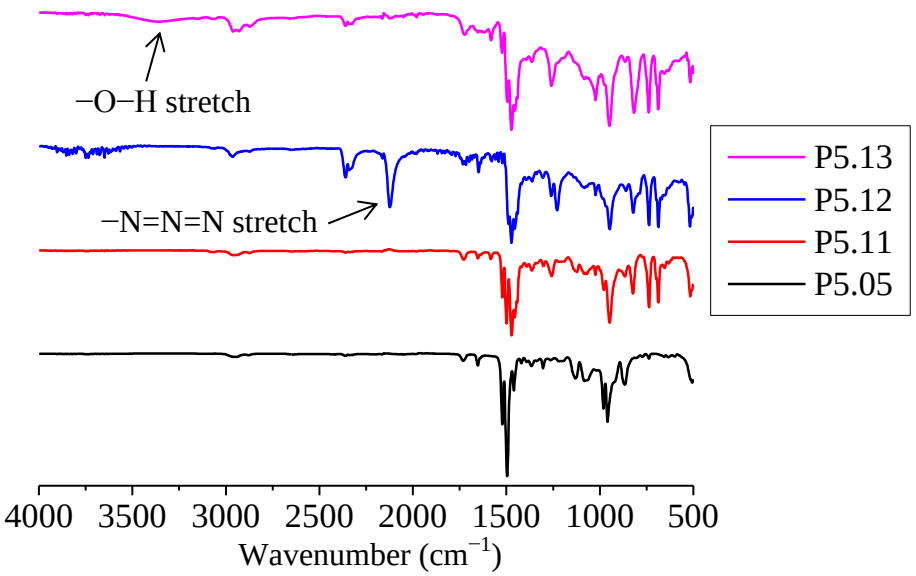

Figure 5.15. FT-IR spectra of P(PFS) before (P5. 05) and after each subsequent functionalisation; *p*-fluoro substitution with TP (P5.11), *p*-fluoro substitution with sodium azide (5.12) and [4+2] cycloaddition of P(ATFS) repeat units with PA (5.13).

FT-IR spectroscopy is particularly useful following the *p*-fluoro substitution with sodium azide as there is a strong characteristic signal at 2123 cm^{-1} for the new azide moiety. Furthermore, after [4+2] cycloaddition of P(ATFS) repeat units with PA there is disappearance of the aforementioned azide peak and appearance of a new broad signal (~3350 cm^{-1}) corresponding to the O-H stretch of the new alcohol moiety (Figure 5.15).

GPC measurements were performed for each subsequent modification of P(PFS) to ensure the resulting polymeric product remained well defined and increased in mass after addition of new functionality. GPC traces of the initial P(PFS) (P5.05) and subsequent modifications (P5.11-13) show a consistent shift towards higher molecular weight (Figure 5.16) and as such an increase in the M_n whilst maintaining low dispersity (<1.25) (Table 5.04).

Table 5.04. GPC characterisation for P(PFS) before (P5.05) and after each subsequent functionalisation; *p*-fluoro substitution with TP (P5.11), *p*-fluoro substitution with sodium azide (5.12) and [4+2] cycloaddition of P(ATFS) repeat units with PA (5.13).

Sample	$M_{n.GPC}^{\alpha}$ (g·mol^{-1})	$M_{w.GPC}^{\alpha}$ (g·mol^{-1})	$Đ^{\alpha}$
P5.05	5400	5700	1.05
P5.11	6000	6500	1.08
P5.12	6100	6600	1.08
P5.13	9600	11900	1.25

$^{\alpha}$DMF + 5 mM NH_4BF_4 eluent, calibrated with PS standards.

As with the other *p*-fluoro substitutions of P5.05 performed in earlier sections, there is formation of a high molecular shoulder that is observable on the GPC traces of P5.11 that persists throughout subsequent modifications (Figure 5.16). The high molecular weight shoulder is believed to form because the residual trithiocarbonate

end group is being converted to a thiol which subsequently substitutes a *p*-fluoro on the P(PFS) and leads to branching. The high molecular weight shoulder is more intense following the cycloaddition of P(ATFS) repeat units and PA to form P5.13 and will be a contributing factor to the higher dispersity measured for P5.13 compared to the previous modifications.

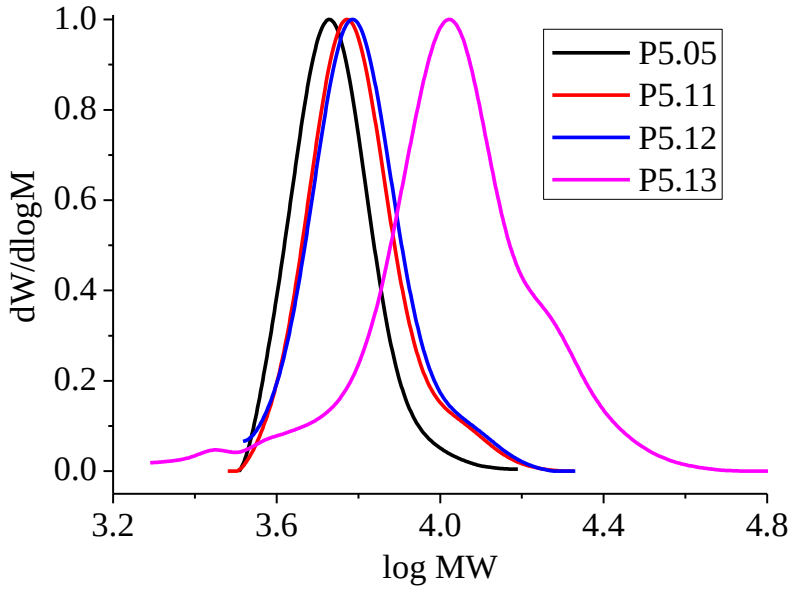

Figure 5.16. GPC traces (RID) of P(PFS) before (P5.05) and after each subsequent functionalisation; *p*-fluoro substitution with TP (P5.11), *p*-fluoro substitution with sodium azide (5.12) and [4+2] cycloaddition of P(ATFS) repeat units with PA (5.13).

This example of multiple subsequent modifications of P(PFS) represents the versatility of P(PFS) as a tuneable material that could be utilised to incorporate multiple functionalities onto a single polymer.

5.3. Synthesis and modification of P[(PFS)-*b*-(iPOx)] block copolymers

In the last section P(PFS) was functionalised multiple times on the same backbone to demonstrate the potential of P(PFS) as a highly tuneable and versatile material. However, a drawback of multiple modifications on the same P(PFS) backbone is that the product is a random copolymer of functionalised repeat units with no control

over the copolymer architecture. Furthermore, synthesise of higher order architectures, such as block copolymers, is not possible using the functionalised P(PFS) from Section 5.2 as the end group was removed and as such not capable of chain extension.

Therefore, a new synthetic methodology was designed to synthesise block copolymers of two reactive monomers; PFS and iPOx. P(PFS) has been demonstrated in previous Sections as a versatile monomer for post-polymerisation modification by thiols, primary amines, sodium azide and then subsequent cycloaddition with an alkyne. iPOx can be polymerised by cationic ring opening polymerisation of the 2-oxazoline or by radical/anionic polymerisation of the α-unsaturation.[37] As iPOx will be combined with PFS polymerised via radical polymerisation, poly(2-isopropenyl-2-oxazoline) (P(iPOx)) will solely refer to iPOx that has been polymerised via the α-unsaturation by radical/anionic polymerisation. Post-polymerisation modification of P(iPOx) has been demonstrated in literature by ring opening the oxazoline side group with thiols and carboxylic acids to the corresponding methacrylamides.[27] Furthermore, P(iPOx) side groups have been converted to salts, by reaction with methyl triflate, and used to initiate cationic ring opening polymerisation of 2-alkyl-2-oxazolines.[37]

Therefore, block copolymers composed of PFS and iPOx will represent a highly functional material capable of many post-polymerisation modifications chemoselective to either the P(PFS) or P(iPOx) block, modification with thiols being the notable exception. Furthermore, owing to the hydrophobic and hydrophilic nature of P(PFS) and P(iPOx), respectively, these block copolymers may exhibit self-assembly properties. Block copolymers composed of P(PFS) and P(iPOx) can be theoretically synthesised by RAFT polymerisation; homopolymerisation of PFS

followed by chain extension with iPOx or vice versa. Section 5.2 demonstrated the effective synthesis of P(PFS) by RAFT polymerisation so an analogous synthesis of P(iPOx) was pursued.

5.3.1. RAFT homopolymerisation of iPOx

Of the CRP techniques available, RAFT polymerisation was utilised for the polymerisation of iPOx. RAFT polymerisation has been demonstrated in the literature as effective technique for the controlled homo and copolymerisation (with MMA and *N*-isopropyl(meth)acrylamide) of iPOx.[27,28] Becer and co-workers have previously screened one RAFT agent from three classes of RAFT agents; trithiocarbonates, dithiobenzoates and dithiocarbamates, to mediate the homopolymerisation of iPOx.[27] The dithiobenzoate gave the best results in terms of P(iPOx) dispersity (1.38) compared to ~1.65 for the other two RAFT agents.[27] However, the trithiocarbonate and dithiocarbamate obtained a higher conversion of iPOx (24%) than the dithiobenzoate (15%).[27] Considering the specific structure of the trithiocarbonate RAFT agent that Becer and co-workers utilised; the R group was a $–CH_2CN$ which is a poor R group when attempting to polymerise monomers containing an α-saturation, such as methacrylates, methacrylamides and iPOx.[38] Therefore, BDTMP may be a more suitable trithiocarbonate as the R group is a $-C(CH_3)_2COOC_4H_9$ and as such more likely to fragment as it will form a tertiary radical. Therefore, iPOx was homopolymerised by the RAFT polymerisation system utilised successfully for PFS, DMA and DMAEA; initiated by V601, mediated by BDTMP, toluene as solvent (equal volume to iPOx) and with a temperature of 70 °C (Scheme 5.09).

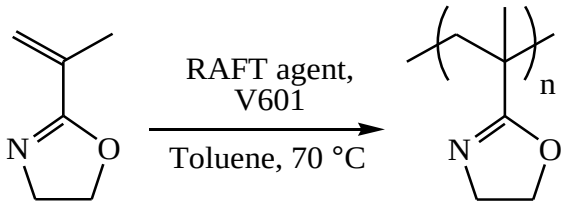

Scheme 5.09. RAFT homopolymerisation of iPOx, initiated by V601 and mediated by either BDTMP, CDSP or CPPA in toluene at 70 °C.

P(iPOx) synthesised by RAFT polymerisation mediated by BDTMP (P5.14) was very poorly defined. This is evidenced by GPC which measured a broad dispersity (1.84) and M_n that was significantly greater than the theoretical M_n (Table 5.05). GPC traces measured by the RID display an unsymmetrical distribution with low molecular weight tailing (Figure 5.17). Furthermore, GPC traces measured by the VWD at 308 nm does not detect any higher molecular weight species, 550 $g \cdot mol^{-1}$ PMMA standard elutes at 19.85 minutes so any species eluting earlier are considered higher molecular weight (Figure 5.18). This implies that radicals did not effectively add to and subsequently fragment BDTMP to synthesise trithiocarbonate terminated P(iPOx). P5.14 essentially proceeded via free radical polymerisation.

Table 5.05. GPC characterisation and iPOx conversion for the RAFT homopolymerisation of iPOx in toluene at 70 °C, mediated by either BDTMP, CDSP or CPPA and initiated by V601.

Sample	RAFT agent	iPOx Conversion$^{\alpha}$ (%)	$M_{n.GPC}{}^{\beta}$ ($g \cdot mol^{-1}$)	$M_{n.Theo}{}^{\gamma}$ ($g \cdot mol^{-1}$)	$Đ^{\beta}$
P5.14$^{\delta}$	BDTMP	32	7300	2200	1.84
P5.15$^{\delta}$	CDSP	37	2900	2500	1.76
P5.16$^{\delta}$	CPPA	31	2800	2100	1.40

$^{\alpha}$Calculated from GC-FID. $^{\beta}$DMF + 5 mM NH_4BF_4 eluent, calibrated with PMMA standards. $^{\gamma}$Calculated from Equation 1. $^{\delta}$Molar equivalents of [iPOx]:[RAFT agent]:[V601] = 50:1:0.1.

BDTMP may be an ineffective RAFT agent for the homopolymerisation of iPOx as the R group was not a relatively good enough radical leaving group compared to P(iPOx) as a radical leaving group. P(iPOx) radicals would not add to and fragment

BDTMP but continue propagating once initiated. Therefore, RAFT homopolymerisation of iPOx was repeated with a different trithiocarbonate, 4-cyano-4-[(dodecylsulfanylthiocarbonyl)sulfanyl] pentanoic acid (CDSP). CDSP bears the following R group; $–C(CN)(CH_3)CH_2CH_2COOH$, this is a better radical leaving group and as such more appropriate for controlling polymerisations of α-methyl containing monomers.[38] P(iPOx) synthesised by RAFT polymerisation mediated by CDSP (P5.15) was still poorly defined but there are indications that CDSP is a more suitable RAFT agent than BDTMP. P(iPOx) dispersity was marginally lower (1.76) and M_n measured by GPC was a much closer match to the theoretical M_n (Table 5.05). Moreover, GPC traces measured by the VWD set to 308 nm does detect higher molecular weight species which implies that P(iPOx) radicals are more effectively adding to and subsequently fragmenting CDSP (Figure 5.18). This may explain why the M_n measured by GPC more closely fits the theoretical M_n.

When utilising trithiocarbonate RAFT agents the resulting P(iPOx) was poorly defined, therefore a dithiobenzoate RAFT agent, 4-cyano-4-(phenylcarbonothioylthio)pentanoic acid (CPPA), was employed to improve the control of iPOx homopolymerisation.[27] CPPA is expected to improve the control of iPOx homopolymerisation as dithiobenzoates have greater transfer coefficients than trithiocarbonates and as such fragmentation will occur more often relative to iPOx propagation.[39] P(iPOx) synthesised by RAFT polymerisation mediated by CPPA (P5.16) was better defined compared to trithiocarbonate mediated polymerisations. P5.16 was measured to have the lowest dispersity (1.40) but this is significantly greater than the dispersity of other polymers synthesised by RAFT polymerisation throughout this and previous Sections (Table 5.05). M_n measured by GPC was again a close match to the theoretical M_n (Table 5.05) and GPC traces measured by the

VWD at 308 nm did detect higher molecular weight species, implying that P(iPOx) radicals are adding to and subsequently fragmenting CPPA (Figure 5.18). These results closely match those reported by Becer and co-workers.[27]

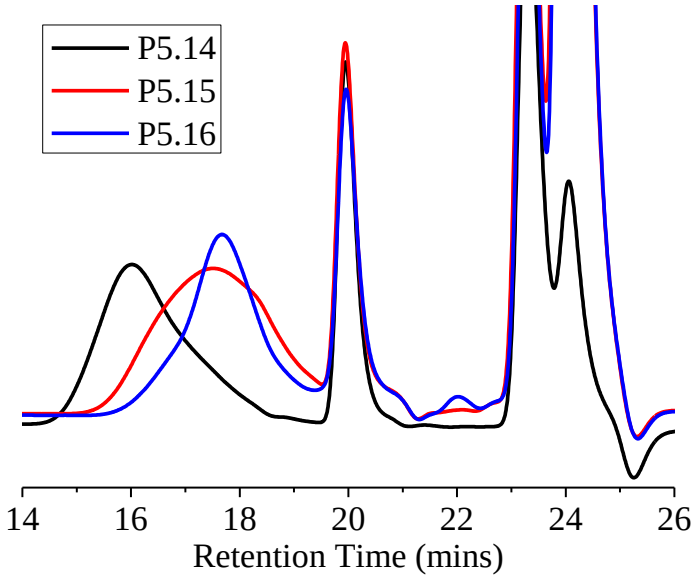

Figure 5.17. GPC traces (RID) of P(iPOx) prepared by RAFT homopolymerisation of iPOx in toluene at 70 °C, mediated by BDTMP (P5.14), CDSP (P5.15), CPPA (P5.16) and initiated by V601.

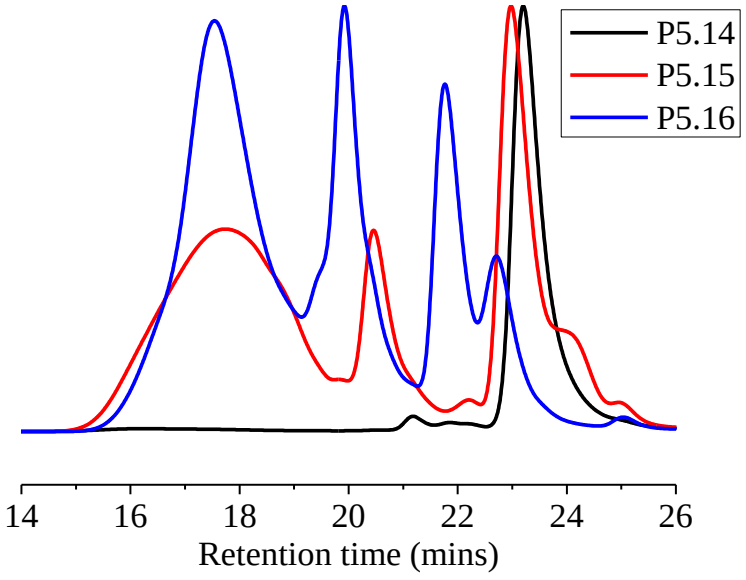

Figure 5.18. GPC traces (VWD) of P(iPOx) prepared by RAFT homopolymerisation of iPOx in toluene at 70 °C, mediated by BDTMP (P5.14), CDSP (P5.15), CPPA (P5.16) and initiated by V601.

Changes in the choice of RAFT agent to mediate the RAFT homopolymerisation of iPOx did provide incremental improvements in terms or dispersity, measured M_n and incorporation of the RAFT agent. However, iPOx conversion remained consistently low (~30%) and the P(iPOx) (P5.14-16) synthesised was not suitably well-defined to be utilised for chain extensions with PFS. Therefore, chain extension of P(PFS) with iPOx was investigated as a means of synthesising the desired block copolymers.

5.3.2. Attempted chain extension of P(PFS) with iPOx

Trithiocarbonate terminated P(PFS) (P5.01) synthesised by RAFT polymerisation in Section 5.2.1 was utilised as a macroRAFT agent for the polymerisation of iPOx; initiated by V601 in toluene at 70 °C, to synthesise P[(PFS)-*b*-(iPOx)] copolymers (Scheme 5.10).

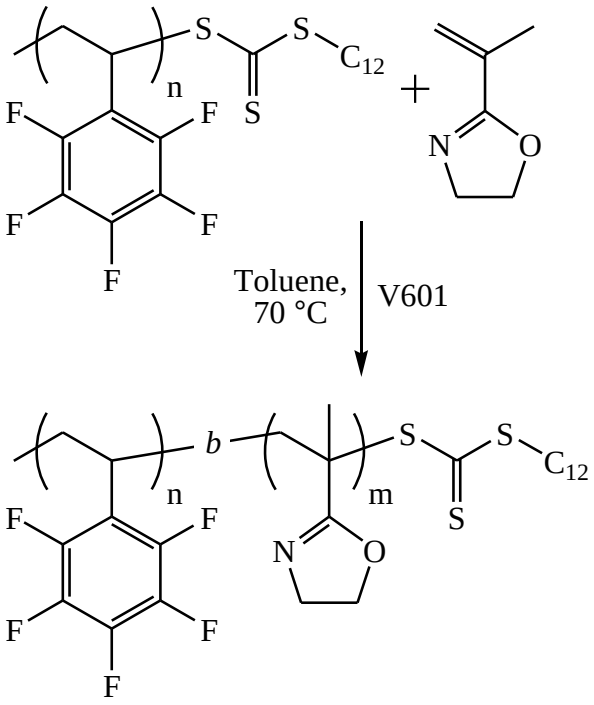

Scheme 5.10. Chain extension of P(PFS) (P5.01) with iPOx in toluene at 70 °C, initiated by V601.

Trithiocarbonate terminated P(PFS) (P5.01) was demonstrated by GPC to be a poor macroRAFT agent for the polymerisation of iPOx (P5.17, Figure 5.19). GPC

provides evidence that P5.01 was not effectively added to and subsequently fragmented by a P(iPOx) radical similar to the results obtained when using BDTMP as RAFT agent for iPOx polymerisation (P5.14). GPC measured by RID shows a bimodal distribution of which the lower molecular weight distribution overlaps with the distribution of P5.01 (Figure 5.19). Furthermore, GPC measured by VWD set to 308 nm observes that the higher molecular weight distribution of P5.17 measured with the RID does not absorb at 308 nm whereas the lower molecular weight distribution of P5.17 and P5.01 does absorb at 308 nm (Figure 5.19). This indicates that the polymerised iPOx does not contain any trithiocarbonate functionality, P5.01 was not chain extended with iPOx and the RID GPC trace of P5.17 displays a mixture of P(PFS) and P(iPOx) homopolymers.

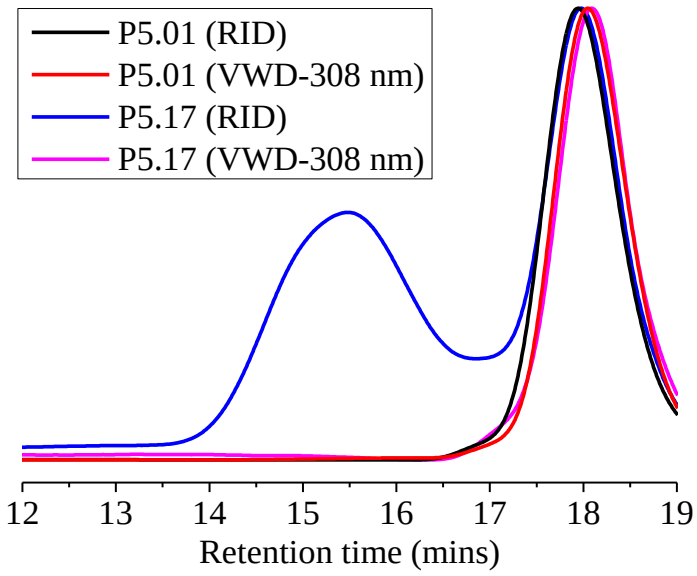

Figure 5.19. GPC traces (RID and VWD-308 nm) of P(PFS) (P5.01) and attempted chain extension with iPOx (P5.17) in toluene at 70 °C and initiated by V601.

P5.01 and BDTMP were equally ineffective as RAFT agents for mediating iPOx homopolymerisation. This is attributed to the R group of both RAFT agents not being sufficiently good radical leaving groups; a $-C(CH_3)_2COOC_4H_9$ for BDTMP

and a P(PFS) chain for P5.01. As such P(iPOx) radicals are unlikely to add to and subsequently fragment these RAFT agents but instead continue propagating in an uncontrolled fashion. Owing to the limitations of chain extending P(PFS) with pure iPOx, chain extensions of P(PFS) with a mixture of iPOx and another comonomer was investigated to determine if greater control could be achieved.

5.3.3. Chain extension of P(PFS) with iPOx and DMA

DMA was selected as the comonomer of iPOx for the chain extension of P(PFS) (P5.01) because, DMA was polymerised in Chapter 4 with good control utilising a trithiocarbonate RAFT agent and P(DMA) radicals will be secondary radicals so more likely to add to/fragment P5.01. Furthermore, DMA is hydrophilic so resulting block copolymers of PFS, DMA and iPOx (P[(PFS)-*b*-((iPOx)-*co*-(DMA))]) should also be amphiphilic block copolymers. P5.01 was utilised as a macroRAFT agent for the copolymerisation of iPOx and DMA; initiated by V601 in toluene at 70 °C, to synthesise P[(PFS)-*b*-((iPOx)-*co*-(DMA))] copolymers (Scheme 5.11).

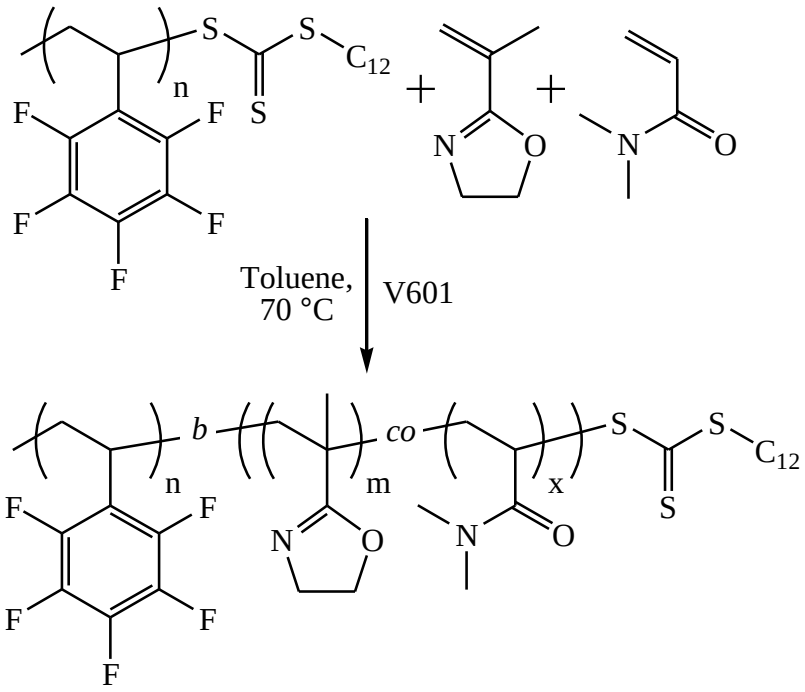

Scheme 5.11. Chain extension of P(PFS) with iPOx and DMA in toluene at 70 °C, initiated by V601.

P5.01 was chain extended with varying ratios of iPOx:DMA, total molar equivalents of iPOx + DMA was either 25 (P5.18, P5.20/21) or 100 (P5.19) relative to P(PFS) (Table 5.06). P5.18, P5.20 and P5.21 copolymerised an increasing percentage of iPOx to DMA; 5%, 10% and 25%, respectively. Each of these chain extensions were successful at synthesising P[(PFS)-*b*-((iPOx)-*co*-(DMA))] (Table 5.06). GPC traces measured by RID and VWD set to 308 nm show clear shifts to higher molecular weight of the initial P5.01 macroRAFT agent (Figure 5.20 and 5.21). As both the RID and VWD GPC traces shift to high molecular weight this indicates that P5.01 is undergoing effective addition of polymeric radicals and subsequent fragmentation to control the copolymerisation. M_n and M_w increased for all three chain extensions of P5.01 and dispersity of each block copolymer remained low (≤1.12) (Table 5.06).

Table 5.06. GPC characterisation and monomer conversions for the chain extension of P(PFS) (P5.01) with iPOx and DMA in toluene at 70 °C, initiated by V601.

Sample	[iPOx]:[DMA] [P(PFS)]$^{\alpha}$:[V601]	iPOx;DMA Conversion$^{\beta}$ (%)	$M_{n.GPC}{}^{\gamma}$ (g·mol^{-1})	$M_{w.GPC}{}^{\gamma}$ (g·mol^{-1})	$Đ^{\gamma}$
P5.18	1.25:23.75:1:0.1	>99;>99	10000	11000	1.10
P5.19	5:95:1:0.l	>99;>99	22900	26600	1.16
P5.20	2.5:22.5:1:0.1	80;54	8300	9100	1.11
P5.21	6.25:18.75:1:0.1	59;37	7000	7800	1.12

$^{\alpha}$P(PFS) M_n = 4400 g·mol^{-1}, M_w = 4800 g·mol^{-1}, $Đ$ = 1.10. $^{\beta}$Calculated from GC-FID. $^{\gamma}$DMF + 5 mM NH_4BF_4 eluent, calibrated with PS standards.

Final conversion of DMA and iPOx decreased as the percentage of iPOx in the chain extension was increased (Table 5.06). Becer and co-workers observed that iPOx conversion plateaued at ~30% when they investigate the kinetics of iPOx RAFT homopolymerisation.[27] They attributed the plateauing of iPOx conversion to the intermediate product during RAFT polymerisation being too stable and not capable

of reinitiating polymerisation.[27] This explanation could explain why increasing the percentage of iPOx resulted in lower overall conversions as more iPOx is incorporated into the block copolymers, they will be less capable of reinitiating and polymerising either iPOx or DMA.

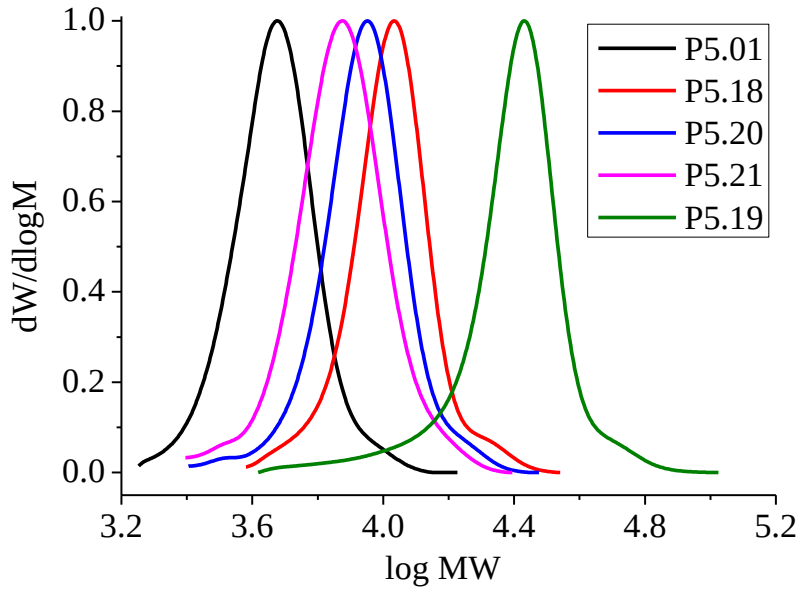

Figure 5.20. GPC traces (RID) of P[(PFS)-*b*-((iPOx)-*co*-(DMA))] (P5.18-21) synthesised by chain extension of P(PFS) (P5.01) with iPOx and DMA in toluene at 70 °C, initiated by V601.

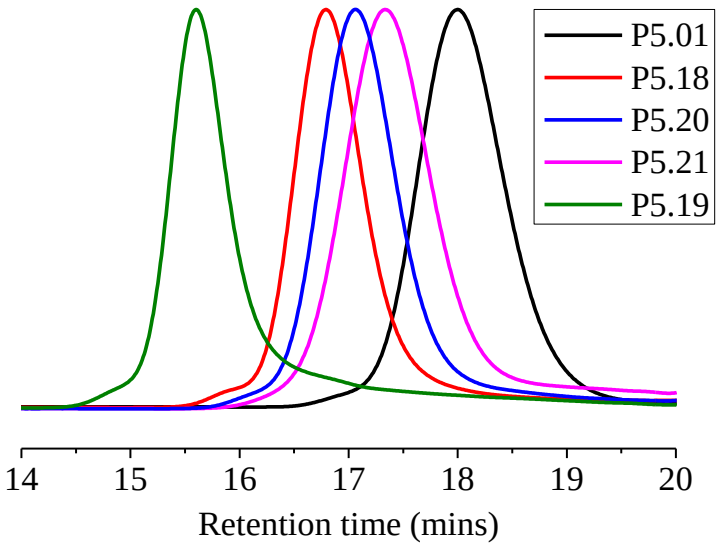

Figure 5.21. GPC traces (VWD-308 nm) of P[(PFS)-*b*-((iPOx)-*co*-(DMA))] (P5.18-21) synthesised by chain extension of P(PFS) (P5.01) with iPOx and DMA in toluene at 70 °C, initiated by V601.

P5.01 was also successfully chain extended with different total equivalents of iPOx + DMA; 25 (P5.18) and 100 (P5.19), whilst maintaining only 5% molar equivalents of iPOx relative to DMA. Both chain extensions proceeded to very high conversions (>99%) of iPOx and DMA whilst maintaining low polymer dispersity (≤1.16). Furthermore, GPC measured by the RID and VWD show clear shifts to higher molecular weight following the chain extension (Figures 5.20 and 5.21).

^{1}H-NMR spectroscopy measurements of precipitated P[(PFS)-*b*-((iPOx)-*co*-(DMA))] samples can be utilised to observe the new P(iPOx) and P(DMA) repeat units added to the P(PFS) macroRAFT agent after chain extension (Figure 5.22). However, when chain extension of P(PFS) was attempted with only iPOx (Section 5.3.2), it was observed that iPOx did not add to but only homopolymerised alongside the P(PFS) macroRAFT agent present (Figure 5.19). GPC and ^{1}H-NMR spectroscopy measurements of P[(PFS)-*b*-((iPOx)-*co*-(DMA))] are good indications that P(PFS) was chain extended as desired but do not definitively prove that the iPOx did chain extend P(PFS) rather than polymerise separately.

Therefore, diffusion ordered spectroscopy (DOSY) was measured for a P[(PFS)-*b*-((iPOx)-*co*-(DMA))] (P5.21) sample to support the expected block copolymer structure (Figure 5.23). DOSY can separate NMR signals according to their respective diffusion coefficients. If P[(PFS)-*b*-((iPOx)-*co*-(DMA))] (P5.21) was a mixture of one or more (co)polymers then DOSY would likely observe NMR signals occurring on multiple diffusion coefficients. DOSY of P[(PFS)-*b*-((iPOx)-*co*-(DMA))] (P5.21) observes that all of the block copolymer NMR signals occur along the same diffusion coefficient ~2.5×10^{-6} (Figure 5.23). This is good evidence that P[(PFS)-*b*-((iPOx)-*co*-(DMA))] (P5.21) has block copolymer architecture. Furthermore, DOSY was measured for the P(PFS) macroRAFT agent to exclude the

possibility that the P(PFS) macroRAFT agent and P[(PFS)-*b*-((iPOx)-*co*-(DMA))] (P5.21) have the same diffusion coefficient. DOSY observes that P(PFS) (P5.01) has a greater diffusion coefficient (~8 × 10^{-6}) than P[(PFS)-*b*-((iPOx)-*co*-(DMA))] (P5.21) and that there is a clear separation between the two samples polymeric NMR signals (Figure 5.23).

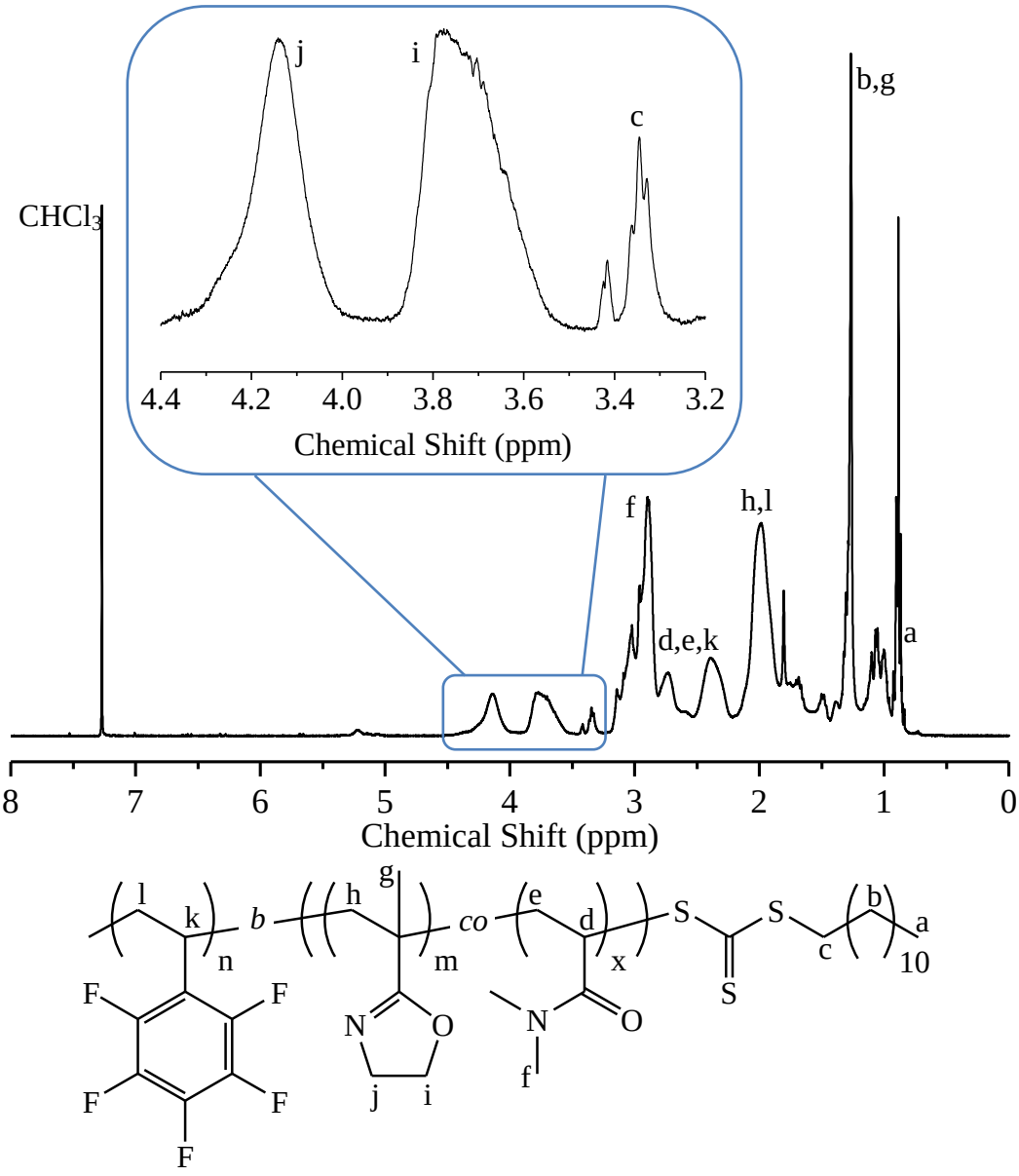

Figure 5.22. ^{1}H-NMR spectrum ($CDCl_3$, 400 MHz, 303 K) of P[(PFS)-*b*-((iPOx)-*co*-(DMA))] (P5.21).

Chain extending P5.01 with iPOx and DMA is an effective means of synthesising P[(PFS)-*b*-((iPOx)-*co*-(DMA))] copolymers with increasing quantities of iPOx in the

second block. Furthermore, iPOx quantity can remain constant and the block length can be tuned relative to the P(PFS) block, this is beneficial when synthesising amphiphilic block copolymers as block lengths can dictate self-assembly behaviour.

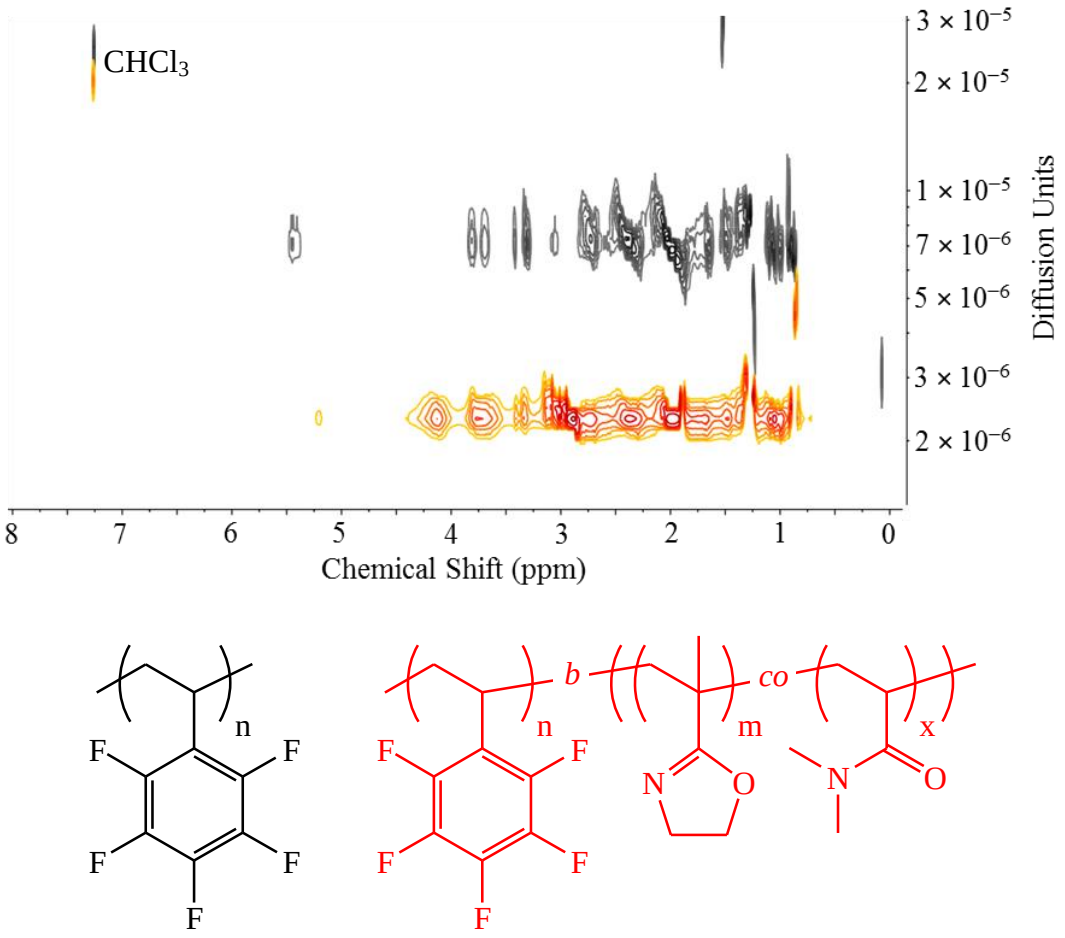

Figure 5.23. DOSY spectra ($CDCl_3$, 400 MHz, 303 K) of P(PFS) (P5.01, black) and P[(PFS)-*b*-((iPOx)-*co*-(DMA))] (P5.21, red).

5.3.4. End group removal of P[(PFS)-*b*-((iPOx)-*co*-(DMA))]

P[(PFS)-*b*-((iPOx)-*co*-(DMA))] was next explored as a material for post-polymerisation modification. P(PFS) repeat units can be functionalised via substitution of the *p*-fluoro with thiols, primary amines and sodium azide. It has been demonstrated that P(iPOx) repeat units can be ring opened by thiols and carboxylic acids to prepare a functional methacrylamide backbone.[27] Therefore, dual functionalisation of P[(PFS)-*b*-((iPOx)-*co*-(DMA))] via *p*-fluoro substitution and

ring opening reactions with TP was performed. Before said functionalisation reactions can be performed the trithiocarbonate end group of P[(PFS)-*b*-((iPOx)-*co*-(DMA))] was removed as a precaution. This is because presence of a trithiocarbonate end group was suspected to be the cause of poor GPC measurements initially observed when first attempting to substitute the *p*-fluoro on trithiocarbonate terminated P(PFS) with thiols (Section 5.2.2). Radical induced addition was again selected to remove the trithiocarbonate end group and the same adapted procedure from literature and Section 5.2.3 was performed on P[(PFS)-*b*-((iPOx)-*co*-(DMA))] (P5.22) (Scheme 5.12).[33] P5.22 was a scaled-up repeat of P5.21 which has a M_n and M_w of 7000 and 8200 g·mol^{-1}, respectively, with dispersity of 1.19 (Table 5.11).

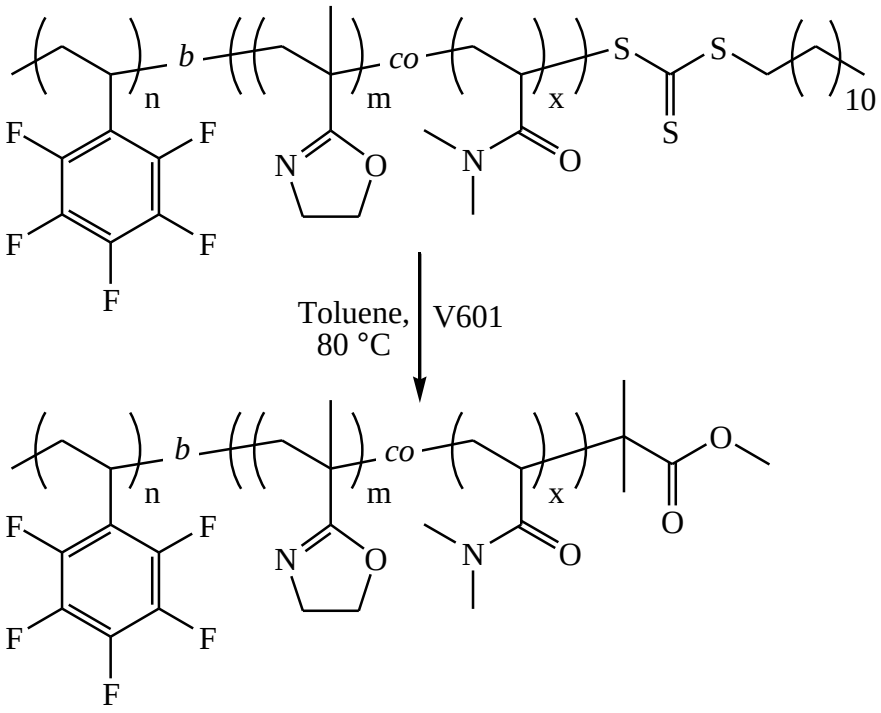

Scheme 5.12. Synthesis of trithiocarbonate end group removed P[(PFS)-*b*-((iPOx)-*co*-(DMA))] (P5.23) by radical induced addition of V601 derived radicals.

P[(PFS)-*b*-((iPOx)-*co*-(DMA))] trithiocarbonate end group removal by radical induced addition was not as efficient as the analogous reaction performed on P(PFS), removing only 52% (measured by ^{1}H-NMR spectroscopy) of the trithiocarbonate after heating for 4 hours at 80 °C with 20 equivalents of V601. Therefore, radical

induced addition was repeated with the partially end group removed P[(PFS)-*b*-((iPOx)-*co*-(DMA))] in an attempt to remove the remaining trithiocarbonate end group. After heating again for 4 hours at 80 °C with 20 equivalents of V601 (essentially a ~40 times excess), total trithiocarbonate end group removal was 76%.

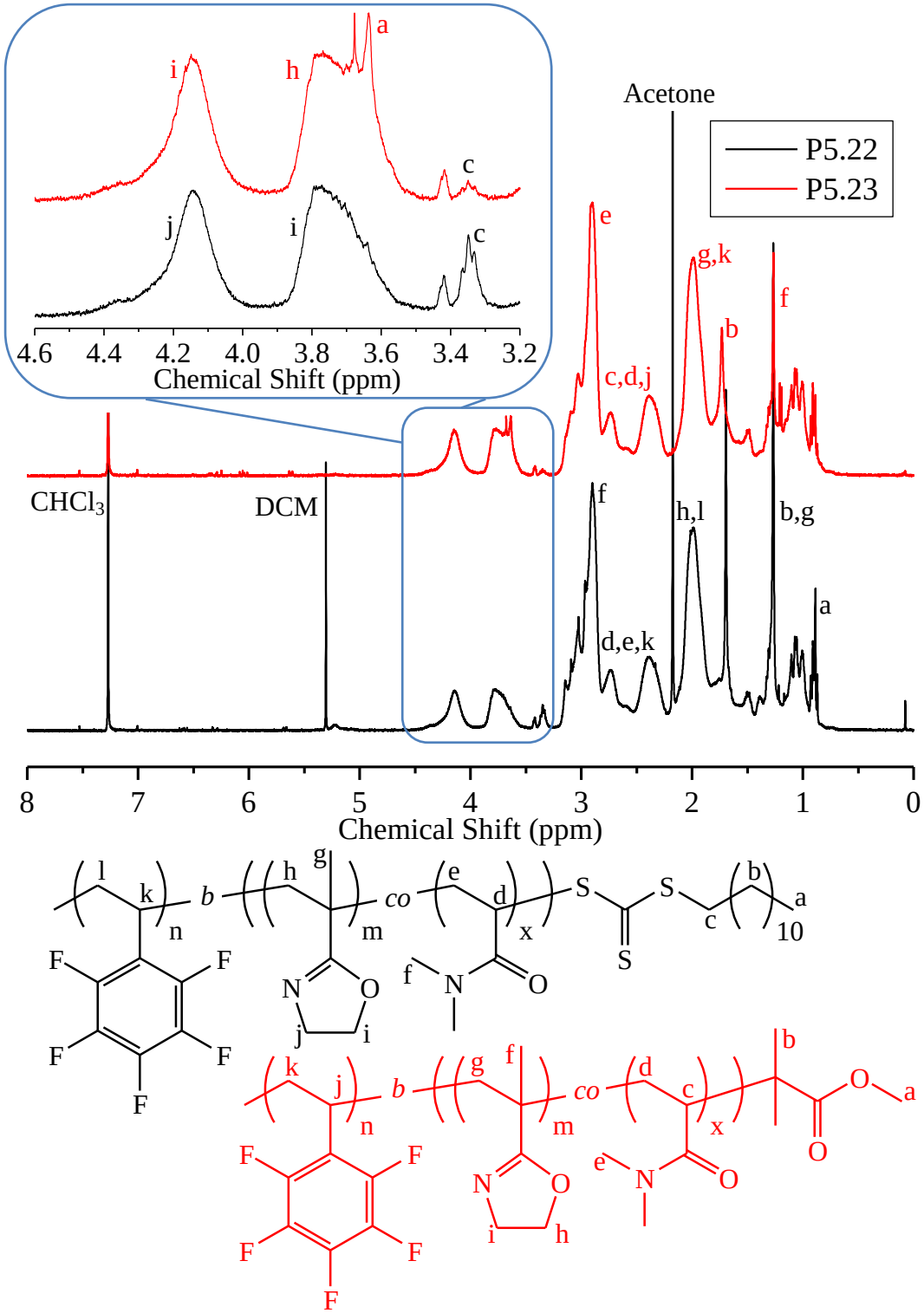

Figure 5.24. ^{1}H-NMR spectrum ($CDCl_3$, 400 MHz, 303 K) of P[(PFS)-*b*-((iPOx)-*co*-(DMA))] with 100% (P5.22) and 24% (P5.23) trithiocarbonate end group.

End group removal can be visualised by disappearance of the triplet at 3.34 ppm which corresponds to the methylene protons (H^c) adjacent to the trithiocarbonate end group (Figure 5.24). Following end group removal, an increase in both the M_n and M_w to 8600 and 9400 g·mol^{-1}, respectively, was measured. Dispersity remained low (1.09) and no high molecular weight shoulder was observed (Figure 5.27). Despite trithiocarbonate end group removal being less efficient for P[(PFS)-*b*-((iPOx)-*co*-(DMA))] than P(PFS), modification of the partially end group removed P[(PFS)-*b*-((iPOx)-*co*-(DMA))] (P5.23) was attempted.

5.3.5. Functionalisation of P[(PFS)-*b*-((iPOx)-*co*-(DMA))] with thiophenol

Modification of P[(PFS)-*b*-((iPOx)-*co*-(DMA))] (P5.23) was performed by the simultaneous functionalisation of P(PFS) and P(iPOx) repeat units with TP, via *p*-fluoro substitution and oxazoline ring opening, respectively. (Scheme 5.13).

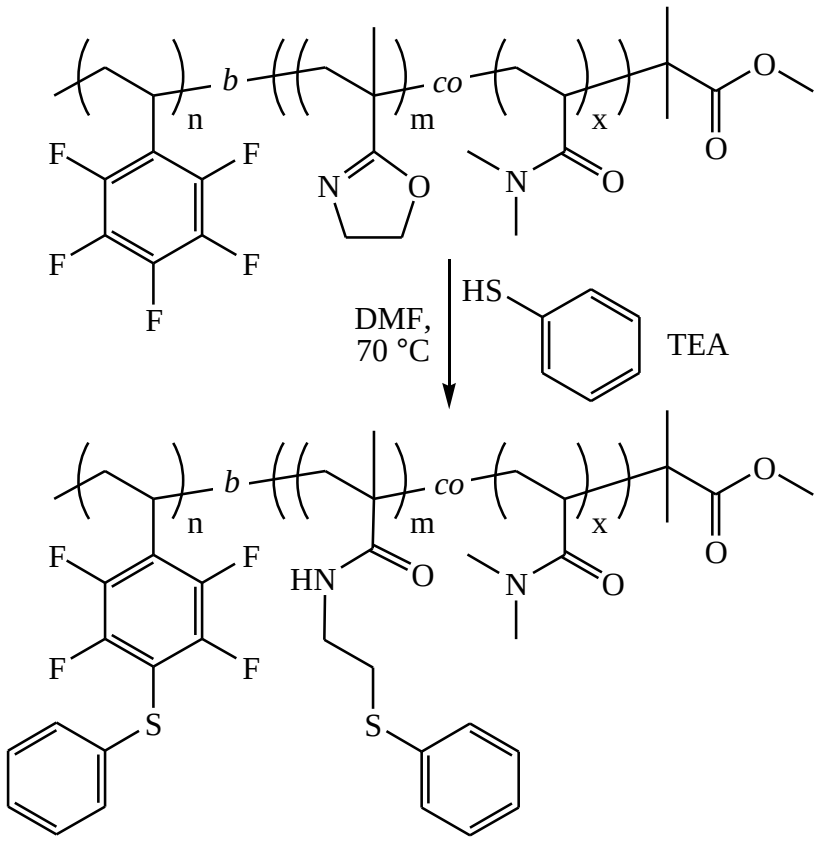

Scheme 5.13. *p*-Fluoro substitution and iPOx repeat unit ring opening of P[(PFS)-*b*-((iPOx)-*co*-(DMA))] (P5.23) with TP.

These conditions were utilised for the modification of P[(PFS)-*b*-((iPOx)-*co*-(DMA))] (P5.23) as they were effective for previous P(PFS) *p*-fluoro substitution with thiols (Section 5.2.3.1). Furthermore, Becer and co-workers have demonstrated these conditions as being effective for P(iPOx) ring opening with TP.[27]

Simultaneous modification of P[(PFS)-*b*-((iPOx)-*co*-(DMA))] was analysed utilising ^{1}H- and ^{19}F-NMR spectroscopy. ^{19}F-NMR spectroscopy demonstrates that *p*-fluoro substitution of the P(PFS) repeat units with TP proceeded to 100%, evidenced by the disappearance of P(PFS) *m*-fluoro and *p*-fluoro resonances at −161 and −154 ppm, respectively, as well as a new *m*-fluoro signal appearing at −133 ppm (Figure 5.25).

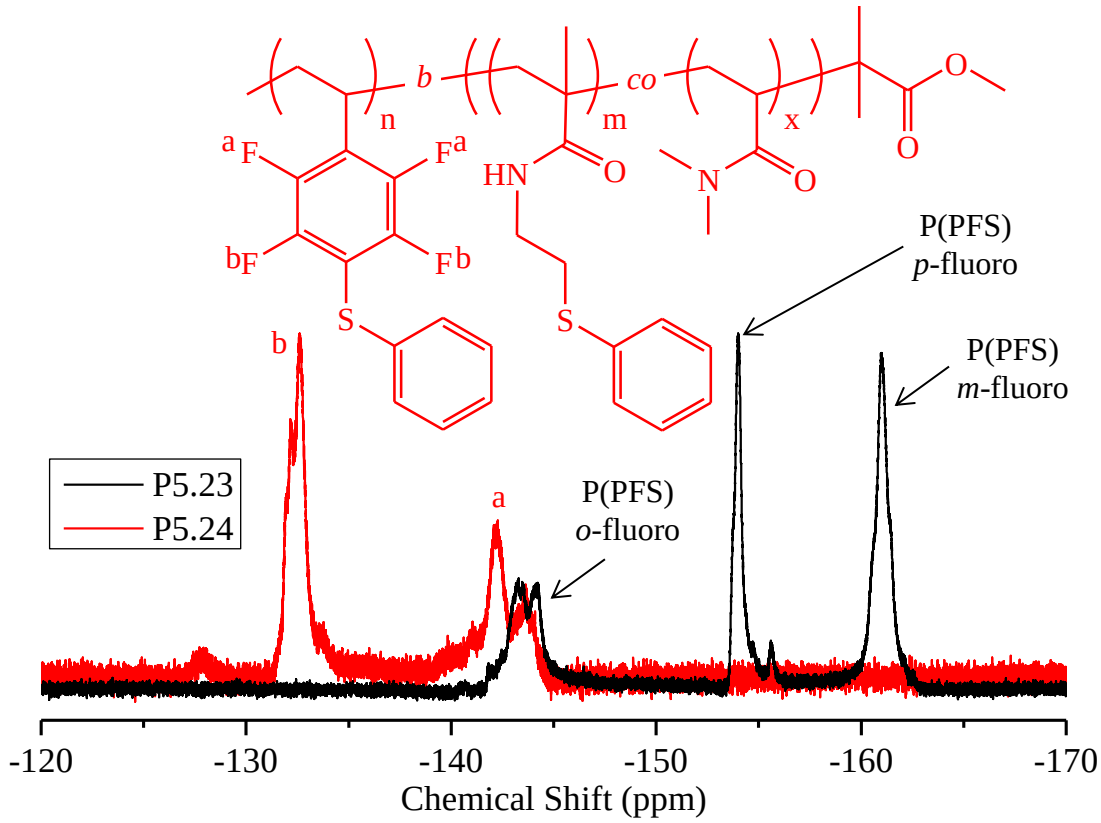

Figure 5.25. ^{19}F-NMR spectra ($CDCl_3$, 400 MHz, 303 K) of P[(PFS)-*b*-((iPOx)-*co*-(DMA))] (P5.23) before (black) and after functionalisation with TP (red, P5.24).

A large signal which is centred at 7.16 ppm is observable on the ^{1}H-NMR spectrum following modification of P[(PFS)-*b*-((iPOx)-*co*-(DMA))], this signal corresponds to the aromatic protons of the added TP functionality (Figure 5.26). However, residual

P(iPOx) repeat unit oxazoline protons are still observed at 3.61 and 4.06 ppm, implying that full conversion of P(iPOx) repeat units to the ring opened derivative was not obtained. Relative integration of residual P(iPOx) repeat unit signal at 4.06 ppm against the merged signal centred at ~1.95 ppm estimates that 52% of the P(iPOx) repeat units have been ring opened (Figure 5.26).

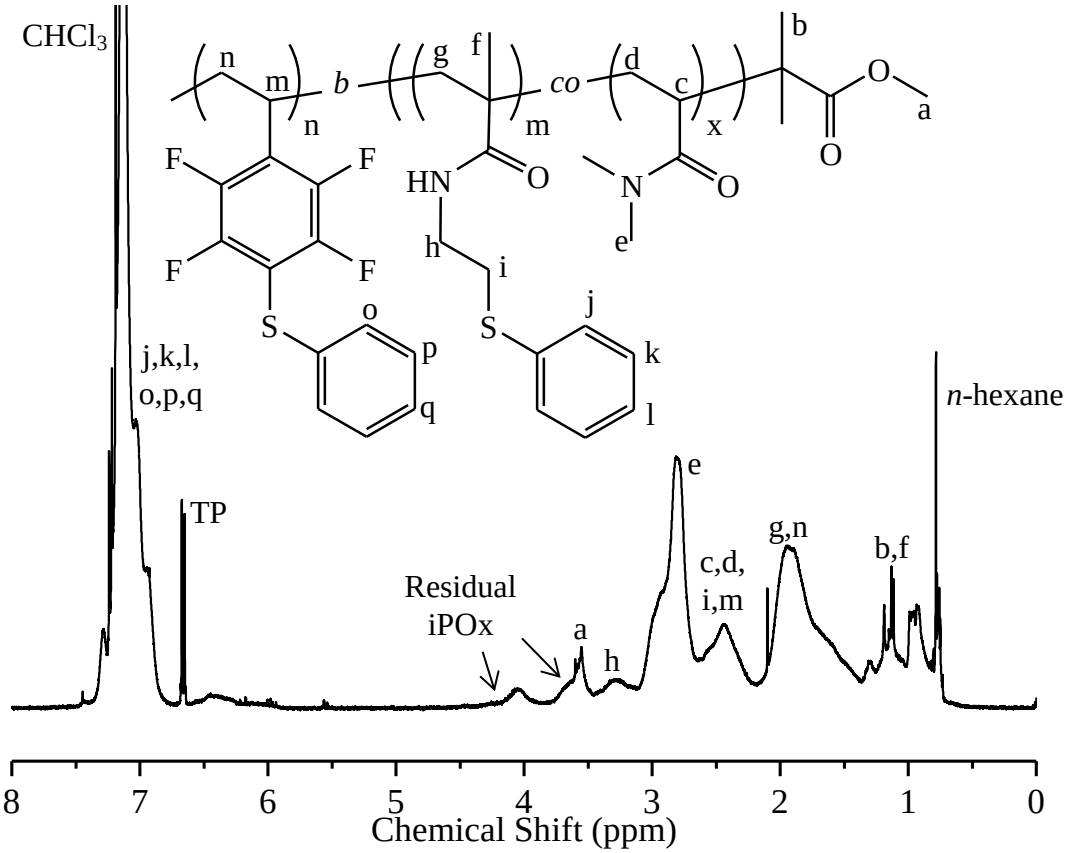

Figure 5.26. ^{1}H-NMR spectra ($CDCl_3$, 400 MHz, 303 K) of P[(PFS)-*b*-((iPOx)-*co*-(DMA))] after functionalisation with TP (P5.24).

Following modification of P[(PFS)-*b*-((iPOx)-*co*-(DMA))] (P5.23) with TP, M_n and M_w increased to 10000 and 11100 g·mol^{-1}, respectively, measured by GPC. Furthermore, final dispersity remained low (1.11) and the GPC trace of TP modified P[(PFS)-*b*-((iPOx)-*co*-(DMA))] shows a shift towards higher molecular weight as well slight formation of a high molecular weight shoulder (Figure 5.27).

Initial modifications of P[(PFS)-*b*-((iPOx)-*co*-(DMA))] with a thiol indicates that *p*-fluoro substitution remains an efficient modification but ring opening of the

P(iPOx) was less efficient and will require further optimisation before this block copolymer's versatility can be fully exploited.

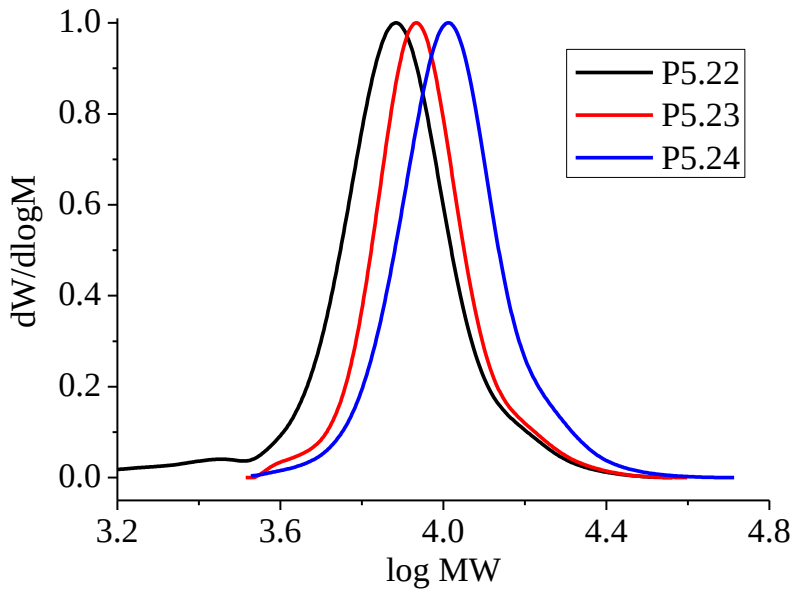

Figure 5.27. GPC traces (RID) of P[(PFS)-*b*-((iPOx)-*co*-(DMA))] with 100% (P5.22) and 24% (P5.23) trithiocarbonate end group and after functionalisation with TP (P5.24).

5.4. Conclusions

The synthetic scope of the already versatile PFS has been expanded upon. PFS was polymerised by RAFT polymerisation with high levels of control; synthesising P(PFS) at variable molecular weights, low dispersity (~1.1), with high PFS conversion (≥69%) and high end group fidelity which was demonstrated by ^{1}H-NMR spectroscopy and chain extensions.

P(PFS) was then utilised for post-polymerisation modification by substitution of the *p*-fluoro with thiols. Initial modifications gave poor results, GPC traces were multimodal and polymer dispersity was much greater than before. These poor GPC measurements following modification were attributed to the trithiocarbonate end group. It is suspected that trithiocarbonate end group may be cleaved by thiols or thiolate anions during modification to furnish a P(PFS) thiol which subsequently

substitutes a *p*-fluoro on the P(PFS) backbone and causes polymer branching. The trithiocarbonate end group was removed by radical induced addition and *p*-fluoro substitution with thiols was repeated. GPC traces were vastly improved when utilising P(PFS) without a trithiocarbonate end group; polymer dispersity remained low (~1.1) and only one very small high molecular weight shoulder was observed. *p*-Fluoro substitution was successful with thiols, a primary amine and sodium azide P(PFS). Multiple subsequent modifications; *p*-fluoro substitution with TP and sodium azide and cycloaddition between ATFS repeat units and PA, were performed on the same P(PFS) backbone to demonstrate the potential versatility of P(PFS).

Synthesis of P[(PFS)-*b*-(iPOx)] block copolymers was investigated. Initial attempts to homopolymerise iPOx by RAFT polymerisation, utilising three different RAFT agents and a P(PFS) macroRAFT agent, all resulted in poorly defined (co)polymers with low iPOx conversion. To overcome this issue P(PFS) was chain extended with a mixture of DMA and iPOx. This was an effective means of synthesising P[(PFS)-*b*-((iPOx)-*co*-(DMA))] block copolymers which could be tuned in composition of DMA to iPOx as well as block length. However, overall monomer conversion decreased as percentage of iPOx increased in the monomer feed.

Finally, post-polymerisation modification of P[(PFS)-*b*-((iPOx)-*co*-(DMA))] was attempted. Trithiocarbonate end group removal by radical induced addition was less efficient (76% removed) despite performing the procedure twice. Modification of P(PFS) repeat units by *p*-fluoro substitution with TP was highly efficient (100%) but oxazoline ring opening of P(iPOx) was less efficient even after 24 hours (52%). However, these initial experiments in conjunction with the novel azide substitution of P(PFS) and multi functionalisation indicate that these materials may be extremely

versatile and future research will focus on broadening the scope of P[(PFS)-*b*-((iPOx)-*co*-(DMA))] post-polymerisation modification.

5.5. Experimental

5.5.1. Instrumentation

5.5.1.1. Gel permeation chromatography

Molecular weight averages and polymer dispersity were determined by GPC. GPC samples were prepared to a concentration of 1mg·mL^{-1} and passed through 0.2 µm nylon filters before injection. GPC measurements were performed on an Agilent 1260 infinity system equipped with 2 PLgel 5 µm mixed-D columns (300 × 7.5 mm), a PLgel 5 mm guard column (50 × 7.5 mm), a RID and variable wavelength detector (VWD). Columns and RID were maintained at 50 °C. The system was eluted with DMF containing 5 mM ammonium tetrafluoroborate at a flow rate of 1 mL·min^{-1} and the RID was calibrated with linear narrow polystyrene and polymethyl methacrylate standards.

5.5.1.2. Nuclear magnetic resonance spectroscopy

^{1}H-NMR, ^{19}F-NMR and ^{13}C-NMR spectra were measured using a Bruker AV-400. Chemical shifts are reported in parts per million (ppm) and all spectra are referenced against the residual solvent peak found in the deuterated NMR solvent. Abbreviations used for peak multiplicity are as follows; s = singlet, d = doublet, t = triplet, q = quartet and m = multiplet.

5.5.1.3. Gas chromatography – flame ionisation detection

GC-FID was used to measure monomer conversions. GC-FID analysis was performed using an Agilent Technologies 7820A. An Agilent J&W HP-5 capillary

column of 30 m × 0.320 mm, film thickness 0.25 μm was used. The oven temperature was programmed as follows: 40 °C (hold for 1 minute) increase at 30 °C min^{-1} to 300 °C (hold for 2.5 minutes). The injector was operated at 250 °C and the FID was operated at 320 °C. Nitrogen was used as carrier gas at flow rate of 6.5 mL min^{-1} and a split ratio of 1:1 was applied. Chromatographic data was processed using OpenLab CDS ChemStation Edition, version C.01.05.

5.5.1.4. Fourier transform infrared spectroscopy

FT-IR spectra were recorded on a Bruker Vector-22 spectrometer using a Golden Gate diamond attenuated total reflection cell. All FT-IR spectra are plotted transmittance against wavenumbers (cm^{-1}).

5.5.2. Materials

Thiophenol (Aldrich, ≥99%), 2-mercaptoethanol (Aldrich, ≥99%), 1-butanethiol (Aldrich, 99%), hexylamine (Aldrich, 99%), sodium azide (Aldrich, ≥99.5%), propagyl alcohol (Aldrich, 99%), triethylamine (Aldrich, ≥99%), 4-cyano-4-[(dodecylsulfanylthiocarbonyl)sulfanyl] pentanoic acid (Aldrich, 97%), 4-cyano-4-(phenylcarbonothioylthio)pentanoic acid (Aldrich, >97%) were all used as received. Dimethyl-2,2′-azobis(isobutyrate) and 3-butyl-2-(dodecylthiocarbonothioylthio)-2-methylpropionate were provided by University of Warwick and used as received. Toluene, *n*-hexane, diethyl ether, *N*,*N*-dimethylformaide, tetrahydrofuran and methanol used were all HPLC grade and used as received.

N,*N*-dimethylacrylamide (Aldrich, 99%) and 2,3,4,5,6-pentafluorostyrene (Aldrich, 99%) were destabilised by passing through a short column of basic aluminium oxide prior to polymerisation. 2-Isopropenyl-2-oxazoline (Aldrich, ≥99%) was vacuum distilled over calcium hydride.

5.5.3. Procedures

5.5.3.1. RAFT homopolymerisation of PFS

PFS, BDTMP, V601 and toluene were charged into a Schlenk tube and degassed by gentle bubbling of Ar gas for 45 minutes. Schlenk tube was submerged into an oil bath at 70 °C. Schlenk tube removed after 70 hours. Reaction mixture was diluted with acetone and P(PFS) was precipitated into a large volume of methanol, filtered and dried overnight in vacuo. Product was a yellow solid.

Table 5.12 shows the quantities of all individual substances (PFS, BDTMP, V601 and toluene) used to synthesise P(PFS) samples (P5.01/02) by the procedure above.

^{1}H-NMR ($CDCl_3$, 400 MHz, 303 K): δ (ppm) 0.83-0.96 (m, (-$SCH_2CH_2(CH_2)_9C\underline{H}_3$ and -$COO\text{-}CH_2CH_2CH_2C\underline{H}_3$), 1.18-1.43 (m, -$SCH_2CH_2(C\underline{H}_2)_9CH_3$ and -$COO\text{-}CH_2CH_2C\underline{H}_2CH_3$), 1.44-1.57 (m, -$COO\text{-}CH_2C\underline{H}_2CH_2CH_3$ and –$C(C\underline{H}_3)_2$), 1.61-1.72 (m, -$SCH_2C\underline{H}_2(CH_2)_9CH_3$), 1.79-2.23 (s, -$C\underline{H}_2CH(C_6F_5)$-), 2.23-2.92 (m, -$CH_2C\underline{H}(C_6F_5)$-), 3.25-3.40 (t, J = 7.4 Hz, -$SC\underline{H}_2CH_2(CH_2)_9CH_3$), 3.63-3.77 (m, -$COOC\underline{H}_3$), 3.77-3.89 (m, -$COO\text{-}C\underline{H}_2CH_2CH_2CH_3$). ^{19}F-NMR ($CDCl_3$, 400 MHz, 303 K): δ (ppm) −162.78-−159.25 (m, -$CH_2CH(C_6\underline{F}_{5meta})$-), −155.50-−152.53 (m, -$CH_2CH(C_6\underline{F}_{5para})$-), −145.44-−141.48 (m, -$CH_2CH(C_6\underline{F}_{5ortho})$-).

Table 5.07. GPC characterisation and PFS conversions for P(PFS)s (P5.01 and P5.02) prepared by RAFT polymerisation.

Sample	PFS Conversion$^{\alpha}$ (%)	$M_{n.GPC}{}^{\beta}$ (g·mol^{-1})	$M_{w.GPC}{}^{\beta}$ (g·mol^{-1})	$M_{n.Theo}{}^{\gamma}$ (g·mol^{-1})	$Đ^{\beta}$
P5.01	85	4400	4800	4500	1.10
P5.02	69	4700	5100	4400	1.08

$^{\alpha}$Calculated from GC-FID. $^{\beta}$DMF + 5 mM NH_4BF_4 eluent, calibrated with PS standards. $^{\gamma}$Calculated from Equation 1.

5.5.3.2. P(PFS) end group removal via radical induced addition

P(PFS) (P5.02, 1 g, 0.227 mmol, 1 eq.), V601 (1.04 g, 4.52 mmol, 20 eq.) and toluene (10 mL) were charged into a Schlenk tube and degassed by gentle bubbling with Ar gas for 45 minutes. Schlenk tube was submerged into an oil bath at 80 °C for 4 hours. P(PFS) (P5.05) was precipitated in methanol. P(PFS) (P5.05) was filtered, dissolved in acetone and precipitated again into methanol before filtering and drying in vacuo. Product was a white powder. ^{1}H-NMR ($CDCl_3$, 400 MHz, 303 K): δ (ppm) 0.87-0.95 (t, J = 7.4 Hz, -COO-$CH_2CH_2CH_2C\underline{H}_3$), 1.23-1.39 (m, -COO-$CH_2CH_2C\underline{H}_2CH_3$), 1.42-1.61 (m, -COO-$CH_2C\underline{H}_2CH_2CH_3$ and –$C(C\underline{H}_3)_2$), 1.78-2.22 (s, -$C\underline{H}_2CH(C_6F_5)$-), 2.22-2.88 (m, -$CH_2C\underline{H}(C_6F_5)$-), 3.55-3.77 (m, -$COOC\underline{H}_3$), 3.77-3.89 (m, -COO-$C\underline{H}_2CH_2CH_2CH_3$). ^{19}F-NMR ($CDCl_3$, 400 MHz, 303 K): δ (ppm) −162.21-−159.79 (m, -$CH_2CH(C_6\underline{F}_{5meta})$-), −155.20-−153.22 (m, -$CH_2CH(C_6\underline{F}_{5para})$-), −145.22-−141.02 (m, -$CH_2CH(C_6\underline{F}_{5ortho})$-). FT-IR (neat): ($cm^{-1}$) 1731 (w), 1653 (w), 1522 (s), 1495 (s), 1460 (m), 1366 (w), 1304 (w), 1131 (m), 1083 (m), 981 (s), 959 (s), 867 (m), 507 (m). GPC: M_n 5400 g·mol^{-1}, M_w 5700 g·mol^{-1}, $Đ$ 1.05.

5.5.3.3. Substitution of P(PFS) *p*-fluoro with thiols

P(PFS) (P5.02 or P5.05), TEA and the selected thiol (TP, BT or ME) were dissolved in DMF and heated at 60 °C for 1 hour in an oil bath. Products were precipitated in methanol and filtered before drying overnight in vacuo.

Table 5.13 shows the quantities of all individual substances (P(PFS), TEA, selected thiol and DMF) used to functionalise P(PFS) by the procedure detailed above.

^{1}H-NMR ($CDCl_3$, 400 MHz, 303 K): δ (ppm) P2.06: 1.77-2.28 (s, -$C\underline{H}_2CH(C_6F_5)$- and -$C\underline{H}_2CH(C_6F_4S(C_6H_5))$-), 2.28-2.95 (m, -$CH_2C\underline{H}(C_6F_5)$- and

-$CH_2C\underline{H}(C_6F_4S(C_6H_5))$-), 6.90-7.54 (s, -$CH_2CH(C_6F_4S(C_6\underline{H}_5))$-). P2.07: 0.86-0.98 (m, -$SCH_2CH_2CH_2C\underline{H}_3$), 1.37-1.64 (m, -$SCH_2C\underline{H}_2C\underline{H}_2CH_3$), 1.77-2.21 (-$C\underline{H}_2CH(C_6F_5)$- and -$C\underline{H}_2CH(C_6F_4S(C_4H_9))$-), 2.21-3.20 (m, -$CH_2C\underline{H}(C_6F_5)$- and -$CH_2C\underline{H}(C_6F_4S(C_4H_9))$- and -$SC\underline{H}_2CH_2CH_2CH_3$).

Table 5.08. GPC characterisation for P(PFS) functionalised via *p*-fluoro substitution with thiols.

Sample	$M_{n.GPC}^{\alpha}$ (g·mol^{-1})	$M_{w.GPC}^{\alpha}$ (g·mol^{-1})	$Đ^{\alpha}$
P5.03	8600	11700	1.36
P5.04	23500	36600	1.56
P5.06	7000	7600	1.09
P5.07	4500	4900	1.09

$^{\alpha}$DMF + 5 mM NH_4BF_4 eluent, calibrated with PS standards.

5.5.3.4. Substitution of P(PFS) *p*-fluoro with hexylamine

P(PFS) (P5.05, 50 mg, 0.258 mmol, 1 eq.) and hexylamine (71 µL, 0.537 mmol, 2.1 eq.) were dissolved in DMF (0.6 mL) and heated at 95 °C for 1 hour in the microwave synthesiser. Product was precipitated in distilled water and filtered before drying overnight in vacuo. ^{1}H-NMR ($CDCl_3$, 400 MHz, 303 K): δ (ppm) 0.82-0.97 (m, -$NHCH_2CH_2(CH_2)_3C\underline{H}_3$), 1.22-1.46 (m, -$NHCH_2CH_2(C\underline{H}_2)_3CH_3$), 1.46-1.67 (m, -$NHCH_2C\underline{H}_2(CH_2)_3CH_3$), 1.67-2.16 (s, -$C\underline{H}_2CH(C_6F_5)$- and -$C\underline{H}_2CH(C_6F_4NHC_6H_{13})$-), 2.16-2.80 (m, -$CH_2C\underline{H}(C_6F_5)$- and -$CH_2C\underline{H}(C_6F_4NHC_6H_{13})$-), 3.19-3.42 (s, -$NHC\underline{H}_2CH_2(CH_2)_3CH_3$), 3.42-3.85 (m, -$N\underline{H}CH_2CH_2(CH_2)_3CH_3$). GPC: M_n 7300 g·mol^{-1}, M_w 7800 g·mol^{-1}, $Đ$ 1.07.

5.5.3.5. Substitution of P(PFS) *p*-fluoro with sodium azide

P(PFS) (P5.05) was dissolved in DMF before the addition of sodium azide. The suspension was stirred at 70 °C for 4 hours. After cooling to room temperature the

reaction mixture was diluted with diethyl ether (50 mL) and extracted with distilled water (10 x 10 mL). Organic layer was dried over magnesium sulfate and filtered before removing all diethyl ether in vacuo.

Table 5.14 shows the quantities of all individual substances (P(PFS), sodium azide and DMF) used to synthesis P[(PFS)-*co*-(ATFS)] samples (P5.09/10) by the procedure detailed above.

^{1}H-NMR ($CDCl_3$, 400 MHz, 303 K): δ (ppm) 1.66-2.15 (s, -C$\underline{H}_2$CH(C_6F_5)- and -C$\underline{H}_2$CH($C_6F_4N_3$)-), 2.21-2.85 (m, -CH_2C$\underline{H}$(C_6F_5)- and -CH_2C$\underline{H}$($C_6F_4N_3$)-). ^{19}F-NMR ($CDCl_3$, 400 MHz, 303 K): δ (ppm) −162.85-−159.91 (m, -CH_2CH($C_6\underline{F}_{5meta}$)-), −155.24-−153.31 (m, -CH_2CH($C_6\underline{F}_{5para}$)-), −153.00-−150.23 (m, -CH_2CH($C_6\underline{F}_{4meta}N_3$)-),−145.37-−141.11 (m, -CH_2CH($C_6\underline{F}_{5ortho}$)- and -$CH_2$CH($C_6\underline{F}_{4ortho}N_3$)-). FT-IR (neat): ($cm^{-1}$) 2123 (s), 1731 (w), 1650 (w), 1522 (m), 1487 (s), 1459 (m), 1365 (w), 1303 (w), 1230 (m), 1123 (w), 961 (s), 864 (m), 786 (w), 738 (w), 671 (w), 504 (m).

Table 5.09. GPC characterisation for P[(PFS)-*co*-(ATFS)] samples (P5.09 and P5.10) prepared by functionalisation of P(PFS) (P5.05) with sodium azide.

Sample	$M_{n.GPC}^{\alpha}$ (g·mol^{-1})	$M_{w.GPC}^{\alpha}$ (g·mol^{-1})	$Đ^{\alpha}$
P5.09	5700	6200	1.10
P5.10	5500	6000	1.11

$^{\alpha}$DMF + 5 mM NH_4BF_4 eluent, calibrated with PS standards.

5.5.3.6. Synthesis of ATFS

PFS (2.5 g, 12.9 mmol, 1 eq.), sodium azide (1.67 g, 25.7 mmol, 2 eq.) and DMF (20 mL) were added to a flask and the resulting suspension was stirred at 70 °C for 3 hours in an oil bath. After cooling to room temperature the reaction mixture was

diluted with diethyl ether (100 mL) and extracted with distilled water (5 × 100 mL). Organic layer was dried over magnesium sulfate and filtered before removing all diethyl ether in vacuo. ^{1}H-NMR ($CDCl_3$, 400 MHz, 303 K): δ (ppm) 5.59 (d, *J* = 11.9 Hz, C$\underline{H}_{cis}H_{trans}$=CH($C_6F_4N_3$)), 5.96 (d, *J* = 18.0 Hz, $CH_{cis}\underline{H}_{trans}$=CH($C_6F_4N_3$)), 6.54 (dd, *J* = 11.9, 18.0 Hz, CH_2=C$\underline{H}$($C_6F_4N_3$)). ^{19}F-NMR ($CDCl_3$, 400 MHz, 303 K): δ (ppm) −153.24 (dd, *J* = 9.9, 20.10 Hz, CH_2=CH($C_6\underline{F}_{4meta}N_3$)), −143.83 (dd, *J* = 9.9, 20.10 Hz, CH_2=CH($C_6\underline{F}_{4ortho}N_3$)). FT-IR (neat): ($cm^{-1}$) 2112 (s), 1645 (w), 1481 (s), 1428 (m), 1408 (m), 1310 (w), 1233 (s), 1104 (w), 1024 (w), 974 (s), 933 (m), 904 (m), 795 (w), 669 (w), 519 (m).

5.5.3.7. Multifunctionalisation of P(PFS)

P(PFS) (P5.05, 56.7 mg, 0.292 mmol, 1 eq.), TEA (24 µL, 0.172 mmol, 0.6 eq.) and TP (15 µL, 0.146 mmol, 0.5 eq.) were dissolved in DMF (1 mL) and stirred at 70 °C for 1 hour in an oil bath. Product (P5.11) was twice precipitated in methanol and filtered before drying overnight in vacuo. ^{1}H-NMR ($CDCl_3$, 400 MHz, 303 K): δ (ppm) 1.76-2.22 (s, -C$\underline{H}_2$CH(C_6F_5)- and -C$\underline{H}_2$CH($C_6F_4S(C_6H_5)$)-), 2.22-2.92 (m, -CH_2C$\underline{H}$(C_6F_5)- and -CH_2C$\underline{H}$($C_6F_4S(C_6H_5)$)-), 7.06-7.38 (s, -CH_2CH($C_6F_4S(C_6\underline{H}_5)$)-). ^{19}F-NMR ($CDCl_3$, 400 MHz, 303 K): δ (ppm) −162.10-−160.15 (m, -CH_2CH($C_6\underline{F}_{5meta}$)-), −155.07-−153.12 (m, -CH_2CH($C_6\underline{F}_{5para}$)-), −145.27-−139.88 (m, -CH_2CH($C_6\underline{F}_{5ortho}$)- and -$CH_2$CH($C_6\underline{F}_{4ortho}S(C_6H_5)$)-),−134.45-−130.71 (m, -CH_2CH($C_6\underline{F}_{4meta}S(C_6H_5)$)-). FT-IR (neat): ($cm^{-1}$) 1729 (w), 1653 (w), 1583 (w), 1521 (m), 1499 (s), 1472 (s), 1456 (s), 1364 (w), 1302 (w), 1257 (w), 1122 (w), 1069 (w), 1024 (w), 979 (m), 948 (s), 866 (w), 823 (m), 737 (m), 687 (m), 517 (m). GPC: M_n 6000 g·mol^{-1}, M_w 6500 g·mol^{-1}, *Đ* 1.08.

P5.11 (40 mg, 0.0645 mmol of P(PFS) repeat units, 1 eq.) was dissolved in DMF (1 mL) before the addition of sodium azide (12.6 mg, 0.194 mmol, 3 eq.) The resulting

suspension was stirred at 70 °C for 12 hours. After cooling to room temperature the reaction mixture was diluted with diethyl ether (50 mL) and extracted with distilled water (10 x 10 mL). Organic layer was dried over magnesium sulfate and filtered before removing all diethyl ether in vacuo to give the product (P5.12). ^{1}H-NMR ($CDCl_3$, 400 MHz, 303 K): δ (ppm) 1.73-2.21 (s, -C<u>H</u>$_2$CH($C_6F_4N_3$)- and -C<u>H</u>$_2$CH($C_6F_4S(C_6H_5)$)-), 2.21-2.98 (m, -CH$_2$C<u>H</u>($C_6F_4N_3$)- and -CH$_2$C<u>H</u>($C_6F_4S(C_6H_5)$)-), 7.02-7.40 (s, -CH$_2$CH($C_6F_4S(C_6$<u>H</u>$_5)$)-). ^{19}F-NMR ($CDCl_3$, 400 MHz, 303 K): δ (ppm) −152.51-−150.47 (m, -CH$_2$CH(C_6<u>F</u>$_{4meta}N_3$)-), −145.18-−139.48 (m, -CH$_2$CH(C_6<u>F</u>$_{4ortho}N_3$)- and -CH$_2$CH(C_6<u>F</u>$_{4ortho}S(C_6H_5)$)-), −134.77-−131.21 (m, -CH$_2$CH(C_6<u>F</u>$_{4meta}S(C_6H_5)$)-). FT-IR (neat): (cm^{-1}) 2360 (m), 2123 (m), 1717 (w), 1648 (w), 1522 (w), 1489 (s), 1473 (s), 1458 (s), 1260 (m), 1229 (m), 1023 (m), 948 (s), 861 (w), 822 (m), 737 (s), 687 (s), 518 (s). GPC: M_n 6100 $g \cdot mol^{-1}$, M_w 6600 $g \cdot mol^{-1}$, $Đ$ 1.08.

P5.12 (27 mg, 0.0429 mmol of P(ATFS) repeat units, 1 eq.) and PA (8 μL, 0.129 mmol, 3 eq.) were dissolved in DMF (1 mL) and stirred at 100 °C for 24 hours. After cooling to room temperature the reaction mixture was diluted with diethyl ether (50 mL) and extracted with distilled water (10 x 10 mL). Organic layer was dried over magnesium sulfate and filtered before removing all diethyl ether in vacuo to give the product (P5.13). ^{1}H-NMR ($CDCl_3$, 400 MHz, 303 K): δ (ppm) 1.80-3.35 (m, -C<u>H</u>$_2$CH($C_6F_4S(C_6H_5)$)-, -C<u>H</u>$_2$CH($C_6F_4(C_2N_3HCH_2OH)$)-, -CH$_2$C<u>H</u>($C_6F_4S(C_6H_5)$)-, -CH$_2$C<u>H</u>($C_6F_4(C_2N_3HCH_2OH)$)-), 4.36-5.00 (m, -CH$_2$CH($C_6F_4(C_2N_3HC$<u>H</u>$_2OH)$)-), 6.88-7.46 (s, -CH$_2$CH($C_6F_4S(C_6$<u>H</u>$_5)$)-), 7.57-8.24 (m, -CH$_2$CH($C_6F_4(C_2N_3$<u>H</u>$CH_2OH)$)-). ^{19}F-NMR ($CDCl_3$, 400 MHz, 303 K): δ (ppm) −147.76-−137.95 (m, -CH$_2$CH(C_6<u>F</u>$_{4ortho}S(C_6H_5)$)-, -CH$_2$CH(C_6<u>F</u>$_{4ortho}(C_2N_3HCH_2OH)$)-, -CH$_2$CH(C_6<u>F</u>$_{4meta}(C_2N_3HCH_2OH)$)-), −134.55-

−130.52 (m, -$CH_2CH(C_6\underline{F}_{4meta}S(C_6H_5))$-). FT-IR (neat): ($cm^{-1}$) 3348 (w, br), 1582 (w), 1520 (w), 1495 (m), 1473 (s), 1456 (m), 1259 (m), 1023 (m), 949 (s), 817 (s), 738 (s), 686 (s), 517 (m). GPC: M_n 9600 $g \cdot mol^{-1}$, M_w 11900 $g \cdot mol^{-1}$, $Đ$ 1.25.

5.5.3.8. RAFT homopolymerisation of iPOx

iPOx, RAFT agent, V601 and toluene were charged into a Schlenk tube and degassed by gentle bubbling of Ar gas for 30 minutes. Schlenk tube was submerged into an oil bath at 70 °C. Schlenk tube removed after 24 hours and placed into liquid N_2 to terminate polymerisation. Reaction mixture was diluted with acetone and P(iPOx) was precipitated into a large volume of diethyl ether, filtered and dried overnight in vacuo.

Table 5.15 shows the quantities of all individual substances (iPOx, RAFT agent, V601 and toluene) used to synthesise P(iPOx) samples (P5.14-16) by the procedure detailed above.

^{1}H-NMR ($CDCl_3$, 400 MHz, 303 K): δ (ppm) 0.91-1.64 (m, -$CH_2C(C\underline{H}_3)$-), 1.64-2.52 (m, -$C\underline{H}_2C(CH_3)$-), 3.60-3.87 (s, -$COC\underline{H}_2$-), 4.02-4.29 (s, -$C{=}NC\underline{H}_2$-).

Table 5.10. GPC characterisation and iPOx conversion for P(iPOx) samples (P5.14-16) prepared by RAFT polymerisation.

Sample	iPOx Conversion$^{\alpha}$ (%)	$M_{n.GPC}{}^{\beta}$ ($g \cdot mol^{-1}$)	$M_{w.GPC}{}^{\beta}$ ($g \cdot mol^{-1}$)	$M_{n.Theo}{}^{\gamma}$ ($g \cdot mol^{-1}$)	$Đ^{\beta}$
P5.14	32	7300	13500	2200	1.84
P5.15	37	2900	5100	2500	1.76
P5.16	31	2800	4000	2100	1.40

$^{\alpha}$Calculated from GC-FID. $^{\beta}$DMF + 5 mM NH_4BF_4 eluent, calibrated with PS standards. $^{\gamma}$Calculated from Equation 1.

5.5.3.9. Chain extension of P(PFS) with iPOx

P(PFS) (P5.01, 0.200 g, 0.0455 mmol, 1 eq.), iPOx (0.5 mL, 4.77 mmol, 100 eq.), V601 (0.0022 g, 0.00955 mmol, 0.2 eq.) and toluene (1 mL) were charged into a Schlenk tube and degassed by gentle bubbling of Ar gas for 15 minutes. Schlenk tube was submerged into an oil bath at 70 °C. Schlenk tube removed after 24 hours and placed into liquid N_2 to terminate polymerisation. GPC: M_n 3800 g·mol^{-1}, M_w 14700 g·mol^{-1}, $Đ$ 3.85.

5.5.3.10. Chain extension of P(PFS) with iPOx and DMA

P(PFS), iPOx, DMA, V601 and toluene were charged into a Schlenk tube and degassed by gentle bubbling of Ar gas for 30 minutes. Schlenk tube was submerged into an oil bath at 70 °C. Schlenk tube removed after 24 hours and placed into liquid N_2 to terminate polymerisation. Reaction mixture was diluted with acetone and P[(PFS)-*b*-((iPOx)-*co*-(DMA))] was twice precipitated into a large volume of *n*-hexane, filtered and dried overnight in vacuo.

Table 5.16 shows the quantities of all individual substances (P(PFS), iPOx, DMA, V601 and toluene) used to synthesise P[(PFS)-*b*-((iPOx)-*co*-(DMA))] samples (P5.18-21) by the procedure detailed above.

^{1}H-NMR ($CDCl_3$, 400 MHz, 303 K): δ (ppm) 1.18-2.15 (m, -C$\underline{H}_2$C(C$\underline{H}_3$)- and -C$\underline{H}_2$CH(C_6F_5)-), 2.22-3.20 (m, -CH$_2$C$\underline{H}$(C_6F_5)- and -C$\underline{H}_2$C$\underline{H}$(CON(C$\underline{H}_3$)$_2$)-), 3.49-3.93 (m, -COC$\underline{H}_2$-), 3.97-4.50 (s, -C=NC$\underline{H}_2$-). ^{19}F-NMR ($CDCl_3$, 400 MHz, 303 K): δ (ppm) −162.79-−159.46 (m, -CH$_2$CH($C_6\underline{F}_{5meta}$)-), −155.16-−153.19 (m, -CH$_2$CH($C_6\underline{F}_{5para}$)-), −146.09-−141.43 (m, -CH$_2$CH($C_6\underline{F}_{5ortho}$)-).

Table 5.11. GPC characterisation and monomer conversions for P[(PFS)-*b*-((iPOx)-*co*-(DMA))] samples (P5.18-22) prepared by chain extension of P(PFS).

Sample	iPOx;DMA Conversion$^{\alpha}$ (%)	$M_{n.GPC}{}^{\beta}$ (g·mol^{-1})	$M_{w.GPC}{}^{\beta}$ (g·mol^{-1})	$Đ^{\beta}$
P5.18	>99;>99	10000	11000	1.10
P5.19	>99;>99	22900	26600	1.16
P5.20	80;54	8300	9100	1.11
P5.21	59;37	7000	7800	1.12
P5.22	66;38	7000	8200	1.19

$^{\alpha}$Calculated from GC-FID. $^{\beta}$DMF + 5 mM NH_4BF_4 eluent, calibrated with PS standards.

5.5.3.11. P[(PFS)-*b*-((iPOx)-*co*-(DMA))] end group removal via radical induced addition

P[(PFS)-*b*-((iPOx)-*co*-(DMA))] (P5.22, 0.786 g, 0.112 mmol, 1 eq.), V601 (0.518 g, 2.25 mmol, 20 eq.) and toluene (10 mL) were charged into a Schlenk tube and degassed by gentle bubbling with Ar gas for 45 minutes. Schlenk tube was submerged into an oil bath at 80 °C for 4 hours. Partially end group removed P[(PFS)-*b*-((iPOx)-*co*-(DMA))] was precipitated in *n*-hexane, filtered and dried in vacuo. Partially end group removed P[(PFS)-*b*-((iPOx)-*co*-(DMA))] (0.529 g, 0.0756 mmol, 1 eq.), V601 (0.347 g, 1.51 mmol, 20 eq.) and toluene (10 mL) were charged into a Schlenk tube and degassed by gentle bubbling with Ar gas for 45 minutes. Schlenk tube was submerged into an oil bath at 80 °C for 4 hours. P[(PFS)-*b*-((iPOx)-*co*-(DMA))] (P5.23) was twice precipitated in *n*-hexane, filtered and dried in vacuo. Product was a white powder. ^{1}H-NMR ($CDCl_3$, 400 MHz, 303 K): δ (ppm) 0.84-2.20 (m, -C$\underline{H}_2$C(C$\underline{H}_3$)- and -C$\underline{H}_2$CH(C_6F_5)- and -C(C$\underline{H}_3$)$_2$COOCH_3), 2.20-3.22 (m, -CH$_2$C$\underline{H}$(C_6F_5)- and -C$\underline{H}_2$C$\underline{H}$(CON(C$\underline{H}_3$)$_2$)-), 3.47-3.93 (m, -COC$\underline{H}_2$- and -C(CH$_3$)$_2$COOC$\underline{H}_3$), 3.93-4.55 (s, -C=NC$\underline{H}_2$-). ^{19}F-NMR ($CDCl_3$, 400 MHz, 303 K):

δ (ppm) −162.39-−159.39 (m, -$CH_2CH(C_6\underline{F}_{5meta})$-), −155.39-−153.38 (m, -$CH_2CH(C_6\underline{F}_{5para})$-), −145.55-−141.53 (m, -$CH_2CH(C_6\underline{F}_{5ortho})$-). GPC: M_n 8600 g·mol^{-1}, M_w 9400 g·mol^{-1}, $Đ$ 1.09.

5.5.3.12. Substitution of P[(PFS)-*b*-((iPOx)-*co*-(DMA))] *p*-fluoro and ring opening of iPOx repeat units with TP

P[(PFS)-*b*-((iPOx)-*co*-(DMA))] (P5.23, 0.101 g, 0.411 mmol, 1 eq. of P(PFS) repeat units and 0.0699 mmol, 0.17 eq. of P(iPOx) repeat units) was dissolved in DMF (3 mL) before addition of TEA (63 µL, 0.452 mmol, 1.1 eq.) and TP (99 µL, 0.962 mmol, 2.34 eq.). Mixture was heating at 70 °C for 24 hours before the product was precipitated in methanol, filtered and dried in vacuo. Product was dissolved in acetone and precipitated in *n*-hexane, filtered and dried in vacuo. ^{1}H-NMR ($CDCl_3$, 400 MHz, 303 K): δ (ppm) 0.78-2.26 (m, -$C\underline{H}_2C(C\underline{H}_3)$- and -$C\underline{H}_2CH(C_6F_5)$- and -$C(C\underline{H}_3)_2COOCH_3$), 2.26-3.19 (m, -$CH_2C\underline{H}(C_6F_5)$- and -$C\underline{H}_2C\underline{H}(CON(C\underline{H}_3)_2)$- and -$CH_2C\underline{H}_2S(C_6H_5)$), 3.19-3.92 (m, -$C\underline{H}_2CH_2S(C_6H_5)$ -$COC\underline{H}_2$- and -$C(CH_3)_2COOC\underline{H}_3$), 3.92-4.45 (s, -C=N$C\underline{H}_2$-), 6.80-7.47 (m, -$CH_2CH_2S(C_6\underline{H}_5)$). ^{19}F-NMR ($CDCl_3$, 400 MHz, 303 K): δ (ppm) −144.75-−139.10 (m, -$CH_2CH(C_6\underline{F}_{4ortho}S(C_6H_5))$-),−134.49-−131.21 (m, -$CH_2CH(C_6\underline{F}_{4meta}S(C_6H_5))$-). GPC: M_n 10000 g·mol^{-1}, M_w 11100 g·mol^{-1}, $Đ$ 1.11.

Table 5.12. PFS, BDTMP, V601 and toluene quantities used to prepare P(PFS) samples P5.01/02 by RAFT polymerisation.

Sample	PFS			BDTMP			V601			Toluene
	(g)	(mmol)	(eq.)	(g)	(mmol)	(eq.)	(mg)	(mmol)	(eq.)	(mL)
P5.01	6	31.0	25	0.521	1.24	1	28	0.124	0.1	6
P5.02	5	25.8	30	0.361	0.858	1	20	0.0869	0.1	5

Table 5.13. P(PFS), thiol, TEA and DMF quantities used to prepare functional polymers (P5.03/04 and P5.06/07) by modification of P(PFS).

Sample	P(PFS)			Thiol			TEA			DMF
	(mg)	(mmol)	(eq.)	(µL)	(mmol)	(eq.)	(µL)	(mmol)	(eq.)	(mL)
P5.03	P5.02 100	 0.515	 1	TP 53	 0.516	 1	72	0.517	1	1
P5.04	P5.02 50	 0.258	 1	ME 18	 0.257	 1	39	0.280	1.1	1
P5.06	P5.05 50	 0.258	 1	TP 29	 0.282	 1.1	43	0.309	1.2	0.5
P5.07	P5.05 50	 0.258	 1	BT 30	 0.280	 1.1	43	0.309	1.2	0.5

Table 5.14. P(PFS), sodium azide and DMF quantities used to prepare functional polymers (P5.09/10) by modification of P(PFS).

Sample	P(PFS)			NaN_3			DMF
	(mg)	(mmol)	(eq.)	(mg)	(mmol)	(eq.)	(mL)
P5.09	P5.05			33	0.508	0.5	5
	199	1.03	1				
P5.10	P5.05			33	0.508	2	1
	50	0.258	1				

Table 5.15. iPOx, RAFT agent, V601 and toluene quantities used to prepare P(iPOx) samples P5.14-16 by RAFT polymerisation.

Sample	iPOx			RAFT agent			V601			Toluene
	(mL)	(mmol)	(eq.)	(g)	(mmol)	(eq.)	(mg)	(mmol)	(eq.)	(mL)
P5.14	0.5	4.77	50	BDTMP			0.0022	0.00955	0.1	1
				0.0401	0.0953	1				
P5.15	0.5	4.77	50	CDSP			0.0022	0.00955	0.1	1
				0.0385	0.0953	1				
P5.16	0.5	4.77	50	CPPA			0.0022	0.00955	0.1	1
				0.0266	0.0953	1				

Table 5.16. iPOx, DMA, P(PFS), V601 and toluene quantities used to prepare P[(PFS)-*b*-((iPOx)-*co*-(DMA))] samples by chain extension of P(PFS).

Sample	iPOx			DMA			P(PFS)			V601			Toluene
	(µL)	(mmol)	(eq.)	(mL)	(mmol)	(eq.)	(g)	(mmol)	(eq.)	(mg)	(mmol)	(eq.)	(mL)
P5.18	13	0.123	1.25	0.24	2.33	23.75	P5.01 0.436	0.0991	1	2.3	0.00999	0.1	1.4
P5.19	27	0.258	5	0.5	4.85	95	P5.01 0.225	0.0511	1	1.2	0.00521	0.1	1.5
P5.20	17	0.162	2.5	0.15	1.46	22.5	P5.01 0.285	0.0648	1	1.5	0.00651	0.1	0.9
P5.21	51	0.486	6.25	0.15	1.46	18.75	P5.01 0.342	0.0777	1	1.8	0.00782	0.1	1.1
P5.22	125	1.19	6.25	0.37	3.59	18.75	P5.02 0.899	0.191	1	4.4	0.0191	0.1	2.8

5.6. References

1. K. Jankova and S. Hvilsted, *Macromolecules*, 2003, **36**, 1753.
2. G. D. Fu, S. J. Phua, E. T. Kang and K. G. Neoh, *Macromolecules*, 2005, **38**, 2612.
3. J.-P. O'Shea, V. Solovyeva, X. Guo, J. Zhao, N. Hadjichristidis and V. O. Rodionov, *Polym. Chem.*, 2014, **5**, 698.
4. C. R. Becer, K. Babiuch, D. Pilz, S. Hornig, T. Heinze, M. Gottschaldt and U. S. Schubert, *Macromolecules*, 2009, **42**, 2387.
5. E. L. Malins, S. Amabilino, G. Yilmaz, F. H. Isikgor, B. M. Gridley and C. R. Becer, *Eur. Polym. J.*, 2015, **62**, 347.
6. C. Ott, R. Hoogenboom and U. S. Schubert, *Chem. Commun.*, 2008, 3516.
7. C. S. Gudipati, M. B. H. Tan, H. Hussain, Y. Liu, C. He and T. P. Davis, *Macromol. Rapid Commun.*, 2008, **29**, 1902.
8. B. H. Tan, C. S. Gudipati, H. Hussain, C. He, Y. Liu and T. P. Davis, *Macromol. Rapid Commun.*, 2009, **30**, 1002.
9. M. Riedel, J. Stadermann, H. Komber, F. Simon and B. Voit, *Eur. Polym. J.*, 2011, **47**, 675.
10. S. Suzuki, M. R. Whittaker, E. Wentrup-Byrne, M. J. Monteiro and L. Grondahl, *Langmuir*, 2008, **24**, 13075.
11. C. R. Becer, K. Kokado, C. Weber, A. Can, Y. Chujo and U. S. Schubert, *J. Polym. Sci. Part A: Polym. Chem.*, 2010, **48**, 1278.
12. A. M. Nyström, J. W. Bartels, W. Du and K. L. Wooley, *J. Polym. Sci. Part A: Polym. Chem.*, 2009, **47**, 1023.
13. N. T. Brummelhuis and M. Weck, *J. Polym. Sci. Part A: Polym. Chem.*, 2014, **52**, 1555.

14. J. Lu, N. T. Brummelhuis and M. Weck, *Chem. Commun.*, 2014, **50**, 6225.
15. K. Jankova and S. Hvilsted, *J. Fluorine Chem.*, 2005, **126**, 241.
16. S. Borkar, K. Jankova, H. W. Siesler and S. Hvilsted, *Macromolecules*, 2004, **37**, 788.
17. L. Valtola, A. Koponen, M. Karesoja, S. Hietala, A. Laukkanen, H. Tenhu and P. Denifl, *Polymer*, 2009, **50**, 3103.
18. J. Ma, C. Cheng, G. Sun and K. L. Wooley, *Macromolecules*, 2008, **41**, 9080.
19. J. Ma, C. Cheng and K. L. Wooley, *Macromolecules*, 2009, **42**, 1565.
20. K. Babiuch, R. Wyrwa, K. Wagner, T. Seemann, S. Hoeppener, C. R. Becer, R. Linke, M. Gottschaldt, J. Weisser, M. Schnabelrauch and U. S. Schubert, *Biomacromolecules*, 2011, **12**, 681.
21. K. Babiuch, D. Pretzel, T. Tolstik, A. Vollrath, S. Stanca, F. Foertsch, C. R. Becer, M. Gottschaldt, C. Biskup and U. S. Schubert, *Macromol. Biosci.*, 2012, **12**, 1190.
22. J. Chen, L. Dumas, J. Duchet-Rumeau, E. Fleury, A. Charlot and D. Portinha, *J. Polym. Sci. Part A: Polym. Chem.*, 2012, **50**, 3452.
23. L. Dumas, E. Fleury and D. Portinha, *Polymer*, 2014, **55**, 2628.
24. N. T. Brummelhuis and M. Weck, *ACS Macro Lett.*, 2012, **1**, 1216.
25. T. Cai, W. J. Yang, K.-G. Neoh and E. T. Kang, *Polym. Chem.*, 2012, **3**, 1061.
26. C. Ott, C. Ulbricht, R. Hoogenboom and U. S. Schubert, *Macromol. Rapid Commun.*, 2012, **33**, 556.
27. C. Weber, T. Neuwirth, K. Kempe, B. Ozkahraman, E. Tamahkar, H. Mert, C. R. Becer and U. S. Schubert, *Macromolecules*, 2012, **45**, 20.
28. F. T. Reyes, E. L. Malins, C. R. Becer and M. A. Kelland, *Energ. Fuel*, 2013, **27**, 3154.

29. X.-P. Qiu and F. M. Winnik, *Macromol. Rapid Commun.*, 2006, **27**, 1648.

30. C. Boyer, A. Granville, T. P. Davis and V. Bulmus, *J. Polym. Sci. Part A: Polym. Chem.*, 2009, **47**, 3773.

31. Y. Wu, Y. Zhou, J. Zhu, W. Zhang, X. Pan, Z. Zhang and X. Zhu, *Polym. Chem.*, 2014, **5**, 5546.

32. A. Postma, T. P. Davis, G. Moad and M. S. O'Shea, *Macromolecules*, 2005, **38**, 5371.

33. S. Perrier, P. Takolpuckdee and C. A. Mars, *Macromolecules*, 2005, **38**, 2033.

34. C. Liu, H. Wang, X. Xing, Y. Xu, J.-A. Ma and B. Zhang, *Tetrahedron Lett.*, 2013, **54**, 4649.

35. Q. Wang, H. Li, Q. Wei, J. Z. Sun, J. Wang, X. A. Zhang, A. Qin and B. Z. Tang, *Polym. Chem.*, 2013, **4**, 1396.

36. J. V. Staros, H. Bayley, D. N. Standring and J. R. Knowles, *Biochem. Bioph. Res. Co.*, 1978, **80**, 568.

37. N. Zhang, S. Huber, A. Schulz, R. Luxenhofer and R. Jordan, *Macromolecules*, 2009, **42**, 2215.

38. Y. K. Chong, J. Krstina, T. P. T. Le, G. Moad, A. Postma, E. Rizzardo and S. H. Thang, *Macromolecules*, 2003, **36**, 2256.

39. J. Chiefari, R. T. A. Mayadunne, C. L. Moad, G. Moad, E. Rizzardo, A. Postma and S. H. Thang, *Macromolecules*, 2003, **36**, 2273.

6. Conclusions and Outlook

This thesis has explored four novel copolymer syntheses that utilise a range of CRP techniques as well as pre/post-polymerisation modification.

Two original synthetic pathways were designed for the synthesis of PIB-*b*-PDMAEMA block copolymers. The first pathway modified primarily *exo*-olefin terminated PIB with an ATRP/SET-LRP initiating group to initiate the SET-LRP of DMAEMA. However, measured M_n of PIB-*b*-PDMAEMA synthesised via this pathway was approximately twice as large as the theoretical M_n. This was attributed to low end group fidelity of the PIB macroinitiator. Therefore, a new synthetic pathway was designed to perform macromolecular coupling between a primary amine terminated PDMAEMA, synthesised by SET-LRP, with PIBSA. This pathway was also successful at synthesising PIB-*b*-PDMAEMA, moreover measured M_n was a better fit with theoretical, dispersity was lower and PDMAEMA block length could be tuned. However, presence of PIBBSA may have resulted in the formation of higher molecular weight species forming as two couplings can occur. Future work will look to perform macromolecular coupling with a PIBSA that contains no PIBBSA (Scheme 1.14).

Olefin terminated PIB was converted to an acrylate macromonomer by end group modification; Friedel-Crafts alkylation of phenol followed by esterification with acryloyl chloride. This modification was highly effective at utilising all end group functionality present on the PIB to synthesise a macromonomer with a single acrylate functionality. RAFT polymerisation was then investigated as a means of homopolymerising DMA, DMAEA and PIBA. P(DMA) and P(DMAEA) synthesised by RAFT homopolymerisation had low dispersity, controlled molecular

weight, reached high monomer conversions but end group fidelity was diminished. P(PIBA) was polymerised to high monomer conversions but dispersity was broad. Finally, RAFT polymerisation was utilised to synthesise statistical and block copolymers of DMA and PIBA. Monomer composition could be adjusted whilst maintaining high monomer conversions and molecular weight increased as more PIBA was incorporated, however copolymer dispersity was broad. Future work will optimise the blocking efficiency of P(DMA) with PIBA and investigate the self-assembly behaviour of these copolymers.

The third project looked to copolymerise MalA with AMS monomers that were functionalised with linear alkyl chains or a tertiary amine. These functionalised AMS monomers were synthesised by reactive coupling of an isocyanate (TMI) and the chosen primary amine. Primary amines coupled were hexylamine, octadecylamine and *N*,*N*-dimethylethylenediamine. Monomer synthesis was very facile; high yields of monomers could be acquired with only filtration required for purification. Functionalised AMS monomers, except for the tertiary amine bearing monomer, were copolymerised via free radical polymerisation to synthesise near-perfectly alternating copolymers. Initiator concentration could be adjusted to influence copolymer M_n without negatively impacted dispersity or monomer conversion. Finally, an example of post-polymerisation modification was demonstrated by imidisation of the MalA repeat units with a primary amine. This functionalisation furnished an alternating difunctionalised copolymer. Future work will look to broaden the scope of post-polymerisation modification to other primary amines as well as alcohols.

A final project demonstrated the synthesis of well-defined P(PFS) via RAFT homopolymerisation. P(PFS) was then modified, by substitution of the *p*-fluoro, with thiols and hexylamine. Trithiocarbonate end group removal was required as presence of this end group is believed to have been the cause of multimodal GPC traces following modification. This end group removal would not be required if P(PFS) had been synthesised via NMP or ATRP. Furthermore, a novel functionalisation of P(PFS) by substituting the *p*-fluoro with sodium azide to furnish a styrenic backbone bearing aromatic azide moieties was developed. This modification was demonstrated for PFS and P(PFS) and was combined with substitution of the *p*-fluoro by TP and subsequent metal-free cycloaddition of the aforementioned polymeric aromatic azides and PA to functionalise a P(PFS) backbone multiple times.

Lastly, well-defined P[(PFS)-*b*-((iPOx)-*co*-(DMA))] was prepared to be utilised as a amphiphilic block copolymer that can undergo post-polymerisation modification via two major pathways; *p*-fluoro substitution and oxazoline ring opening. An Initial attempt at simultaneous *p*-fluoro substitution and oxazoline ring opening with TP demonstrated that *p*-fluoro substitution remained efficient but oxazoline ring opening was less efficient and only obtained 52% conversion. Future work will examine the scope of modifications possible as well as optimising the modification of P[(PFS)-*b*-((iPOx)-*co*-(DMA))] with thiols.

Publications

"Investigations on the Combination of Cationic Ring Opening Polymerization and Single Electron Transfer Living Radical Polymerization to Synthesize 2-Ethyl-2-Oxazoline Block Copolymers". R. A. Young, E. L. Malins and C. R. Becer, *Aust. J. Chem.*, 2012, **65**, 1132.

"Non-amide kinetic hydrate inhibitors: performance of a series of polymers of isopropenyloxazoline on structure II gas hydrates" F. T. Reyes, E. L. Malins, C. R. Becer and M. A. Kelland, *Energ. Fuel*, 2013, **27**, 3154.

"Precise insertion of clickable monomer along polymer backbone by dynamic temperature controlled radical polymerization" E. L. Malins, S. Amabilino, G. Yilmaz, F. H. Isikgor, B. M. Gridley and C. R. Becer, *Eur. Polym. J.*, 2015, **62**, 347.

"Alternating copolymers of functionalized α-methyl styrene monomers and maleic anhydride" E. L. Malins, C. Waterson and C. R. Becer, *Polym. Chem.*, 2015, **6**, 6543.

"Controlled synthesis of amphiphilic block copolymers based on poly(isobutylene) macromonomers" E. L. Malins, C. Waterson and C. R. Becer, *J. Polym. Sci. Part A: Polym. Chem.*, 2015, DOI: 10.1002/pola.20150544R1, accepted.

"Slow Chlorine Releasing Compounds: A Viable Sterilisation Method for Bioabsorbable Nanocomposite Biomaterials" N. Naderi, M. Griffin, E. L. Malins, C. R. Becer, A. Mosahebi, I. S. Whitaker and A. M. Seifalian, *J. Biomater Appl.*, accepted.